

An mRNA degradation complex in *Bacillus subtilis*

Dissertation

for the award of the degree
“Doctor rerum naturalium” (Dr.rer.nat.)
Division of Mathematics and Natural Sciences
of the Georg-August-Universität Göttingen

submitted by

Martin Lehnik-Habrink

from Berlin

Göttingen 2011

Prof. Dr. Jörg Stülke (Supervisor and 1st Reviewer)

(Institute for Microbiology and Genetics / Department of General Microbiology / University of Göttingen)

Prof. Dr. Kai Tittmann (2nd Reviewer)

(Albrecht-von-Haller-Institute for Plant Science / Department of Bioanalytics / University of Göttingen)

PD Dr. Wilfried Kramer

(Institute for Microbiology and Genetics / Department of Molecular Genetics and preparative Microbiology / University of Göttingen)

Date of oral examination: 26.10.2011

I hereby declare that the doctoral thesis entitled, "An mRNA degradation complex in *Bacillus subtilis*" has been written independently and with no other sources and aids than quoted.

Martin Lehnik-Habrink

Danksagung

Als erstes möchte ich mich ganz herzlich bei Prof. Dr. Jörg Stülke für die sehr gute Betreuung bedanken. Von seiner unterstützenden und offenen Art haben diese Arbeit und auch ich persönlich sehr profitiert. Vielen Dank!

Des Weiteren möchte ich Prof. Dr. Kai Tittmann für die Übernahme des Korreferates danken. Ihm und PD Dr. Wilfried Kramer möchte ich auch für die Teilnahme an meinem thesis committee danken. PD Dr. Boris Görke, Prof. Ralf Ficner und PD Dr. Michael Hoppert gilt mein Dank für Ihre Teilnahme an meiner Prüfungskommission. In diesem Zusammenhang sei auch den GGNB-Mitarbeitern für die Unterstützung gedankt.

Bei Dr. Ulrike Mäder möchte ich mich für die sehr angenehme und schöne Zusammenarbeit bedanken. Ebenfalls möchte ich mich bei allen Leuten aus der Abteilung von Prof. Dr. Richard Lewis aus Newcastle für die gute Zusammenarbeit bedanken.

Natürlich gilt ein besonders großer Dank allen Leuten aus dem Labor. Hierbei vor allem Christina Herzberg. Ihre liebenswerte und begeisternde Art half mir durch viele Hochs und Tiefs des alltäglichen (Labor-)Lebens. Ohne ihre Unterstützung wäre diese Arbeit niemals so entstanden. Vielen Dank!

Weiterhin möchte ich Dr. Nico Pietack, für seine Unterstützung in der Anfangsphase danken. Außerdem sei meinen Kollegen Fabian Rothe und Frederik Meyer für eine sehr heitere Büroatmosphäre gedankt. Dr. Katrin Gunka will ich besonders für ihre vielen Hilfen und Tipps im Labor danken. Christine Diethmaier will ich ebenfalls für ihre Hilfe danken. Auch bei Felix Mehne und Arne Schmeisky möchte ich mich für die Unterstützung bedanken. Allen Leuten, die hier genannt wurden, möchte ich noch einmal für einen wirklich sehr angenehmen und offenen Umgang im Labor danken. Außerdem sei dem ganzen Mycoplasmenlabor für die Hilfe gedankt.

Weiterhin möchte ich mich besonders bei meinen zu betreuenden Bachelor-, Master-, bzw. Diplomstudenten/innen: Leonie Rempeters, Henrike Pförtner und Dominik Tödter für die tatkräftige Unterstützung bedanken. Außerdem möchte ich allen Leuten in der Abteilung, welche hier nicht namentlich aufgeführt sind, danken.

Ein besonderer Dank gilt meinen Eltern, die mir stets Rückhalt und Unterstützung geboten haben, Vielen Dank!

Table of content

List of publication	I
List of abbreviations	II
Summary	IV
1. Introduction	1
1.1. RNA degradation in <i>E. coli</i>	3
1.2. The RNA degradosome of <i>E. coli</i>	4
1.3. <i>Bacillus subtilis</i>	9
1.4. RNases in <i>B. subtilis</i>	10
1.5. RNA processing in <i>B. subtilis</i>	13
1.6. DEAD-box RNA helicases in <i>B. subtilis</i>	17
2. Novel activities of glycolytic enzymes in <i>Bacillus subtilis</i>	19
3. CshA - the major RNA helicase in the degradosome of <i>Bacillus subtilis</i>	42
4. Multiple roles of the DEAD-box RNA helicase CshA in <i>Bacillus subtilis</i>	65
5. Characterization of RNase Y in <i>Bacillus subtilis</i>	95
6. Identification of targets of RNase Y in <i>Bacillus subtilis</i>	118
7. The role of YmdB in <i>Bacillus subtilis</i>	144
8. Discussion	167
8.1. RNase Y: the missing endoribonuclease of <i>Bacillus subtilis</i>	167
8.2. Re-fining the structure of RNase Y	172
8.3. The RNA degradosome of <i>B. subtilis</i>	174
8.4. mRNA degradation in <i>B. subtilis</i>	176
8.5. Which is the chief-endoribonuclease, RNase J1 vs RNase Y?	176
8.6. A model for the mRNA degradation in <i>B. subtilis</i>	179
8.7. CshA: A versatile RNA helicase of <i>B. subtilis</i>	183
9. References	188
10. Appendix	213
10.1. Oligonucleotides	213
10.2. Plasmids	237
10.3. Strains	247
10.4. Analysis of the DEAD-box helicases CshB, DeaD and YfmL in <i>B. subtilis</i>	252
10.5. Supplementary material for RNase Y microarray analysis	257
10.6. Curriculum vitae	276

List of publication

Commichau, F. M., Rothe, F. M., Herzberg, C., Wagner, E., Hellwig, D., **Lehnik-Habrink, M.**, Hammer, E., Völker, U. & Stülke, J. (2009). Novel activities of glycolytic enzymes in *Bacillus subtilis*: interactions with essential proteins involved in mRNA processing. *Mol. Cell. Proteomics* 8: 1350-1360.

Lehnik-Habrink, M., Pförtner, H., Rempeters, L., Pietack, N., Herzberg, C. & Stülke, J. (2010). The RNA degradosome in *Bacillus subtilis*: identification of CshA as the major RNA helicase in the multiprotein complex. *Mol. Microbiol.* 77: 958-971.

Lehnik-Habrink, M., Newman, J., Rothe, F. M., Solovyova, A. S., Rodrigues, C., Herzberg, C., Commichau, F. M., Lewis, R. J. & Stülke, J. (2011). RNase Y in *Bacillus subtilis*: a natively disordered protein that is the functional equivalent to RNase E from *Escherichia coli*. *J. Bacteriol.* 193: 5431-5441.

Lehnik-Habrink, M., Schaffer, M., Mäder, U., Diethmaier, C., Herzberg, C. & Stülke, J. (2011). RNA processing in *Bacillus subtilis*: identification of targets of the essential RNase Y. *Mol. Microbiol.* 81: 1459-1473.

Diethmaier, C., Pietack, N., Gunka, K., Wrede, C., **Lehnik-Habrink, M.**, Herzberg, C., Hübner, S. & Stülke, J. (2011). A Novel Factor Controlling Bistability in *Bacillus subtilis*: The YmdB Protein Affects Flagellin Expression and Biofilm Formation. *J. Bacteriol.* in press

List of abbreviations

% (vol/vol)	% (volume/volume)
% (wt/vol)	% (weight/volume)
ADP	adenosine diphosphate
Amp	ampicillin
AP	alkaline phosphatase
ATP	adenosine triphosphate
<i>B.</i>	<i>Bacillus/Bordetella</i>
B2H	bacterial two-hybrid
CD	catalytic domain
CDP*	disodium 2-chloro-5-(4-methoxyspiro {1,2-dioxetane-3,2'-(5'-chloro)tricyclo[3.3.1.1 ^{3,7}]decan}-4-yl) phenyl phosphate
Cm	chloramphenicol
CTD	C-terminal domain
DNA	deoxyribonucleic acid
<i>E.</i>	<i>Escherichia</i>
EDTA	ethylenediaminetetraacetic acid
Em	erythromycin
FA	formaldehyde
Fig.	figure
fwd	forward
Glc	glucose
IPTG	isopropyl- β -D-thiogalactopyranoside
LB	Luria Bertani (medium)
LFH-PCR	Long Flanking Homology PCR
Lin	Lincomycin
mRNA	messenger RNA
OD _x	optical density , measured at the wavelength $\lambda = x$ nm
ONPG	ortho-Nitrophenyl- β -galactoside
<i>ori</i>	origin of replication
<i>P</i>	promoter
PAGE	polyacrylamide gel electrophoresis
PCR	polymerase chain reaction
pH	power of hydrogen

PVDF	polyvinylidene difluoride
rev	reverse
RNA	ribonucleic acid
S	Succinate
<i>S.</i>	<i>Saccharomyces</i>
SD	Shine-Dalgarno
SDS	sodium dodecyl sulfate
SP	sporulation medium
Spec	Spectinomycin
SPINE	Strep-protein interaction experiment
Tab.	Table
Tet	Tetracycline
Tris	tris(hydroxymethyl)aminomethane
U	units
WT	wild type
X-Gal	5-bromo-4-chloro-3-indolyl- β -D-galactopyranoside
YFP	yellow fluorescent protein

Summary

In every organism the degradation of mRNAs is a fundamental process. This step not only recycles nucleotides but also adjusts gene expression due to the availability of the mRNA templates. The main players in this process are RNases which can function as single enzymes or in multiprotein complexes, the so-called RNA degradosomes. Recently, the existence such an RNA degradosome was demonstrated in the Gram-positive model organism *Bacillus subtilis*. The investigation of the complex and detailed analyses of some of its members was the aim of this work.

The initial model of the RNA degradosome of *B. subtilis* consists of RNases and glycolytic enzymes. The central RNase of the complex is the endoribonuclease RNase Y. To assess the impact of RNase Y on mRNA decay we performed microarray analysis demonstrating that depletion of the enzyme affects the degradation of transcripts on global scale. Further analysis of several targets revealed that RNase Y is indeed crucial for the turnover of the transcripts resulting in remarkably increased half lives upon depletion of the enzyme. These experiments highlight RNase Y as a key player in the mRNA degradation of *B. subtilis*.

Due to its high significance in the mRNA decay process we further investigated RNase Y for its physiological and biochemical properties. We studied its domain organization and revealed that the protein contains substantial regions of intrinsic disorder. Furthermore we demonstrated that the membrane localization of RNase Y is essential for survival.

As mentioned, the initial model of the RNA degradosome contained only RNases and glycolytic enzymes. In contrast to homolog complexes in other bacteria, a DEAD-box RNA helicase was not present in our model. Therefore we re-addressed this issue and revealed that the DEAD-box RNA helicase CshA has the ability to interact with all enzymes of the complex, especially with the important RNase Y. The suggested participation of CshA in the RNA degrading complex is underlined by the fact that deletion of *csHA* affects the abundance of hundreds of mRNAs. In addition to its participation in the RNA degradosome, we found that CshA is implicated in the biogenesis of ribosomes and the adaption to low temperatures.

In conclusion, the analysis of RNase Y and CshA as members of the RNA degradosome revealed the impact of both enzymes for the physiology of *B. subtilis* and pave the way for further investigations.

1. Introduction

mRNA turnover – a general introduction

One of the keystones in molecular biology is the central dogma: DNA > RNA > proteins, first articulated by Francis Crick in 1958. Even though this idea was challenged by several exceptions it is still valid for the considerable majority of lifestyles of most organisms. One of the main consequences of the statement is that the flow of information from the DNA (blueprint of life) to the proteins (players of life) is carried out via RNA (Crick, 1970). This highlights the importance of RNA in the overall process of life.

In general the bacterial cell contains three major types of RNA: messenger (mRNA), ribosomal RNA (rRNA) and transfer RNA (tRNA). Messenger RNAs carry the information for the amino acid composition of a protein from the DNA to the ribosome, the site of protein synthesis or translation. This large macromolecular complex is composed of proteins and RNA molecules, the ribosomal RNAs. Transfer RNAs are involved in the process of translation as they are adaptor molecules that bridge the three-letter-genetic code in mRNAs with the twenty-letter code of amino acids in proteins. Therefore rRNA and tRNA are involved in the process of protein synthesis itself whereas mRNAs are the blueprint of the individual proteins. This difference in the function of the molecules is reflected by the stability of the species. Because rRNA and tRNA are involved in the process of protein biosynthesis the molecules are rather stable, as degradation would affect the whole cellular physiology. In contrast, mRNAs are quite unstable molecules as the cell has to constantly adapt to its environment and therefore adjusts its mRNA and in turn protein composition.

Importance of mRNA turnover

As a result of a longstanding interplay between bacteria and a continuously changing set of environmental stimuli, a very complex adaptational and regulatory network has been developed. The aim of all regulatory processes is it to provide the cell with a best protein setting that enables the bacterium to cope with the stimuli and to promote growth (Hecker, 2003). In general, the synthesis of a certain protein is predominantly regulated by the abundance of the corresponding mRNA. Because the cellular concentration of a given transcript itself depends on the rates of its synthesis and degradation, both transcription and degradation control the level of proteins in the cell.

Whereas extensive work has been devoted to transcriptional regulation, regulation of RNA degradation is much less elucidated.

One of the main features of bacterial RNA degradation is the short half life of transcripts. Compared to eukaryotes, exhibiting mRNA half-lives in the range of hours, bacteria show considerable mRNA instability *in vivo*. This property is part of the bacterial strategy to respond to changing environmental conditions as protein synthesis can be rapidly reprogrammed by changes in the mRNA pattern of the cell (Rauhut & Klug, 1999).

Players of mRNA turnover

The main players in the process of mRNA turnover are ribonucleases. These enzymes catalyze the degradation of RNA into smaller pieces and ultimately to nucleotides. RNases exhibit a broad range of properties in terms of substrate specificity and interaction ability. While some RNases only act on specific targets, others have an impact on a global scale; some of them are essential whereas others exhibit a functional overlap and are interchangeable. Furthermore several RNases exclusively work as single enzymes; whereas others cooperate with distinct enzymes and form large macromolecular complexes. Despite this high variance, all ribonucleases can be classified into two groups depending of their site of action. Endoribonucleases cleave mRNAs within the body of the transcript whereas exoribonucleases degrade the molecules from either the 5' or the 3' end. It is important to note that, in the process of mRNA decay, RNases do not simply act as molecular killers, degrading every transcript equally. In contrast, they act according to the requirements of the cell (Arraiano *et al.*, 2010).

The well studied Gram negative model organism *E. coli* often served as a paradigm to understand fundamental processes of gene regulation. Therefore it is assumed that fundamental mechanisms of mRNA turnover derived from *E. coli* are valid for many other bacteria, too.

The generally accepted model of mRNA turnover, derived from studies done in *E. coli*, is thought to proceed by a combination of series of endonucleolytic cleavages, followed by exonucleolytic degradation of the resulting fragments from the 3' end (Kushner, 2002). The absence of a 5'-3' exonuclease activity that can degrade transcripts from the beginning and the fact that 3' ends of mRNAs are often protected by secondary structures like transcription terminators support this idea. To circumvent this obstacle RNA decay is initiated by an endonucleolytic cleavage. The major endoribonuclease involved in this process is RNase E (Babitzke & Kushner, 1991). RNase E binds the 5' end

of the transcript and scans the mRNA for further cleavage sites. The process of initial endonucleolytic cleavages is thought to be the rate limiting step in the mRNA decay in *E. coli*. Degradation from the 5' end is favorable as it rapidly separates the ribosome binding site and start codon from the rest of the mRNA resulting in inactivation of the message for translation. Even though RNase E is the major player, a number of other endoribonucleases exists, but their participation in overall mRNA turnover is only minor (Carpousis *et al.*, 2009; Jain, 2002; Kushner, 2002).

1.1. RNA degradation in *E. coli*

Following the initial endonucleolytic cleavage, degradation of the products occurs by exoribonucleases in 3'-5' direction. The three main enzymes involved in this process are polynucleotide phosphorylase (PnpA), RNase R and RNase II. Interestingly, inactivation of one of these enzymes has no effect on growth at normal temperature, suggesting functional overlap *in vivo*. The advantage of having preceding endonucleolytic cleavage steps lies in the fact that several mRNAs have protected 3' ends due to secondary structures. An initial endonucleolytic cut results in the formation of a new unprotected 3' end inside of the mRNA serving as an entry site for different exoribonucleases. This subsequent degradation by exoribonucleases results in the release of oligonucleotides in *E. coli*. These residual products are digested to mononucleotides by the oligonuclease (Niyogi & Datta, 1975). This exoribonuclease prefers very short RNA oligomers. In the absence of the enzyme very short nucleotides with a length 2-5 nt accumulate significantly (Ghosh & Deutscher, 1999). Interestingly the oligonuclease is one out of the three essential RNases of *E. coli* (Jain, 2002).

RNase E in *E. coli*

RNA turnover in *E. coli* is tightly connected to RNase E. This protein was initially described to be required for the processing of the 9S rRNA of *E. coli* (Ghora & Apirion, 1978). Later on, it was shown that the enzyme also has a strong impact on bulk mRNA turnover (Babitzke & Kushner, 1991). The list of targets where RNase E cleavage occurs was extended considerably in the following years encompassing: processing of 5S rRNA gene (Misra & Apirion, 1979), the 16S RNA gene (Li *et al.*, 1999), several tRNAs (Ow & Kushner, 2002), transfer mRNAs (Lin-Chao *et al.*, 1999) and the M1 RNA component of the RNase P ribozyme (Ko *et al.*, 2008). Very recently, tiling array studies revealed that mutations in RNase E affect about 40 % of the mRNAs in *E. coli* (Stead *et al.*, 2011).

RNase E is a quite large enzyme with a molecular weight of 118 kDa comprising two functional domains (see Fig. 1). The amino terminal part harbors the catalytic activity and is well conserved among bacteria expressing RNase E homologues (Marcaida *et al.*, 2006). Crystal structure determinations of this part revealed that the subdomain encompassing the active site is structurally similar to a desoxyribonuclease (Callaghan *et al.*, 2005). In contrast, the C-terminal half is poorly conserved, largely unstructured and has no catalytic activity (Callaghan *et al.*, 2004).

RNase E acts as a single-stranded, non specific endoribonuclease with a preference for cleaving A/U rich sequences (McDowall *et al.*, 1995). At least *in vitro*, its activity is highly dependent on the 5' end of its substrates. RNAs with terminal 5' triphosphates groups are poorly cleaved, whereas 5' monophosphorylated substrates are strongly preferred (Mackie, 1998). The preference for monophosphorylated substrates was further supported by the finding that the enzyme RppH, which removes pyrophosphates from the 5' end of triphosphorylated RNA can contribute to the overall decay process (Celesnik *et al.*, 2007; Deana *et al.*, 2008). However, the cellular levels of the majority of transcripts seemed to be largely unaffected by deleting *rppH* (Deana *et al.*, 2008). Furthermore, a number of targets are degraded irrespective of their phosphorylation status. Therefore a model called "direct entry" was proposed, which suggests the existence of a 5' end-independent mechanism of mRNA degradation (Baker & Mackie, 2003; Kime *et al.*, 2010).

1.2. The RNA degradosome of *E. coli*

The RNA degradosome of *E. coli* is a multiprotein complex involved in RNA degradation. It was first discovered in attempts to purify RNase E from *E. coli*. In this and further experiments three proteins co-purified in stoichiometric amounts. These proteins were the exoribonuclease polynucleotide phosphorylase (PnpA), the DEAD-box RNA helicase RhlB and the glycolytic enzyme enolase (Miczak *et al.*, 1996; Py *et al.*, 1994). In the following years it was demonstrated that the unstructured carboxy-terminal half of RNase E forms an organizing scaffold domain that tethers the degradosome components (Vanzo *et al.*, 1998). Even though this domain has little intrinsic structure, four isolated segments were characterized with increased structural propensity (see Fig. 1). The first segment localizes the degradosome to the inner cytoplasmic membrane (Khemici *et al.*, 2008). The second segment is important for the binding of RhlB (Chandran *et al.*, 2007). The third and fourth segments are important for the binding of enolase and polynucleotide phosphorylase (Callaghan *et al.*, 2004; Chandran & Luisi, 2006).

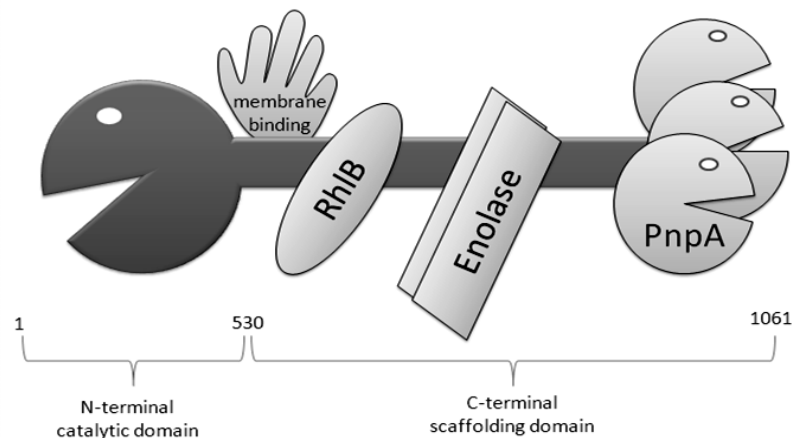


Fig. 1. Schematic cartoon of *E. coli* RNase E with the assembled proteins RhIB, Enolase and PnpA. RNase E contains two distinct domains: the N-terminal comprises the endonucleolytic activity; the C-terminal part is involved in direct protein-protein interactions for the formation of the RNA degradosome. The membrane binding domain tethers the complex to the inner cytoplasmatic membrane.

Determinations of the overall molecular weight of the RNA degradosome are quite difficult. In the current model the degradosome would be a 4.1 mega Dalton complex in which three RNase E tetramers bind to four PnpA trimers. Adding the glycolytic enolase and the RNA helicase RhIB the complex would comprise a 12:12:24:12 stoichiometry (RNase E: PnpA: enolase: RhIB) (Carpousis, 2007; Marcaida *et al.*, 2006).

The polynucleotide phosphorylase of *E. coli*

One of best studied 3'-5' exoribonucleases in *E. coli* is the polynucleotide phosphorylase. This enzyme can be found in most bacteria as well as eukaryotic organelles, i.e. mitochondria and chloroplasts. PnpA is a homotrimeric protein with a structural core, containing the catalytic domain, and the two carboxy terminal RNA-binding domains, KH and S1 (Stickney *et al.*, 2005). The three subunits associate via trimerization interfaces of the core domain, forming a central channel (Symmons *et al.*, 2000). *In vitro*, PnpA is able to catalyze the processive 3'-5' phosphorolytic degradation as well as the reverse polymerization reaction. *In vivo*, the enzyme has been shown to be indeed implicated in both degradation and polyadenylation of RNAs (Carzaniga *et al.*, 2009; Mohanty & Kushner, 2000). Consistently with these versatile properties, PnpA is involved in many aspects of RNA metabolism. It is the major exoribonuclease for degrading mRNA decay intermediates and small noncoding RNAs, particularly the

structured regions of these molecules (Kushner, 2002; Xu & Cohen, 1995). Although *E. coli* encodes several exoribonucleases degrading RNA in 3' -5' direction, PnpA is somehow special as double mutations affecting PnpA and RNase II (Donovan & Kushner, 1986), or PnpA and RNase R are lethal (Cheng *et al.*, 1998), whereas strains devoid of RNase II and RNase R are viable (Wu *et al.*, 2009). Very recently it was discovered that the metabolite citrate and the signaling molecule c-di-GMP can alter the activity of the enzyme (Nurmohamed *et al.*, 2011; Tuckerman *et al.*, 2011).

The DEAD-box RNA helicase RhlB of *E. coli*

DEAD-box RNA helicases are a ubiquitous family of ATPases involved in RNA metabolism. They are characterized by nine conserved sequence motifs including the name-giving DEAD motif (Asp-Glu-Ala-Asp) forming the catalytic core of the enzyme (Rocak & Linder, 2004). Structural studies have shown that this core folds into two 'RecA-like domains' separated by a flexible linker, with the conserved motifs being involved in the binding of ATP or RNA or in inter-domain contacts (Sengoku *et al.*, 2006). Additionally, C- or N-terminal extensions can be found, conferring substrate or interaction partner specificity. In general, DEAD-box RNA helicases function in the cell in processes of rearranging RNAs and ribonucleoprotein structures (Fairman *et al.*, 2004).

E. coli encodes five different RNA helicases. Functional analysis of strains deleted in one of the enzymes revealed that four out of the five RNA helicases are important for the proper assembly of ribosomes (Iost & Dreyfus, 2006; Jain, 2008). Interestingly, the RhlB helicase is not involved in this process, but contributes significantly to the mRNA turnover of the cell. Even though deletion of *rhlB* increased overall mRNA only slightly, the steady-state abundances of hundreds of mRNAs were affected significantly (Bernstein *et al.*, 2004). *In vitro*, RhlB has no detectable RNA-dependent ATPase activity. This activity is restored when RNase E (or the polypeptide containing the RhlB binding site) is added to the reaction, suggesting that RNase E is necessary to stimulate ATPase activity (Vanzo *et al.*, 1998). However, RhlB is not the only RNA helicase having the ability to bind to RNase E. During cold shock, the RNA helicase CsdA also associates with the degradosome. Functional assays using reconstituted minimal degradosomes showed that CsdA can fully replace the resident RNA helicase of the RNA degradosome, RhlB. Furthermore it was shown that other helicases also have the potential to interact with RNase E *in vitro* (Prud'homme-Généreux *et al.*, 2004). The reasons for an alternative RNA degradosome in response to cold shock remain to be clarified (Carpousis, 2007).

Enolase of *E. coli*

The glycolytic enzyme enolase is universally conserved in organisms of all domains of life. In glycolysis it forms phosphoenolpyruvate from 2-phosphoglycerate. Pull-down experiments revealed that about one-tenth of the cellular enolase is bound to RNase E and therefore most likely participates in the RNA degradosome (Liou *et al.*, 2001). The role of this metabolic enzyme in the complex is not well understood. However, it was shown that enolase is involved in the degradation of the transcript for the major glucose transporter under certain conditions (Morita *et al.*, 2004). A global microarray study revealed that deletion of enolase affected the steady-state abundances of mRNAs encoding proteins involved in energy-generating pathways (Bernstein *et al.*, 2004). Therefore it was hypothesized that the glycolytic enzyme serves a sensor to link the metabolic status of the cell to mRNA degradation.

The physiological role of the RNA degradosome

As the RNA degradosome of *E. coli* is formed at the C-terminal end of the protein, truncation of this part would prevent the formation of the complex. Even though full length RNase E is essential, strains expressing C-terminal truncated RNase E variants are viable, suggesting that the catalytic activity causes the essentiality of the enzyme (Kaberdin *et al.*, 1998). Furthermore none of the other enzymes of the complex are essential. Nevertheless, in a genome-wide study it was demonstrated that the assembly of the RNA degradosome is crucial for normal mRNA decay. Deletions of the individual components of the complex (RhlB, PnpA and Eno) were compared with a mutant strain that expressed a C-terminal truncated RNase E variant. It was revealed that in a mutant strain expressing the truncated form of RNase E (which is viable as it contained the catalytic site) mRNA turnover was corrupted anyhow. For several genes a clear overlap of altered mRNA amounts between single deletions of PnpA, RhlB or Eno and the RNase E C-terminal truncation strain could be demonstrated, representing mRNAs that are probably specific target of the RNA degradosome (Bernstein *et al.*, 2004).

Another evidence for the physiological relevance of the RNA degradosome comes from the degradation of REP elements (repeated extragenic palindrome). REP elements (or REP stabilizers) are structural elements in polycistronic messages that protect 5' proximal cistrons from 3'-5' exonucleolytic degradation. It was demonstrated that under certain conditions mutations in *rhlB* as well as *pnpA* stabilized mRNAs containing these

REP elements. Interestingly, truncation of the C-terminus of RNase E which still contain the catalytic site (but no longer can bind RhlB or PnpA) exhibited the same pattern of REP stabilization as the single *rhlB* and *pnpA* deletions, suggesting that the formation of the RNA degradosome is crucial for the turnover of the REP structures (Carpousis, 2007; Khemici & Carpousis, 2004).

RNA degradation by macromolecular complexes

The presence of RNase E homologs in many bacteria suggested that the RNA degradosome is not unique to *E. coli*. However, prediction of such a complex is quite difficult, as sequence alignments of different RNase E homologous revealed, that conservation of the complex coordinating C-terminal half of the protein is rather low in other bacteria. Nevertheless experimental verification for the existence of an RNA degradosome was successful in several cases. *Caulobacter crescentus*, a Gram negative α -proteobacterium harbors a complex consisting of an RNase E homolog, a DEAD-box RNA helicase, PnpA and the Krebs cycle enzyme aconitase (Hardwick *et al.*, 2011). Further complexes with RNase E as the central protein were reported (Ait-Bara & Carpousis, 2010; Erce *et al.*, 2010).

The degradation of RNA by macromolecular machines is not a unique feature of bacteria. Archea and Eukaryotes also contain ribonucleolytic complexes. These so-called exosomes were first described in *Saccharomyces cerevisiae* (Mitchell *et al.*, 1997). This complex endowed with ribonucleolytic activity is present in both the nucleus and cytoplasm. The exosome in the nucleus is involved in the maturation of stable RNA molecules, such as rRNA. Cytoplasmic exosome participates in the mRNA turnover and degradation of mRNA interference intermediates (Tomecki *et al.*, 2010). Interestingly, despite the presence of several catalytic sites, the exosome is almost entirely inactive without the aid of cofactors. Several of these cofactors (Mtr4 or Ski-proteins) are DEAD-box RNA helicases which somehow activate the complex or simply recruit the exosome to the specific RNA substrate (Liu *et al.*, 2006).

In analogy to the eukaryotic exosome, a structurally similar complex was discovered in archea, too (Evguenieva-Hackenberg *et al.*, 2003). The overall quaternary structure of both exosomes (the one from eukaryotes as well as the one of archea) exhibit high similarity to the bacterial polynucleotide phosphorylase (PnpA) suggesting an evolutionary conservation of this complex in all domains of life (Hartung & Hopfner, 2009). In agreement with this idea is the finding that even in *E. coli* a PnpA-mediated

complex with the DEAD-box protein RhlB exists independent of RNase E (Lin & Lin-Chao, 2005). Therefore in terms of evolutionary conservation it is probably not the RNase E-mediated RNA degradosome itself that is conserved, but a complex with a structure, resembling homology to PnpA (Lin-Chao *et al.*, 2007).

1.3. *Bacillus subtilis*

Over several decades, *B. subtilis* emerged as a model organism for Gram positive bacteria and basic cell differentiation (endospore formation). Working with *B. subtilis* has several advantages, making it easy to handle the bacterium in the daily lab routine: it is non-pathogenic, naturally competent and its genome was one of first that was sequenced (Kunst *et al.*, 1997).

It is generally assumed that the natural habitat of *B. subtilis* is the upper layer of the soil, a quite challenging environment. Therefore the bacterium evolved some elaborate adaptation mechanisms to cope with changing water, nutrient or oxygen supply and fluctuating temperatures (Hecker & Völker, 1998; Hecker *et al.*, 2007). Furthermore under condition of severe nutrient starvation the bacterium is able to form endospores. When *B. subtilis* is sporulated the bacterium is still “alive”, but somehow dormant. Endospores are bacterial structures that withstand high temperatures, drying out, freezing or total nutrient depletion; thus, conditions that would easily kill a vegetative cell. Nevertheless spores are not dead cells; they still sense the environment and when conditions improve they undergo germination and become vegetative cells, again (Piggot & Hilbert, 2004).

RNA degradation in *Bacillus subtilis*

Studies in the Gram negative enterobacterium *E. coli* have served several times as a paradigm to understand fundamental cellular processes in other organisms. Therefore, the publication of the genome sequence of *B. subtilis* in 1997 was somewhat surprising with respect to RNA decay (Kunst *et al.*, 1997). Sequence alignments of the two genomes revealed that *B. subtilis* did not contain homologs for some of the most important enzymes of the RNA degradation machinery of *E. coli*. Especially the absence of a homolog for the essential endoribonuclease RNase E was surprising. Furthermore, no homologs for the important exoribonuclease RNase II and the essential oligoribonuclease were found. Therefore, *B. subtilis* contains either a different mechanism of RNA turnover compared to *E. coli* or, at least a different set of proteins fulfills the function (Bechhofer, 2009).

Another fundamental difference was already found several decades ago. It was demonstrated that RNA decay in *B. subtilis* happens first of all phosphorolytically whereas *E. coli* degrades RNA mainly hydrolytically (Chaney & Boyer, 1972; Duffy *et al.*, 1972). This means that in *B. subtilis* the removal of a nucleotide from the end of an mRNA occurs by addition of a phosphate and not water. Therefore RNA degradation in *B. subtilis* results in nucleotide diphosphates whereas *E. coli* gives nucleotide monophosphates. This discrepancy is caused by different enzymatic activities of two RNases (Deutscher & Reuven, 1991). While in *E. coli* 90% of the degrading activity comes from the hydrolytic enzyme RNase II, in *B. subtilis* the major contributor to this decay is the phosphorolytic enzyme PnpA (Wang & Bechhofer, 1996). This fundamental difference was explained by the distinct habitats the two organisms live in. *E. coli* occupies an energy-rich environment (the gut) whereas *B. subtilis* has to cope with energy-poor conditions (the soil). The phosphorolytic decay, with its retention of phosphate bond energy in the breakdown products, might be particularly advantageous for *B. subtilis* (Bechhofer, 2009; Deutscher & Reuven, 1991).

A third and very significant difference was discovered only recently. *B. subtilis* contains a 5'-3' exonuclease (Mathy *et al.*, 2007). This enzymatic activity was long anticipated and in theory is most beneficial with respect to suppress translation. Whereas digestion products of 3'-5' exonucleases would be translated until the very end (the translation initiation region would be degraded at last), 5'-3' exonucleolytic attack would eliminate the ribosome binding sites at the very beginning avoiding wasteful protein translation.

1.4. RNases in *B. subtilis*

B. subtilis contain 18 different RNases, 12 endoribonucleases and 7 exoribonucleases (RNase J1 counts in both categories as it contains endonucleolytic and exonucleolytic activities). Several of the endoribonucleases exhibit specificity to a certain substrate (RNase P and RNase Z are involved in tRNA maturation, RNase Mini-III and RNase M5 cleave rRNA) (Condon, 2003). Most interesting in terms of gene expression and regulation, are globally acting mRNA-specific RNases. Next, two endoribonucleases are introduced that have the capability to cleave several mRNAs. Furthermore the polynucleotide phosphorylase (a 3'-5' exonuclease) of *B. subtilis* is presented.

RNase J1/J2

The two J-type RNases J1 and J2 were first discovered in the search for the endoribonuclease responsible for the cleavage of the *thrS* leader sequence (Even *et al.*, 2005). When this leader sequence is transferred to *E. coli* it is processed in an RNase E dependent manner, suggesting that identification of the endoribonuclease in *B. subtilis* responsible for the cleavage will reveal the functional homolog of RNase E of *E. coli* (Condon *et al.*, 1997). To identify the enzyme in *B. subtilis*, crude extracts were fractionated until two proteins were left exhibiting this activity *in vitro*. These so far unknown proteins YkqC and YmfA, were renamed RNase J1 and J2 (Even *et al.*, 2005). A sequence alignment of the two enzymes revealed 49 % identity. The close relationship of the two enzymes is underlined by two-hybrid experiments demonstrating an interaction of both proteins (Commichau *et al.*, 2009). Further gel-filtration experiments suggested a hetero-tetrameric complex. Interestingly, the complex of the two proteins had altered target site specificity as compared to the isolated enzymes alone (Mathy *et al.*, 2010). In addition, RNase J1 and J2 exhibited a high level of redundancy in terms of substrate specificity. Microarray analysis revealed that inactivation of either one enzyme had only little effect on mRNA turnover, whereas inactivation of both enzymes led to 300 mRNAs with increased and 300 mRNA with decreased amounts (Mäder *et al.*, 2008). Although the transcriptome results showed a rather significant impact on mRNA turnover, the inactivation of both enzymes had only little effects on bulk mRNA degradation (Even *et al.*, 2005). Despite the similarities of the two enzymes, it is interesting to note that only RNase J1 is essential in *B. subtilis*.

Even though RNase J1 was first described as an endoribonuclease, further research revealed a second catalytic activity. It was demonstrated that maturation of the 5' end of *B. subtilis* 16S ribosomal RNA occurs via a 5'-3' exonucleolytic pathway and that this process is catalyzed by RNase J1. Therefore RNase J1 is not only an endoribonuclease but also contains 5'-3' exonucleolytic activity. This activity was so far only known from eukaryotic organisms. Interestingly, the 5'-3' exonucleolytic activity is blocked by 5' triphosphates, whereas the endonucleolytic activity of J1 is measured even in the presence of a triphosphate at the 5' end. Analysis of the crystal structure of the RNase J1 homolog of *Thermus thermophilus* revealed that a binding pocket coordinating the phosphate and base moieties of the nucleotide in the vicinity of the catalytic center provides an explanation for the 5' monophosphate-dependent 5'-3' exoribonucleolytic activity. In addition, it was shown that despite the lack of sequence homology the overall tertiary structure of the enzyme is quite similar to that of the catalytic domain of RNase E from *E. coli* (Li de la

Sierra-Gallay et al., 2008). A so far unanswered question is, whether the endonucleolytic or the exonucleolytic activity of RNase J1 makes the enzyme essential.

RNase Y

Even though RNase J1/J2 affected the steady state level of several mRNAs, the impact of both enzymes on bulk mRNA turnover is only minor. Just recently a new endoribonuclease named RNase Y was discovered. A first investigation of the protein, at a time when the ribonucleolytic activity was only annotated, showed that the protein is essential. The prolonged depletion of RNase Y (at this time called YmdA) in a conditional mutant resulted in abnormalities on cell and chromosome morphology already suggesting a significant impact of the protein (Hunt *et al.*, 2006).

A first hint that RNase Y (YmdA) is probably endowed with ribonucleolytic activity derived from analysis of the *gapA* operon. It was demonstrated that depletion of the protein resulted in the stabilization of the full length transcript of the *gapA* operon (Commichau *et al.*, 2009)(for detail see processing of the *gapA* operon). In the same study another interesting feature of RNase Y (YmdA) was discovered. Using a pull-down approach to identify interaction partners of glycolytic enzymes binding of enolase and phosphofructokinase to several RNases was revealed, among them RNase Y (YmdA). To verify these potential interactions, a large two-hybrid screen was conducted, suggesting a degradosome-like complex in *B. subtilis*. The hypothesized model comprised the RNases Y, J1, J2 and PnpA and the two glycolytic enzymes enolase and phosphofructokinase (Commichau *et al.*, 2009). In this model RNase Y (YmdA) is the only enzyme that is able to bind to all other proteins of the complex (except RNase J2), suggesting a major role in the formation of the postulated RNA degradosome.

The biochemical verification that RNase Y indeed possesses endoribonucleolytic activity was brought in the same year. In an attempt to identify the endoribonuclease responsible for the turnover of the *yitJ* riboswitch, RNase Y was discovered to initiate the process, as none of the other endoribonucleases of *B. subtilis* (RNase J1/J2, RNase III) exhibited a stabilizing effect on the riboswitch leader. Further *in vitro* experiments suggested that the enzyme is a 5' dependent endoribonuclease with a preference for monophosphorylated ends. However, RNase Y was not only important for the turnover of the *yitJ* leader but also acted on all riboswitches controlled by the S-box mechanism. This more global effect of the enzyme was highlighted by the fact that RNase Y depletion increases bulk mRNA abundance more than twofold (Shahbadian *et al.*, 2009).

Polynucleotide phosphorylase

The polynucleotide phosphorylase of *B. subtilis* is a large enzyme of 77 kDa and belongs to the family of the phosphate-dependent exoribonucleases. This family is widely distributed in several organisms. It is suggested that most PnpA enzymes are likely to form trimers (Symmons *et al.*, 2000). Even though the enzymatic activity is phosphorolytic, under conditions of excess nucleosides, the reverse reaction can be catalyzed (Mitra *et al.*, 1996). *In vivo* a *pnpA* mutant strain exhibits several phenotypes like filamentous growth, cold sensitivity and competence deficiency (Wang & Bechhofer, 1996). The reason for these phenotypes is unknown, but it is assumed that PnpA is involved in the degradation of mRNAs encoding proteins involved in these processes. Despite the fact, that PnpA plays a major role in the mRNA turnover of *B. subtilis*, a *pnpA* deletion strain is viable (Bechhofer, 2009).

A well-known target of PnpA is the *trp* leader sequence. In wild type cells PnpA degrades the leader and by this, releases the regulatory RNA binding protein TRAP. If PnpA is absent, TRAP remains bound to the leader and is subsequently titrated away so expression is no longer regulated (for further details see 'Processing of the *trp* operon'). Further investigation demonstrated that PnpA poorly binds the native 3' end of the *trp* leader which contained a secondary structure and 6 single stranded nucleotides (Deikus *et al.*, 2004). The extension of several nucleotides at the end of the leader enables PnpA to bind, but the enzyme has still difficulties to degrade recessively through the secondary structure present at the 3' end. Therefore it is hypothesized that PnpA does not bind and degrade mRNAs from their native 3' ends. It is more likely that the enzyme needs entry sites generated by endonucleolytic cleavages.

1.5. RNA processing in *B. subtilis*

RNA processing is an event in which cleavage occurs in the body of the transcript. In *E. coli* this endonucleolytic cleavage produces entry sites for further degradation by exoribonucleases. It is assumed that the initial endoribonucleolytic cut is the rate-limiting step in the overall mRNA turnover. However, processing is more than a simple door opener for mRNA decay. Here, three examples are presented where endonucleolytic cleavage is important for regulatory mechanisms; the recycling of a regulator (*trp*), adjustment of different expression levels of two proteins encoded in the same operon (*gapA*) and the modulation of RNA stability in response to nutrient availability (*thrS*).

Processing of the *trp* operon mRNA

The *trp* operon encodes proteins needed for the *de novo* biosynthesis of the aromatic amino acid tryptophan. This operon is regulated by a premature transcription termination decision occurring in the untranslated 5' region of the operon, the *trp* leader site. When cells grow in media with high amounts of tryptophan, excess tryptophan can bind the regulatory protein TRAP (*trp* RNA-binding attenuation protein). Binding of tryptophan enables the TRAP protein to bind to its recognition sites on the *trp* leader, resulting in the formation of a terminator structure so transcription stops right behind the leader. Therefore the presence of tryptophan leads to the repression of the operon encoding the proteins needed for its synthesis of the amino acid (Gollnick *et al.*, 2005).

A key event in the tryptophan-mediated termination mechanism is the binding of TRAP to the leader sequence. Interestingly, the amount of TRAP protein in the cell is quite low and binding to the leader site is very strong. On the other hand, the promoter in front of the *trp* operon is rather strong. Therefore it is critical for the whole mechanism to proceed, that bound TRAP is released quickly from the *trp* leader to ensure continuous transcription termination (Deikus *et al.*, 2004). This is achieved by the combined action of two RNases (see Fig. 2). RNase J1 initiates the degradation of the leader with an endoribonucleolytic cleavage producing an entry site for the exoribonuclease PnpA. Therefore strains devoid of PnpA are not able to recycle TRAP from the leader and *trp* transcription becomes deregulated (Deikus *et al.*, 2008).

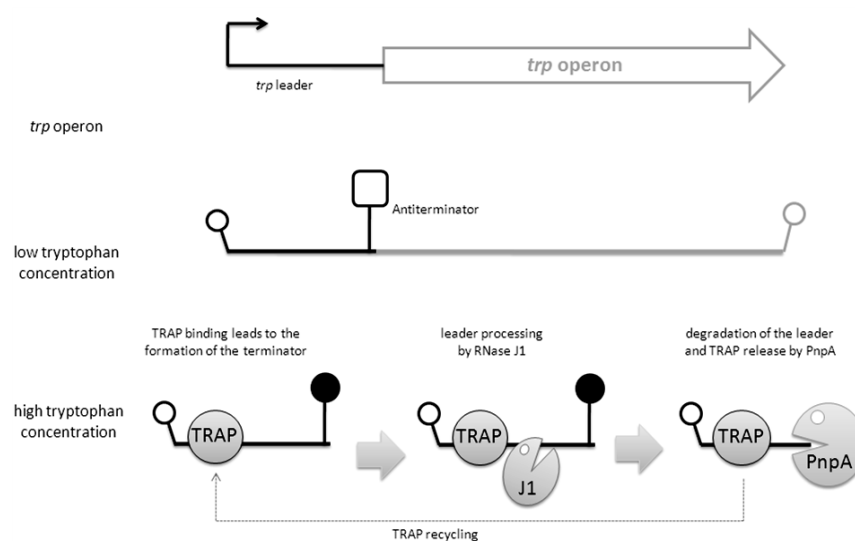


Fig. 2. Regulation of the *trp* operon by the *trp* leader RNA degradation. Under conditions of low intracellular tryptophan, the operon is transcribed by the constitutive promoter in front of the genes. If the

tryptophan concentration in the cell rises, excess tryptophan binds TRAP. This binding of the amino acid enables TRAP to bind the *trp* leader RNA, which favors the formation of a transcriptional terminator structure. To release TRAP from the leader RNA, RNase J1 endonucleolytically processes the leader and produces an entry site for PnpA. The exoribonuclease degrades the leader and therefore recycles TRAP (The figure is adapted from Condon and Bechhofer, 2011).

Processing of the *gapA* operon mRNA

The *gapA* operon of *B. subtilis* is a hexacistronic operon, encoding five glycolytic enzymes and the transcriptional regulator CggR. The operon is organized in a way, that *cggR* is located at the 5' end of the transcript followed by the gene encoding the glyceraldehyde 3-phosphate dehydrogenase (GapA). Downstream and separated by a weak terminator and an internal promoter are the genes encoding the phosphoglycerate kinase, triose phosphate isomerase, phosphoglycerate mutase and enolase (Ludwig *et al.*, 2001). While GapA is an enzyme needed in glycolysis, CggR is a regulatory protein with only one target, the *gapA* operon itself. Therefore the amounts of the proteins needed in the cell to fulfill their properties are quite different. Indeed, quantitative Western blot analysis demonstrated that the cell contained about 230 molecules CggR but 25.000 molecules of GapA (Meinken *et al.*, 2003). Nevertheless both genes are located right next to each other on the same transcript. The differential expression of CggR and GapA is achieved among other things by an endonucleolytic cleavage of the mRNA between *cggR* and *gapA*. This processing first separates both genes and importantly produces two mRNAs with completely different half-lives. Whereas the resulting *gapA* mRNA is quite stable the upstream *cggR* transcript is extremely unstable (Ludwig *et al.*, 2001). Therefore internal mRNA cleavage leading to different stability of the final processing products is one factor accounting for a more than a 100-fold difference in protein amounts between the CggR repressor protein and the glycolytic enzyme glyceraldehyde-3-phosphate dehydrogenase. Even though this processing event was known for years the endonuclease responsible for the cleavage was unknown until recently. Years later, it could be shown that the protein YmdA (later RNase Y) is responsible for the initial cleavage of the mRNA. Even though it was not clear at this time whether YmdA was indeed an RNase, experiments strongly suggested this notion, as depletion of the protein resulted in the accumulation of the primary and unprocessed transcript (Commichau *et al.*, 2009) (for further details see 'Commichau *et al.* 2009').

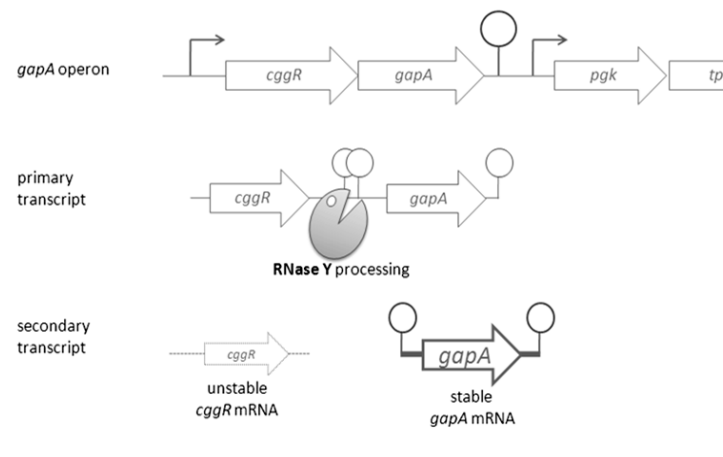


Fig. 3. Regulation of the bicistronic *cggR-gapA* transcript by RNase Y processing. The transcriptional regulator CggR and the glycolytic enzyme glyceraldehyde-3-phosphate dehydrogenase (GapA) are transcribed in a bicistronic operon. Even though the genes are co-transcribed both proteins are needed in different amounts to fulfill their cellular functions. One mechanism to achieve the differential protein levels is the processing of the operon by an endoribonucleolytic cleavage. RNase Y cleaves upstream of *gapA*, producing two new transcripts with different stabilities. Whereas the *cggR* mRNA is very unstable the *gapA* transcript is stabilized due to the stem-loop at the 5' end (for the sake of simplicity the transcripts reaching into the downstream genes are not presented).

Processing of the *thrS* mRNA

The *thrS* gene of *B. subtilis* encodes the major threonyl-tRNA synthetase. This gene contains a 300 nt long 5' untranslated region (5' UTR) where the so-called T-box is located (Putzer *et al.*, 1992). T-boxes are highly structured RNA sequences, important for a mechanism that responds to levels of uncharged cognate tRNAs (Green *et al.*, 2010). Under conditions of high threonine supply, transcription terminates in the *thrS* leader due to the formation of a transcriptional attenuator. In contrast, under conditions of low threonine, the uncharged tRNA^{Thr} binds to the 5' UTR, resulting in the formation of an antiterminator. The formation of the antiterminator structure has a second effect. In addition, processing of this secondary structure by an endoribonuclease amplifies the positive effect of uncharged tRNA^{Thr} binding by generating a new 5' end that forms a protective stem loop structure and contributes to the increased half life of the mRNA (Condon *et al.*, 1996). Even though *in vitro* experiments suggested the participation of RNase J1 in this cleavage event no *in vivo* data is available (Condon & Bechhofer, 2011).

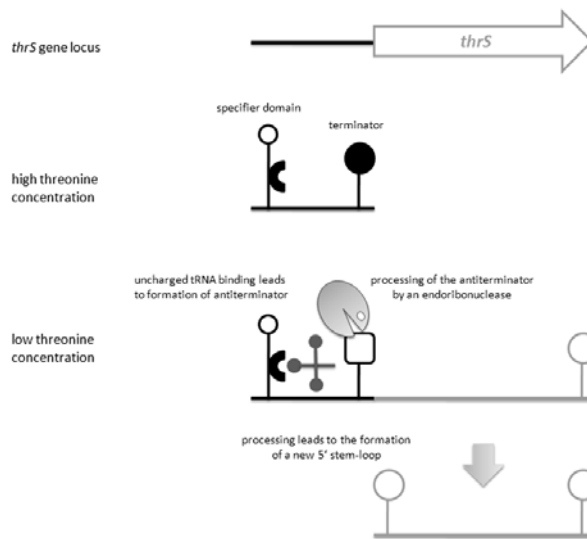


Fig. 4. Regulation of the *thrS* mRNA stability. Under conditions of high threonine, transcription from the constitutive promoter in front of the gene ends due to the formation of a terminator structure. When threonine concentration is low, the uncharged tRNA binds on the 5' UTR, inducing the formation of an antiterminator. The effect is further amplified by a processing event on the emerged antiterminator leading to an increased half life of the mRNA by the formation of a new stem loop at the 5' end (The figure is adapted from Condon and Bechhofer, 2011).

1.6. DEAD-box RNA helicases in *B. subtilis*

DEAD-box RNA helicases are enzymes that utilize ATP to bind and remodel RNA or ribonucleoprotein complexes. The enzymes consist of a catalytic core and an optional N- or C-terminal extensions. In *E. coli* RNA helicases are involved in the process of ribosome assembly, mRNA turnover and growth at lower temperatures (Iost & Dreyfus, 2006).

B. subtilis encodes four different DEAD-box RNA helicases. The RNA helicases CshA and CshB were both suggested to be involved in process of cold adaption. The mRNAs of the enzymes are slightly induced under conditions low temperature (Budde *et al.*, 2006). Nevertheless deletion of either *cshA* or *cshB* exhibited no growth defect at decreased temperatures compared to the wild type (Hunger *et al.*, 2006). In contrast, a double mutant strain was not viable. The participation of CshA and CshB in the process of low temperature adaption was suggested by fluorescence microscopy experiments demonstrating that the two RNA helicases colocalizes with cold shock proteins and ribosomes. Further FRET analysis showed that the RNA helicase CshB interacted with the cold shock protein CspB (Hunger *et al.*, 2006). A second reports dealing with CshA verified the RNA helicase activity of the protein by *in vitro* experiments (Ando & Nakamura, 2006). In contrast to previous finding that deletion of *cshA* did not result in any phenotype

(Hunger *et al.*, 2006) this study demonstrated that a mutant strain devoid of *cshA* had a severe growth defect at decreased temperatures (Ando & Nakamura, 2006). Furthermore CshA was also found to interact with the RNA polymerase, even though the physiological relevance of this interactions remained to be elucidated (Delumeau *et al.*, 2011).

The RNA helicase DeaD/YxiN was investigated extensively with respect to its biochemical properties (Aregger & Klostermeier, 2009; Theissen *et al.*, 2008). The protein consists of a helicase core and a C-terminal domain comprising an RNA recognition motif. It was shown that the enzyme is able to bind to the hairpin 92 in the 23S rRNA (Kossen *et al.*, 2002). The physiological relevance of this binding is still unclear, as no phenotype of a *deaD* mutant is reported. The role of the fourth RNA helicase YfmL in *B. subtilis* is completely unknown.

2. Novel activities of glycolytic enzymes in *Bacillus subtilis*

The results described in this chapter were published in:

Commichau, F. M., Rothe, F. M., Herzberg, C., Wagner, E., Hellwig, D., **Lehnik-Habrink, M.**, Hammer, E., Völker, U. & Stülke, J. (2009). Novel activities of glycolytic enzymes in *Bacillus subtilis*: interactions with essential proteins involved in mRNA processing. *Mol Cell Proteomics* **8**, 1350-1360.

Author's contribution:

MLH performed the Northern blot analysis of the *gapA* operon.

Abstract

Glycolysis is one of the most important metabolic pathways in heterotrophic organisms. Several genes encoding glycolytic enzymes are essential in many bacteria, even under conditions when neither glycolytic nor gluconeogenic activities are required. In this study, a screening for *in vivo* interaction partners of glycolytic enzymes of the soil bacterium *Bacillus subtilis* was employed to provide a rationale for essentiality of glycolytic enzymes. Glycolytic enzymes proved to be in close contact with several other proteins, among them a high proportion of essential proteins. Among these essential interaction partners, other glycolytic enzymes were most prominent. Two-hybrid studies confirmed interactions of phosphofructokinase with phosphoglyceromutase and enolase. Such a complex of glycolytic enzymes might allow direct substrate channelling of glycolytic intermediates. Moreover, we found associations of glycolytic enzymes with several proteins known or suspected to be involved in RNA processing and degradation. One of these proteins, Rny (YmdA), that has so far not been functionally characterized, is required for the processing of the mRNA of the glycolytic *gapA* operon. Two-hybrid analyses confirmed the interactions between the glycolytic enzymes phosphofructokinase and enolase and the enzymes involved in RNA processing RNase J1, Rny and polynucleotide phosphorylase. Moreover, RNase J1 interacts with its homologue RNase J2. We suggest that this complex of mRNA processing and glycolytic enzymes is the *B. subtilis* equivalent of the RNA degradosome. Our findings suggest that the functional interaction of glycolytic enzymes with essential proteins may be the reason why they are indispensable.

Introduction

Glycolysis is a central metabolic pathway that has appeared early in the evolution of life (Canback *et al.*, 2002). Major functions of the glycolytic pathway are the generation of precursors for anabolic reactions and the conservation of energy that is needed to fuel all other cellular processes. The glycolytic pathway is conventionally divided into two parts: (i) the upper part, also referred to as the preparatory phase of glycolysis since the reactions of this part consume energy to convert the incoming sugars to triose phosphates and (ii), the lower part or pay-off phase that is characterized by the net gain of energy and the formation of reduction equivalents. Although glycolysis is highly conserved from archaea and bacteria to man not all organisms use this pathway for the oxidization of glucose. *Escherichia coli* is able to oxidize glucose *via* glycolysis, but the Entner-Doudoroff and the pentose phosphate pathways may replace the preparatory phase. In contrast to *E.*

coli, the Entner-Doudoroff pathway is not present in *Bacillus subtilis* (Stülke & Hillen, 2000). Interestingly, the enzymes of the upper glycolytic part seem to be completely absent in many archaea (Dandekar *et al.*, 1999; Siebers & Schönheit, 2005). These few examples show that there is a high plasticity in how archaea and bacteria can feed glucose into the triose phosphate part of glycolysis. This plasticity is in good agreement with the observation that the genes encoding the enzymes of the upper glycolytic part are less conserved than those for the enzymes of the lower part (Dandekar *et al.*, 1999). The great importance of the enzymes of the three-carbon part of glycolysis is underlined by the fact that two of the enzymes, *i. e.* glyceraldehyde-3-phosphate dehydrogenase (GAPDH) and phosphoglycerate kinase (PGK), catalyze reactions of the Calvin cycle. Moreover, the PGK and the enolase (ENO) are among the about 30 proteins that are universally conserved in all organisms that have been sequenced so far (www.microbesonline.org). Thus, these two enzymes seem to be of key importance for all extant life!

A systematic inactivation of *B. subtilis* genes revealed that 271 of the approximately 4100 genes are essential (Kobayashi *et al.*, 2003). Surprisingly, several of these essential genes encode glycolytic enzymes. It turned out that the two genes *pfkA* and *fbaA* encoding 6-phosphofructokinase (PFK) and fructose-1,6-bisphosphate aldolase (FBA) of the upper part and the five genes *tpiA*, *gapA*, *pgk*, *pgm* and *eno* encoding the triose phosphate isomerase (TPI), GAPDH, PGK, phosphoglycerate mutase (PGM) and ENO of the lower part of glycolysis are essential in *B. subtilis* (see Fig. 4) (Kobayashi *et al.*, 2003; Thomaidis *et al.*, 2007). This is a striking observation since the systematic gene inactivation was performed in complex growth medium (Luria-Bertani medium containing glucose) in which neither glycolysis nor gluconeogenesis are expected to be necessary. Glycolytic enzymes are also essential in bacteria belonging to other phylogenetic branches. In *E. coli*, the aldolase FBA, GAPDH, ENO and PGK are encoded by essential genes (Baba *et al.*, 2006), and in *Corynebacterium glutamicum* the genes for six (FBA, TPI, GAPDH, PGK, PGM and ENO) out of the nine glycolytic enzymes are essential (Suzuki *et al.*, 2006).

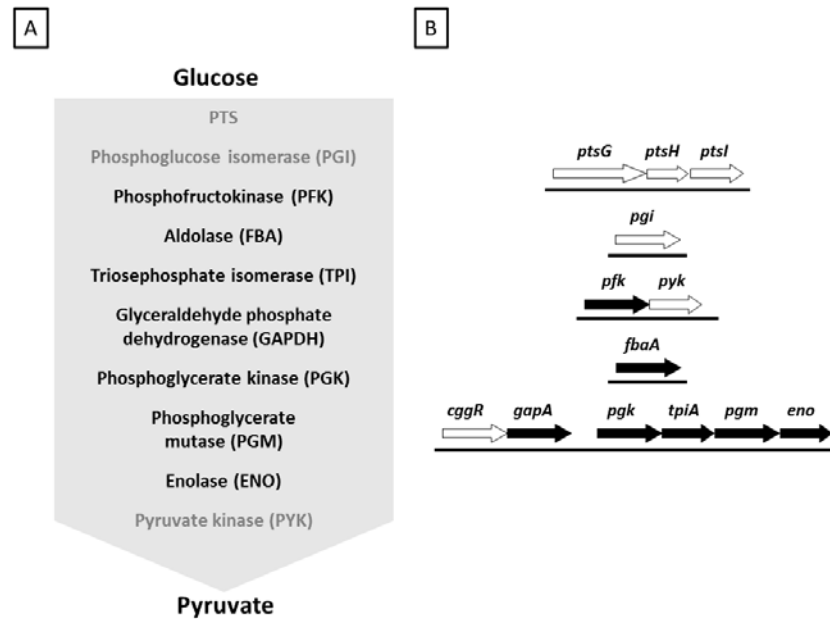


Fig. 4. Schematic illustration of glycolysis and the glycolytic genes of *B. subtilis* (A). Glycolytic enzymes involved in glucose catabolism. Enzymes encoded by non-essential and essential genes are depicted in grey and black, respectively. The abbreviations for the essential glycolytic enzymes are indicated. PTS, phosphotransferase system. (B). Genetic organization of the glycolytic genes of *B. subtilis*. Non-essential genes are illustrated by white arrows and essential genes are illustrated by black arrows.

These observations suggest that glycolytic enzymes play an essential role in the bacterial cell that may not be related to their enzymatic activity! It is thus tempting to speculate that these enzymes might have functions in addition to their catalytic role in metabolism. Such enzymes with additional functions that are not directly related to their primary (enzymatic) tasks in metabolism are collectively termed moonlighting proteins (Jeffery, 1999). It is well established that several glycolytic enzymes in eukaryotic organisms have moonlighting functions (Gancedo & Flores, 2008; Kim & Dang, 2005). In eukaryotes the hexokinase, GAPDH, ENO and the lactate dehydrogenase are active in transcriptional regulation (Kim & Dang, 2005). Moreover, the two isoforms of ENO encoded by *ENO1* and *ENO2* are involved in vacuolar protein traffic and in mitochondrial tRNA import, respectively, in yeast (Decker & Wickner, 2006; Entelis *et al.*, 2006). In addition, GAPDHs from all domains of life are able to cleave RNA *in vitro* (Evguenieva-Hackenberg *et al.*, 2002). In *E. coli*, ENO is part of a complex mRNA degradation machinery, the degradosome. The degradosome is a large multi-protein complex that consists of the major endoribonuclease RNase E, the polynucleotide phosphorylase (PNPase), the ATP-dependent RNA helicase RhlB, and ENO (Carpousis, 2007). The role of ENO within the

complex has been enigmatic until recently. This enzyme plays a crucial role in the regulation of the *ptsG* mRNA stability in response to metabolic stress. Thus, glycolytic activity might be linked to RNA metabolism by a regulatory protein-protein interaction *via* ENO (Morita *et al.*, 2004). In contrast to *E. coli* and eukaryotes, much less is known about moonlighting functions of glycolytic enzymes in *B. subtilis*. A recent work shows that there might be a link between enzymes of the lower glycolytic part and DNA replication in *B. subtilis* (Janni re *et al.*, 2007).

We are interested in basic metabolism and its regulation in *B. subtilis*. Among the genes encoding glycolytic enzymes, those for the glucose transporter, *ptsG*, and for the GAPDH, *gapA*, are only expressed in the presence of glucose (Fig. 4) (Ludwig *et al.*, 2001). The *gapA* gene is the second gene of the hexacistronic *cggR gapA pgk tpi pgm eno* operon (the *gapA* operon). In the absence of glucose or other sugars, expression of the *gapA* operon is repressed by CggR, the product of the first gene (Fillinger *et al.*, 2000). Interestingly, the intracellular amount of GAPDH exceeds that of CggR by a factor of 100, even though the two proteins are encoded by consecutive genes in one operon! This differential expression of the two genes is largely caused by an mRNA cleavage event between the *cggR* and *gapA* open reading frames resulting in a substantial stabilization of the mature *gapA* transcript (Ludwig *et al.*, 2001; Meinken *et al.*, 2003). The RNase responsible for this processing event has so far not been identified.

Recently, we have established that a class of metabolic enzymes, the trigger enzymes, have moonlighting activities in the regulation of gene expression in *B. subtilis* and many other bacteria (Commichau *et al.*, 2007; Commichau & St lke, 2008). In this work, we wanted to define why the genes encoding glycolytic enzymes are essential in *B. subtilis*. We considered the idea that these enzymes might be involved in essential interactions in the cell most attractive. Indeed, we found that PFK and ENO interact with the essential RNase J1 and with a novel protein that is encoded by the essential gene *ymdA*. In addition, the polynucleotide phosphorylase PnpA and RNase J2 interact with glycolytic enzymes. RNases J1 and J2, PnpA and YmdA are involved in RNA metabolism in *B. subtilis* suggesting the formation of a complex equivalent to the *E. coli* degradosome. Moreover, it turned out that several glycolytic enzymes, i. e. PFK, ENO and PGM form a complex *in vivo*.

Results

Identification of potential interaction partners of the essential glycolytic enzymes in *B. subtilis*

To isolate the glycolytic enzymes together with their potential interaction partners we used the SPINE (Strep-protein interaction experiment) method (Herzberg *et al.*, 2007). Briefly, the bait proteins were fused to a Strep-tag and the fusion proteins were expressed in *B. subtilis*. In vivo protein complexes were cross-linked by formaldehyde, purified by affinity chromatography and the cross-links were broken. Finally, the proteins were analysed by SDS-PAGE and the interaction partners were identified by mass spectrometry. Those potential interaction partners that were detected with ten or more peptides were regarded as significant in this study.

This procedure was performed for PFK, FBA, TPI, GAPDH, PGK, PGM and ENO. As an example, Fig. 5 shows the purification of TPI with its potential interaction partners. Only those proteins are shown for which at least ten different peptides were identified (the complete list of all proteins identified is available at the MCP homepage, supplementary Table 3 → <http://www.mcponline.org/content/8/6/1350/suppl/DC1>). As can be seen, the application of the purification scheme to a control strain carrying the empty vector did not reveal appreciable protein enrichment/ purification. In contrast, distinct bands in addition to the bait protein (Strep-TPI) were observed in the strain carrying the expression vector. These bands were identified as PGK, TPI, and transketolase (Tkt). For PFK we identified 180 proteins that were cross-linked and co-purified with the bait. Of these, 48 proteins are encoded by essential genes. However, many of these potential interaction partners were identified only with a few peptides. 25 potential interaction partners, among them 6 essential proteins exceeded the threshold of ten peptides (see below). Unfortunately, for FBA, no purification was achieved. For GAPDH, 59 proteins were co-purified with the bait, but only the chromosomally encoded GAPDH itself was above the threshold.

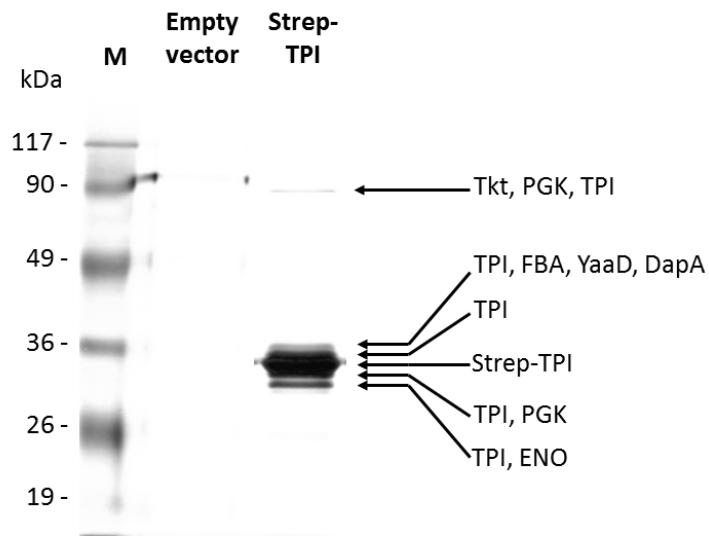


Fig. 5. Identification of potential interaction partners of the triosephosphate isomerase TPI. The protein complex was isolated from the *B. subtilis* wild type strain 168 carrying either pGP380 (empty vector) or the vector pGP89 (expressing TPI). All strains were grown in CSE-Glc minimal medium containing glucose and glutamate as carbon and nitrogen sources, respectively. 15 of the first elution fractions from each purification were loaded on a 12.5% SDS-PAA gel. Protein bands were visualized by silver staining. M, prestained protein molecular weight marker, Fermentas.

For PGK, no distinct protein bands were obtained with the SPINE procedure suggesting that this enzyme interacts with many partners. Therefore, the interaction partners of PGK were isolated without *in vivo* cross-linking. With all bait proteins, we obtained multiple potential interaction partners that had been cross-linked to the glycolytic enzymes. PGK seems to interact with a wide variety of proteins. In total, we identified 186 potential interaction partners for PGK. 44 potential partners of PGK, among them seven essential proteins, yielded at least ten different peptides in mass spectrometry. With PGM as the bait, only PGM itself and PFK were co-purified in significant amounts. Finally, 110 potential partners were identified for ENO, among them were only five proteins above the threshold. Three of these proteins are encoded by essential genes.

The essential proteins that were co-purified with the glycolytic enzymes and that were detected in high abundance are listed in Table 1. Interestingly, the glycolytic enzymes themselves form the largest group of these proteins. The glycolytic enzymes were all cross-linked to their own variant carrying a Strep-tag. This observation is in good agreement with the fact that these enzymes form dimers or tetramers (Erlandsen *et al.*, 2000). In addition, several of the glycolytic enzymes were co-purified with multiple other

glycolytic enzymes. This finding suggests the existence of a complex of glycolytic enzymes in the cell (see below). Moreover, Tkt, an enzyme of the pentose phosphate pathway that feeds into the lower part of glycolysis was co-purified with TPI. Together with PFK, we also purified two translation elongation factors, glutamyl-tRNA synthetase and a protein involved in the biosynthesis of iron-sulphur clusters, whereas two ribosomal proteins were cross-linked to PGK. Finally, ENO was found to interact with the translation elongation factor Ts, the β -subunit of the RNA polymerase (RpoB), and PGK was co-purified with an essential factor of lipid biosynthesis (PlsX) and a so far unknown protein, YmdA (see below).

Table 1. Essential proteins that interact with glycolytic enzymes^a

Protein	Bait enzyme	Function
<i>Basic carbon metabolism (glycolysis, pentose phosphate pathway)</i>		
PFK	PFK, PGM	phosphofructokinase
TPI	TPI	triose phosphate isomerase
GAPDH	PFK, GAPDH, PGK	glyceraldehyde 3-phosphate dehydrogenase
PGK	TPI, PGK	phosphoglycerate kinase
PGM	PGM	phosphoglycerate mutase
ENO	PGK, ENO	enolase
Tkt	TPI	transketolase
<i>Translation</i>		
FusA	PFK	elongation factor G
RplE	PGK	ribosomal protein L5
RpsB	PGK	ribosomal protein S2
Tsf	PFK, ENO	elongation factor Ts
GltX	PFK	glutamate-tRNA synthetase
<i>Transcription</i>		
RpoB	ENO	RNA polymerase, β subunit
<i>Lipid biosynthesis</i>		
PlsX	PGK	acyl carrier protein:phosphate acyltransferase
<i>Other functions</i>		
YmdA (Rny)	PGK	RNA processing factor, previously unknown
YurU	PFK	involved in the synthesis of FeS clusters

^a The Table lists all those proteins encoded by essential genes, that were abundant in the SPINE analysis (10 identified peptides). The first column gives the name of the interacting proteins, the second column the glycolytic enzymes with which these proteins eluted.

Analysis of primary protein-protein interactions among the glycolytic enzymes of *B. subtilis*

The SPINE approach is highly efficient to isolate protein complexes but it does not allow to determine the primary interactions in a protein complex that is composed of more than two proteins. We used the bacterial two hybrid (B2H) system to analyze the primary protein-protein interactions among the glycolytic enzymes. In the B2H system, the T25 and the T18 fragments of the catalytic domain of the *B. pertussis* adenylate cyclase were fused to full-length copies of all glycolytic enzymes of *B. subtilis*. The leucine zipper of the yeast GCN4 transcription factor served as a control (Karimova *et al.*, 1998). The results of the B2H analysis are shown in Fig. 6. As expected, the leucine zipper of GCN4 showed strong self-interaction but failed to interact with any of the glycolytic enzymes. With the exception of the GAPDH, all glycolytic enzymes gave positive signals when they were fused to both the N- and C-terminal domains of the *B. pertussis* adenylate cyclase. This observation corresponds to the formation of dimers (or larger oligomers) and is in good agreement with the results of the SPINE assay and the published evidence (Erlandsen *et al.*, 2000). The GAPDH did not interact with any other protein in the B2H assay. This might indicate that the GAPDH fusion proteins are not correctly folded or that they have lost their potential to interact with other proteins. In contrast, we observed direct interactions between PFK and both PGM and ENO. Thus the B2H analysis supports the hypothesis of a glycolytic complex in *B. subtilis*.

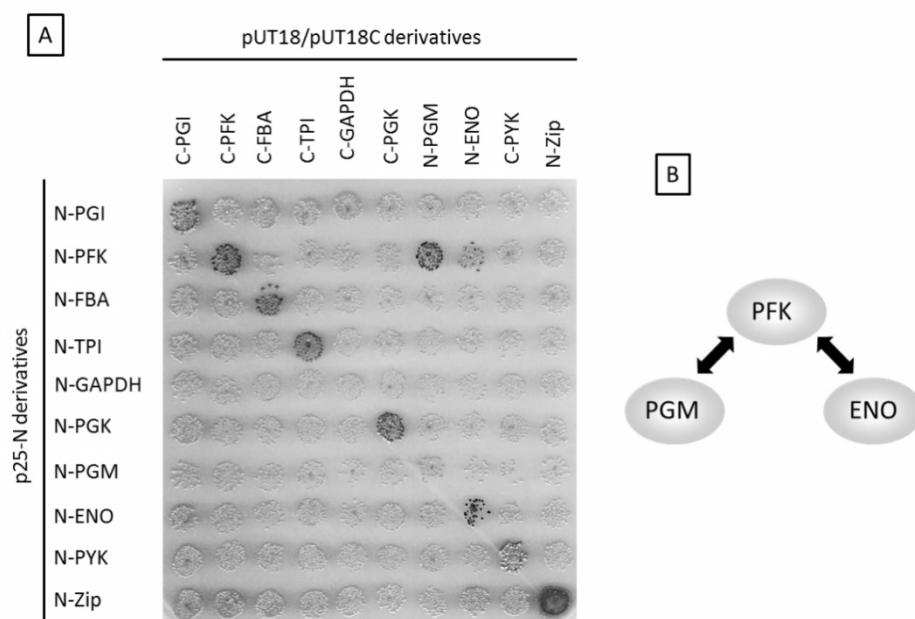


Fig. 6. Analysis of interactions among glycolytic enzymes of *B. subtilis*. (A) Bacterial two hybrid (B2H) analysis to identify interactions among the glycolytic enzymes of *B. subtilis*. All genes were cloned in the plasmids pUT18, pUT18C and p25-N. Plasmids pUT18 and pUT18C allow the expression of the glycolytic enzymes fused either to the N- or the C-terminus of the T18 domain of the *B. pertussis* adenylate cyclase, respectively. Plasmid p25-N allows the expression of the glycolytic enzymes fused to the N-terminus of the T25 domain of the adenylate cyclase. The *E. coli* transformants were incubated for 48 h at 28°C. (B) Schematic summary of the outcome of the B2H analysis.

The essential protein YmdA is involved in the maturation of the *gapA* operon mRNA

Using the SPINE approach, we identified several essential interaction partners for the glycolytic enzymes. Among these proteins was a protein of unknown function, YmdA (see Table 1). YmdA contains KH (ribonucleoprotein K homology) and HD (His-Asp-containing phosphohydrolase) domains. Both domains are found in many nucleic acid-binding proteins and are characteristic for a family of metal-dependent phosphohydrolases (Aravind & Koonin, 1998; Hunt *et al.*, 2006). It was therefore hypothesized that YmdA might act as an RNase (Condon, 2003). In addition, the RNases III (Rnc), J1 (RnjA), and J2 (RnjB) were present in a complex with PFK, and the phosphonucleotide phosphorylase PnpA was identified as an interaction partner of ENO (see supplementary Table 3). This coincidence suggested that YmdA might indeed be involved in mRNA processing.

Since none of the known *B. subtilis* RNases is responsible for the endonucleolytic processing of the *gapA* operon mRNA, we considered the possibility that YmdA might be required for this RNA maturation event. In order to test this hypothesis, we analyzed the effect of a YmdA depletion on the *gapA* operon mRNA maturation. For this purpose we used the *B. subtilis* strain GP193 in which the *ymdA* gene is expressed under control of a xylose-inducible promoter. The strain was grown in the presence and absence of xylose. Growth in the absence of xylose resulted in a depletion of the YmdA protein. The effect of the YmdA depletion on the *gapA* operon mRNA maturation was monitored by Northern blot analysis using *cggR*- and *gapA*-specific riboprobes. The primary and the mature transcripts of the hexacistronic *gapA* operon are shown in Fig. 7 A. First, we analyzed the transcription of the *gapA* operon in the presence of xylose reflecting the wild type situation. As expected, two mRNAs of 2.2 kb and 1.0 kb were detected using the *cggR* probe (Fig. 7 B). The 2.2 kb mRNA represent the primary transcripts of the *gapA* operon whereas the faint 1.0 kb mRNA corresponds to the processed *cggR* transcript (Fig. 7 B). These results are in good agreement with the previous transcriptional analysis of the *gapA*

operon (Ludwig *et al.*, 2001; Meinken *et al.*, 2003). The depletion of YmdA resulted in a significant accumulation of the 7.2 kb and 2.2 kb primary transcripts, whereas the 1.0 kb *cggR* mature transcript was barely detectable (Fig. 7). These results clearly demonstrate that the processing of the *gapA* mRNA is severely impaired upon YmdA depletion.

Using the *gapA*-specific riboprobe three mRNAs of about 6.2 kb, 2.2 kb and 1.2 kb were detected when the cells were grown in the presence of xylose (Fig. 7 B). The intense 6.2 kb and 1.2 kb mRNAs correspond to the mature *gapA pgk tpiA pgm eno* and the *gapA* transcripts, respectively. The 2.2 kb transcript represents the primary *cggR gapA* mRNA which was also detected with the *cggR*-specific riboprobe (Fig. 7 B). Again, these results are in good agreement with previous observations (Ludwig *et al.*, 2001; Meinken *et al.*, 2003). As shown in Fig. 7 B, the effect of a YmdA depletion on the maturation of the *gapA* operon mRNA using the *gapA*-specific riboprobe is quite similar to the results obtained with the *cggR*-specific riboprobe. As a consequence of the YmdA depletion, the mature 6.2 kb transcript was less intense than in the presence of the YmdA. Moreover, the unprocessed hexacistronic *cggR gapA pgk tpiA pgm eno* transcript of the *gapA* operon significantly accumulated due to the depletion of the YmdA protein. These results unequivocally confirm the implication of YmdA in the processing of the *gapA* mRNA. Therefore, we suggest re-designating the *ymdA* gene as *rny* and the gene product as Rny.

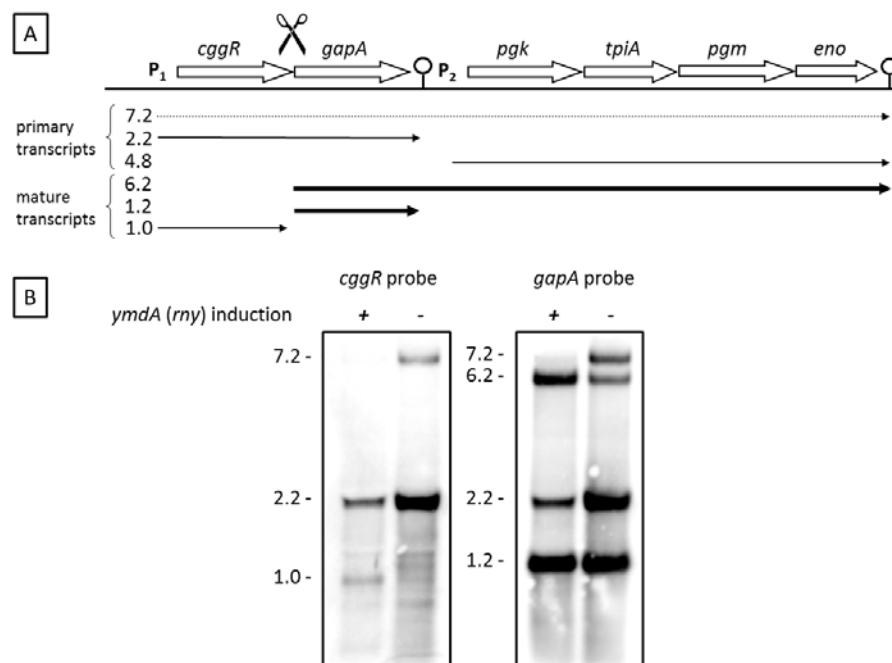


Fig. 7. Effect of Rny depletion on the maturation of the *gapA* operon mRNA. (A) Schematic illustration of the primary and mature transcripts of the *gapA* operon. The first promoter (P₁) of the *gapA* operon is located in front of the *cggR* gene and the second promoter (P₂) is located between a terminator and the *pgk* gene. The

cleavage site of the *gapA* operon mRNA is located at the end of the *cggR* open reading frame. (B) Northern blot analysis to test the effect of Rny depletion on the maturation of the *gapA* operon mRNA. The *rny* gene was placed under control of an xylose-inducible promoter. The strain was grown in LB medium in the presence (+) and in the absence (-) of xylose. Primary and mature transcripts of the *gapA* operon were detected with *cggR* and *gapA* specific riboprobes.

Evidence for a degradosome-like protein complex in *B. subtilis*

As presented above, the SPINE approach identified the mRNA processing factor Rny and the polynucleotide phosphorylase PnpA as potential interaction partners of the glycolytic enzymes PGK and ENO, respectively. In addition, we found that Rny, the RNases III, J1 and J2 as well as PnpA were co-purified with PFK. Interestingly, these proteins are all involved in RNA metabolism in *B. subtilis*, suggesting that there might be a direct link between carbon metabolism and RNA processing. In *E. coli*, ENO is part of the degradosome, a multi-protein complex consisting of the PNPase, RNase E and the helicase RhlB (Carpousis, 2007). Nothing is known about the existence of such a protein complex in *B. subtilis*. Inspired by the co-purification of Rny, three RNases and PnpA with glycolytic enzymes, we considered the possibility that a degradosome-like protein complex might also exist in *B. subtilis*.

Using the B2H system, we analyzed the primary protein-protein interactions between the bait proteins PFK, ENO and PGK and their potential interaction partners PnpA, Rny, and the RNases J1, J2 and III. As shown in Fig. 8 A, the B2H analysis confirmed the strong self-interactions of the glycolytic enzymes (see also Fig. 6). In addition, the B2H analysis also revealed strong self-interactions of PnpA, Rny, and the RNases J1, J2 and III, suggesting that these proteins dimerize or even multimerize *in vivo*.

The B2H experiment showed a direct and reciprocal interaction between PFK, ENO and Rny. As observed with the SPINE approach, the B2H analysis confirmed that PFK directly interacts with the polynucleotide phosphorylase PnpA, Rny and RNase J1 (Fig. 8A). Moreover, direct and reciprocal interactions were observed between RNase J1 and PnpA, RNase J1 and Rny, the RNases J1 and J2, as well as Rny and PnpA (Fig. 8 A). The B2H analyses did not support an interaction of Rny and ENO with PGK (data not shown), which were observed in the SPINE analysis (see Table 1). Thus, the complex between Rny and PGK observed upon *in vivo* cross-linking might be the result of indirect interaction involving other proteins such as ENO and PFK. Finally, RNase III did not interact with any of the tested candidates in the B2H screen (see Fig. 8 A).

Taken together, the results of the B2H analyses confirm the observations of the SPINE approach and clearly demonstrate that PFK, ENO and the four proteins PnpA, Rny, RNase J1 and J2, which are involved in RNA metabolism in *B. subtilis*, form a complex *in vivo* (Fig. 8 B). This complex is very reminiscent of the *E. coli* degradosome since it contains four enzymes involved in RNA processing and the glycolytic enzyme ENO. The interaction of PFK and ENO with essential proteins that mediate mRNA processing might also account for the essentiality of the *pfkA* and *eno* genes, respectively.

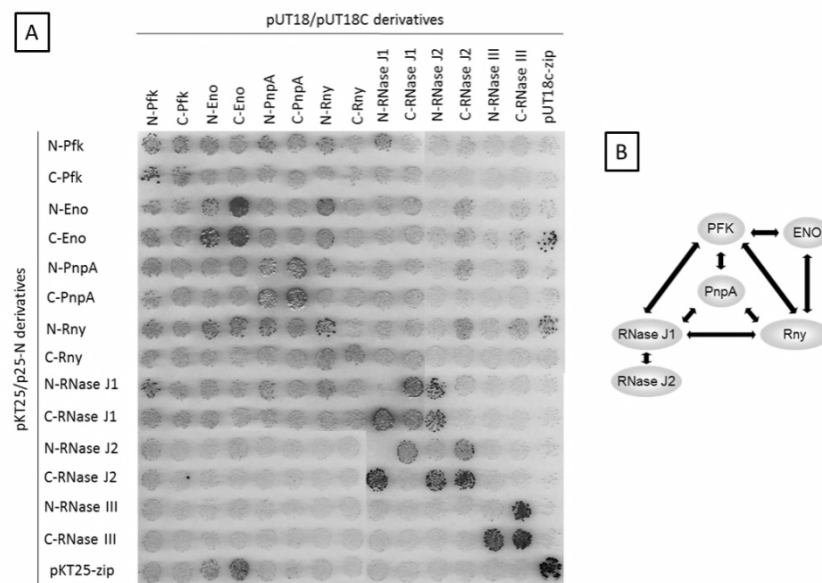


Fig. 8. Analysis of interactions among glycolytic enzymes and enzymes involved in RNA metabolism. (A) Bacterial two hybrid (B2H) analysis to identify interactions among the glycolytic enzymes and enzymes involved in RNA metabolism. All genes were cloned in the plasmids pUT18, pUT18C, p25-N and pKT25. Plasmids pUT18 and pUT18C allow the expression of the selected enzymes fused either to the N- or the C-terminus of the T18 domain of the *B. pertussis* adenylate cyclase, respectively. Plasmids p25-N and pKT25 allow the expression of the selected enzymes fused either to the N- or the C-terminus of the adenylate cyclase, respectively. The *E. coli* transformants were incubated for 48 h at 28°C. (B). Schematic summary of the outcome of the B2H analysis.

Phylogenetic distribution of the RNA processing factor Rny – The phylogenetic distribution of the novel processing factor Rny was analyzed by using the MicrobesOnline web site for comparative genomics (<http://www.microbesonline.org>). The distributions of the PNPase and of enzymes of the E/G or the J1/J2 RNase families were included in this analysis (Condon & Putzer, 2002).

As shown in Table 2, the gene encoding Rny is conserved in the groups *Aquifex*, *Thermotoga*, *Deinococcus/ Thermus*, the flavobacteria and the ϵ -group of the

proteobacteria. Moreover, Rny is highly conserved within the firmicutes. The gene is present in all bacilli, lactobacilli and the clostridia. Since Rny is an essential enzyme in *B. subtilis*, one may speculate that this enzyme might play an important role also in other bacteria that belong to the firmicutes. Despite its high conservation, the *rny* gene is absent in some members of the mollicutes. The complete absence of a homologous gene in *Mycoplasma genitalium* and *Mycoplasma pneumoniae* might be due to a severe genome reduction that these two bacteria have experienced. Similarly to Rny, the PNPase is also less conserved among the mollicutes. Rny is barely conserved within the spirochaetes, the actinobacteria and the δ -proteobacteria and it is completely absent in the *Chloroflexus* group, the chlamydiae, the cyanobacteria and the α - γ groups of the proteobacteria. Most of the groups listed in Table 2 that do not contain a Rny homologue possess at least one enzyme that belongs either to the E/G or the J1/J2 family of RNases. Interestingly, some bacteria such as *Leptospira interrogans*, *Legionella pneumophila* and *Stigmatella aurantiaca* belonging to the spirochaetes and proteobacteria, respectively, possess neither Rny nor an RNase that is homologous to the E/G or the J1/J2 RNases, suggesting that these bacteria might have other enzymes with so far not identified ribonucleolytic activities.

Table 2. Phylogenetic distribution of proteins involved in mRNA processing^a

Group	P	E/G	J1/J2	Rny
<i>Aquifex</i>	●	●	○	●
<i>Thermotoga</i>	●	●	○	●
<i>Chloroflexus</i>	●	●	●	○
Chlamydiae	●	●	○	○
<i>Deinococcus/ Thermus</i>	●	○	●	●
Flavobacteria	●	●	○	●
Spirochaetes	●	○	○	●
Cyanobacteria	●	●	●	○
Actinobacteria	●	●	●	●
Firmicutes: Bacilli	●	●	●	●
Firmicutes: Lactobacilli	●	○	●	●

Firmicutes: Clostridia	●	●	●	●
Firmicutes: Mollicutes	●	○	●	●
α -Proteobacteria	●	●	●	○
β -Proteobacteria	●	●	○	○
γ -Proteobacteria	●	●	○	○
δ -Proteobacteria	●	●	●	●
ϵ -Proteobacteria	●	○	●	●

^a Abbreviations: P, PNPase; E/G, RNases E, G or E/G; J1/J2, RNases J1 or J2. The black dots indicate the presence of the enzyme in all representatives of the group, the grey dots indicate the presence of the enzyme in some representatives of a group, whereas a white dot indicates absence of the enzyme from a bacterial group.

Taken together, the phylogenetic analysis shows that the equipment of bacteria with essential RNases is highly diverse. Moreover, Rny is widely distributed among different phylogenetic branches, but it is highly conserved among the firmicutes.

Discussion

Glycolysis and its variations such as gluconeogenesis are among the key metabolic pathways in most organisms. The importance of this pathway is underlined by the observation that several glycolytic enzymes are essential in many bacteria. The reason for this essentiality has so far remained unknown since the systematic gene inactivation experiments have been performed under conditions where neither glycolytic nor gluconeogenic activities are required (i. e. in LB medium containing glucose) (Kobayashi *et al.*, 2003). In this work, we tested the hypothesis that the glycolytic enzymes are involved in essential interactions. Indeed, it turned out that all of the essential glycolytic enzymes of *B. subtilis* form complexes with essential proteins *in vivo* (see Table 1). The most prominent class of essential interaction partners are glycolytic enzymes themselves suggesting the existence of protein complexes that perform glycolysis (see below). In addition, PFK, PGK and ENO interact with proteins involved in translation and transcription. PFK was also cross-linked to YurU, a protein involved in the biosynthesis of iron-sulphur clusters. Moreover, PGK was present in complexes with PlsX, a protein involved in lipid biosynthesis, and Rny (YmdA), a previously unknown protein that was

identified as an essential RNA processing factor in this work. While Table 1 lists only those essential proteins that were found in large abundance, there may be other essential proteins interacting with glycolytic enzymes that were present in smaller amounts in the purified complexes. Recently, it has been reported that glycolytic enzymes are also linked to replication (Janni re *et al.*, 2007). Most interestingly, we observed interactions between glycolytic enzymes and replication proteins. The leading and lagging strand polymerases PolC and DnaE were found to be cross-linked to ENO and GAPDH, respectively, and the β -clamp of DNA polymerase III, DnaN, was present in a complex with PGK. These observations support the existence of a direct link between glycolysis and DNA replication that has been suggested based on genetic evidence (Janni re *et al.*, 2007). It is, however, unknown whether the observed interactions are (i) direct and (ii) relevant. The *in vivo* cross-linking approach used in this study does not allow distinguishing between primary interactions and those that are mediated by intermediary partners. However, there are indications that suggest that our observations are meaningful: First, the SPINE strategy has already successfully been applied to identify the regulatory interaction between the transcription activator GltC and the glutamate dehydrogenase RocG (Commichau *et al.*, 2007). Moreover, the presence of glycolytic as well as degradosome-like complexes was verified by the two-hybrid analysis. This analysis does also provide insights into the primary interactions that may differ from the outcome of the SPINE experiment.

All studies at the global level may give valuable insights into the functions of so far unknown proteins. In this work, we focussed our attention on Rny (YmdA), the only essential protein that interacts with glycolytic proteins for which no function had been annotated. We could demonstrate that this protein is required for the processing of the *gapA* operon mRNA. So far, RNases J1 and J2 have been described as the functional equivalents of *E. coli* RNase E (Even *et al.*, 2005). However, neither RNase J1 nor RNase J2 are involved in the processing of the *gapA* mRNA (M ader *et al.*, 2008). Therefore, other endoribonucleases must exist in *B. subtilis*. Our data are in good agreement with the idea that Rny is this RNase. However, we were so far unable to demonstrate this function *in vitro*. This may be difficult due to the presence of Rny in a large protein complex (this work) and because of the requirement for membrane insertion of Rny for proper activity (our unpublished results).

RNA degradation by large multiprotein complexes seems to be a general rule. In archaea and eukaryotes, the exosome forms a macromolecular cage for RNA degradation (B uttner *et al.*, 2006; Evguenieva-Hackenberg *et al.*, 2003). In several proteobacteria such as *E. coli* and *Rhodobacter capsulatus* as well as in the actinobacterium *Streptomyces*

coelicolor, RNase E is the key component of the RNA degradosome. In addition to RNase E, the degradosome may contain a RNA helicase, the phosphonucleotide phosphorylase and other factors such as RNase R, the transcription factor Rho or the glycolytic enzyme ENO (Evguenieva-Hackenberg *et al.*, 2002; Jäger *et al.*, 2001; Lee & Cohen, 2003; Marcaida *et al.*, 2006). In *B. subtilis*, RNases J1, J2 and Rny might play the role of RNase E. The two-hybrid analysis revealed the formation of a complex of these three proteins with PnpA as well as with the glycolytic enzymes PFK and ENO. This composition is very reminiscent of the degradosomes in the other organisms. It should be noted that *E. coli* and *B. subtilis* are so far the only bacteria with glycolytic enzymes in their degradosomes. The function of these enzymes in the *B. subtilis* degradosome will be the subject of further studies. The observation of a RNA degradosome with key players different from RNase E supports the striking importance of protein complexes for mRNA processing and degradation. It is tempting to speculate that such complexes may be present in all bacteria. It has not escaped our attention that the interaction pattern of the RNases J1 and J2 immediately suggests why the *rnjA* gene encoding RNase J1 is essential in *B. subtilis* whereas *rnjB* (RNase J2) is not. RNase J1 is part of the core of the degradosome. In contrast, RNase J2 is connected to the degradosome only via J1. In a *rnjA* mutant, no J-type RNase could assemble with the other degradosome components whereas functional degradosomes containing RNase J1 can assemble in *rnjB* mutants.

The analysis of proteins encoded by essential genes has recently attracted much attention. Several studies have been devoted to the identification and functional characterization of essential genes and proteins in *B. subtilis* (Hunt *et al.*, 2006; Kobayashi *et al.*, 2003; Thomaidis *et al.*, 2007). The study of these proteins helps to eliminate uncharted territories on the map of our knowledge. In addition, these proteins are excellent candidates for being novel drug targets (Bumann, 2008). This is specifically true for essential proteins that do not have counterparts in eukaryotes. However, it is difficult to design assays for essential proteins of unknown function. Essential unknown proteins are therefore regarded as low priority candidates for drug development (Payne *et al.*, 2007). The identification of a biological activity for Rny makes it an excellent candidate. With the exception of some *Mycoplasma* species, Rny is present in all firmicutes including many severe pathogens such as *Staphylococcus aureus* that are often resistant to many common antibiotics. Moreover, a recent study has shown that Rny is also essential in *Mycoplasma pulmonis* (French *et al.*, 2008), suggesting an important role in those mollicutes that retained the *rny* gene.

Another interesting result of this study is the observation of a complex of glycolytic enzymes. Such a complex, called the glycosome, has previously been reported for some protozoans of the genera *Trypanosoma* and *Leishmania* (Michels *et al.*, 2006). Similarly, clustered association of glycolytic enzymes was also observed in human and murine erythrocytes and in yeast (Campanella *et al.*, 2005; Campanella *et al.*, 2008; Persson & Johansson, 1989). Our work provides compelling evidence for a complex composed of PFK, PGM, and ENO. However, we cannot rule out the possibility that other proteins are present in this complex. In the two-hybrid screen, the GAPDH did not interact with any protein. However, GAPDH was found to be present in a complex with PFK, PGK and ENO in the SPINE analysis. It is possible, that the GAPDH carrying protein tags is unable to participate in productive interactions. The observation of a complex between glycolytic enzymes raises the question of the physiological significance of such a complex. It has been suggested that the glycolytic intermediates can be directly transferred from one enzyme to the next in the complex. This metabolic or substrate channelling may be advantageous for glycolytic fluxes as compared to free diffusion of the intermediates. The relevance of metabolic channelling in glycolysis is controversially discussed (Cornish-Bowden & Cardenas, 1993; Welch & Easterby, 1994). Alternatively, the complexes of glycolytic enzymes might facilitate fine-tuning of the enzymes' activities. Clearly, new experimental approaches to address this important issue are urgently required. Compartmentalization of enzymes of one metabolic pathway has also been observed for purine biosynthesis (the "purinosome") and branched-chain amino acid catabolism in human cells (An *et al.*, 2008; Islam *et al.*, 2007). The analysis of branched-chain amino acid utilization supports the idea of a specific metabolic unit with substrate channeling between the components (Islam *et al.*, 2007). A recent *in silico* study suggests that flux through glycolysis in terms of pyruvate production is more efficient if the glycolytic enzymes form a complex as compared to non-associated glycolytic enzymes (Amar *et al.*, 2008).

The work presented here demonstrates that glycolytic enzymes are involved in many protein-protein interactions in *B. subtilis*. This observation opens many new fields for further research: Does the complex of glycolytic enzymes contribute to metabolic efficiency? What is the biochemical activity of Rny? Can Rny be useful to isolate new drugs against multiresistant staphylococci? What are the functions of the glycolytic enzymes in the RNA degradosome? What is the relevance of those interactions that were observed but not further addressed in this work? The answers to these questions are not only important for our understanding of the biology of *B. subtilis*, but also for the general understanding of metabolic and regulatory networks.

Acknowledgements

We are grateful to Harald Putzer for helpful discussions and for sharing data prior to publication. We wish to thank Henning Urlaub for the help with the identification of PGM's interaction partners. Sebastian Hübner and Sven Halbedel are acknowledged for advice with some experiments and critical reading of the manuscript, respectively. This work was supported by grants of the Deutsche Forschungsgemeinschaft and the Federal Ministry of Education and Research SYSMO network (PtJ-BIO/0313978D and 0313978A) to J. S. and U.V. F.M.C. and J.S. were additionally supported by the Fonds der Chemischen Industrie.

Experimental procedures

Bacterial strains and growth conditions - *B. subtilis* 168 (*trpC2*, laboratory collection) was used for the purification of glycolytic enzymes with their potential interaction partners. *B. subtilis* GP193 (*trpC2* Ω *ymdA::pGP774(p_{xyIA}-ymdA cat)*) was used to test the effect of the YmdA depletion on the *gapA* operon mRNA processing. *E. coli* DH5 α , XL1-Blue and BTH101 (Karimova *et al.*, 1998; Sambrook *et al.*, 1989) were used for cloning experiments and bacterial two-hybrid (B2H) analyses. *B. subtilis* was grown in LB and in CSE minimal medium containing succinate and glutamate/ ammonium as basic sources of carbon and nitrogen, respectively (Faires *et al.*, 1999). The media were supplemented with auxotrophic requirements (at 50 mg/l) and glucose (0.5% (w/v)). *E. coli* was grown in LB medium. LB and SP plates were prepared by addition of 17 g Bacto agar/l (Difco) to LB and SP, respectively (Commichau *et al.*, 2007; Sambrook *et al.*, 1989).

DNA manipulation - Transformation of *E. coli* and plasmid DNA extraction were performed using standard procedures (Sambrook *et al.*, 1989). Restriction enzymes, T4 DNA ligase and DNA polymerases were used as recommended by the manufacturers. DNA fragments were purified from agarose gels using the Qiaquick Gel Extraction kit (Qiagen, Germany). *Pfu* DNA polymerase was used for the polymerase chain reaction as recommended by the manufacturer. All primer sequences are provided as supplementary material (supplementary Table 1). DNA sequences were determined using the dideoxy chain termination method (Sambrook *et al.*, 1989). Chromosomal DNA of *B. subtilis* was isolated as described (Commichau *et al.*, 2007).

Transformation and phenotypic analysis - Standard procedures were used to transform *E. coli* (Faires *et al.*, 1999) and transformants were selected on LB plates containing either ampicillin (100 µg/ml) or kanamycin (50 µg/ml). *B. subtilis* was transformed with plasmid DNA according to the two-step protocol (Commichau *et al.*, 2007). Transformants were selected on SP plates containing erythromycin plus lincomycin (Em 2 µg/ml and Lin 25 µg/ml).

Plasmid constructions - Plasmids for the overexpression and purification of the glycolytic enzymes PFK, FBA, TPI, GAPDH, PGK, PGM, and ENO from *B. subtilis* were constructed as follows. The coding sequence of each gene was amplified by PCR with gene specific primers (listed in supplementary Table 1) using chromosomal DNA of *B. subtilis* 168 as the template. The PCR products were digested with *Bam*HI and *Sal*I and cloned into the expression vector pGP380 (Herzberg *et al.*, 2007). These plasmids allowed the expression of the glycolytic enzymes carrying a N-terminal strep-tag. The resulting plasmids are listed in supplementary Table 2. To obtain the plasmids for the B2H analyses the coding sequences of the genes *pgi*, *pfkA*, *fbaA*, *tpiA*, *gapA*, *pgk*, *pgm*, *eno*, *pykA*, *pnpA*, *rnjA*, *rnjB*, *rnc* and *ymdA* were amplified by PCR using chromosomal DNA of *B. subtilis* 168. The gene specific primers are listed in supplementary Table 1. The PCR products were digested with *Xba*I and *Kpn*I, and the resulting fragments were cloned into each of the four plasmids p25-N, pKT25, pUT18 and pUT18c (Claessen *et al.*, 2008; Karimova *et al.*, 1998), digested with the same enzymes. The resulting plasmids used for the B2H analyses are listed in supplementary Table 2. All plasmid inserts were verified by DNA sequencing.

Construction of a B. subtilis strain that allows controlled depletion of ymdA - To express the *ymdA* gene under the control of the strongly regulated promoter of the *B. subtilis* *xyl* operon, plasmid pGP774 was constructed as follows. A 423 bp PCR fragment covering the region of the *ymdA* translational start was generated using the primers DH11 (5' AAAGGATCCGCAACAACCAAGTTCATAGCAAG) and DH12 (5' AAAGGATCCGCTTTCATCTCTTCAATATGTTG). The resulting PCR product was digested with *Bam*HI and ligated into plasmid pX2 (Mogk *et al.*, 1997) linearized with *Bam*HI. The identity of the cloned insert was verified by sequencing. *B. subtilis* 168 was transformed with the resulting plasmid pGP774, and transformants were selected on SP plates containing chloramphenicol and xylose (1%, w/v). The resulting strain GP193 was unable to grow in the absence of xylose confirming that the *ymdA* gene is essential for *B. subtilis*.

Purification of glycolytic enzymes with their potential interaction partners from B. subtilis - *B. subtilis* 168 served as host for the overexpression of the glycolytic enzymes. A

first preculture was grown in LB medium for 10 hours at 28°C. Four ml of this preculture were used to inoculate 100 ml of CSE medium containing 0.5% glucose. This second preculture was grown overnight at 28°C. Then, we inoculated 1 liter of the same medium with the second preculture to an OD₆₀₀ of 0.1. This culture was grown at 37°C until the OD₆₀₀ had reached the value of 1.0. Cells were harvested and lysed using a French press (20,000 p.s.i., 138,000 kPa; Spectronic Instruments, UK). After lysis the crude extracts were centrifuged at 100,000 *g* for 1 h. For purification of the *Strep*-tagged proteins the resulting supernatants were passed over a Streptactin column (IBA, Göttingen, Germany) (1.0 ml bed volume). The recombinant proteins were eluted with desthiobiotin (IBA, Göttingen, Germany, final concentration 2.5 mM). After elution the fractions were tested for the desired protein using 12.5% SDS PAGE gels. Protein concentrations were determined using the Bio-Rad dye-binding assay with Bovine serum albumin as the standard. To facilitate the isolation of glycolytic enzymes together with their potential interaction partners, cells expressing these enzymes were treated with formaldehyde (0.6% w/v, 20 min) (Herzberg *et al.*, 2007). After cross-linking, the cells were harvested and washed once with a buffer containing 50 mM Tris-HCl (pH 7.5) and 200 mM NaCl. As control, we used the *B. subtilis* wild type strain carrying the empty vector pGP380 (Herzberg *et al.*, 2007). The cells were disrupted using a French press and the glycolytic enzymes were purified using a Streptactin column as described above. Aliquots of the different fractions were subjected to SDS-PAGE and visualized by silver staining. Prior to electrophoresis, the protein samples were boiled for 20 minutes in Laemmli buffer to reverse the cross-links.

Protein identification by mass spectrometry - Silver nitrate stained gel slices were destained by incubation in 30 mM K₃[Fe(CN)₆]/ 100 mM Na₂S₂O₃ until colourless and washed three times in water before processing of gel slices as previously described (Thiele *et al.*, 2007). Briefly, gel pieces were washed twice with 200 µl 20 mM NH₄HCO₃/ 50% (v/v) acetonitrile (ACN) for 30 min, at 37°C and dried by adding 200 µl ACN two times for 15 min. Trypsin solution (10 ng/µl trypsin in 20 mM ammonium bicarbonate) was added until gel pieces stopped swelling and digestion was allowed to proceed for 16 to 18 hours at 37°C. Peptides were extracted from gel pieces by incubation in an ultrasonic bath for 30 min in 40 µl 0.1% (v/v) acetic acid followed by a second extraction with 40 µl 50% ACN in 0.05% acetic acid. The supernatants containing peptides were collected, combined, ACN depleted by evaporation, and transferred into micro vials for mass spectrometric analysis. Peptides were separated by a non-linear water-acetonitrile gradient in 0.1% acetic acid on a PepMap reverse phase column (75-µm I. D. x 150 mm, LC Packings, Idstein, Germany)

with a MDLC nano-HPLC (GE Healthcare, Freiburg, Germany) coupled on-line with a LTQ-Orbitrap mass spectrometer (Thermo Electron, Bremen) operated in data-dependent MS/MS mode. Proteins were identified by searching all MS/MS spectra in .dta format against a *B. subtilis* protein database (4106 entries, extracted from SubtiList (genolist.pasteur.fr/SubtiList/) using SEQUEST (Bioworks 3.2/Sequest v. 2.7 rev. 11, Thermo Electron) on an IBM cluster with eight dual nodes. Initial mass tolerance for peptide identification on MS and MS/MS peaks were 10 ppm and 1 Da respectively. Up to two missed tryptic cleavages were allowed. Methionine oxidation (+15.99492 Da) and propionamide modification on cysteine (+71.037109 Da) were set as variable modifications. Protein identification results were evaluated by determination of probability for peptide and protein assignments provided by PeptideProphet and ProteinProphet (ISI Seattle, WA, USA) incorporated in the Scaffold software package rel. 2.01 (Proteome Software, Portland, OR, USA). Proteins were identified by at least two peptides with peptide probability > 90% reflecting protein probability of >99%.

B2H assay – Primary protein-protein interactions were identified by bacterial two-hybrid (B2H) analysis (Karimova *et al.*, 1998). The B2H system is based on the interaction-mediated reconstruction of adenylate cyclase (CyaA) activity from *Bordetella pertussis* in *E. coli*. The CyaA enzyme consists of two complementary fragments T18 and T25 that are not active when physically separated. Fusion of these fragments to interacting proteins results in functional complementation between the T18 and T25 fragments and the synthesis of cAMP. cAMP production can be monitored by measuring the β -galactosidase activity of the cAMP-CAP-dependent promoter of the *E. coli lac* operon. Thus, a high β -galactosidase activity reflects the interaction between the hybrid proteins. Plasmids pUT18 and p25-N allow the expression of proteins fused to the N-terminus of the T18 and T25 fragments of the CyaA protein, respectively, and the plasmids pUT18C and pKT25 allow the expression of proteins fused to the C-terminus of the T18 and T25 fragments of the CyaA protein, respectively (Claessen *et al.*, 2008; Karimova *et al.*, 1998). The plasmids pKT25-*zip* and pUT18C-*zip* served as positive controls for complementation. These plasmids express T18-*zip* and T25-*zip* fusion proteins that can associate due to the leucine zipper motifs resulting in an active CyaA enzyme and a high β -galactosidase activity. The plasmids constructed for the B2H assay (see supplementary Table 2) were used for cotransformations of *E. coli* BTH101 and the protein-protein interactions were then analyzed by plating the cells on LB plates containing ampicillin (100 μ g/ml), kanamycin (50 μ g/ml), X-Gal (40 μ g/ml) (5-bromo-4-chloro-3-indolyl- β -D-galactopyranoside) and

IPTG (0.5 mM) (isopropyl- β -D-thiogalactopyranoside), respectively. The plates were incubated for a maximum of 36 h at 30°C.

Northern blot analysis – To test the effect of the YmdA depletion on the *gapA* operon mRNA processing we used *B. subtilis* GP193 in which the *ymdA* gene is expressed under control of a xylose-inducible promoter. This strain was grown overnight at 37°C in LB containing 0.25% glucose and 1% xylose. This preculture was used to inoculate two cultures containing 20 ml LB to an OD₆₀₀ of 0.1. One culture contained 1% xylose to allow the expression of the *ymdA* gene. Both cultures were grown to an OD₆₀₀ of 1.5 – 2.0. The cells were then washed twice in fresh LB and used to inoculate two main cultures (100 ml each). One culture contained 1% xylose to induce *ymdA* expression. The cells were grown to an OD₆₀₀ of 0.5 – 0.8 and harvested for RNA isolation. Preparation of total RNA and Northern blot analysis were carried out as described previously (Ludwig *et al.*, 2001). Digoxigenin (DIG) RNA probes were obtained by *in vitro* transcription with T7 RNA polymerase (Roche Diagnostics) using PCR-generated DNA fragments as templates. The primer pair *gapfor/gaprev* (30) was used to amplify a DNA fragment specific for *gapA*. The reverse primer contained a T7 RNA polymerase recognition sequence. *In vitro* RNA labelling, hybridization and signal detection were carried out according to the instructions of the manufacturer (DIG RNA labelling kit and detection chemicals; Roche Diagnostics). The sizes of the RNA molecular weight marker I (Roche Diagnostics) were as follows: 6.9, 4.7, 2.6, 1.8, 1.5, 1.0, 0.57, 0.48 and 0.31 kb.

3. CshA - the major RNA helicase in the degradosome of *Bacillus subtilis*

The results described in this chapter were published in:

Lehnik-Habrink, M., Pförtner, H., Rempeters, L., Pietack, N., Herzberg, C. & Stülke, J. (2010). The RNA degradosome in *Bacillus subtilis*: identification of CshA as the major RNA helicase in the multiprotein complex. *Mol Microbiol* **77**, 958-971.

Author's contribution:

The study was designed and interpreted by MLH and JS. MLH together with CH and LR performed the *in vitro* CshA interaction experiments. The *in vivo* pull down experiments were done by MLH, LR and CH. Experiments concerning the subcellular localization of CshA were done by MLH. The analysis of the expression of CshA and CshB was done by MLH and CH. Analysis of the C-terminal domain was done by MLH and CH. HP performed most of the B2H experiments and the PnpA pull down. The paper was written by MLH and JS.

Abstract

In most organisms, dedicated multiprotein complexes, called exosome or RNA degradosome, carry out RNA degradation and processing. In addition to varying exo- or endoribonucleases, most of these complexes contain a RNA helicase. In the Gram-positive bacterium *Bacillus subtilis*, a RNA degradosome has recently been described, however, no RNA helicase was identified. In this work, we tested the interaction of the four DEAD box RNA helicases encoded in the *B. subtilis* genome with the RNA degradosome components. One of these helicases, CshA, is able to interact with several of the degradosome proteins, *i. e.* RNase Y, the polynucleotide phosphorylase, and the glycolytic enzymes enolase and phosphofructokinase. The determination of *in vivo* protein-protein interactions revealed that CshA is indeed present in a complex with polynucleotide phosphorylase. CshA is composed of two RecA-like domains that are found in all DEAD box RNA helicases and a C-terminal domain that is present in some members of this protein family. An analysis of the contribution of the individual domains of CshA revealed that the C-terminal domain is crucial both for dimerisation of CshA and for all interactions with components of the RNA degradosome, including RNase Y. A transfer of this domain to CshB allowed the resulting chimeric protein to interact with RNase Y suggesting that this domain confers interaction specificity. As a degradosome component, CshA is present in the cell in similar amounts under all conditions. Taken together, our results suggest that CshA is the functional equivalent of the RhlB helicase of the *Escherichia coli* RNA degradosome.

Introduction

In all living cells, RNA turnover is essential for controlling the steady-state concentration of any given mRNA. Moreover, direct mRNA processing events may contribute to the differential regulation of genes encoded in the same operon.

In the model bacterium *Escherichia coli*, the enzymes responsible for RNA degradation and processing are able to assemble into a large multi-protein complex, the RNA degradosome. This complex consists of RNase E, the polynucleotide phosphorylase PnpA, the RNA helicase RhlB and the glycolytic enzyme enolase. In this complex RNase E and PnpA have the endo- and exoribonucleolytic activities, respectively, whereas RhlB unwinds double-stranded RNAs and makes them accessible to the RNases (Carpousis, 2007; Py *et al.*, 1994). The precise function of enolase in the complex is unknown, however, it is required for the degradation of the mRNA of the glucose transporter *ptsG* upon phosphosugar stress (Morita *et al.*, 2004). In addition to its function as a

ribonuclease, RNase E does also act as the scaffold to organize the interactions with the components of the degradosome (Vanzo *et al.*, 1998).

Protein complexes that are functionally equivalent to the *E. coli* RNA degradosome have been identified in several bacterial species such as *Pseudomonas syringae*, *Rhodobacter capsulatus*, and *Streptomyces coelicolor* (Jäger *et al.*, 2001; Lee & Cohen, 2003; Purusharth *et al.*, 2005). Similarly, RNA-degrading complexes called exosome are present in archaea and eukaryotes (Büttner *et al.*, 2006; Evguenieva-Hackenberg & Klug, 2009). In all these complexes, a ribonuclease and a RNA helicase are present even though the actual composition can differ substantially between species (Lin-Chao *et al.*, 2007). This conservation suggests that these enzymes are essential for any RNA-degrading protein complex.

We are interested in RNA processing in the Gram-positive soil bacterium *Bacillus subtilis*. This bacterium does not possess a protein homologous to RNase E suggesting that the mechanisms of RNA processing and degradation differ substantially from those described for *E. coli*. Two paralogous RNases, J1 and J2, with both endonucleolytic and 5'-3' exonucleolytic activity have been identified in *B. subtilis* (Even *et al.*, 2005). These RNases contribute to the maturation of 16S rRNA and to that of the small cytoplasmic RNA as well as to the turnover of the *trp* operon leader mRNA (Britton *et al.*, 2007; Deikus *et al.*, 2008; Yao *et al.*, 2007). A transcriptome analysis revealed that they are globally implicated in the control of the accumulation of mRNAs in *B. subtilis* (Mäder *et al.*, 2008). Very recently, a RNA degradosome was identified in *B. subtilis*. This complex is composed of the newly discovered RNase Y, the RNases J1 and J2, the polynucleotide phosphorylase PnpA and the two glycolytic enzymes enolase (Eno) and phosphofructokinase (PfkA) (Commichau *et al.*, 2009). RNase Y is required for the processing of the mRNA of the glycolytic *gapA* operon, and subsequently it was shown to be necessary for the initiation of the S-box riboswitch and bulk mRNA turnover (Commichau *et al.*, 2009; Shahbadian *et al.*, 2009). In contrast to the RNA-degrading protein complexes from all other organisms, no RNA helicase was reported for the *B. subtilis* RNA degradosome. This might indicate that either the principal mechanisms of RNA degradation differ substantially between *B. subtilis* and all other species studied in this respect or that the RNA helicase(s) component has escaped its identification in the initial analysis of the degradosome.

Three RNA helicases have so far been studied in *B. subtilis*. These proteins, CshA, CshB, and DeaD, are all members of the DEAD box family of RNA helicases. The members of this family are found in all domains of life. They are involved in many important cellular

processes such as RNA splicing in the spliceosome, mRNA export from the nucleus to the cytoplasm, ribosome biogenesis or RNA degradation (Rocak & Linder, 2004). The DEAD box helicases are composed of two RecA-like domains that are both required for catalytic activity. In the first domain, they contain the conserved characteristic Asp-Glu-Ala-Asp motif that gave rise to the name of this protein family. The biochemical activity of the DEAD box helicases is the unwinding of double-stranded RNA driven by ATP hydrolysis. The ATPase activity of many DEAD box helicases is stimulated by RNA binding (Cordin *et al.*, 2006). In *E.coli*, the principal RNA helicase of the RNA degradosome is RhlB. This helicase may be replaced by CsdA, another member of the DEAD box family, upon cold shock (Prud'homme-Généreux *et al.*, 2004).

The *B. subtilis* DEAD box helicases CshA and CshB were first identified in an analysis of cold-induced genes (Beckering *et al.*, 2002). Subsequently, it was shown that they are required for adaptation to low temperature and that they exert an essential function even at moderate temperature since *cshA cshB* double mutants are not viable (Hunger *et al.*, 2006). CshB interacts with the cold shock RNA chaperone CspB and may facilitate the unwinding of folded RNAs at low temperatures to ensure continued translation (Hunger *et al.*, 2006). The CshA and DeaD (alternative designation: YxiN) helicases have been characterized biochemically. As observed for other proteins of the DEAD box family, they exhibit RNA-stimulated ATPase activity and have RNA unwinding activity (Ando & Nakamura, 2006; Kossen & Uhlenbeck, 1999). It is interesting to note that CshA, CshB and DeaD possess an additional C-terminal domain that is not characteristic for the whole DEAD box helicase family. In DeaD, this C-terminal domain is a RNA-binding domain. If attached to another DEAD box helicase, it confers the same RNA-binding property (Kossen *et al.*, 2002). The function of the corresponding domains in CshA and CshB is unknown.

In this work, we have studied the interaction of DEAD box RNA helicases with components of the *B. subtilis* degradosome. We demonstrate that CshA interacts with RNase Y and polynucleotide phosphorylase. Thus, the principal structure of the *B. subtilis* degradosome is similar to that of other RNA degrading machines in all domains of life. Moreover, we provide evidence for a specific function of the C-terminal domain of CshA in mediating protein-protein interactions. The transfer of this domain to CshB did also transfer the ability to interact with RNase Y, the major component of the *B. subtilis* degradosome.

Results

Potential RNA helicases encoded in the genome of *B. subtilis*.

RNA helicases are essential for resolving stable structures during RNA folding or processes of functional RNA utilization. In *B. subtilis*, three DEAD-box RNA helicases have been studied so far. These are the cold shock proteins CshA and CshB and the DeaD helicase. In addition, we found another potential RNA helicase of the DExD type. This is the YfmL protein. YfmL shares 32% to 35% and 56% to 58% identical and similar amino acid residues with the three other RNA helicases and contains a threonine as the variable amino acid in the DExD motif. Interestingly, YfmL is significantly shorter than the other helicases (376 amino acids) and it lacks the C-terminal domain that is present in the other RNA helicases. This domain is required and sufficient for specific RNA binding of DeaD (Wang *et al.*, 2006). Thus, it is likely that YfmL acts as a non-specific RNA helicase.

Interactions between RNA helicases in *B. subtilis*.

So far, nothing is known about the oligomerisation of RNA helicases in *B. subtilis*. The cold shock helicases CshB was shown to interact with the cold shock RNA chaperone CspB (Hunger *et al.*, 2006), but so far nothing is known about the oligomerisation of RNA helicases in *B. subtilis*.

Here, we used a bacterial two-hybrid (B2H) system to address the possibility of helicase homodimerization or formation of heterodimers between different *B. subtilis* RNA helicases. In the B2H system, the T25 and the T18 fragments of the catalytic domain of the *Bordetella pertussis* adenylate cyclase were fused to full-length copies of the four RNA helicases of *B. subtilis*. If fusions of one protein to either domain (and the other protein to the alternative adenylate cyclase domain) result in a productive interaction, this interaction is called reciprocal thus providing a higher level of confidence that an interaction actually takes place. The leucine zipper of the yeast GCN4 transcription factor served as a control (Karimova *et al.*, 1998). The results of the B2H analysis are shown in Fig. 9. As expected, the leucine zipper of GCN4 exhibited strong self-interaction but failed to interact with any of the RNA helicases (data not shown). As illustrated in Fig. 9, CshA showed a strong self-interaction suggesting that this helicase may be capable of forming dimers or oligomers. Moreover, both CshA and CshB interacted directly and reciprocally with DeaD. In contrast, YfmL showed only faint and non-reciprocal interaction signals with

itself and with CshA. Thus the B2H analysis suggests that some of the DEAD-box RNA helicases of *B. subtilis* have the potential to interact with each other.

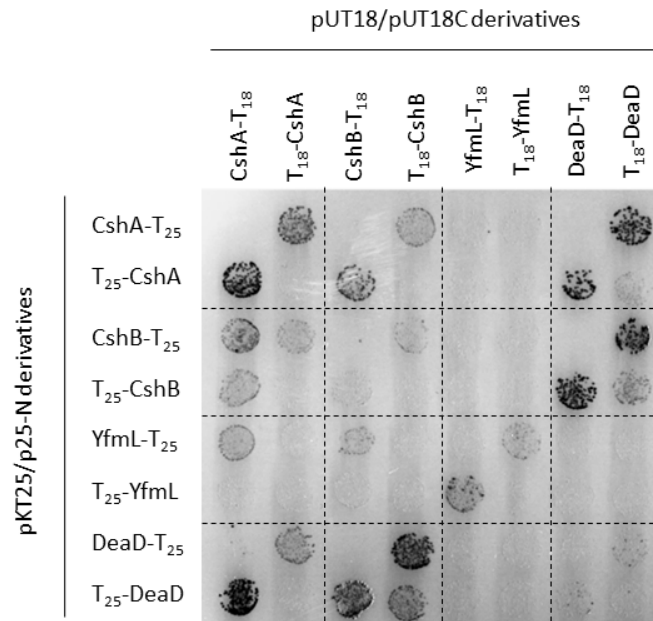


Fig. 9. Bacterial two-hybrid analysis of interactions among RNA helicases of *B. subtilis*. All genes were cloned in the plasmids pUT18, pUT18C, p25-N and pKT25. Plasmids pUT18 and pUT18C allow the expression of the selected enzymes fused either to the N- or the C-terminus of the T18 domain of the *B. pertussis* adenylate cyclase, respectively. Plasmids p25-N and pKT25 allow the expression of the selected enzymes fused either to the N- or the C-terminus of the T25 domain of the adenylate cyclase, respectively. The *E. coli* transformants were incubated for 48 h at 30°C. Degradation of X-Gal (blue colour) indicates the presence of a functional adenylate cyclase owing to the interaction of the two proteins of interest.

The dimerisation of DEAD-box RNA helicases has been a matter of debate (Callaghan *et al.*, 2004; Klostermeier & Rudolph, 2009; Liou *et al.*, 2002). To get further support for self-association of CshA, we expressed CshA carrying an N-terminal His-tag and a C-terminal FLAG-tag in *E. coli* and *B. subtilis*, respectively. After co-incubation of both extracts and affinity purification of His₆-CshA, CshA-FLAG was co-eluted demonstrating the formation of CshA dimers or oligomers (Fig. 10). His₆-GlcT was used as a control protein to exclude the possibility of non-specific interaction. As shown in Fig. 10, CshA-FLAG was not detected upon GlcT affinity purification suggesting that the assay was specific.

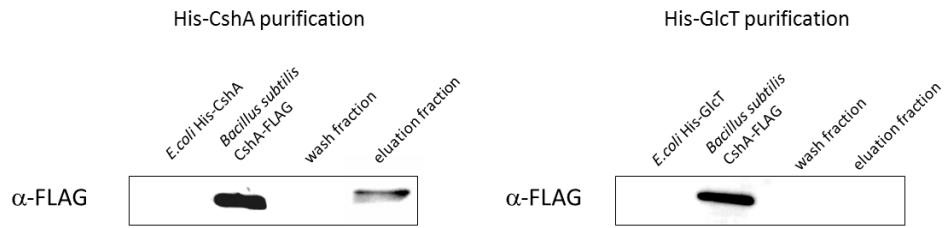


Fig. 10. Self-interaction of the DEAD-box helicase CshA. Extracts of *E. coli* cells expressing His-CshA (pGP1386) and *B. subtilis* cells expressing CshA-FLAG (GP1010) were mixed and His-CshA was purified by affinity chromatography. The elution fraction was separated by SDS-PAGE and blotted onto a PVDF-membrane. Self interaction was confirmed by detection of co-purified CshA-FLAG. His-GlcT (pGP124) purification served as a control to exclude non-specific protein-protein interaction of CshA-FLAG.

Interaction of RNA helicases with the components of the *B. subtilis* RNA degradosome.

In a previous study, we have shown that RNase Y, the RNases J1 and J2, the polynucleotide phosphorylase PnpA and the glycolytic enzymes enolase and phosphofructokinase form a protein complex, the RNA degradosome (Commichau *et al.*, 2009). The RNA degradosomes of other bacteria do usually also contain at least one RNA helicase (Carpousis, 2007; Marcaida *et al.*, 2006). It was therefore tempting to speculate that the *B. subtilis* RNA degradosome might also contain a RNA helicase.

Using the B2H system, we analyzed the primary protein-protein interactions between the bait proteins CshA, CshB, YfmL, and DeaD and their potential interaction partners PfkA, Eno, PnpA, and the RNases Y, J1, and J2. As shown in Fig. 11, the B2H analysis revealed direct and reciprocal interactions between CshA and the two proteins PnpA and RNase Y. In addition, we observed non-reciprocal interactions between CshA and Eno and PfkA, and of CshB to PfkA. Finally, DeaD showed a strong non-reciprocal interaction with PnpA. YfmL was not involved in any interaction.

Taken together, the results of the B2H analyses clearly demonstrate that CshA is capable of interacting with several components of the RNA degradosome *in vivo* suggesting that it is part of this complex. Moreover, it is interesting to note that PnpA seems to be able to interact with all three DEAD-box RNA helicases of *B. subtilis*.

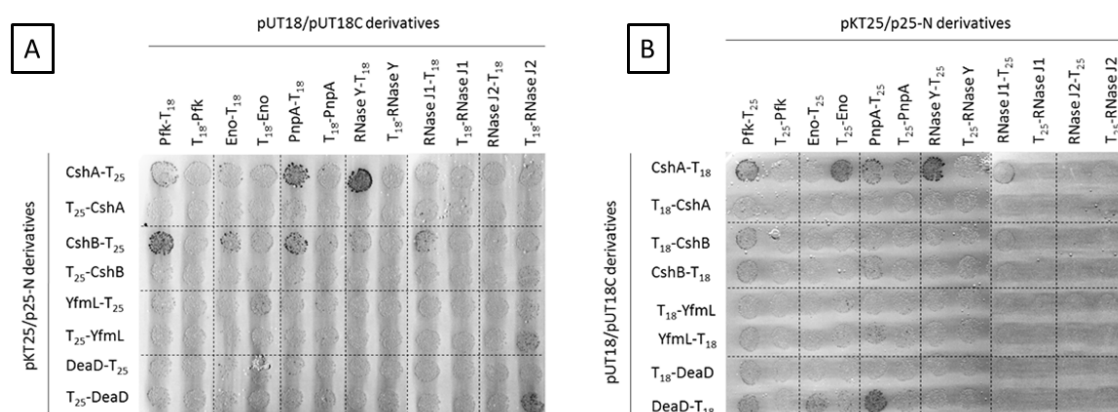


Fig. 11. Interactions among RNA helicases and components of the RNA degradosome of *B. subtilis*. All genes were cloned into the B2H system using the complementation of the *B. pertussis* adenylate cyclase (for details see Fig. 9). (A) Genes encoding the components of the degradosome of *B. subtilis* were present in the high-copy plasmids (pUT18 and pUT18C), whereas the genes encoding the four RNA helicases were present in the low-copy vectors (p25N and pKT25). (B) Genes encoding the RNA helicases were present in the high-copy vectors (pUT18 and pUT18C) whereas the RNA degradosome components were present in the low-copy plasmids (p25N and pKT25).

***In vivo* evidence for the interaction of CshA with degradosome components.**

The two hybrid analyses presented above demonstrate that the helicases have the potential to interact with each other and some or several degradosome components but they cannot reveal whether these interactions occur *in vivo* in the *B. subtilis* cell. To test whether such interactions take place, we used the SPINE approach in which Strep-tagged bait proteins are cross-linked to their potential interaction partners *in vivo* (Herzberg *et al.*, 2007). In a previous study that was aimed at the identification of the glycolytic interactome, we observed cross-linking of PfkA and Eno with CshA (Commichau *et al.*, 2009). This observation prompted us to investigate the *in vivo* interactions of CshA with RNA-degrading proteins.

To facilitate the detection of interacting proteins, we constructed a strain expressing CshA fused to a C-terminal Strep-Tag from its native promoter. This strain, GP1026, was then transformed with integrative plasmids resulting in the expression of degradosome components carrying a C-terminal triple FLAG-tag. The resulting strains (see Fig. 12) were grown in LB medium and a snapshot of protein-protein interaction was obtained by formaldehyde-mediated cross-linking of proteins. As shown in Fig. 12, all proteins tested for interaction with CshA were expressed under our experimental conditions as judged from the Western-blot signals obtained with the crude extracts. In

excellent agreement with the results obtained in the two-hybrid analysis, all potential components of the RNA degradosome, *i. e.* the glycolytic enzymes enolase and phosphofruktokinase as well as the RNase Y, J1, and PnpA were found to interact with CshA. In contrast, two control proteins, GltC and the malic enzyme YtsJ were not cross-linked with CshA. To be sure of the specificity of the experiments, GltC was assayed in each strain carrying one of the FLAG-tag constructs, and none of the strains yielded a signal. YtsJ carrying a C-terminal FLAG-tag was used to exclude the possibility that CshA might interact with the FLAG-tag rather than with the target proteins. Taken together, these observations suggest that CshA does specifically interact *in vivo* with the other proteins of the RNA degradosome.

strain		crude extract	-FA	+FA
GP1029	α -PnpA*			
GP1028	α -RNase J1*			
GP1031	α -RNase Y*			
GP1026	α -Eno			
GP1027	α -PfkA*			
GP1026	α -GltC			
GP1032	α -YtsJ*			

Fig. 12. Confirmation of the *in vivo* interaction of CshA and the degradosome components PnpA, RNase J1, RNase Y, Eno and PfkA. The RNA-helicase CshA fused to a C-terminal Strep-tag and expressed at its native locus was purified with its interaction partners from various *B. subtilis* strains (indicated in the first column) carrying triple FLAG tags attached to the putative interaction partners. All strains were grown in LB medium. CshA-Strep was purified in the absence and presence of the cross-linker formaldehyde (FA). 25 μ l of the first elution fraction of each purification were loaded onto a 12.5% SDS-polyacrylamide gel. After electrophoresis and blotting onto a polyvinylidene difluoride membrane, interaction partners were detected by FLAG-tag (indicated by asterisk) or polyclonal antibodies. GltC and YtsJ were used as negative controls.

To provide further evidence for the *in vivo* interaction between CshA and degradosome components, we performed a reverse experiment using RNase Y and PnpA as the baits and FLAG-tagged CshA as the prey. For this purpose, we constructed strain GP1010 that codes for a CshA protein carrying a triple FLAG-tag at its C-terminus. The biological activity of the FLAG-tagged CshA protein was tested by transforming the strain GP1010 with chromosomal DNA of the $\Delta cshB$ mutant strain CB40. This experiment yielded viable transformants. In contrast, a *cshA cshB* double mutant is not viable (Hunger *et al.*,

2006). Thus, the FLAG-tagged CshA protein has retained its activity. Strain GP1010 and its isogenic *pnpA* mutant GP1017 were transformed with the empty vector pGP380 or either plasmids pGP775 or pGP1342 that allow the expression of Strep-tagged versions of RNase Y and PnpA, respectively. The transformed strains were cultivated and *in vivo* protein complexes were cross-linked by formaldehyde, purified by affinity chromatography and the cross-links were broken. Finally, the proteins were analysed by SDS-PAGE and crosslinked CshA was detected by Western blotting. For RNase Y, no purification was obtained. This may be due to the fact that RNase Y is a membrane-bound protein (Hunt *et al.*, 2006). For PnpA, a protein recognized by the anti-FLAG antibody and corresponding to the molecular weight of CshA was co-purified upon cross-linking. As a control, the presence of the GltC protein in the protein fraction cross-linked to PnpA was assayed. No signal was observed although the GltC protein was present in the crude extract (see Fig. 13). Thus, the specific interaction between CshA and PnpA could be confirmed by an alternative approach.

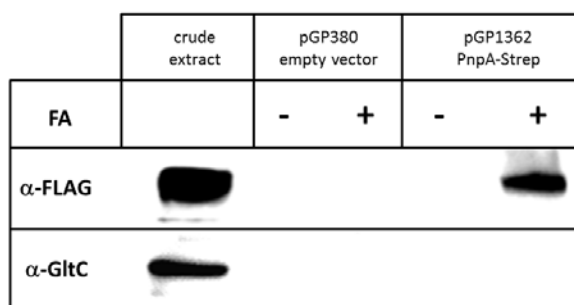


Fig. 13. Confirmation of the *in vivo* interaction between PnpA and CshA. The polynucleotide phosphorylase carrying a N-terminal Strep-tag was purified with its interaction partners from the *B. subtilis* strain GP1017 Δ *pnpA::aphA3 cshA-FLAG* carrying either pGP380 (empty vector) or the vector pGP1342 (expressing Strep-PnpA). Both strains were grown in CSE minimal medium containing 0.5% glucose. Strep-PnpA was purified from cultures that were grown in the absence and in the presence of the cross-linker formaldehyde (FA). 15 μ l of the first elution fractions from each purification were loaded onto a 12.5% SDS-polyacrylamide gel. After electrophoresis and blotting onto a polyvinylidene difluoride membrane, the FLAG-tag was detected using rabbit polyclonal antibodies. GltC was detected by rabbit polyclonal antibodies raised against GltC and served as a control.

Our results show that all the proteins hypothesized to form the RNA degradosome interact with CshA *in vivo*. This implicates that these proteins must have the same subcellular localization. It is known from previous studies that RNase Y, one of the principal components of the complex, is a membrane protein (Hunt *et al.*, 2006; Zweers *et al.*, 2009). To address the localization of CshA, the cell components of strain GP1010

expressing the FLAG-tagged CshA were fractionated and the localization of CshA was studied by Western blot analysis. CggR, a cytoplasmic protein, served as a control. In good agreement with previous results, CggR and RNase Y were exclusively present in the cytoplasmic and membrane fractions, respectively (Fig. 14). Thus our assay reliably differentiated proteins present in the two subcellular fractions. The CshA protein was detected only in the membrane fraction (Fig. 14).

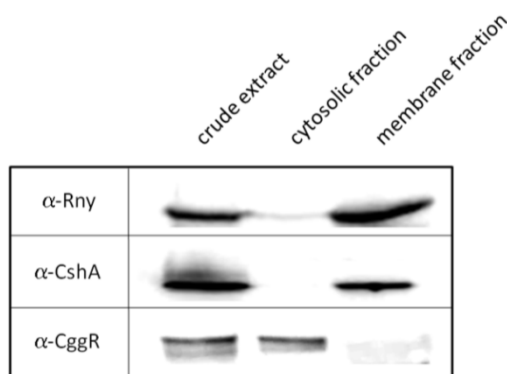


Fig. 14. Subcellular localization of RNase Y, CshA and CggR. Strain GP1010 (*cshA*-3xFLAG *spc*) was grown in LB medium to an OD₆₀₀ of 1.0. Cytosolic and membrane fractions were separated by ultracentrifugation and subjected to SDS-PAGE (12.5% PAA), followed by Western blotting. Anti-CggR was used as a control for a cytoplasmic protein.

Taken together, CshA and RNase Y interact *in vivo* and co-purify with the cellular membrane fraction, supporting the notion that both are components of the *B. subtilis* RNA degradosome.

Expression of CshA and CshB.

The results presented above suggest that CshA is the major RNA helicase in the RNA degradosome of *B. subtilis*. Transcriptome analyses revealed that both CshA and CshB are induced upon cold shock (Beckerling *et al.*, 2002). Since transcriptome studies do not report on changes in protein expression, we decided to analyze the expression of CshA and CshB by Western blotting. For this purpose, we grew the strains GP1010 and GP1011 that express the FLAG-tagged helicases under the control of their native promoters in complex and minimal media and determined the amounts of the fusion proteins by Western blot analysis of cell extracts. As shown in Fig. 15A, both CshA and CshB were present in LB medium, however, CshB was expressed at a lower level. In minimal medium, the expression of CshA was similar to that observed in LB. In contrast, CshB was not detectable in cells grown in minimal medium. Interestingly, the amounts of both helicases

were similar at 16°C and 37°C suggesting that temperature plays only a minor role in controlling their expression. The temporal patterns of *cshA* and *cshB* expression were studied during growth of GP1010 and GP1011 in LB medium. As shown in Fig. 15B, the amounts of CshA were constant throughout growth. In contrast, CshB was present at highest levels during logarithmic growth, but its amounts decreased upon entry into stationary phase and the protein disappeared during extended stationary phase.

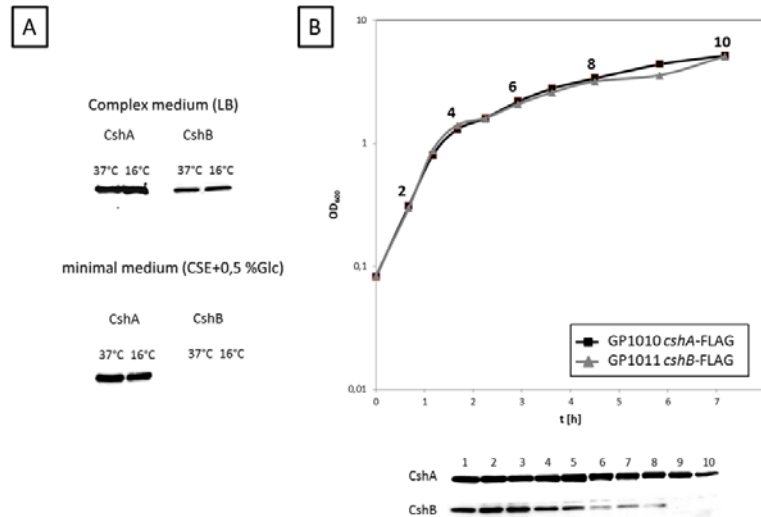


Fig. 15. Cellular amounts of CshA and CshB. (A) Crude extracts were isolated from the *B. subtilis* strains GP1010 (*cshA*-FLAG) and GP1011 (*cshB*-FLAG) grown in minimal medium (CSE containing 0.5% glucose) and complex medium (LB) at low (16°C) and moderate (37°C) temperatures. 10 µg crude extract of each culture was loaded on a 12.5% sodium dodecyl sulfate-polyacrylamide gel. After electrophoresis and blotting onto a polyvinylidene difluoride membrane, the FLAG-tag was detected using rabbit polyclonal antibodies. All cultures were harvested in the exponential phase. (B) Cellular amounts of CshA and CshB throughout growth. The *B. subtilis* strains GP1010 (*cshA*-FLAG) and GP1011 (*cshB*-FLAG) were grown in LB medium at 37°C. Each second time point of sampling is labeled by the sample number. Western blot analysis was performed as described in (A).

Taken together, these results show that *cshA* is constitutively expressed. On the other hand, *cshB* expression is controlled by the medium composition and the growth phase. Based on the differential availability of the two helicases in the cell, it seems safe to conclude that only CshA may play a major role in the RNA degradosome throughout growth.

Contributions of the domains of CshA to the different interactions.

As other RNA helicases of the DEAD box family, CshA contains two RecA-like helicase domains that are required for ATP binding, RNA binding and catalytic activity. Moreover, CshA carries an additional domain at its C-terminus (see Fig. 16A). The corresponding domain of the homologous protein DeaD was shown to bind RNA (Wang *et al.*, 2006). We were interested in defining the role of these domains for self-interaction of CshA and for the different interactions with the other RNA helicases and the degradosome components. For this purpose, the different portions of CshA were tested in the B2H system.

First, we addressed self-interactions among the domains of CshA. The RecA-like domains as well as the C-terminal domain did not participate in any interaction with itself or the other domains when they were present as isolated domains (data not shown). Of the isolated domains, only the C-terminal domain interacted with the full-length CshA protein (Fig. 16B). Similarly, an N-terminally truncated variant of CshA (consisting of only the second RecA-like and C-terminal domains) showed an interaction with full-length CshA. These results demonstrate that the C-terminal domain makes the major contribution to CshA dimerisation or oligomerisation.

In a similar manner, we studied the contributions of the domains of CshA for the interactions with its partners in the *B. subtilis* RNA degradosome, i. e. the phosphofructokinase PfkA, the enolase Eno, the polynucleotide phosphorylase PnpA and RNase Y. As shown in Fig. 16B, only the full-length CshA protein and the protein consisting of the second RecA-like and the C-terminal domains were able to interact with the partners in the degradosome. It should be noted that efficient interaction with PfkA required the presence of all three domains. As observed for the dimerisation of CshA, the C-terminal domain is essential for the protein-protein interactions, however, is not sufficient for the interactions with the other degradosome components. Our results furthermore demonstrate that, with the exception of PfkA, the first RecA-like domain of CshA is dispensable for the protein-protein interactions.

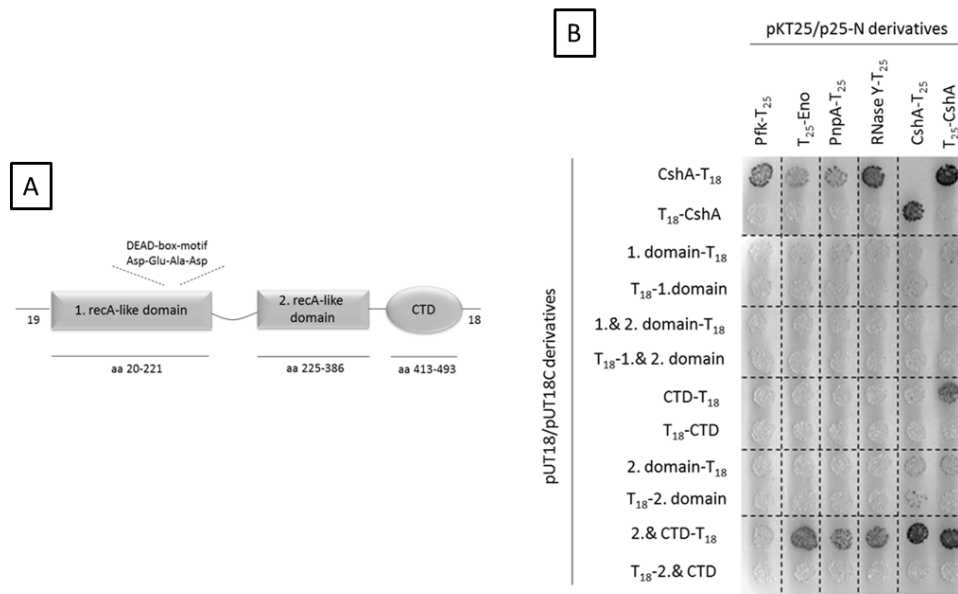


Fig. 16. Interactions among truncated variants of the RNA helicase CshA and components of the *B. subtilis* RNA degradosome. (A) Domain organisation of the RNA helicase CshA. As a member of the DEAD box family, CshA contains the helicase core that includes all conserved helicase motifs such as the conserved DEAD motif and an additional C-terminal domain. The core consists of two RecA-like domains. (B) B2H interaction analysis of truncated variants of CshA and enzymes of the RNA degradosome. Genes encoding components of the RNA degradosome and full length CshA were present in the high-copy plasmids pUT18 and pUT18C. Truncated variants of CshA, as well as the full-length protein were cloned into the low-copy plasmids p25-N and pKT25 (for details of the B2H analysis see Fig. 9). CTD, C-terminal domain.

The C-terminal domain of CshA confers interaction with RNase Y.

As described above, CshA interacts with RNase Y, the key component of the *B. subtilis* RNA degradosome whereas no interaction between CshB and RNase Y was observed. The results shown in Fig. 16B demonstrate that the C-terminal domain of CshA that is not required for helicase activity is implicated in the interaction with RNase Y. We therefore considered the possibility that the function of this domain is to mediate protein-protein interactions, and that transfer of this domain to CshB might allow the latter helicase to interact with RNase Y. To test this hypothesis, we constructed a hybrid gene that encodes the two RecA-like domains of CshB and the C-terminal domain of CshA. The interaction properties of this hybrid protein (CshB_{CshA}) were assayed in the B2H system. As shown in Fig. 17, CshB_{CshA} was indeed able to interact with RNase Y, and was in this respect indistinguishable from the CshA protein. In contrast and in good agreement with the results reported above, CshB was not capable of interacting with RNase Y. Thus, the C-

terminal domain of CshA is a major determinant for the specific interaction with RNase Y. This finding may explain why CshA but not CshB is associated with the RNA degradosome.

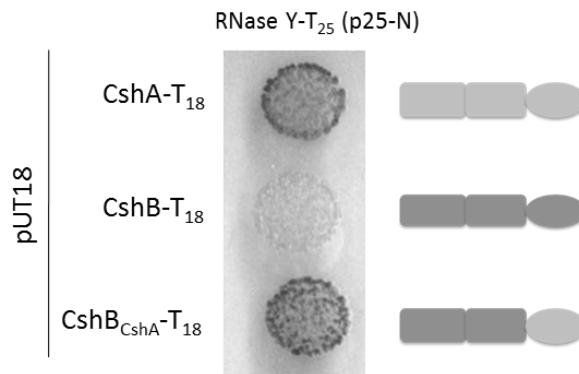


Fig.17. Contribution of the C-terminal domain of CshA to the specific interaction with RNase Y. The gene encoding RNase Y was present in p25N, whereas the coding sequences of CshA, CshB and the CshB_{CshA} chimera were cloned into pUT18 (for details of the B2H analysis see Fig. 9) CshB_{CshA} is a chimeric protein composed of the RecA-like domains that comprise the helicase core of CshB and the C-terminal domain of CshA.

Discussion

RNA degradation is an important cellular process that involves multiprotein complexes. In *B. subtilis*, such a complex, the RNA degradosome, was discovered only recently (Commichau *et al.*, 2009). However, the initially described assembly did not include a RNA helicase, a component found in most archaeal, bacterial, and eukaryotic RNA degradation machines. Here, we presented evidence that the DEAD box RNA helicase CshA is capable of interacting with multiple subunits of the *B. subtilis* degradosome and that this interaction does indeed occur *in vivo*. This evidence implies that CshA is an integral component of the *B. subtilis* degradosome.

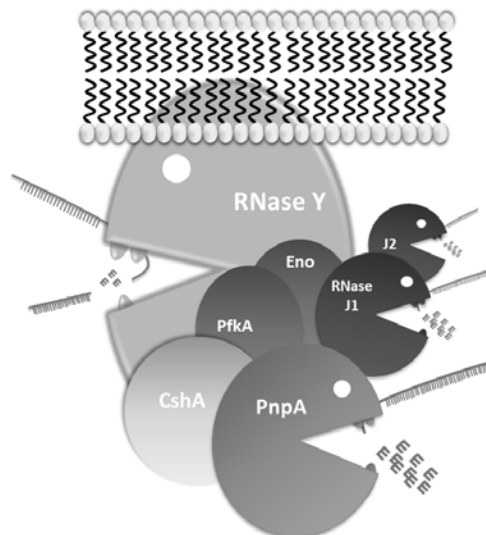


Fig. 18. The current model of the *B. subtilis* RNA degradosome. The membrane-bound RNase Y coordinates the RNA degradosome. This protein binds to the RNases PnpA and J1 (shown in grey). Additionally, RNase Y interacts with the glycolytic enzymes enolase (Eno) and phosphofructokinase (PfkA) (shown in blue). As demonstrated in this study, the RNA helicase CshA (yellow) is the central helicase in the complex and contacts RNase Y, PnpA, PfkA and Eno. RNase J2 is associated to the degradosome due to its interaction with RNase J1 (Commichau *et al.*, 2009; Mathy *et al.*, 2010). In agreement with recently published evidence, RNase Y may perform the initial endonucleolytic attacks on mRNA substrates whereas the exonucleases PnpA and RNase J1/J2 degrade the RNA fragments from the 3' and 5' ends, respectively (Shababian *et al.*, 2009; Condon, 2010; Yao and Bechhofer, 2010).

RNases and RNA helicases are the key components of all RNA degradation complexes studied so far. Our work shows that this is also the case for the RNA degradosome of *B. subtilis*. However, there is a wide variation in the RNases and in additional proteins that may be part of the complex. In *E. coli* and *R. capsulatus*, the endonuclease RNase E is the major constituent of the complex that does also provide the backbone to organise the assembly of the other partners (Marcaida *et al.*, 2006). However, RNase E is not encoded in the genome of *B. subtilis* and many other bacteria. In *B. subtilis*, the novel and essential RNase Y is a central component of the degradosome. A peculiarity of the RNA degradosomes of *E. coli* and *B. subtilis* that has not been observed in any other species is the presence of glycolytic enzymes in the RNA degradosome. However, the precise function of these enzymes in the protein complex is so far unknown.

The only constants in the different RNA degrading machineries are the presence of 3' to 5' exoribonucleases, such as polynucleotide phosphorylase, and DEAD box RNA helicases. This has two implications for the interaction properties of these proteins: First, during evolution these two classes of proteins must have adapted to a wide variety of different partners such as several unrelated endoribonucleases, glycolytic enzymes or other accessory degradosome components. Such a potential for differing interactions in different species is not unprecedented: The HPr and PII proteins involved in the control of carbon and nitrogen metabolism, respectively, interact with a large number of unrelated proteins (Deutscher *et al.*, 2006; Forchhammer, 2008). Second, polynucleotide phosphorylase and RNA helicases must have co-evolved, at least with respect to their interaction sites. Two lines of evidence support this idea: In *E. coli*, PnpA and the helicase RhlB form a distinct exoribonucleolytic complex (Lin & Lin-Chao, 2005). Moreover, our results show interactions of PnpA with two DEAD box helicases, *i. e.* CshA and DeaD.

The RNA helicases are particularly important when RNA secondary structures become more stable, *i. e.* at low temperatures. In *E. coli*, the cold shock helicase CsdA

becomes a member of the degradosome during cold acclimatisation (Prud'homme-Généreux *et al.*, 2004). In *B. subtilis*, transcriptome studies revealed that the expression of both CshA and CshB is increased upon a cold shock. In contrast, expression of the other RNA helicases, DeaD and YfmL, is not affected (Beckering *et al.*, 2002). However, a proteome analysis revealed substantial accumulation of CshA even at 37°C (Eymann *et al.*, 2004). To clarify this issue, we analysed the expression patterns of CshA and CshB in different media and at low (16°C) and moderate (37°C) temperatures. In agreement with the observation of Eymann *et al.* (2004) we found that CshA is well expressed at 37°C, and the expression is similar under all conditions tested in our study. For CshB, we found that the temperature does not affect the expression, but that CshB is not expressed in our minimal medium, and that the expression in complex medium declines after entry into the stationary phase (see Fig. 15). The mRNA amounts of *cshA* and *cshB* might be increased at low temperatures as observed by Beckering *et al.* (2002) to compensate the reduced translation efficiency due to the formation of secondary structures in the mRNAs.

Another interesting result of our study is the observation that CshA may form dimers or even oligomers (see Fig. 9, 10). This is rather unusual for RNA helicases of the DEAD box family. Conflicting results have been reported with respect to the ability of *E. coli* RhlB to form dimers. While Liou *et al.* (2002) reported dimer formation; Callaghan *et al.* (2004) did not observe any dimerisation. Recently, the analysis of the crystal structure of the *Thermus thermophilus* DEAD box RNA helicase Hera revealed that this protein also forms dimers (Klostermeier & Rudolph, 2009) and oligomerization of *E. coli* RhlB was observed *in vitro* (Taghbalout & Yang, 2010). It is, however, not known whether di- or oligomerisation of these proteins is a prerequisite that helps them to fulfil their specific tasks. The domain analysis of both *T. thermophilus* Hera and *B. subtilis* CshA revealed that the C-terminal domain of the proteins is required for efficient dimerisation. This domain is not involved in the catalytic activity of the RNA helicases. Moreover, such C-terminal domains are present only in a subset of DEAD box helicases. The corresponding domain of DeaD is a RNA-binding domain that recognizes 23S rRNA (Kossen *et al.*, 2002).

Unlike the other DEAD box RNA helicases, CshA does also interact with multiple components of the RNA degradosome. In this respect, CshA resembles its *E. coli* counterpart RhlB that can bind both RNase E and the polynucleotide phosphorylase (Chandran *et al.*, 2007; Lin & Lin-Chao, 2005). The analysis of the contribution of the three domains of CshA to the different interactions showed that the C-terminal domain is crucial for all interactions. This domain is sufficient for self-interaction, and a fragment containing both the second RecA-like domain and the C-terminal domain efficiently interacts with all

partners except PfkA (see Fig. 16). A similar result has been obtained for the interaction of the *E. coli* RNA helicase RhlB with RNase E (Liou *et al.*, 2002). The significance of the C-terminal domain is underlined by the fact that it can confer recognition of RNase Y to CshB (Fig. 17). Moreover, YfmL, the only DEAD box helicase in *B. subtilis* that is devoid of a C-terminal domain does not participate in any of the interactions studied in this work. All these findings strongly suggest that the C-terminal domains determine the interactions to which the different DEAD box helicases can contribute. This can be interactions with a specific RNA as in the case of DeaD, dimerization as observed for Hera and CshA or specific interactions with other proteins as described here for CshA and RNase Y.

The constitutive expression of CshA, its *in vivo* interaction with all degradosome components, and the demonstration that CshA and RNase Y are exclusively present in the cell membrane fraction, strongly supports the idea that CshA acts as the constitutive RNA helicase of the *B. subtilis* RNA degradosome. However, our findings do not rule out the possibility that also CshB and DeaD associate with the degradosome, at least transiently under specific conditions, to assist RNA unwinding. Such interactions might depend on the presence of specific RNA substrates as suggested by the specific recognition of 23S rRNA by DeaD (Wang *et al.*, 2006). The functional analysis of the interactions described here will be the subject of further analyses.

Acknowledgements

Martin Arnold, Daniel Hellwig, Frederik Meyer and Fabian M. Rothe are acknowledged for the help with some experiments. We are grateful to Mohamed Marahiel and Thomas Wiegert for providing us with strain CB40 and plasmid pAL-FLAG-*rsiW*, respectively. We wish to thank Fabian M. Commichau for helpful discussions in the initial phase of this project. This work was supported by grants of the Deutsche Forschungsgemeinschaft and the Fonds der Chemischen Industrie to J. S..

Experimental procedures

Bacterial strains and growth conditions - All *B. subtilis* strains used in this work are derived from the laboratory wild type strain 168. They are listed in Table 1. *B. subtilis* CB40 (*cshB::ermC*; (Hunger *et al.*, 2006)) was used to assay the activity of FLAG-tagged CshA. For this purpose, CB40 was transformed with chromosomal DNA of GP1010. Transformants were selected for resistance to erythromycin and spectinomycin. The

absence of the *cshB* gene was verified by PCR using the primer pair HP7/HP8. *E. coli* DH5 α , XL1-Blue and BTH101 (Karimova *et al.*, 1998; Sambrook *et al.*, 1989) were used for cloning experiments and bacterial two-hybrid (B2H) analyses, respectively. *B. subtilis* was grown in CSE minimal medium containing succinate and glutamate/ ammonium as basic sources of carbon and nitrogen, respectively (Faires *et al.*, 1999). The medium was supplemented with auxotrophic requirements (at 50 mg/l) and glucose as indicated. *E. coli* was grown in LB medium and transformants were selected on plates containing ampicillin (100 μ g/ml). LB, SP and CSE plates were prepared by the addition of 17 g Bacto agar/l (Difco) to LB, SP or CSE medium, respectively.

DNA manipulation and transformation - Transformation of *E. coli* and plasmid DNA extraction were performed using standard procedures (Sambrook *et al.*, 1989). Restriction enzymes, T4 DNA ligase and DNA polymerases were used as recommended by the manufacturers. DNA fragments were purified from agarose gels using the Nucleospin Extract kit (Macherey and Nagel, Germany). *Phusion* DNA polymerase was used for the polymerase chain reaction as recommended by the manufacturer. All primer sequences are provided as supplementary material. DNA sequences were determined using the dideoxy chain termination method (Sambrook *et al.*, 1989). All plasmid inserts derived from PCR products were verified by DNA sequencing. Chromosomal DNA of *B. subtilis* was isolated as described (Kunst & Rapoport, 1995).

E. coli transformants were selected on LB plates containing ampicillin (100 μ g/ml) or kanamycin (50 μ g/ml). *B. subtilis* was transformed with plasmid or chromosomal DNA according to the two-step protocol described previously (Kunst & Rapoport, 1995). Transformants were selected on SP plates containing kanamycin (Km 10 μ g/ml), spectinomycin (Spc 150 μ g/ml), or erythromycin plus lincomycin (Em 2 μ g/ml and Lin 10 μ g/ml).

Expression analysis - To monitor the expression patterns of CshA and CshB, vector pGP1331 was designed to fuse both proteins to a triple FLAG-tag at their C-terminus. For this purpose the 3 \times FLAG-tag sequence was amplified with primers ML5 and ML6 using vector pAL-FLAG-rsiW (Schöbel *et al.*, 2004) as a template. The product was ligated into the *Hind*III restriction site of pUS19 (Benson *et al.* 1993) giving pGP1331. Next, the 3'-ends of *cshA* and *cshB* were amplified using primer pairs ML11/ML12 and ML13/ML14 and cloned into pGP1331 using the *Bam*HI and *Sa*II restriction sites. The resulting plasmids were pGP1332 (*cshB*-3 \times FLAG) and pGP1333 (*cshA*-3 \times FLAG). Both plasmids integrate by

single crossing-over into the chromosome of *B. subtilis* leading to strains GP1010 (*cshA*::pGP1333) and GP1011 (*cshB*::pGP1332).

Growth experiments with the *B. subtilis* strains GP1010 and GP1011 were carried out as follows: LB or CSE (supplemented with 0.5% Glc) media were inoculated with an overnight culture of the corresponding strains. These cultures were grown at 37°C. At an OD₆₀₀ of 1.0, these cultures were used to inoculate new cultures in the same media to an OD₆₀₀ of 0.1. These cultures were grown under vigorous agitation at 16°C or 37°C. Samples for Western blot analysis were taken throughout growth.

Preparation of membrane fractions - Cultures of *B. subtilis* were harvested by centrifugation (4,400 x *g*, 10 min, 4°C). The following steps were done as described previously (Coutts *et al.*, 2002). Briefly, the cells were lysed by sonication, the cellular debris removed, and the fractions of the cell extract were separated by ultracentrifugation. The membrane pellet was washed for three times and finally resuspended in phosphate buffer (50 mM Na₂HPO₄, 50 mM NaH₂PO₄, pH6.8). To assess the quality of the preparations, the fractions were analyzed for the presence of CggR and RNase Y using polyclonal rabbit antibodies raised against these proteins (Meinken *et al.*, 2003; Zweers *et al.*, 2009).

Western blotting - For Western blot analysis, proteins were separated by 12.5% SDS-PAGE and transferred onto polyvinylidene difluoride (PVDF) membranes (Bio-Rad) by electroblotting. Rabbit anti-FLAG polyclonal antibodies (Sigma-Aldrich; 1:10 000), anti-GltC (1:25,000) (Commichau *et al.*, 2007), and anti-CggR (1:10,000), anti-RNase Y (1:50,000), and anti-Eno (1:30,000) served as primary antibodies. The antibodies were visualized by using anti-rabbit immunoglobulin G-alkaline phosphatase secondary antibodies (Promega) and the CDP-Star detection system (Roche Diagnostics), as described previously (Commichau *et al.*, 2007).

B2H assay - Primary protein-protein interactions were identified by bacterial two-hybrid (B2H) analysis (Karimova *et al.*, 1998). The B2H system is based on the interaction-mediated reconstruction of adenylate cyclase (CyaA) activity from *Bordetella pertussis* in *E. coli*. The CyaA enzyme consists of two complementary fragments T18 and T25 that are not active when physically separated. Fusion of these fragments to interacting proteins results in functional complementation between the T18 and T25 fragments and the synthesis of cAMP. cAMP production can be monitored by measuring the β-galactosidase activity of the cAMP-CAP-dependent promoter of the *E. coli lac* operon. Thus, a high β-galactosidase activity reflects the interaction between the hybrid proteins. Plasmids

pUT18 and p25-N allow the expression of proteins fused to the N-terminus of the T18 and T25 fragments of the CyaA protein, respectively, and the plasmids pUT18C and pKT25 allow the expression of proteins fused to the C-terminus of the T18 and T25 fragments of the CyaA protein, respectively (Claessen *et al.*, 2008; Karimova *et al.*, 1998). The plasmids pKT25-*zip* and pUT18C-*zip* served as positive controls for complementation. These plasmids express T18-*zip* and T25-*zip* fusion proteins that can associate due to the leucine zipper motifs resulting in an active CyaA enzyme and a high β -galactosidase activity. DNA fragments corresponding to the helicase genes and their domains were obtained by PCR (for primers, see supplementary material). The PCR products were digested with KpnI and XbaI and cloned into the four vectors of the two-hybrid system that have been linearized with the same enzymes. The resulting plasmids (see supplementary Table S2) were used for cotransformations of *E. coli* BTH101 and the protein-protein interactions were then analyzed by plating the cells on LB plates containing ampicillin (100 μ g/ml), kanamycin (50 μ g/ml), X-Gal (40 μ g/ml) (5-bromo-4-chloro-3-indolyl- β -D-galactopyranoside) and IPTG (0.5 mM) (isopropyl- β -D-thiogalactopyranoside), respectively. The plates were incubated for a maximum of 48 h at 30°C.

The *cshB-cshA* hybrid gene was constructed by two-step PCR. For step one PCR products using primer pairs HP7/ML37 and ML36/HP6 were generated. The resulting fragments were mixed and used as template with the primer pair HP7/HP6 to generate the *cshB-cshA* product, which was subsequently cloned into the two hybrid vectors using *XbaI* and *KpnI*.

In vivo detection of protein-protein interactions - The isolation of protein complexes from *B. subtilis* cells was performed by the SPINE technology (Herzberg *et al.*, 2007). To express the CshA protein fused to a C-terminal Strep-tag from its native locus we first amplified the 3'-end of *cshA* using primers ML11/ML93. The PCR product was digested with BamHI and SalI and ligated to vector pGP382 (Herzberg *et al.*, 2007). The resulting plasmid was pGP1387. To introduce the *cshA*-Strep-tag fusion into the chromosome of *B. subtilis* 168, we applied the long flanking homology PCR technique (Wach, 1996). For this purpose, the *cshA*-Strep-tag fusion was amplified using primer pair ML93/ML94 using pGP1387 as a template. The *aphA3* resistance cassette was obtained from plasmid pDG780 (Guerout-Fleury *et al.*, 1995). For the amplification of the downstream *ydbS* gene we used the primers ML95/ML96. The joining of the three fragments was performed by a second round of PCR using primers ML93/ML96. The PCR product was directly used to transform *B. subtilis* 168 resulting in the introduction of the kanamycin resistance cassette between

the open reading frame of *cshA* and the downstream gene *ydbS* replacing *cshA* with the *cshA*-Strep-tag fusion. This strain was designated GP1026.

To facilitate the detection of CshA interaction partners by Western blot analysis, we fused RNase Y, PfkA, RNase J1, PnpA, and YtsJ to a C-terminal triple FLAG tag using plasmid pGP1331 as described above for *cshA* and *cshB*. The resulting plasmids were pGP1388 (*rny*), pGP1375 (*pfkA*), pGP1376 (*rnjA*), pGP1377 (*pnpA*), and pGP1758 (*ytsJ*).

To express RNase Y and PNPase with an N-terminal Strep-tag the coding sequences of both genes were amplified by PCR with primer pairs DH13/DH14 and HP11/HP12 using chromosomal DNA of *B. subtilis* 168 as the template. The PCR products were digested with *Bam*HI and *Sal*I and cloned into the expression vector pGP380 (Herzberg *et al.*, 2007) giving pGP775 (Strep-*rny*) and pGP1342 (Strep-*pnpA*). *B. subtilis* 168 and the *pnpA* mutant GP1017 served as host for the overexpression of the bait proteins. To construct strain GP1017, we used chromosomal DNA of the *B. subtilis* GP584. This strain was obtained by long flanking homology PCR as outlined above. DNA fragments of about 1,000 bp flanking the *pnpA* region at its 5' and 3' ends were amplified using the primer pairs NP64/NP66 and NP67/NP68. The 3' end of the upstream fragment as well as the 5' end of the downstream fragment extended into the *pnpA* gene in a way that all expression signals of genes up- and downstream remained intact. The joining of the two fragments to the *aphA3* resistance cassette (see above) was performed using the primer pair NP64/NP68. The PCR product was directly used to transform *B. subtilis*. The integrity of the regions flanking the integrated resistance cassette was verified by sequencing PCR products of about 1,000 bp amplified from chromosomal DNA of the resulting mutant GP584 ($\Delta pnpA::aphA3$). Transformation of strain GP1010 expressing a CshA protein fused to a triple FLAG-tag with chromosomal DNA of GP584 yielded *B. subtilis* GP1017.

For cultivation one liter LB culture was inoculated to an OD₆₀₀ of 0.1 with an overnight culture. This culture was grown at 37°C until OD₆₀₀ 1.0 and divided. One half was harvested immediately, and the other was treated with formaldehyde (0.6% w/v, 20 min) to facilitate the cross-linking (Herzberg *et al.*, 2007). After cross-linking, the cells were also harvested and washed with a buffer containing 50 mM Tris-HCl (pH 7.5) and 200 mM NaCl. The pellets were lysed using a French press (20,000 p.s.i., 138,000 kPa; Spectronic Instruments, UK). After lysis the crude extracts were centrifuged at 100,000 *g* for 1 h. For purification of the Strep-tagged proteins the resulting supernatants were passed over a Streptactin column (IBA, Göttingen, Germany) (0.5 ml bed volume). The recombinant proteins were eluted with desthiobiotin (IBA, Göttingen, Germany, final

concentration 2.5 mM). Aliquots of the different fractions were subjected to SDS-PAGE. Prior to electrophoresis, the protein samples were boiled for 20 minutes in Laemmli buffer to reverse the cross-links. As a control, the *B. subtilis* strain carrying the empty vector pGP380 was used.

In vitro pull-down experiments - The self-interaction of CshA analyzed according to a published procedure (Chai *et al.*, 2010b). For this purpose we constructed plasmid pGP1386 that allows the expression of CshA carrying an N-terminal His-tag in *E. coli*. Briefly, the *csHA* gene was amplified using the primer pair HP13/ML120, digested with BamHI/ HindIII and ligated with pWH844 (Schirmer *et al.*, 1997) cut with the same enzymes. Crude extracts of *E.coli* DH5 α /pGP1386 and of *B. subtilis* GP1010 expressing His₆-CshA CshA-3xFLAG, respectively, were mixed and purified via the His-tag. Co-purification of FLAG-CshA was detected with α -FLAG antibodies. For *E.coli* we grew the cells in LB to an OD₆₀₀ of 0.6 and induced the protein expression with IPTG (final concentration 1 mM). The cells we harvested after 2.5 h, resuspended in disruption buffer (50 mM Tris-HCl pH 7.5, 200 mM NaCl) and disrupted by a French press. For *B. subtilis*, the cells were grown in LB to an OD₆₀₀ of 1.0. The cells were centrifuged, resuspended in disruption buffer and broken by a French Press, too. The cell debris of both preparations were removed by centrifugation at 8000 rpm. Both crude extracts were mixed and incubated for 45 min at 4°C to facilitate CshA self-interaction. For purification of the recombinant His₆-tagged protein the supernatant fraction was loaded onto a 1 ml bed volume of Ni²⁺-NTA resin (Qiagen) in a Poly-Prep Chromatography Column (Biorad, Munich, Germany). The Ni²⁺-NTA resin had been pre-equilibrated with 10 ml disruption buffer. After extensive washing with 10 ml of disruption buffer containing 10 mM imidazole (Roth, Karlsruhe, Germany) and 20 ml with 20 mM imidazole, the His₆-tagged protein was eluted (0.5 M imidazole). Overproduction of His₆-GlcT (pGP124) (Langbein *et al.*, 1999) was used as a control.

4. Multiple roles of the DEAD-box RNA helicase CshA in *Bacillus subtilis*

Martin Lehnik-Habrink, Leonie Rempeters, Christina Herzberg, Ákos T. Kovács, Dominik Tödter, Christoph Wrede, Claudia Baierlein, Michael Hoppert, Heike Krebber, Oscar P. Kuipers and Jörg Stülke

Author's contribution: MLH, CH and DT performed the analysis of the impact of CshA for the growth at low temperatures. Phase contrast microscopy was performed by MLH, electron microscopy by CW. The pull down analysis was done by MLH and CH. The bacterial two hybrid analysis concerning the cold shock proteins was done by DT, analysis concerning the ribosomal proteins was done by MLH. The ribosomal profiles were prepared by LR, with the help of CB. Microarray analyses were conducted by AK. The Northern blot experiments performed LR. The experiments were designed and interpreted by MLH and JS.

Abstract

DEAD-box RNA helicases are enzymes that remodel secondary structures on RNA molecules. In this study we investigate the physiological role of the RNA helicase CshA in *Bacillus subtilis*. We demonstrate that the deletion of *csHA* results in a severe growth defect at low temperatures. This growth defect is accompanied by an altered cell morphology probably caused by a cell separation deficiency. Furthermore we reveal that CshA interacts with ribosomal proteins *in vivo* and that loss of the RNA helicase impairs the cells ability for proper ribosome biogenesis. In addition we elucidate the role of CshA as the major RNA helicase in the RNA degradosome of *B. subtilis*. Therefore we conducted transcriptome analysis revealing that deletion of *csHA* changes the abundance of over 200 mRNAs. The experiments presented in this study suggest that the DEAD-box RNA helicase CshA has multiple roles in the physiology of *B. subtilis*.

Introduction

RNA molecules are often illustrated as a single-stranded species released by the RNA polymerase in the process of transcription. Even though it is possible that the nascent molecule is just a long stretch, RNA molecules inside of the cell are faced with a number of different proteins or other nucleic acids that have the capability to interact with it. Additionally, the RNA molecule itself is highly biased to form intramolecular interactions. While some of these interactions are necessary and essential for survival of the cell, others have negative consequences (Rocak & Linder, 2004). To avoid undesirable intra- and intermolecular interactions of RNA molecules, the cell encodes a variety of proteins helping the RNA to fold properly. One of the largest protein classes in RNA metabolism are RNA helicases (Anantharaman *et al.*, 2002). Such RNA helicases are highly conserved enzymes utilizing ATP to bind and remodel RNA or ribonucleoprotein complexes (Tanner & Linder, 2001). As RNA molecules are a fundamental part of all known organisms, RNA helicases are found in all domains of life (Anantharaman *et al.*, 2002).

On the basis of sequence alignments RNA helicases are classified into different superfamilies. Within superfamily II, the DEAD-box proteins represent the largest family of RNA helicases (Gorbalenya & Koonin, 1993). All DEAD-box proteins contain a high conserved catalytic core and optionally a variable N- or C-terminal extension. The catalytic core is composed of two RecA-like domains comprising nine conserved motifs (Rocak &

Linder, 2004). The Asp-Glu-Ala-Asp or DEAD (one-letter-code) motif gave the protein family its name.

As RNA molecules are an integral part of every cell, RNA helicases are involved in a variety of different processes. In eukaryotic cells, RNA helicases are involved in transcription, splicing, mRNA export, ribosome biogenesis, translation and mRNA decay (for review see (Rocak & Linder, 2004)). The importance of these enzymes is underlined by the fact that yeasts like *Saccharomyces cerevisiae* harbor 26 DEAD-box genes, of which 18 are essential (Linder *et al.*, 2000).

RNA helicases also play a central role in bacterial cells. The Gram negative model organism *E. coli* encode five DEAD-box proteins. They are mainly involved in ribosome assembly, mRNA decay or both. For example, the RNA helicase RhIB is an integral part of the RNA degradosome of *E. coli*, a protein complex involved in the degradation of mRNA. Deletion of the gene results in a slightly elevated overall RNA stability and regulation of steady-state levels of hundreds of mRNAs (Bernstein *et al.*, 2004). While RhIB participates solely in mRNA decay, other RNA helicases are more versatile. The DEAD-box RNA helicase CsdA has the unique ability of being implicated in the three different cellular processes: mRNA decay, ribosome biogenesis and translational initiation. Its involvement in mRNA decay was demonstrated by the fact that overexpression of the protein yielded in the stabilization of the *cspA* mRNA, encoding the cold shock protein A (CspA) (Brandi *et al.*, 1999). Furthermore *csdA* deletion strains are impaired in the proper formation of the large ribosomal subunit and *in vitro*; CsdA helps in the translation initiation process when the mRNA harbors secondary structures.

While *E. coli* encodes five different RNA helicases, the Gram positive model organism *B. subtilis* contains four enzymes: CshA, CshB, DeaD and YfmL. All four RNA helicases contain the conserved catalytic core and, with the exception of YfmL, an additional C-terminal domain.

CshA is the largest of the four RNA helicases with a distinct domain at its C-terminus. This protein is the functional homolog of RhIB of *E. coli* with respect to its ability to bind to the RNA degradosome (Lehnik-Habrink *et al.*, 2010). Furthermore, it was demonstrated that the C-terminal domain of CshA confers the interaction specificity to the essential endoribonuclease RNase Y. CshA, as well as the RNA helicase CshB, are involved in the cold adaptation process of the cell (Hunger *et al.*, 2006). It was demonstrated that the deletion of one of the RNA helicases had no effect on growth whereas the loss of both helicases was lethal. Moreover both proteins localized around the nuclei, a pattern

reminiscent of that of ribosomes or cold-shock proteins (CSP). Further FRET analysis using CshB and the cold shock protein B (CspB) demonstrated interaction of the two proteins suggesting that the RNA helicase CshB is involved in the cold adaptation process of the cell (Hunger *et al.*, 2006). In a second report dealing with the RNA helicase CshA, it was demonstrated that the enzyme indeed possesses RNA unwinding activity (Ando & Nakamura, 2006). In contrast to the previous finding that a deletion of *cshA* has no effect on growth at lower temperatures, this publication demonstrated that deletion of *cshA* resulted in a growth defect at 22 °C, but not at higher temperatures (Ando & Nakamura, 2006). In support of this result, the deletion in the corresponding *cshA* homolog of *Bacillus cereus* was shown to have a severe growth defect at lower temperatures, too (Pandiani *et al.*, 2010). A further analysis of the CshA and CshB homologs of *B. cereus* revealed that the RNA helicases are also involved in the process of growth at a basic pH and oxidative conditions (Pandiani *et al.*, 2011).

Another RNA helicase of *B. subtilis* is DeaD/YxiN. This enzyme was extensively investigated with a focus on the molecular mechanisms of its catalytic function, whereas nothing is known about the physiological role of the protein, except that it has the ability to bind the 23S rRNA (Karow & Klostermeier, 2009; Kossen & Uhlenbeck, 1999; Theissen *et al.*, 2008). The role of the RNA helicase YfmL in the physiology of *B. subtilis* is completely unknown.

In this study we investigated the multiple roles CshA in the physiology of *B. subtilis*. We reveal that CshA is essential for the growth at low temperatures and mutant cells devoid of the RNA helicase exhibit an aberrant morphology at this temperature. Furthermore we show that CshA interacts with ribosomal proteins of the large subunit. Interestingly, the deletion of *cshA* leads to a changed ribosomal profile. Finally we elucidate the impact of the loss of *cshA* on the transcriptome by microarray analysis.

Results

Analysis of the growth behavior of a *cshA* deletion strain at lower temperatures

To get insight into the physiological role of CshA, a mutant strain (GP1083) was constructed by long flanking homology PCR. This strain devoid of *cshA* grew indistinguishable in comparison to the wild type under standard laboratory conditions (37°C, rich medium).

One of the main functions of DEAD-box RNA helicases is the binding and subsequent remodeling of secondary structures on RNA molecules by the utilization of ATP. The formation of these secondary structures is thermodynamically favored at lower temperatures. Therefore RNA helicases play an important role for the adaptation process to the cold (Phadtare & Severinov, 2010). To test whether CshA is involved in this process we compared growth of wild type with isogenic *cshA* mutant strains. As shown in Fig. 19 the wild type grew well at 20°C on LB-agar-plates. In contrast, no growth was visible for the *cshA* mutant after 24 h and 48 h at 20°C. To exclude the possibility that our mutation had any secondary effects on the genetic context of *cshA*, we also constructed a complemented *cshA* mutant strain (GP1084), harboring a second copy of *cshA* in the *lacA* locus. Expression of *cshA* in this ectopic site restored the growth in the $\Delta cshA$ background, demonstrating that only the loss of the *cshA* causes the cold sensitivity of mutant strain.

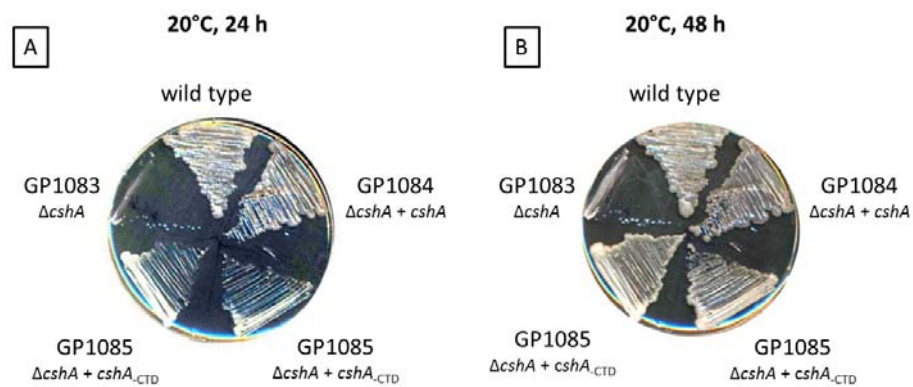


Fig. 19. Impact of CshA and its C-terminal domain on growth at low temperatures. *B. subtilis* wild type, a *cshA* mutant strain and two *cshA* mutant strains either complemented with full length *cshA* or a *cshA* variant devoid of the C-terminal domain were incubated at 20°C for 24 h (A) or 48 h (B) on LB-agar-plates supplemented with 2% xylose.

Impact of the C-terminal domain on the growth at low temperatures

CshA is a DEAD-box RNA helicase comprising three domains, two RecA-like domains forming the catalytic core of the protein and an additional C-terminal domain. This C-terminal part is important for direct protein-protein interactions and confers the interaction specificity to RNase Y (Lehnik-Habrink *et al.*, 2010). To investigate whether the C-terminal domain is essential for the growth at lower temperatures we constructed a strain in which the *cshA* deletion is complemented with a truncated variant of the protein devoid of the C-terminal domain.

As shown in Fig. 19, our growth experiments reveal that the C-terminal domain of CshA is not essential for the growth at lower temperatures. While the complemented strain harboring full length CshA (GP1084) behaves like the wild type, the C-terminal truncated mutant (GP1085) grows significantly slower. Nevertheless, after two days no difference between the strains is visible on the LB-agar-plates.

Consequences of a *cshA* deletion on the morphology of the cell

The deletion of the gene for the RNA helicase CshA resulted in a severe growth defect when cells were grown at lower temperatures. To investigate whether this growth defect is accompanied by altered morphology of the cells, the *cshA* mutant strain was grown at 18°C in LB medium and phase contrast microscopy was conducted.

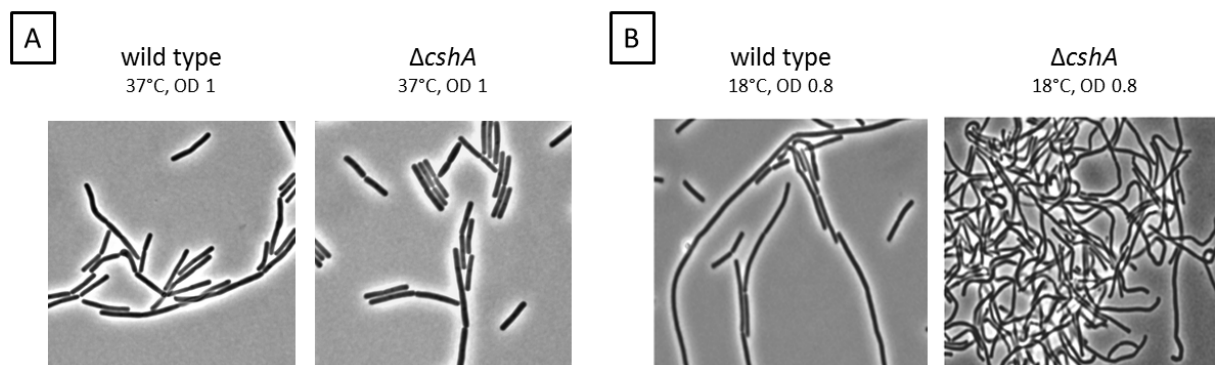


Fig 20. Influence of deletion of *cshA* on the cell morphology at lower temperature. *B. subtilis* wild type and the isogenic *cshA* mutant strain were grown in LB medium at 37°C and 18°C. At an optical density of about one the cells morphology was analyzed by phase contrast microscopy.

Analyzing the morphology of wild type and the *cshA* mutant cells at 37°C did not reveal any difference in the shape of the bacteria. In contrast, growing the cells at 18°C leads a drastically altered phenotype with wrinkled and elongated cells in the *cshA* mutant strain. Therefore the growth defect of the *cshA* mutant strain at lower temperature is accompanied by a significant change in the morphology of the cell. In contrast to the previous experiment (growth on LB-agar-plates at 20°C), the *cshA* mutant is able to grow at 18°C in liquid LB medium. This apparent contradiction of different growth behavior of RNA helicase mutants in liquid medium compared to solid medium was already observed in *E. coli* (Charollais *et al.*, 2004).

To investigate this aberrant morphology of the cells in more detail we further conducted electron microscopy. This analysis revealed that the long and wrinkled cells that were observed in the phase contrast microscopy represent chains of cells that are impaired in their ability to separate (see Fig. 21). In addition, the *cshA* mutant cells contained a remarkable thickened cell wall. Therefore the loss of *cshA* leads to a change in the morphology of the cells which is probably caused by an interference with the process of proper cell separation.

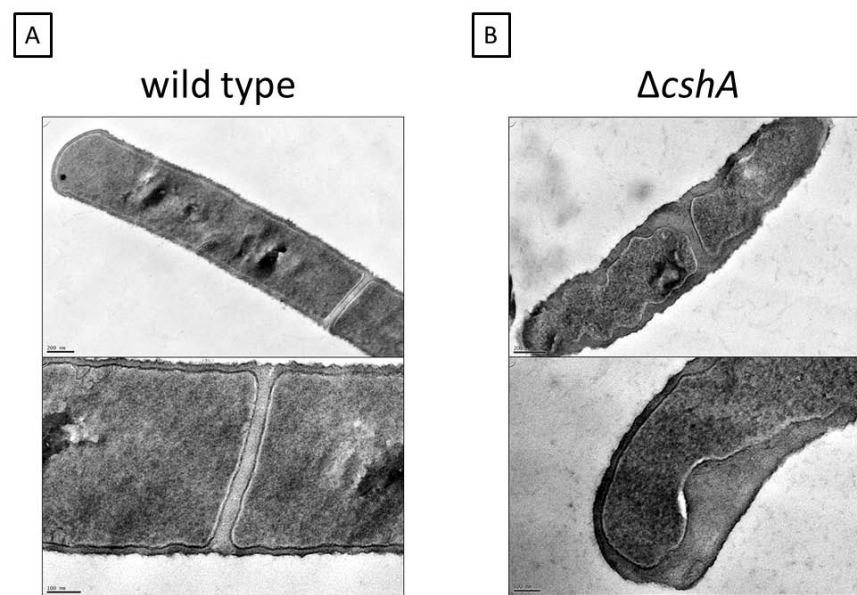


Fig 21. Detailed analysis of the loss of *cshA* on the morphology of *B. subtilis* cells. Transmission electron micrographs of *B. subtilis* wild type (A) and *cshA* mutant cells (B) were conducted. Both strains were cultivated in LB-medium at low temperatures.

Interaction of CshA with cold shock proteins (CSPs)

The experiments presented before demonstrated that *cshA* is essential for growth at lower temperatures. Previously it was shown that the RNA helicase CshB interacts with the cold shock protein B (CspB), suggesting that both proteins work in conjunction to rescue misfolded mRNA molecules and maintain proper initiation of translation at low temperatures in *B. subtilis* (Hunger *et al.*, 2006). To investigate whether such an interaction is unique to the RNA helicase CshB or also applies to CshA we performed bacterial two hybrid analysis. Therefore we cloned the genes of the cold shock proteins CspB, CspC and CspD into the plasmids of the two hybrid system and tested the resulting constructs for their interaction ability towards CshA.

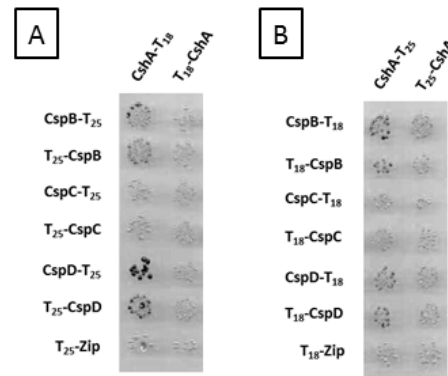


Fig 22. Analysis of interactions among the RNA helicases CshA and the cold shock proteins in *B. subtilis*.

All genes were cloned in the vectors of the bacterial two hybrid system. These plasmids allow the expression of the gene of interest fused to either the N- or C-terminus to the T18 or T25 domain of the *B. pertussis* adenylate cyclase. The *E. coli* transformants harboring both vectors were incubated for 48 h at 30°C. Degradation of Xgal indicates interaction due to the presence of a functional adenylate cyclase. (A) The gene encoding the RNA helicases CshA was present in the high copy vectors (pUT18 and pUT18C), whereas the genes encoding the three cold shock proteins CspB, CspC and CspD were present in the low-copy vectors (p25N and pKT25). (B) Genes coding for the cold shock proteins were present in the high copy vectors, whereas the *cshA* gene was present in the in low-copy vectors.

Our two-hybrid analysis revealed strong interaction between the cold shock protein CspD and the RNA helicase CshA. Even though slightly colored colonies were visible for CshA and CspB this interaction did not meet our stringency criteria. Therefore CshA is able to directly interact with the RNA chaperone CspD, suggesting a conjoint function of both enzymes to rescue misfolded mRNA in the cold.

Identification of interaction partners of CshA *in vivo*

In vitro, most RNA helicases exhibit only a low substrate specificity and catalytic activity. In contrast, *in vivo* these enzymes function very fast and specific. This contradiction is explained by the strong dependence of RNA helicases on interaction partners for full catalytic activity (Silverman *et al.*, 2003). Thus, the identification of proteins interacting with RNA helicases is of particular interest. In this study, we performed a pull down assay with CshA as a bait protein. To minimize secondary effects that can occur by overexpression from a plasmid strain GP1026 was constructed. This strain expressed a CshA variant that contained a Strep-tag at its C-terminal end in its original locus under the control of the natural promoter (Lehnik-Habrink *et al.*, 2010). To facilitate the identification of interaction partners we added formaldehyde prior to the

harvest of the cells (Herzberg *et al.*, 2007). The elution fraction of the CshA pull down was stained with silver nitrate and five bands were excised and analyzed by mass spectrometry.

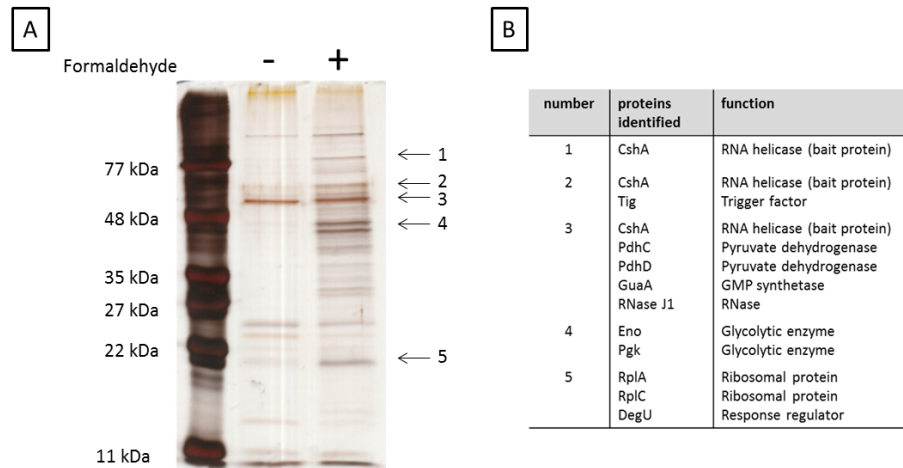


Fig. 23. Identification of interaction partners of the RNA helicase CshA. (A) The protein complex was isolated from the *B. subtilis* strain GP1026 encoding CshA-Strep. The strain was grown in minimal medium. 25 μ l of the elution fraction of the purification was loaded on a 12.5% SDS-PAGE gel. Gel bands were visualized by staining with silver nitrate. Array mark the gel bands analyzed by mass spectrometry. (B) Results of the mass spectrometric analysis.

As shown in Fig. 23, the amount of co-purified proteins increased upon the addition of formaldehyde. The identification of RNase J1 and enolase was anticipated and is in good agreement with the fact that CshA as well as RNase J1 and enolase are part of the RNA degradosome of *B. subtilis* (Lehnik-Habrink *et al.*, 2010). PdhC and PdhD are both subunits of the pyruvate dehydrogenase complex. Tig is a propyl isomerase, GuaA a GMP synthase and Pgk the glycolytic enzyme phosphoglycerate kinase. In the lower molecular range the two ribosomal proteins RplA and RplC were identified. Moreover, the response regulator DegU was found.

Verification of direct protein-protein interactions between CshA and ribosomal proteins RplA and RplC

The pull down experiment revealed a potential interaction of CshA with the ribosomal proteins RplA and RplC, both part of the large subunit of the ribosome. To

investigate whether these interactions are direct protein-protein interactions, bacterial two-hybrid analyses were conducted.

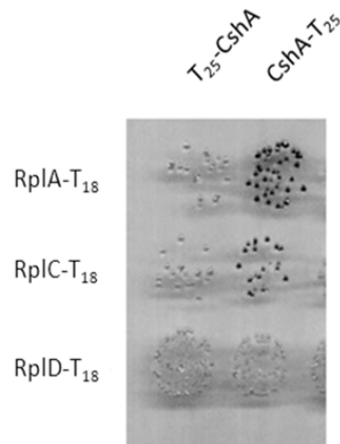


Fig. 24. Analysis of interactions among CshA and the ribosomal proteins RplA and RplC. The gene encoding CshA was cloned in the low-copy plasmid p25N and pKT25 and the genes encoding the ribosomal proteins RplA and RplC in the high-copy plasmids pUT18 and pUT18C. These plasmids allow the expression of the gene of interest fused to either the N- or C-terminus to the T18 or T25 domain of the *B. pertussis* adenylate cyclase. The *E. coli* transformants harboring both vectors were incubated for 48 h at 30°C. Degradation of Xgal indicates interaction due to the presence of a functional adenylate cyclase.

As shown in Fig. 24, CshA interacts with RplA and RplC. The RplD protein served as a negative control, as the protein was not identified in the pull down experiment before (Fig. 23B) and also no interaction in the two hybrid analysis was observed (Fig. 24). This experiment demonstrated that the interaction between CshA and RplA and RplC are direct.

Effect of *cshA* deletion on the ribosome biogenesis

Our previous experiment showed that CshA directly interacts with the ribosomal proteins RplA and RplC suggesting a particular role of the RNA helicase in the biogenesis of ribosomes. To elucidate whether this interaction has physiological relevance we compared the ribosome profiles of the wild type and cells lacking *cshA*. Therefore we grew the strains in LB medium at 20°C, lysed the cells and separated the ribosomal particles by sucrose gradient sedimentation under conditions preserving ribosome association.

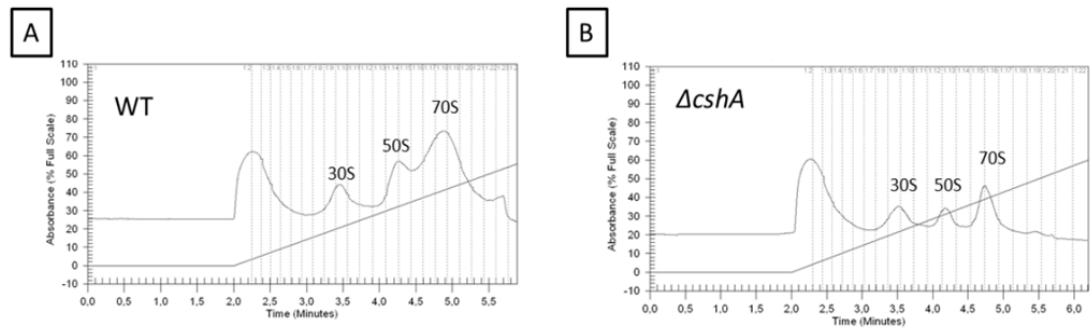


Fig. 25. Absence of *cshA* leads to a deficiency in the free 50S ribosomal subunits and a decrease of assembled ribosomes. The wild type (A) and the isogenic *cshA* mutant strain (B) were grown in LB medium at 20°C. Ribosomal profiles were analyzed as described in the material and methods section of this chapter. Peaks of the free 30S and 50S ribosomal subunits and 70S ribosomes are indicated.

As shown in Fig. 25 the main fraction of the ribosomal particles of the wild type form the assembled ribosome as illustrated by the large 70S peak in the spectrogram. Furthermore the signal for the large subunit (50S) is significantly stronger than for the small subunit (30S). In contrast to the wild type, the *cshA* mutant strain exhibited a considerably decreased proportion of fully assembled ribosomes and also reduced amounts of the large subunit (50S). The signal for the small 30S subunit is comparable to that of the wild type.

Together with the previous experiments we reveal that CshA is involved in the biogenesis of the ribosome, especially the large subunit. The binding of RplA and RplC (both proteins of the large subunit) probably helps the RNA helicase to find its target sites.

Consequences of the deletion of *cshA* on the transcriptome of *B. subtilis*

The degradation of mRNAs in *E. coli* and *B. subtilis* can be conducted by multi-enzyme complexes called RNA degradosome (Carpousis, 2007; Commichau *et al.*, 2009). In *B. subtilis* the RNA helicase CshA is part of this assembly suggesting a significant role in the mRNA turnover process (Lehnik-Habrink *et al.*, 2010). To get further insight into the function of CshA in mRNA decay of *B. subtilis*, microarray analyses were performed comparing the wild type and the isogenic *cshA* mutant strain in the exponential phase. To achieve the most reliable data both strains were cultivated at 37°C to avoid secondary effects due to different growth rates at lower temperatures.

Our microarray analysis revealed that over 200 mRNAs were changed in abundance under these conditions (see Table 3). In detail, we observed an increase of

steady-states levels for 118 mRNAs and a decrease of 103 mRNAs upon deletion of the *cshA* gene. Especially mRNAs encoding proteins involved in competence development were increased in abundance. The most strongly regulated target overall is the mRNA for the antiholing-like protein YsbA which is almost sixty times more abundant in the *cshA* mutant strain. mRNAs exhibiting decreased amounts in the *cshA* mutant strains are the *dhbACEBF* and *ykuNOP* operons which are both members of the Fur regulon. Furthermore mRNAs encoding proteins involved in the biosynthesis of arginine as well as the operon coding for proteins that are involved in the utilization of fructosamines are less abundant.

A complete list of the mRNAs affected by *cshA* deletion is listed in the supplemental material section of this chapter.

In the previous chapter we revealed CshA as the major RNA helicase of the RNA degradosome of *B. subtilis* (Lehnik-Habrink *et al.*, 2010). We demonstrated that CshA was the only RNA helicase that was able to interact with RNase Y, the major mRNA decay-initiating enzyme of *B. subtilis* (Lehnik-Habrink *et al.*, 2011b; Shahbadian *et al.*, 2009). As RNA helicases like CshA contain no inherent RNA cleaving activity changes in the abundance of mRNAs due to deletion of *cshA* has to be indirect. However, DEAD-box proteins are able to alter the stability of mRNAs by making the transcript more or less amenable for the degradation by RNases. In agreement with this idea we should observe a considerable overlap in the targets of CshA and RNase Y. Comparing both lists of altered transcripts we found that 78 mRNAs were affected by the deletion of *cshA* that were also changed in abundance due to the depletion of RNase Y. This is one-third of the total of the affected mRNAs by the *cshA* deletion (78 mRNAs out of the total of 220 mRNAs). About a half of the 78 overlapping mRNAs exhibited the same direction of change, whereas the other half was altered in the opposite direction (the overlapping targets are highlighted in gray in Table 3).

In conclusion, our microarray analysis revealed that deletion of *cshA* alters the abundance of more than 200 mRNAs. About third of these targets are also affected by RNase Y suggesting a conjoint function of both enzymes on the amounts of the transcripts.

Table 3. Effect of *cshA* deletion on the steady-state levels of mRNAs in *B. subtilis* in the exponential phase.

Transcription unit¹	Function²	Remarks	Fold regulation upon <i>cshA</i> deletion
<i>mRNAs with increased amounts upon deletion of cshA</i>			
<i>ysbA-ysbB</i>	Putative anti-holin		58
<i>ytnP</i>	NA		15
<i>yoaR-yozF</i>	NA		6
<i>yrrMNO-udk</i>	NA		4.8
<i>comEAB</i>	genetic competence	ComK regulon	4.8
<i>yvgK</i>	transporters		4.7
<i>narGHIJ</i>	respiration	Fnr regulon	4.5
<i>hxlR</i>	transcription factors		3.9
<i>comFABC-yvyF-flgM-yvyG-flgKL</i>	genetic competence, motility and chemotaxis	ComK regulon	3.7
<i>narK-fnr</i>	transporters	Fnr regulon	3.7
<i>yfmQ</i>	NA		3.6
<i>sigW-rsiW</i>	sigma factor and anti-sigma factor (cell envelope stress)	SigW regulon	3.6
<i>bioWAFDBI-ytbQ</i>	biosynthesis of cofactors		3.5
<i>nucA-nin</i>	genetic competence	ComK regulon	3.5
<i>bmrCD</i>	ABC transporters		3.1
<i>mmgABCDE-yqiQ</i>	sporulation proteins	CcpA regulon, SigE regulon	3.0
<i>spsABCDEF-spsGHIJKL</i>	sporulation proteins	SigK regulon	3
<i>spoVAABCDEFGF-lysA</i>	sporulation proteins	SigG regulon, SpoVT regulon	2.9
<i>ycnK</i>	trace metal homeostasis (Cu, Zn, Ni, Mn)	AbrB regulon	2.8
<i>ytgP</i>	cell wall synthesis		2.7
<i>yvyE-yvhJ</i>	NA	Spo0A regulon	2.7
<i>sacXY</i>	phosphotransferase systems	SacY regulon	2.7
<i>lmrAB</i>	drug-export protein	LmrA regulon	2.7

ywzB-ywmB	NA		2.7
comGABCDEFGF-yqzE	genetic competence	comK regulon	2.7
comC	genetic competence (processing protease)	ComK regulon	2.7
rnmV-ksgA	RNase		2.5
maf	cell division inhibitor in competent cells	ComK regulon	2.5
yhjE	NA	LexA regulon	2.5
<hr/> <i>mRNAs with decreased amounts upon deletion of cshA</i> <hr/>			
frlBONMD-frlR-yurJ	utilization of specific carbon sources	FrlR regulon	-50
cshA	DEAD-box RNA helicases	deleted in the strain	-20
ykuNOP	electron transport/ other	Fur regulon	-14
argCJBD-carAB-argF	biosynthesis of amino acids	AhrC regulon	-11
dhbACEBF	acquisition of iron	Fur regulon	-5.88
sdpRI	toxins, antitoxins and immunity against toxins	SdpR regulon	-5.88
yvcIJKL-crh-yvcN	DNA repair/ recombination/ based on similarity	CcpA regulon	-5.26
argGH	biosynthesis of amino acids	AhrC regulon	-4.8
yvgO	general stress proteins (controlled by SigB)	SigB regulon	-4.8
rocB	utilization of amino acids	AhrC regulon, RocR regulon,	-4.4
yusZ	NA		-4.2
ytzD	NA		-3.7
metIC	biosynthesis of amino acids	S-box	-3.6
ytxGHJ	general stress proteins	SigB regulon	-3.6
psdRSAB	ABC transporters	PsdR regulon	-3.5
gspA	general stress proteins	SigB regulon	-3.5
ypuE-ribDEAHT	biosynthesis of cofactors	FMN-box	-3.3

<i>gin</i>	sigma factors and their control	SigF regulon	-3.3
<i>opuBABCD</i>	ABC transporters		-3.3
<i>metE</i>	methionine synthase	S-box	-3.1
<i>ilvBHC-leuABCD</i>	biosynthesis of amino acids	T-box, TnrA regulon	-3.0
<i>ypzE</i>	NA		-3.0
<i>mtnU</i>	NA		-2.9
<i>yybF</i>	transporters		-2.9
<i>yufOPQ</i>	ABC transporters		-2.9
<i>sdpABC</i>	toxins, antitoxins and immunity against toxins	Rok regulon, Spo0A regulon	-2.9
<i>yaaC</i>	NA		-2.8
<i>ctsR-mcsAB-clpC-radA-disA</i>	transcription repressor	CtsR regulon, SigB regulon	-2.6
<i>yycD</i>	general stress proteins	SigB regulon	-2.6
<i>spo0M</i>	sporulation/ other		-2.6
<i>yoaB</i>	transporters/ other	S-box	-2.6

¹ Genes with factors ≥ 2.5 are shown in boldface.

² Functional information is based on the *SubtiWiki* database (Lammers *et al.*, 2010).

Northern blot analysis of the individual targets of CshA

Our microarray analysis revealed that deletion of *cshA* affected a large number of mRNAs in abundance. Therefore we conducted Northern blot analysis of to get more insight into the effect of CshA on certain transcripts.

The most strongly affected target of our microarray analysis was the *ysbA* transcript. As shown in the Northern blot presented in Fig. 26A, using an RNA probe directed against *ysbA*, we detected a signal of about 1.4 kb. Most likely *ysbA* is cotranscribed with its downstream gene *ysbB*. This bicistronic operon structure is also suggested by tiling array analysis (Rasmussen *et al.*, 2009). The bicistronic mRNA strongly accumulated upon the deletion of *cshA*, confirming our results of the microarray analysis.

The most affected target upon *cshA* deletion exhibiting reduced amount is the *frlB* gene. The gene for FrlB is suggested to be part of a large *frlBONMD* operon. Our Northern blot analysis revealed three distinct signals. One signal, in the range of 1.4 kb, most likely represents the monocistronic transcript of *frlB*. A second signal in the range of 2.5 kb

probably contains *frlB* and the downstream gene *frlO*. The last signal in the range of 7.5 kb supposedly contains the complete *frlBONMD* cluster, the downstream gene for the regulator of the operon *frlR* and *yurJ*. As revealed by our microarray analysis all three transcripts were less abundant in the *cshA* mutant strain compared to the wild type.

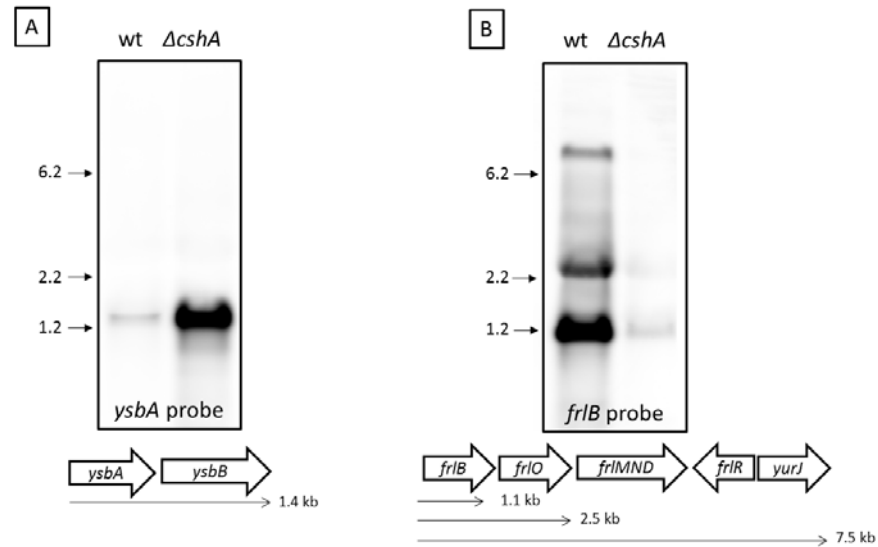


Fig. 26. Effects of the deletion of the RNA helicase *cshA* on the *ysbA* (A) and *frlB* (B) mRNAs. Total RNA was isolated from the wild type and the isogenic *cshA* deletion strain. RNA was prepared from cells grown in minimal medium supplemented with 0.5% glucose. 5 μ g of total RNA was loaded per lane. A schematic illustration of the operon structure is given below each Northern blot.

We further investigated the amounts of the mRNAs for *ytnP*, *dhbA*, and *argG*. In contrast to our microarray analysis we found that the abundance of *ytnP* and *dhbA* were not altered by the loss of *cshA*. Furthermore while the mRNA for *argG* is significantly decreased in the microarray analysis our Northern blot analysis revealed a considerable increase in the amount of the mRNA. The reasons for these conflicting results have to be further elucidated.

Discussion

Even though RNA helicases are extensively studied in eukaryotic organisms like yeast or the Gram negative bacterium *E. coli*, little is known about these proteins in *B. subtilis*. Here, we present evidence that the DEAD-box RNA helicase CshA has multiple roles in the physiology of *B. subtilis* (see Fig. 27).

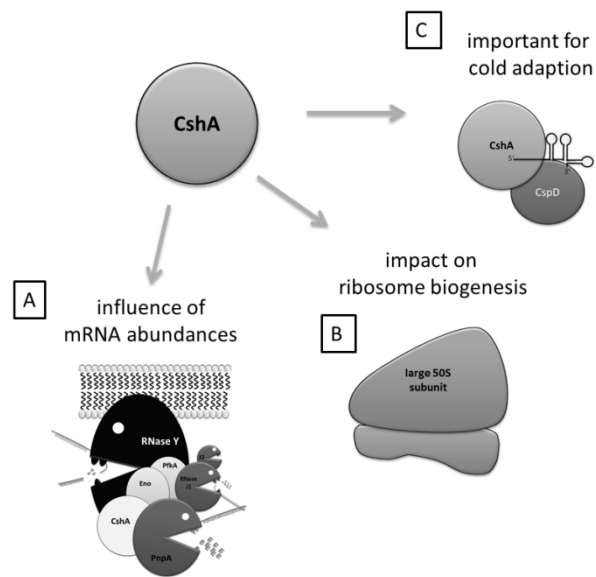


Fig 27. Illustration of the multiple role of CshA in *B. subtilis*.(A) CshA influences the amount of several transcripts. CshA is the major RNA helicase in the RNA degradosome of *B. subtilis*. Microarray analysis revealed that deletion of *cshA* altered the abundances of a large number of mRNAs. (B) CshA is important for the ribosome biogenesis. Pull down experiments and two hybrid analyses demonstrated that CshA interacts with the ribosomal proteins RplA and RplC. Analysis regarding the formation of ribosomes demonstrated an aberrant ribosomal profile in the *cshA* mutant strain. (C) CshA is important for the cells ability of growth at low temperatures. Loss of the RNA helicase *cshA* leads to a growth defect and altered cell morphology in the cold. Furthermore CshA is able to interact with the cold shock protein CspD, probably to rescue misfolded RNA especially formed at low temperatures.

To get functional insight into the physiological role of the RNA helicase CshA we constructed a mutant strain devoid of the helicase. While no difference in growth between the wild type and the *cshA* mutant was observed at 37°C, decreasing the temperature severely impaired the growth of the *cshA* mutant strain in the cold. We further demonstrate that the C-terminal domain of CshA is dispensable for the growth at low temperatures. Analysis of the morphology of the cells devoid of *cshA* in the cold revealed a remarkable change in the morphology of the cells. In detail experiments of these impaired cells demonstrated that the long chained cells had a severe separation deficiency.

The involvement of RNA helicases in the adaption process of bacteria to reduced temperatures is well known. This dependency is most likely based on the fact that the formations of secondary structures in RNA species are thermodynamically favored under these conditions. The deletion of the RNA helicases *csdA* and *srmB* in *E. coli* also results in impaired growth at lower temperatures. Furthermore deletion of *csdA* resulted in

aberrant cell shapes (Jones *et al.*, 1996). In analogy, the growth defect in the cold of our *B. subtilis* cells devoid of *cshA* was also accompanied by altered cell morphologies. The same properties of a *cshA* deletion were previously demonstrated for a Δ *cshA* mutant in *B. cereus* (Pandiani *et al.*, 2010). The formation of aberrant long chained cells as seen in all three organisms can be caused by different mechanisms, e.g. deficiency in cells separation or cell division. Our experiments indicate that not cell division but the loss of the ability to properly separate causes this altered morphology. This cell separation defect in the *cshA* mutant strain can result from an mRNA that is present in increased or decreased amounts which encodes a protein that is involved in the cell separation. Our microarray analysis together with Northern blots experiments revealed that *ysbA* and *ysbB* are strongly increased upon *cshA* deletion. Both genes are closely related to the *lrgAB* genes of *Staphylococcus aureus*. In *S. aureus* *lrgA* and *lrgB* encode holin- and antiholin-like proteins. The deletion of the genes significantly affects the murein hydrolase activity of cells (Groicher *et al.*, 2000). It is therefore possible that higher expression of the proteins due to the strongly increased abundance of the mRNA in the *cshA* mutant also affects the murein hydrolytic activity of *B. subtilis*. This in turn can cause the separation deficiency of the *cshA* mutant in the cold. We also noted that our finding that the deletion of *cshA* results in a growth defect and an alter cell morphology in the cold is in contradiction with one report from *B. subtilis* demonstrating that the knockout of *cshA* in *B. subtilis* did have any effect on growth or cell shape (Hunger *et al.*, 2006).

RNA helicases are highly dependent on the presence of an interaction partner for their proper function in the cell (Silverman *et al.*, 2003). Therefore the identification of partner proteins is insightful. Using pull-down experiments with CshA proteins as bait we were able to identify several interaction partners. The interaction of CshA with RNase J1 and the glycolytic enzyme enolase was expected as CshA is part of the RNA degradosome of *B. subtilis* (Lehnik-Habrink *et al.*, 2010). However, we failed to identify RNase Y, another protein of the RNA degradosome, in this experiment. This could be explained by the fact, that we did not analyze all bands present in the SDS-PAGE. Therefore it is quite likely that RNase Y was present in the CshA elution fraction, but we failed to excise the corresponding band containing RNase Y.

An interesting finding of this experiment was the identification of the ribosomal proteins RplA and RplC as interaction partners. Both proteins are part of the large subunit of the ribosome. This interaction was also verified by two hybrid analysis suggesting that the protein-protein interaction is direct. To elucidate the physiological relevance, we compared the ribosomal profiles of wild type and *cshA* mutant cells. Our analysis revealed

that the *cshA* mutant is impaired in the formation of the large 50S subunit and probably in turn of the completely assembled ribosome. The involvement of DEAD-box RNA helicases in the biogenesis of ribosomes is well established. For example, deletion of the RNA helicase *csdA* and *smrB* in *E. coli* leads to a mis-assembled 50 S subunit (Charollais *et al.*, 2003; Charollais *et al.*, 2004). In case of SrmB, the RNA helicase is able to contact its target, the large subunit of the ribosome, by interacting with the protein L4 and L24 (Trubetskoj *et al.*, 2009).

Furthermore, the identification of proteins of the pyruvate dehydrogenase complex (PdhC/D) and the trigger factor (Tig) is intriguing. Both proteins are suggested to be part of the cold-shock response of *E. coli* (Jones & Inouye, 1994; Kandror & Goldberg, 1997; Phadtare & Severinov, 2010). Herein, we demonstrated that growth at lower temperatures strongly dependent on the presence of CshA, the bait protein of the pull-down. However, it is currently not clear, whether and to what extent the interactions of these three proteins (CshA, Tig and PdhC/D) influences the ability of the cell to cope with decreased temperatures. In addition using the bacterial two hybrid system we revealed interactions between the cold shock proteins CspD and the RNA helicases CshA. This interaction is probably in analogy to the previously reported interaction of CshB and CspB (Hunger *et al.*, 2006). These interactions between RNA helicases and cold shock proteins are thought to be beneficial for the cell as the two enzymes probably work in conjunction to rescue misfolded mRNA molecules.

The RNA helicase CshA is part of the RNA degradosome in *B. subtilis*. To define the role of CshA in the mRNA turnover of *B. subtilis* we performed microarray analysis. A total over 200 mRNAs were affected in abundance by deleting *cshA* suggesting a significant impact of the RNA helicase in mRNA decay. It is assumed that RNA helicases assist the RNases that are present in the complex to degrade the mRNAs by unwinding secondary structures. These secondary structures are thought to impede the activity of the cleaving enzymes. Most likely the 100 mRNAs that are increased in abundance are good candidates for this kind of regulation. In contrast the deletion of *cshA* also had a negative effect on almost 100 mRNAs. In this case the *cshA* deletion affects mRNA abundances more indirectly possibly by altering the turnover of the transcripts encoding a transcriptional regulator. This could be true for the numerous of *arg* genes (encoding proteins involved in the biosynthesis of arginine) that are negatively regulated. Here the mRNA of the regulator AhrC is present in fewer amounts in the cell. As the protein represses the genes for the arginine biosynthesis its decrease should result in the upregulation of the *arg* operon (Miller *et al.*, 1997). In contrast, mRNA encoding genes involved in the synthesis of the

amino acid are also downregulated. This result suggests a second effect of *cshA* deletion on the *arg* operon. Due to the technical limitation of the method small non coding RNAs escaped our microarray analysis. Therefore it is possible that some of the effects are mediated by these kinds of species. The regulation of small non-coding RNAs by RNA helicases was already shown for the RNA helicase CsdA of *E. coli* where the enzyme is involved in the activation of the alternative sigma factor RpoS at low temperatures. Here, CsdA is needed to unfold the small RNA DsrA which can bind to the *rpoS* mRNA and subsequently enables its translation. Therefore deletion of the *csdA* represses the activation of *rpoS* at low temperatures (Resch *et al.*, 2010). Effects of RNA helicase deletion on the regulation by small non coding RNAs is probably an explanation for the number of mRNAs with decreased mRNA amounts. This is perhaps also true for the *arg* operon regulation as SR1, a small non-coding RNA also was shown to influence the *ahrC* mRNA (Heidrich *et al.*, 2006). In total, microarray analysis demonstrates that CshA is involved in the mRNA decay of a large number of targets. The nature of the impact (stabilization, effects due to small RNA regulation) remains to be elucidated.

CshA as an RNA helicase did not contain hydrolytic activity of mRNA molecules. Nevertheless the enzyme can render the structure of mRNA making them more or less accessible for cleaving ribonucleases. The comparison of the results of the microarray analyses of the *cshA* deletion and with the one of the RNase Y depletion revealed that about one third of the transcripts overlap between both enzymes. This considerable overlap suggests a conjoint function of both enzymes on the adjustment of amount of several mRNAs in the cell. The detailed analysis of this teamplay between CshA and other RNase (especially RNase Y) will be an interesting task for future investigations.

In conclusion, we demonstrate that the RNA helicase CshA is important for the growth of *B. subtilis* cells at low temperatures. Furthermore we demonstrated that CshA is involvement in biogenesis of ribosomes and loss of the enzyme influences the amount of over 200 mRNAs. All these finding suggests that CshA has multiple roles in the physiology of *B. subtilis*.

Acknowledgments

We wish to thank Tiziana Guerra for her help with some experiments.

Experimental procedures

Growth conditions - *B. subtilis* was grown in LB medium and in CSE minimal medium containing succinate and glutamate/ ammonium as basic sources of carbon and nitrogen, respectively (Wacker *et al.*, 2003). The medium was supplemented with auxotrophic requirements (at 50 mg/l) and glucose as indicated. Plates were prepared by the addition of 17 g Bacto agar/l (Difco) to the liquid medium. For the growth experiments at different temperatures, *B. subtilis* wild type and mutant strains were streaked on LB-agar-plates and incubated overnight at 42°C to ensure comparable conditions at the starting point of the experiment. The next day, the fresh cells were streaked again on LB-agar-plates and incubated at the indicated temperature.

Long flanking homology PCR (LFH-PCR) - *B. subtilis* strain GP1083 carrying single deletions of $\Delta cshA$ was obtained by applying the long flanking homology PCR (LFH-PCR) technique (Wach, 1996). For the construction of the $\Delta cshA$ mutant, an *aphA3* resistance cassette was amplified from plasmid pDG780 (Guerout-Fleury *et al.*, 1995). DNA fragments of about 1,000 bp flanking the *cshA* region at their 5' and 3' end was amplified, too. Chromosomal DNA of *B. subtilis* 168 served as the template. The 3' end of the upstream fragment as well as the 5' end of the downstream fragments extended into the respective gene region, in a way that all expression signals of genes up- and downstream remained intact. The joining of the two fragments to the resistance cassette was performed in a second PCR. The PCR product was directly used to transform *B. subtilis* 168. The integrity of the regions flanking the integrated resistance cassettes was verified by sequencing.

Pull-down analysis - The isolation of CshA interaction partners from *B. subtilis* strain GP1026 was performed by the SPINE technology (Herzberg *et al.*, 2007; Lehnik-Habrink *et al.*, 2010). Briefly, 1 l of culture in CSE minimal medium supplemented with 0.5 % glucose was grown at 37°C until OD₆₀₀ 1.0 and divided. One half was harvested immediately, and the other was treated with formaldehyde (0.6 % w/v, 20 min) for 20 min to facilitate cross-linking (Herzberg *et al.*, 2007) and harvested, too. After lysis of the cells by French press, the crude extracts were centrifuged at 100.000 × g for 1 h. For the purification of the Strep-tagged proteins, the resulting supernatants were passed over a Strep-tactin column (IBA, Göttingen, Germany) (0.5 ml bed volume). The recombinant proteins were eluted with desthiobiotin (IBA, final concentration 2.5 mM). Aliquots of the elution fractions were subjected to SDS-PAGE. Prior to electrophoresis, the protein

samples were boiled for 30 min in Laemmli buffer to reverse the cross-links. The protein gels were stained with silver nitrate (Blum *et al.*, 1987).

Bacterial-two hybrid assay - To reveal direct protein-protein interactions, the bacterial two-hybrid system was used (Claessen *et al.*, 2008; Karimova *et al.*, 1998). For construction of the plasmids harboring the genes of interest, the PCR products were digested with KpnI and XbaI and cloned into the vectors pUT18, pUT18C, p25N and pKT25 of the two-hybrid system that had been linearized with the same enzymes. The primers and plasmids are listed in the supporting material of this chapter.

Complementation analysis - To elucidate the impact of the C-terminal domain of CshA to the growth at lower temperatures a mutant strain devoid of the *csHA* was complemented with the full length protein and a C-terminal truncation. To construct this strain the *csHA* was amplified using primers HP3 + ML255 (full length *csHA*) and HP3 + ML256 (*csHA* without the C-terminal domain). The PCR product was digested with XbaI and KpnI. The digested PCR fragments were subsequently ligated into plasmid pGP888 that was digested with the same restriction enzymes (Diethmaier *et al.*, 2011). The resulting plasmids were transformed after linearization with SacI into strain GP1083 ($\Delta csHA::cat$). All strains, plasmids and primer sequences are listed in supplemental part of this chapter.

Preparation of Ribosome profiles - Relative amounts of 30S, 50S and 70S Ribosomes were investigated by sucrose density centrifugation of cell extract. *B. subtilis* cells were grown to an OD₆₀₀ of 0.4 to 0.6 in 75 ml of LB medium at 20°C. 100 µg/ml chloramphenicol was added to the culture five minutes prior to harvesting to avoid ribosome run off. Cells were pelleted by centrifugation and washed in a minimum of 30 ml magnesium washing puffer (10mM Tris-HCl, 10 mM MgCl₂, 60 mM KCl). Pelleted cells were stored at -20°C until further use or directly resuspended in 1.3 ml lysis buffer (10 mM Tris-HCl pH 7.5, 60 mM KCl, 20 mM MgCl₂, 0.5% Sodium Deoxycholate, 0.5% Tween 20, 1 mM DTT, 10 U/ml DNase I). The sodium deoxycholate contained in this puffer is prone to precipitate. It should be the last component added to the buffer and all other components should be properly mixed. Cells were lysed using a french press. Extracts were clarified by centrifugation at 18.000 × g for 15 min. The RNA concentration was measured at 260 nm using the Nanodrop. 12.5 A₂₆₀ units were applied to a pre-cooled linear sucrose gradient of 10% to 40% sucrose (10 mM Tris-HCl buffer pH 7.5 with 15 mM MgCl₂, 50 mM NH₄Cl and 1 mM DTT). These gradients were prepared by applying a 10% and a 40% sucrose solution to the ISCO640 gradient fractionator. Loaded gradients were centrifuged for 16 hours and 15 minutes at 22.000 rpm at 4°C using a TH-641 rotor.

Absorbance of the sucrose gradients was continuously monitored at 254 nm with the ISCO640 gradient fractionator.

Northern blot analysis - Preparation of total RNA and Northern blot analysis were carried out as described previously (Ludwig *et al.*, 2001). Digoxigenin (DIG) RNA probes were obtained by *in vitro* transcription with T7 RNA polymerase (Roche Diagnostics) using PCR-generated DNA fragments as templates. The primer pairs used to amplify DNA fragments specific for *ysbA* and *frlB* are listed in the supplementary section of this chapter. The reverse primers contained a T7 RNA polymerase recognition sequence. *In vitro* RNA labelling, hybridization and signal detection were carried out according to the instructions of the manufacturer (DIG RNA labelling kit and detection chemicals; Roche Diagnostics). The sizes of the transcripts were estimated based on the transcripts of the *gapA* operon. On each gel, a RNA sample from a culture grown in CSE minimal medium containing glucose was separated and analysed with a probe specific for *gapA*.

List of mRNAs that are affected in abundance by the deletion of *cshA* in **exponential phase**

mRNA with increased abundance			mRNA with decreased abundance		
gene	ratio	function	gene	ratio	function
<i>comGABCDEFGG-</i>					
<i>yqzE</i>	2.44	genetic competence	<i>ahrC-recN</i>	-2.44	biosynthesis/ acquisition of amino acids
<i>radC</i>	2.43	DNA repair/ recombination	<i>wapA-yxxG</i>	-2.44	cell wall/ other
<i>ctaO</i>	2.39	biosynthesis of cofactors	<i>ydhB</i>	-2.44	NA
<i>bmrC</i>	2.39	ABC transporters	<i>dhaS</i>	-2.44	NA
<i>ywpH-glcR</i>	2.35	transcription factors and their control	<i>yufN</i>	-2.44	NA
<i>yusQ</i>	2.28	NA	<i>metIC</i>	-2.38	biosynthesis/ acquisition of amino acids
<i>yhdW</i>	2.26	utilization of lipids	<i>aroA</i>	-2.27	biosynthesis/ acquisition of amino acids
<i>yukC</i>	2.24	NA	<i>yydD</i>	-2.27	NA
<i>ybdK</i>	2.23	protein modification	<i>yxzC</i>	-2.27	NA
<i>ybxA</i>	2.22	ABC transporters	<i>yxiG</i>	-2.27	NA
<i>cotSA-cotS-ytxO</i>	2.2	sporulation proteins	<i>mtnKA</i>	-2.22	biosynthesis/ acquisition of amino acids
<i>codV-clpQY-</i>			<i>yxbBA-yxnB-</i>		
<i>codY</i>	2.18	DNA condensation/ segregation	<i>asnH-yxaM</i>	-2.22	NA
<i>ftsW-pycA</i>	2.15	cell division	<i>glnRA</i>	-2.17	biosynthesis/ acquisition of amino acids

yraJ	2.13	NA	serA	-2.17	biosynthesis/ acquisition of amino acids
yckB	2.12	ABC transporters	skfABCEFGH	-2.17	toxins, antitoxins and immunity against toxins
bkdR	2.09	utilization of amino acids	wprA	-2.13	cell wall/ other
recU-ponA	2.08	DNA repair/ recombination	ytpl	-2.13	NA
ywfA	2.08	resistance against toxins/ antibiotics/ based on similarity	yfmH	-2.13	NA
resABCDE	2.08	respiration	yusI	-2.13	resistance against toxic metals/ based on similarity
queC	2.08	translation	yclM	-2.08	biosynthesis/ acquisition of amino acids
ssbB	2.07	DNA replication	ybaR	-2.08	NA
yqgS	2.06	cell wall synthesis	thrZ-ywhA	-2.08	transcription factors and their control
ydzA	2.06	NA	yfmG	-2.04	NA
cotD	2.06	sporulation proteins	yycCB	-2.04	NA
yllB-mraW-ftsL-pbpB	2.04	cell division	cysHP-sat-cysC-ylnDEF	-2.04	sulfur metabolism
coiA	2	genetic competence	safa-coxA	-2.04	sporulation proteins
ytpA	1.99	cell envelope stress proteins (controlled by SigM, W, X, Y)	trpS	-2.00	translation

		cell envelope stress proteins (controlled by			
<i>pssA-ybfM-psd</i>	1.99	SigM, W, X, Y)	<i>appDFABC</i>	-2.00	ABC transporters
<i>cdd-era</i>	1.97	translation	<i>yoaC</i>	-2.00	NA
<i>yhdV</i>	1.92	NA	<i>yfhB</i>	-2.00	NA
<i>ylbN</i>	1.9	NA	<i>gabP</i>	-2.00	transporters/ other
<i>nrdIEF-ymaB</i>	1.89	biosynthesis/ acquisition of nucleotides	<i>yxbCD</i>	-1.96	NA
<i>usd-spolIID-mbl-</i>					
<i>flhOP</i>	1.89	cell shape	<i>yitJ</i>	-1.96	NA
<i>ytsJ</i>	1.89	utilization of specific carbon sources	<i>serC</i>	-1.92	biosynthesis/ acquisition of amino acids
<i>rapA-phrA</i>	1.88	protein modification	<i>yuiA</i>	-1.92	NA
<i>yorH</i>	1.87	SP-beta prophage	<i>sat</i>	-1.92	sulfur metabolism
		cell envelope stress proteins (controlled by			
<i>yqeZ-yqfA-yqfB</i>	1.86	SigM, W, X, Y)	<i>pheST</i>	-1.85	translation
			<i>ytmIJKLMNO-</i>		
<i>ycnJ</i>	1.84	transporters/ other	<i>ytnIJ-ribR-ytnLM</i>	-1.85	NA
<i>thiUVWX</i>	1.82	ABC transporters	<i>ldh-lctP</i>	-1.85	transporters/ other
<i>yerB</i>	1.77	NA	<i>nadBCA</i>	-1.82	biosynthesis of cofactors
<i>sboAX-</i>					
<i>albABCDEFG</i>	1.76	miscellaneous metabolic pathways	<i>hisZGDBHAFI</i>	-1.79	biosynthesis/ acquisition of amino acids

<i>cdsA</i>	1.76	biosynthesis of lipids	<i>trpP</i>	-1.69	transporters/ other
<i>recO</i>	1.76	DNA repair/ recombination	<i>besA</i>	-1.67	acquisition of iron
<i>ydgD</i>	1.76	NA			
<i>sunA</i>	1.75	miscellaneous metabolic pathways			
		electron transport/ other/ based on			
<i>yojN</i>	1.71	similarity			
<i>ypuGHI</i>	1.69	translation			
<i>citZ-icd-mdh</i>	1.69	carbon core metabolism			
<i>ispC</i>	1.65	biosynthesis of lipids			
<i>sunT-bdbA-yolJ- bdbB</i>	1.64	ABC transporters			
<i>ylxM-ffh</i>	1.64	NA			
<i>gapB-speD</i>	1.59	carbon core metabolism			
<i>ctaA</i>	1.45	biosynthesis of cofactors			

Supporting material**Plasmids used in this study.**

Plasmid	Relevant characteristics	Primers	References
<i>Plasmids for bacterial two-hybrid analysis</i>			
pKT25	<i>P_{lac}-cyaA-mcs kan</i>		Karimova <i>et al.</i> , 1998
p25N	<i>P_{lac}-mcs-cyaA kan</i>		Claessen <i>et al.</i> , 2008
pGP1601	pUT18- <i>cshA</i>		Lehnik-Habrink <i>et al.</i> , 2010
pGP1336	p25N- <i>rplA</i>	ML165+ML18	This study
pGP1337	pKT25- <i>rplA</i>	ML165+ML18	This study
pGP1340	p25N- <i>rplC</i>	ML169+ML29	This study
pGP1341	pKT25- <i>rplC</i>	ML169+ML29	This study
pGP1397	p25N- <i>rplD</i>	ML167+ML19	This study
pGP1398	pKT25- <i>rplD</i>	ML167+ML19	This study
<i>Plasmid for bacterial two-hybrid analysis: the cold shock proteins CspB, CspC and CspD</i>			
pGP1874	pUT18- <i>cspB</i>	ML229+ML230	This study
pGP1875	pUT18- <i>cspB</i>	ML229+ML230	This study
pGP1876	p25N- <i>cspB</i>	ML229+ML230	This study
pGP1877	pKT25- <i>cspB</i>	ML229+ML230	This study
pGP1878	pUT18- <i>cspC</i>	ML231+ML232	This study
pGP1879	pUT18- <i>cspC</i>	ML231+ML232	This study
pGP1880	p25N- <i>cspC</i>	ML231+ML232	This study
pGP1881	pKT25- <i>cspC</i>	ML231+ML232	This study
pGP1882	pUT18- <i>cspD</i>	ML233+ML234	This study
pGP1883	pUT18- <i>cspD</i>	ML233+ML234	This study
pGP1884	p25N- <i>cspD</i>	ML233+ML234	This study
pGP1885	pKT25- <i>cspD</i>	ML233+ML234	This study
<i>Plasmids for complementation analysis</i>			
pGP888			Diethmaier <i>et al.</i> 2011
pGP1886	<i>lacA Pxl-cshA</i>	HP3+ML255	This study
pGP1887	<i>lacA Pxl-cshA_{-CTD}</i>	HP3+ML256	This study

Primers used in this study.

Primer	Sequence	Restriction sites
<i>Bacterial two-hybrid experiments</i>		
ML18	5'- TTTGGTACCCGTTTTACGTTAAAAGTTGAAGAGTCTACTTTGA C	KpnI
ML19	5'- TTTGGTACCCGTGCAAGCACCTCCTCTACTTTTTTC	KpnI
ML29	5'- TTTGGTACCCGTTTAGATTTAACAGCACTTTTAACAGTGATTA AAG	KpnI
ML165	5'- AAATCTAGAGATGGCTAAAAAAGGTAAAAAGTACGTTG	XbaI
ML167	5'- AAATCTAGAGATGCCAAAAGTAGCATTATACAACCAAAACG	XbaI
ML169	5'- AAATCTAGAGATGACCAAAGGAATCTTAGGAAGAAAAATTGG	XbaI
<i>Construction of the cshA deletion strain</i>		
ML129	5'- CCTATCACCTCAAATGGTTCGCTGCTCCTTCTAATTGCTGTTTC AGTAAT	
ML130	5'- ATGCATACAGCTGCCAGAC	
ML131	5'- CGAGCGCTACGAGGAATTTGTATCGCCTATGACAAAAAGCGT TCAAACG	
ML132	5'- CGTATTCATTGTTTGAATCCGATCAA	
<i>Complementation analysis</i>		
HP3	5'- AAATCTAGAGGTGGTAAATCACGACATTACTGAAACAGCAATT AG	XbaI
ML255	5'- TTTGGTACCCGTTATTAGTAAGATTTTTTCTGGCGTCTGTCCAC CTG	KpnI
ML256	5'- AAAGGTACCCGTTATTAAGTAACCTGTTGCTGACCTTCTAACG CTT	KpnI
<i>Northern blot analysis</i>		
<i>ysbA probe</i>		
LR1	5'- GAGTGCTAAAAAAGTGTACGGGTTTTTAACAC	
LR2	5'- CTAATACGACTCACTATAGGGAGAATGGTGAACGAGTTCGTTA TTGTTCTGC	
<i>frlB probe</i>		
LR11	5'-GGCCACAGCAAAAAGTAAATCGTGAGG	
LR12	5'- CTAATACGACTCACTATAGGGAGATCTCCTCTGCCAGCTCGTC TGC	

Strains constructed in this study.

Construction of *cshA* mutant with listed with used oligos.

Strain	Genotype	Construction	Oligos
GP1083	<i>trpC2 ΔcshA::cat</i>	LFH →168	ML129/ML130 + ML131/ML132

Further mutant strains used in this study.

Strain	Genotype	Construction
<i>Construction of cshA complementation strains</i>		
GP1084	<i>trpC2 ΔcshA::cat lacA::cshA aphA3</i>	pGP1886 → GP1083
GP1085	<i>trpC2 ΔcshA::cat lacA::cshA-CTD aphA3</i>	pGP1887 → GP1083
<i>Construction of the cshA-Strep strain for pull down experiments</i>		
GP1026	<i>trpC2 cshA-Strep spc</i>	Lehnik-Habrink <i>et al.</i> 2010

5. Characterization of RNase Y in *Bacillus subtilis*

The results described in this chapter were published in:

Lehnik-Habrink, M., Newman, J., Rothe, F. M., Solovyova, A. S., Rodrigues, C., Herzberg, C., Commichau, F. M., Lewis, R. J. & Stülke, J. (2011). RNase Y in *Bacillus subtilis*: a natively disordered protein that is the functional equivalent to RNase E from *Escherichia coli*. *J Bacteriol* **193**, 5431-5441.

Author's contribution:

The experiments were designed and interpreted by MLH, FMC, JN, RL and JS. The *in silico* analysis of RNase Y was performed by MLH, JN and RL. MLH, together with CH and FR performed the experiments concerning the complementation analysis of RNase Y truncations and the contributions of the domains to intra- and intermolecular interactions. The *in vivo* pulls down experiments were done by MLH and CH. The analysis of the transmembrane domain was done by MLH and CH, too. JN and RL made the biochemical experiments concerning the disordered structure of RNase Y. The paper was written by MLH, JN, RL and JS.

Abstract

The control of mRNA stability is an important component of regulation in bacteria. Processing and degradation of mRNAs are initiated by an endonucleolytic attack, and the cleavage products are processively degraded by exoribonucleases. In many bacteria, these RNases, as well as RNA helicases and other proteins are organized in a protein complex called the RNA degradosome. In *Escherichia coli*, the RNA degradosome is assembled around the essential endoribonuclease E. In *Bacillus subtilis*, the recently discovered essential endoribonuclease RNase Y is involved in the initiation of RNA degradation. Moreover, RNase Y interacts with other RNases, with the RNA helicase CshA and the glycolytic enzymes enolase and phosphofructokinase in a degradosome-like complex. In this work, we have studied the domain organization of RNase Y, and the contribution of the domains for protein-protein interactions. We provide evidence for the physical interaction between RNase Y with the degradosome partners *in vivo*. We present experimental and bioinformatic data which indicate the RNase Y contains significant regions of intrinsic disorder and discuss the possible functional implications of this finding. The localization of RNase Y in the membrane is essential both for the viability of *B. subtilis* as well as for all interactions that involve RNase Y. The results presented in this study provide novel evidence for the idea that RNase Y is the functional equivalent of RNase E even though the two enzymes do not share any sequence similarity.

Introduction

Messenger RNAs transmit the genetic information from DNA to proteins. In contrast to the high stability of transfer RNA and ribosomal RNA, bacterial mRNAs are readily degraded. This crucial feature ensures the ability of bacteria to respond quickly to changing environmental conditions by adding an extra layer of control in addition to the regulation of transcription and enzymatic activities of proteins (Arraiano *et al.*, 2010). Moreover, mRNA processing allows the adjustment of different expression levels for genes encoded in one operon, as observed for the *ilv* operon and the glycolytic *gapA* operon of the Gram-positive soil bacterium *Bacillus subtilis* (Homuth *et al.*, 1999; Ludwig *et al.*, 2001; Meinken *et al.*, 2003).

The enzymes that process and degrade RNAs are called ribonucleases. In the two model organisms *Escherichia coli* and *B. subtilis* a set of about twenty ribonucleases have been described thus far, but only a small fraction of these are common to both bacteria (Condon, 2003). Some of these RNases are necessary for the maturation of one specific

target (e.g. RNase M5 or RNase-Mini III in *B. subtilis*), whereas others (e.g. RNase J1 or RNase Y in *B. subtilis*) are more promiscuous and have a more global impact on RNA metabolism (Condon, 2003; Mäder *et al.*, 2008; Shahbadian *et al.*, 2009). The individual RNases differ not only in their respective amino acid sequences and in their number of substrates, but also in their enzymatic mode of action. Two different classes of RNases can be defined: exoribonucleases, which remove RNA nucleotides one at a time from either the 3'- or the 5'-end, and endoribonucleases, which cleave within the RNA molecule. For the degradation of mRNAs, the concerted action of both enzyme classes is necessary as 5'-ends are protected by their native triphosphates whereas decay from the 3'-end is often impeded by RNA secondary structural elements (e.g. transcriptional terminators) (Celesnik *et al.*, 2007). For instance, in *E. coli* the endoribonuclease RNase E acts processively on the mRNA transcript producing smaller fragments that are subsequently cleaved by exoribonucleases like polynucleotide phosphorylase (PNPase) or RNase II (Kushner, 2002). The key step in this process is the initial endonucleolytic cleavage by RNase E, perhaps explaining the essential nature of this enzyme for *E. coli*.

RNase E is a large protein of 1061 amino acids comprising two distinct functional domains. The N-terminal half (residues 1-530) comprises the catalytic core. This part of the protein is structured and well conserved amongst different prokaryotes. The structure of the catalytic domain is already known (Callaghan *et al.*, 2005). By contrast, the C-terminal half of RNase E has little intrinsic order, rendering its structure solution impossible. The unstructured part of RNase E is very important for function as it serves as an organizing centre for the binding of the exoribonuclease PNPase, the DEAD-box RNA helicase RhlB and the glycolytic enzyme enolase (Carpousis, 2007). Together these four proteins form a protein complex called the RNA degradosome, a molecular machine devoted to RNA degradation. The importance of processing and degradation of RNA by protein complexes is underlined by the fact that degradosome-like complexes are found in bacteria and also in archaea and eukaryotes, where they are called exosomes (Carpousis, 2007; Evguenieva-Hackenberg *et al.*, 2011).

An RNA degradosome was found only recently in *B. subtilis*, and it consists of the novel essential endoribonuclease RNase Y, the essential endo/exoribonuclease RNase J1 and its non-essential paralog RNase J2, the polynucleotide phosphorylase PNPase, the DEAD-box RNA helicase CshA and the two glycolytic enzymes enolase and phosphofructokinase (Commichau *et al.*, 2009; Lechnik-Habrink *et al.*, 2010). The relevance of a degradosome in *B. subtilis* is also supported by the fact that RNase Y, RNase J1 and PNPase are all involved in the turnover of identical targets such as the *rpsO* mRNA or the

yitJ riboswitch (Shahbadian *et al.*, 2009; Yao & Bechhofer, 2010). The discovery of an RNA degradosome in *B. subtilis* was somewhat surprising, as the genomes of Gram positive bacteria do not encode for homologues of RNase E. However, the newly identified RNase Y in *B. subtilis* appears to be the functional counterpart of RNase E in *E. coli*, even though the two RNases do not share any sequence similarity. The functional similarity between the two enzymes is intriguing: both enzymes are essential endoribonucleases preferring 5'-monophosphorylated substrates (Celesnik *et al.*, 2007; Shahbadian *et al.*, 2009) and they are the only RNases shown, thus far, to have a major impact on bulk mRNA degradation in their host organisms (Bernstein *et al.*, 2004; Shahbadian *et al.*, 2009). Finally, both are central members of their respective RNA degradosomes and both are integral membrane proteins (Hunt *et al.*, 2006; Khemici *et al.*, 2008; Liou *et al.*, 2001).

While RNase E has been the subject of intensive investigation for several years (see 8 for a recent review), the analysis of RNase Y is still in the initial stages. RNase Y is required to control the degradation of bulk mRNA in *B. subtilis*, and the mRNAs of *rpsO* and the *gapA* operon as well as the *yitJ* riboswitch have been identified as targets (Commichau *et al.*, 2009; Shahbadian *et al.*, 2009; Yao & Bechhofer, 2010). Based on the initial target analyses, it was suggested that RNase Y requires 5' monophosphorylated RNA and prefers substrates with downstream secondary structures (Shahbadian *et al.*, 2009). From the amino acid sequence, RNase Y seems to comprise at least three domains. First, a short N-terminal transmembrane domain mediates the membrane localisation of the protein (Hunt *et al.*, 2006). Second, a KH-domain is required for RNA binding and finally a HD-domain contains the catalytic apparatus (Condon, 2003; Hunt *et al.*, 2006). The importance of the HD-domain has already been demonstrated, as a strain carrying a single point mutation in the catalytic site is not viable (Hunt *et al.*, 2006).

In this work, we have studied the domain organization of RNase Y and its interactions with the other components of the RNA degradosome. Using biochemical techniques we have shown that RNase Y is a natively disordered protein that forms dimers in solution. We have refined further the domain analysis *in silico*. Based on this new domain definition, we have analysed the contribution of the single domains in the context of protein-protein interactions and cell viability. Our observation that a variant of RNase Y without the transmembrane domain (which is catalytically competent *in vitro*) could not complement *in vivo*, revealed that membrane localization is essential for RNase Y activity *in vivo*. Using bacterial two hybrid analysis we also demonstrated that the intact, full-length protein was required to interact with the other components of the RNA

degradosome. Together, our new data provide further compelling evidence that RNase Y is the functional equivalent of RNase E.

Results

In silico analysis of RNase Y

An *in silico* analysis of the domain structure of RNase Y detected an N-terminal trans-membrane domain (residues 5-24) and two central KH and HD domains (residues 210-280 and 330-430, respectively), in agreement with previous analyses (Commichau *et al.*, 2009; Shahbadian *et al.*, 2009). The relevance of the trans-membrane domain of RNase Y is supported by the membrane localisation of the protein (Hunt *et al.*, 2006; Zweers *et al.*, 2009). Similarly, the importance of the catalytic residues in the HD domain has been demonstrated both *in vivo* and *in vitro* (Hunt *et al.*, 2006; Shahbadian *et al.*, 2009). Our analysis additionally revealed the presence of a coiled-coiled domain with the potential to form a leucine zipper, spanning residues 30 to 150 (Fig. 28), and a C-terminal domain (residues 430-520) that has not been described previously, but that is conserved in all RNases Y.

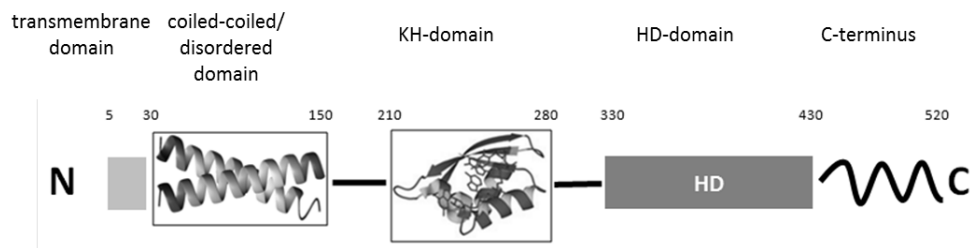


Fig. 28. Domain arrangement of RNase Y. The N-terminal 30 amino acids of RNase Y form a transmembrane spanning α -helix. Using the program COILS, a coiled-coiled region is predicted between amino acids 30 and 150. The KH domain (RNA binding) and HD domain (catalytic activity) spans from amino acids 210-280 and 330-430, respectively. No functional domain is predicted for the C-terminus of the protein (amino acids 430-520); however, this sequence is well conserved in RNase Y proteins from different bacteria.

To extend the domain analysis of RNase Y, we have submitted the amino acid sequence to the web servers PONDR-FIT (64) and metaPrDOS (Ishida & Kinoshita, 2008) which predict specifically the presence of naturally disordered regions of proteins, an important and still emerging facet of protein function (Dyson & Wright, 2005). PONDR-FIT and metaPrDOS are both “meta predictors” which incorporate the results of several individual bioinformatic tools to output a consensus score with greater accuracy than the best performing individual tools (Xue *et al.*, 2010). As can be seen from Fig 29A, both tools

predict a single, large contiguous stretch of disorder near the N-terminus of RNase Y with high disorder propensity. The exact boundaries of this region vary depending both on the type of predictor and the strictness of criteria used, with estimates of length ranging from 158 residues (amino acids 34-192) to just 76 (amino acids 70-146), with the general consensus being in the range of 100 amino acids. A sharp decrease in the disorder propensity can be observed around residue 190 which we believe to be a good estimate of the upper limit of the disordered region, with the lower limit being less well defined. A number of the individual bioinformatic tools predicted additional shorter disordered regions which importantly lie in between the ordered domains identified *in silico*. Thus it is possible that additional regions of RNase Y are disordered but the shorter length and inconsistent predictions mean that little confidence can be assigned to these predictions. Charge-hydrophathy analysis (Uversky *et al.*, 2000) of the amino acid sequence using the domain boundaries previously identified shows that both the HD, KH and C-terminal domains fall clearly in the region of the plot occupied by folded proteins, which is in contrast to the N terminal disordered region that clearly belongs to the distribution of disordered proteins (Fig. 29B).

The N-terminal disordered region overlaps significantly with the predicted coiled-coil domain identified using the COILS program (Lupas *et al.*, 1991) which predicts a strong tendency to form coiled coils (> 0.92 confidence score throughout) for residues 31-153 (Fig. 29C). The high confidence levels assigned to this region by both programs, and the accuracy for disorder prediction algorithms for the prediction of long disordered regions, <0.4% error rate for 40 consecutive residues (Dunker *et al.*, 2001), lead us to suggest that this region may form a flexible coiled coil like structure that is also significantly disordered and is able to occupy many different conformational states. Indeed, purified RNase Y is highly sensitive to proteolysis and is rapidly and completely digested in the time course of a limited trypsinolysis experiment (data not shown).

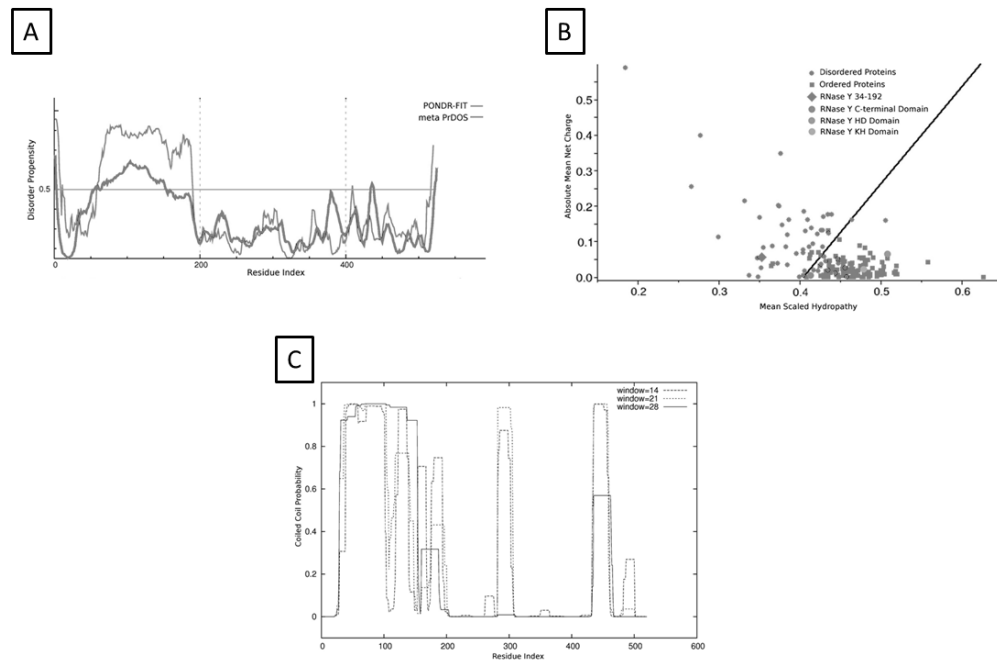


Fig. 29. *In silico* and *in vitro* analysis of RNase Y. (A) Disorder propensity analysis of RNase Y calculated using the program PONDR using the VL-XT neural network predictor, plotted as a function of the RNase Y amino acid sequence. Continuous regions of disorder > 30 amino acids long are considered significant. (B) Hydrophobicity charge analysis of RNase Y domains, mean net charge is plotted as a function of mean hydrophobicity for a set of 105 ordered (shown as blue squares) and 54 disordered proteins (shown as red spheres). Disordered proteins are expected to possess a higher proportion of charged residues and a lower content of hydrophobic amino acids causing them to cluster towards the upper left hand side of this plot. The individual domains of RNase Y are plotted on the graph as indicated in the inset panel. The solid line represents a boundary dividing ordered and disordered regions. (C) Output from the COILS coiled-coil prediction server for RNase Y, plotted as a function of residue number.

RNase Y is disordered in solution and forms dimers

Previous interaction studies with RNase Y using the bacterial two-hybrid system had suggested that the protein is capable of self-interaction (Commichau *et al.*, 2009). However, the nature of these oligomers, whether they were dimers, trimers or higher level oligomers, was unknown. To address this question, we have analyzed purified protein that lacks the N-terminal trans-membrane domain by size exclusion chromatography. A significant proportion of the protein seemed to be in an aggregated form with the molecular mass of the non-aggregated form estimated at 280 kDa (Fig. 30A). To characterize RNase Y in solution further we analyzed the hydrodynamic properties of the enzyme by sedimentation velocity AUC (Fig. 30B). Analysis of the velocity data using a continuous $c(s)$ distribution model revealed that a mixture of two species are present in solution, a major peak at $S = 4.5$ and a minor fraction at $S = 7.6$ corresponding to molecular

weights of 100 and 200 kDa, which most likely represent dimers and tetramers, respectively (Fig. 30C). The relative abundance of these two species does not appear to change with protein concentration under the conditions tested, between 0.37 and 1.5 mg/ml. The value of the frictional ratio, f/f_0^{shape} , was 1.41, which is significantly greater than the value (1.0) expected for a perfectly spherical particle. These data indicate that RNase Y adopts an extended, non-globular conformation in solution, a property common to intrinsically disordered proteins and to proteins with coiled-coil domains. The apparent discrepancy between the major 100 kDa dimeric species identified by AUC and the apparent mass of RNase Y observed by size exclusion chromatography of 280 kDa can also be explained by the fact that RNase Y adopts an extended non-globular structure in solution with a larger Stokes radius than a globular protein of equal mass. The elongated nature of RNase Y would cause it to elute earlier in size exclusion with a consequent overestimation of its apparent molecular mass. It is also not clear at present whether this single peak corresponds to a very elongated dimer or a slightly elongated tetramer. The sedimentation data are also consistent with the *in silico* predictions that RNase Y contains extensive regions of intrinsic disorder, which presumably, and classically, will become ordered upon the interaction with other proteins.

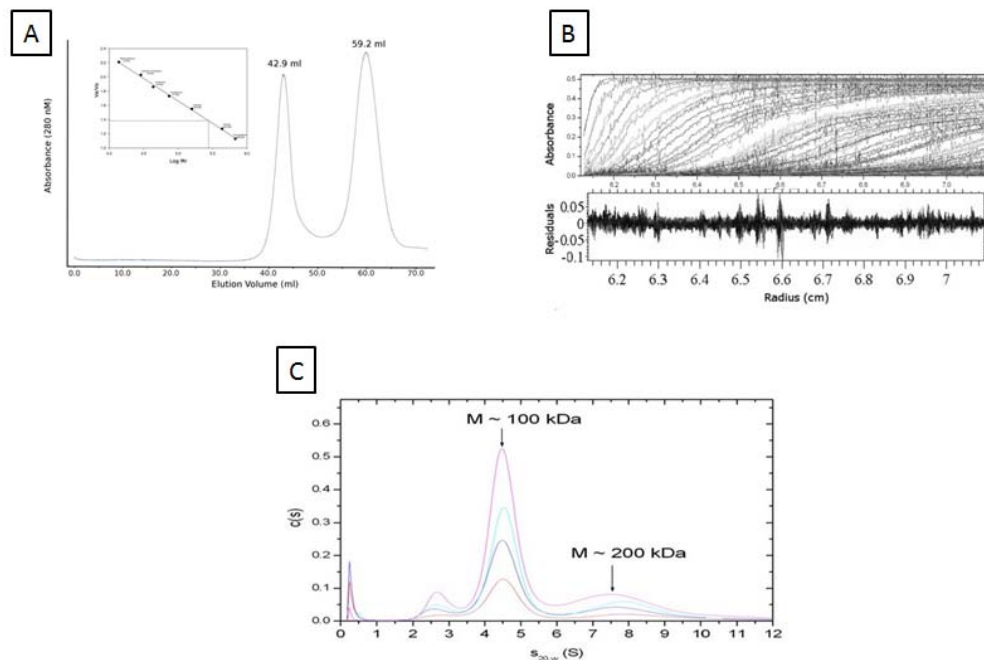


Fig. 30 Hydrodynamic analysis of RNase Y in solution. (A) Gel filtration chromatography of purified RNase Y the non aggregated form was found to elute at ~59 ml which corresponds to an expected molecular weight of 280 kDa for a globular protein (calculated from calibration curve shown in insert). (B) Sedimentation velocity AUC of RNase Y, the top panel shows the raw absorbance data overlaid with the fit using a continuous distribution for sedimentation coefficient model $c(s)$. The residuals are shown in the bottom panel. (C)

Normalised sedimentation coefficient values calculated from the data with different dilutions represented as coloured lines. RNase Y appears to exist as two species in solution, a major smaller species $S_{20,w=4.5}$ (corresponding to an approximate molecular weight of 100 kDa) and a minor larger species $S_{20,w=7.6}$ (corresponding to an approximate molecular weight of 200 kDa); these two species would correspond to dimers and tetramers of RNase Y respectively.

Complementation analysis of the domains of RNase Y

To assess the functional properties of RNase Y *in vivo*, we performed a complementation assay using truncated fragments of the RNase. The *rny* gene encoding RNase Y is essential for the growth of *B. subtilis* (Hunt *et al.*, 2006). We have constructed a *B. subtilis* strain, GP1092, in which *rny* expression is controlled by the xylose repressor and, therefore, this strain is unable to grow in the absence of xylose. Strain GP1092 was transformed with a series of plasmids that encode the full-length or truncated variants of the *rny* gene and growth of the bacteria was recorded. As shown in Fig. 31, transformation of GP1092 with the empty vector pBQ200 allowed growth of the bacteria only in the presence of xylose, confirming the essentiality of RNase Y for *B. subtilis* in this genetic background. Transformation with plasmid pGP1201, which allows expression of the full-length *rny* gene, resulted in xylose-independent growth, suggesting that the plasmid-borne RNase Y effectively complements the chromosomal copy that is repressed in the absence of xylose. By contrast, all truncated variants of the *rny* gene were unable to complement RNase Y depletion (Fig. 31). The lack of growth might be due to poor expression or instability of the truncated proteins, or to their functional inactivity. To distinguish between these possibilities, we studied the accumulation of the different RNase Y variants by Western blot analysis. As shown in Fig. 31C, all truncated variants were expressed as detected with antibodies raised against RNase Y. However, using the anti-Rny antibody, it was difficult to distinguish chromosomally expressed RNase Y from plasmid-encoded variants for those proteins that were similar in size to the wild type protein. Therefore, we constructed additional plasmids that expressed FLAG-tagged variants of those proteins, and detected their expression using anti-FLAG antibodies (see Fig. 31D). Again, these proteins were expressed in *B. subtilis*. Taken together, the data demonstrate that both the trans-membrane and the C-terminal domains of RNase Y are essential for the function of the protein in the organism. As a consequence, we then assessed the roles of the various domains of RNase Y in membrane association, for self-assembly into dimers and for the interaction with other proteins in the degradosome.

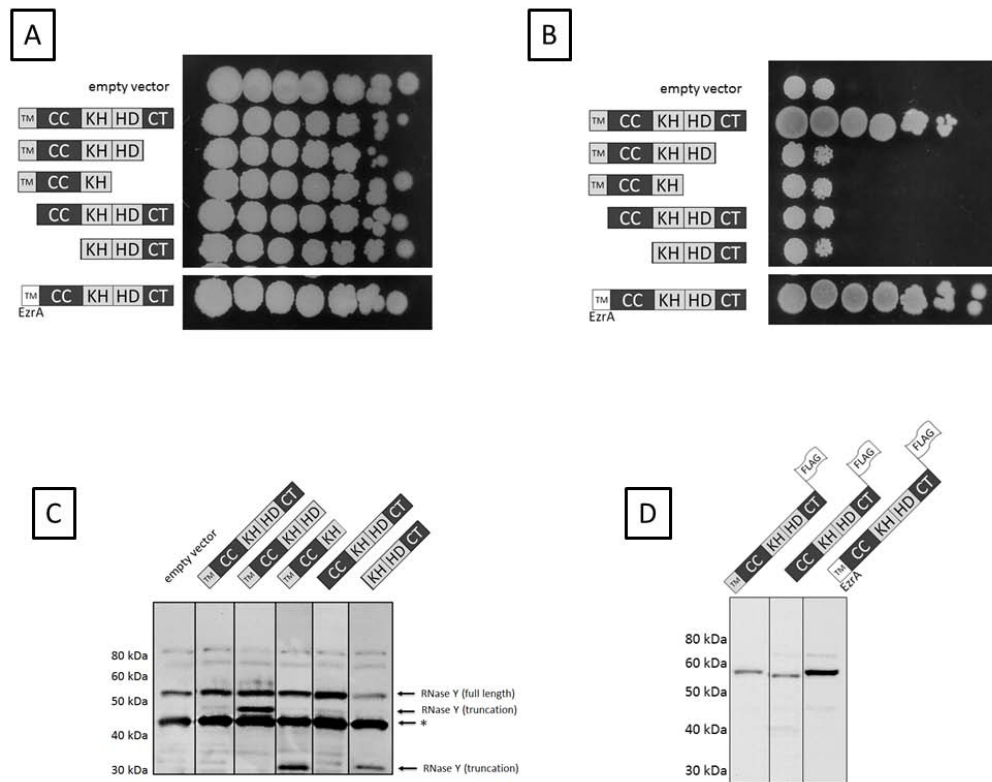


Fig. 31. Functional complementation by truncated RNase Y proteins *in vivo*. RNase Y was truncated N- and C-terminally with respect to the protein domains annotated in FIG. 28. The truncated proteins were expressed from an overexpression vector in strain GP1016. In this strain the chromosomal copy of *rny* is under the control of a xylose-inducible promoter. Fresh cells (optical density of 1.0) were spotted in tenfold dilution on LB-agar-plates with (A) and without xylose (B) to facilitate or impede chromosomal *rny* expression. To verify the expression of the RNase Y variants Western blot analysis were performed with α -RNase Y (C) and α -FLAG (D) antibodies. A band that results from non-specific interaction of one protein with the antibodies raised against RNase Y is marked by an asterisk (C).

The trans-membrane domain of RNase Y can be substituted by a heterologous domain

The trans-membrane domain of RNase Y comprises residues 5 to 24 (Fig. 28) and is predicted to form a single trans-membrane α -helix, but its amino acid sequence does not conform to the signal peptide paradigm ((Tjalsma *et al.*, 2004; Tjalsma & van Dijk, 2005), Fig 32A), consistent with RNase Y being a membrane rather than a secreted protein. Furthermore, our complementation data indicated that the trans-membrane domain is crucial for the function of RNase Y in *B. subtilis* (Fig. 31). To probe the membrane association of this domain of RNase Y, we replaced the trans-membrane region with the analogous domain of an unrelated protein, the divisome protein EzrA (Levin *et al.*, 1999). First, we tested the ability of the chimeric protein to replace RNase Y in the *rny*

depletion strain, GP1092. As shown in Fig. 31 transformants of GP1092 with a plasmid expressing the EzrA-RNase Y chimera grew well in both the presence and the absence of xylose. By contrast, the RNase Y lacking the N-terminal trans-membrane domain was unable to grow when the wild type *rny* gene was depleted by xylose limitation. The strain that expressed the EzrA-RNase Y chimera grew at higher dilution rates in comparison to the strain expressing the wild type RNase Y (see Fig. 31), suggesting that the chimeric EzrA-RNase Y might be even more active and/or more stable than wild type RNase Y. Indeed, Western blot analyses on the accumulation of the RNase Y variants demonstrated that the EzrA-RNase Y protein was present at higher levels in comparison to the full-length, wild type protein (Fig. 31D).

Recently, we have also shown that RNase Y is required for the full expression of the *epsA-O* and *tapA-sipW-tasA* operons that encode the proteins required for extracellular polysaccharide synthesis and the matrix protein TasA, *i. e.* the major contributors to biofilm formation (36). Moreover, over-expression of RNase Y was sufficient to induce biofilm formation even in the laboratory strain *B. subtilis* 168 (Lehnik-Habrink *et al.*, 2011b). We therefore examined the morphology of *B. subtilis* GP1092, a derivative of *B. subtilis* 168, in the presence of the plasmid, pGP1352, which expresses the EzrA-RNase Y chimera. The strain carrying the empty vector, pBQ200, did not form complex colonies (Fig 32B). In good agreement with a previous report (36), overexpression of wild type RNase Y resulted in the formation of complex colonies (Fig. 32B). The complexity of the colonies was even more pronounced in the presence of the EzrA-RNase Y chimera (Fig. 32B). In conclusion, the trans-membrane domain of the divisome protein EzrA can replace the cognate trans-membrane domain of RNase Y and the functional, chimeric protein seems to accumulate to higher levels than the wild type protein.

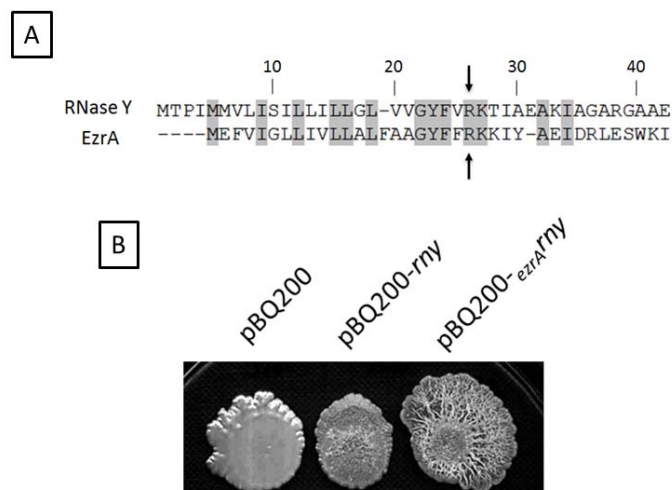


Fig. 32. Influence of a heterologous N-terminal domain in RNase Y on colony morphology. (A) Alignment of the first amino acids of RNase Y and EzrA. The first 26 amino acids of RNase Y (comprising the transmembrane segment of the enzyme) were exchanged by the N-terminus of the unrelated EzrA protein. The arrows at amino acid 26 of RNase Y mark the endpoint of the domain exchange. (B) Phenotypic characterization of the strain GP193 (P_{xyI} -*rny*) harbouring the empty vector pBQ200 (A), an *rny* overexpression plasmid (B), and a variant of *rny* with a heterologous transmembrane segment (C). This chimeric protein is more abundant in the cell (see Western blot Fig 30D) leading to the formation of a more pronounced biofilm. All strains were spotted on LB-agar plates supplemented with xylose and inoculated at 22°C for six days.

Contributions of the domains to the dimerization of RNase Y

The ability of RNase Y to form both dimers and tetramers led us to investigate the contributions of the individual domains to oligomerisation. For this purpose, the N- and C-terminal domains of *Bordetella pertussis* adenylate cyclase were fused to the domains of RNase Y, and the restoration of adenylate cyclase activity upon interaction of the fusion partners was investigated. As shown in Fig. 33, and consistent with the sedimentation velocity data (Fig. 30), full-length RNase Y showed a strong self-interaction. Moreover, all individual domains, with the exception of the KH domain, were capable of interacting with the full-length protein suggesting that all the domains contribute to dimerization (Fig 33). The analysis of the interaction of the isolated domains with each other revealed a different picture: only the trans-membrane and the coiled-coiled domains showed self-interactions, suggesting that the KH, the HD and the C-terminal domains make only minor contributions to the oligomerisation (Fig. 33). The observation that the coiled-coil domains showed the strongest self-association is in good agreement with the well-established role of these domains for the self-interaction of many proteins.

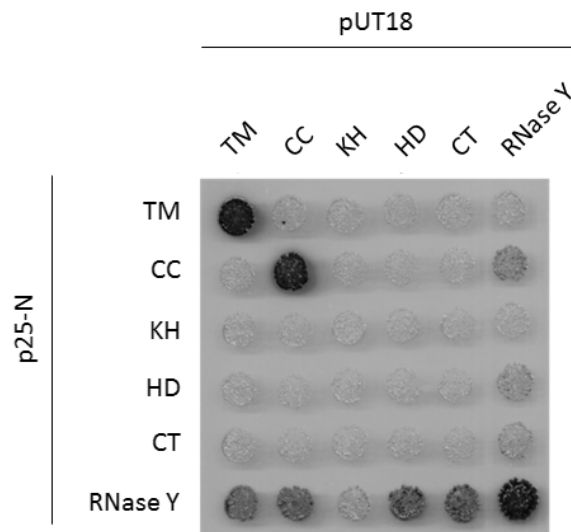


Fig. 33. Bacterial two-hybrid analysis to study the interactions among the single domains of RNase Y and with full length protein. All genes were cloned in the plasmids pUT18, pUT18C, p25-N and pKT25. Plasmids pUT18 and pUT18C allow the expression of the selected truncations fused either to the N- or C-terminus of the T18 domain of the *B. pertussis* adenylate cyclase respectively. Plasmids p25-N and pKT25 allow the expression of the selected enzymes fused either to the N- or C-terminus of the T25 domain of the adenylate cyclase respectively. The *E. coli* transformants were incubated for 48 h at 30°C. The degradation of XGal (blue colour) indicates the presence of a functional adenylate cyclase owing to the interaction of the two proteins of interest. (Abbreviation: TM=transmembrane domain, CC=coiled-coiled/ disordered domain, KH=KH-domain, HD=HD-domain, CT=C-terminal domain, for further details see Fig. 28).

***In vivo* evidence for the interaction of RNase Y with the other components of the degradosome**

Previously, we have observed interactions between several RNases, the RNA helicase CshA, and the glycolytic enzymes enolase and phosphofructokinase in a bacterial two-hybrid assay and in affinity co-purification experiments with glycolytic enzymes and CshA (Commichau *et al.*, 2009; Lehnik-Habrink *et al.*, 2010). The binary interactions in the degradosome have also been the focus of recent *in vitro* biochemical and biophysical studies (Newman *et al.*, unpublished results). The observation of multiple protein-protein complexes has led us to propose that these proteins form a complex that is the *B. subtilis* equivalent of the RNA degradosome, with the novel RNase Y as the central component. To provide evidence for the *in vivo* interaction of RNase Y with other members of the degradosome, we attempted to purify RNase Y together with its interaction partners. To facilitate detection of components of the degradosome, strains expressing RNase Y with a C-terminal Strep-tag under the control of its native promoter and the potential

degradosome components carrying a C-terminal triple FLAG-tag were constructed. A strain expressing the malic enzyme, YtsJ, fused to a FLAG-tag was used as control. As shown in Fig. 34, all potential degradosome proteins as well as YtsJ were expressed under the conditions employed to isolate the protein complexes. With Strep-tagged RNase Y as the bait, the polynucleotide phosphorylase PNPase, the RNases J1 and J2, the DEAD box RNA helicase CshA and the glycolytic enzymes Eno and PfkA were co-purified after cross-linking. By contrast, a very faint signal was observed for YtsJ suggesting that the degradosome proteins do indeed form a complex with RNase Y whereas YtsJ does not (see Fig. 34). These findings are in excellent agreement with previous results of bacterial two hybrid assays that suggested binary protein-protein interactions of RNase Y with all components of the degradosome (Commichau *et al.*, 2009; Lehnik-Habrink *et al.*, 2010), with the common association of the degradosome proteins to the cytoplasmic membrane (Hahne *et al.*, 2008; Lehnik-Habrink *et al.*, 2010), and with a recent study on an RNase Y homologue from *Streptococcus pyogenes*, which was demonstrated to interact with enolase (Kang *et al.*, 2010).












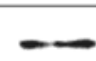


strain	α -FLAG	crude extract	co-purification
GP1016	PNPase		
GP1024	RNase J1		
GP1039	RNase J2		
GP1022	CshA		
GP1023	PfkA		
GP1040	Eno		
GP1025	YtsJ		

Fig. 34. Confirmation of the *in vivo* interaction of RNase Y with the degradosome components. RNase Y fused to a C-terminal Strep-tag and expressed at its native locus was purified with its interaction partners from various *B. subtilis* strains (indicated in the first column) carrying triple FLAG tags attached to the putative interaction partners. All strains were grown in LB medium. 25 μ l of the first eluting fraction from each purification were loaded onto a 12.5% SDS polyacrylamide gel. After electrophoresis and blotting onto a polyvinylidene difluoride membrane, interaction partners were detected by FLAG-tag polyclonal antibodies. YtsJ was used as a negative control.

Contributions of the RNase Y domains to the interactions with the partners in the degradosome

Our data are consistent with RNase Y forming a mixture of mostly dimers, but some tetramers (Fig. 30) and suggest that this self-association is driven primarily by the trans-membrane and coiled-coil domains (Fig. 33). We have extended the domain analysis of RNase Y to address the contribution of these domains for the interaction with several other proteins that are found in a protein complex called the RNA degradosome (Commichau *et al.*, 2009; Lehnik-Habrink *et al.*, 2010). The truncated variants of RNase Y described above were used in an *in vivo* complementation experiment. In good agreement with previous reports (Lehnik-Habrink *et al.*, 2010), full-length RNase Y interacted with all the different members of the degradosome (Fig. 34). By contrast, truncations of RNase Y at the N- or C-terminus resulted in a loss of interaction with the other degradosome proteins. To exclude the possibility that a lack of interaction reflected poor expression or stability of the truncated variants, we tested the interaction of the truncated versions with full-length RNase Y. All truncated variants showed a strong interaction with RNase Y, suggesting that the truncated proteins retain the ability to interact (Fig. 34). Thus, the loss of interaction seen upon deleting domains from either the N- or the C-terminus of RNase Y suggests that these domains are essential for the interactions with other degradosome partners, but not for dimerization of RNase Y. By contrast, and quite unexpectedly, the N-terminal trans-membrane region is required *in vivo* for all the properties of RNase Y tested; for cell viability, and for the interaction with the other components in the degradosome.

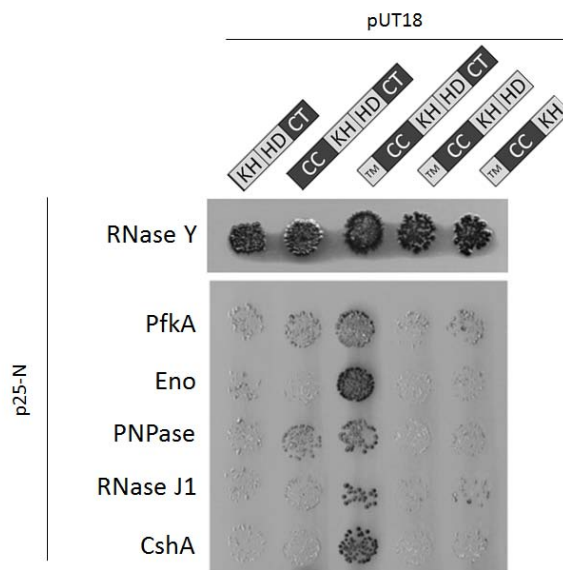


Fig. 34. Bacterial two-hybrid analysis to study the interactions among full length RNase Y and its fragments with the other components of the degradosome. The gene encoding RNase Y and its fragments

were cloned into p25N, whereas the coding sequences of the other degradosome components PfkA (phosphofructokinase), Eno (enolase), PNPase (polynucleotide phosphorylase), RNase J1, CshA were cloned into pUT18 (for further details of the B2H analysis see Fig. 32).

Discussion

Although it was discovered only two years ago (Commichau *et al.*, 2009; Shahbadian *et al.*, 2009), the accumulating evidence suggests that RNase Y is a key player in RNA processing and degradation in *B. subtilis* and most likely also in other Gram-positive bacteria. This is supported by the notion that RNase Y shares a growing list of similarities with the RNase E from *E. coli* and other Gram-negative bacteria even though the two proteins do not share any sequence similarity. Moreover, RNase Y is found to occur in more bacterial phyla that lack RNase E than any other endoribonuclease (Kaberdin *et al.*, 2011). The list of similarities between RNase Y and RNase E is extended by the results reported in this study. Both proteins are endoribonucleases with a preference for 5' monophosphorylated mRNA ends (Mackie, 1998; Shahbadian *et al.*, 2009), both have a major impact on the global RNA stability (Bernstein *et al.*, 2004; Shahbadian *et al.*, 2009), both are attached to the membrane (Hunt *et al.*, 2006; Khemici *et al.*, 2008; Lehnik-Habrink *et al.*, 2010; Zweers *et al.*, 2009) and both interact with other proteins involved in RNA processing in a protein complex called the RNA degradosome (Carpousis, 2007; Commichau *et al.*, 2009; Roux *et al.*, 2011). This work provides evidence for the importance of the membrane localization of RNase Y, and for the presence of disordered regions of RNase Y. Both of these features are shares with RNase E, although both the way in which membrane localization is achieved and the distribution of ordered and disordered domains is distinct between the two enzymes.

The prediction by bioinformatics and the observation by direct experimentation that RNase Y contains disordered regions will fundamentally alter our understanding of this important enzyme. Disordered regions within proteins have been found to play key roles in interaction networks as they allow rapid evolution of protein recognition 'microdomains' without the structural and thermodynamic constraints of protein folding and stability. They also allow the evolution of high specificity, low affinity interactions where the free energy of the interaction is used for protein folding (Dyson & Wright, 2005); it is thus likely that RNase Y adopts an ordered structure upon binding to its interaction partners. This disorder to order transition is not uncommon in proteins (Fong *et al.*, 2009). For instance, a C-terminal region of the HPr kinase/phosphorylase adopts an ordered structure only upon binding its target protein, phosphorylated HPr (Fieulaine *et*

al., 2002). The discovery of unstructured regions of RNase Y in the *B. subtilis* degradosome extends the already extensive functional similarities with RNase E in the *E. coli* degradosome. In RNase E, the unstructured C-terminus is used as a scaffold to facilitate and to co-ordinate the organization and activities of the enzymes in the *E. coli* degradosome (Kaberdin *et al.*, 1998); we suggest an equivalent role for the unstructured regions of RNase Y.

The results of our domain analysis suggest that the coiled coil domain may be important for oligomerisation. The involvement of coiled-coiled domains in protein self-interaction is very common (Grigoryan & Keating, 2008; Rigden *et al.*, 2008) and oligomerization of RNases is widespread (Callaghan *et al.*, 2003; Shi *et al.*, 2008). In the case of RNase Y, self-association may be of special importance for the assembly of the RNA degradosome and for contacting other degradosome components. The formation of higher oligomeric structures extends significantly the potential interaction interface for binding other proteins.

Previous reports of the interactions of RNase Y with the members of the RNA degradosome of *B. subtilis* were based mainly on two-hybrid studies in a heterologous host (Commichau *et al.*, 2009; Lehnik-Habrink *et al.*, 2010). To verify that RNase Y physically interacts with these proteins inside the cell, we froze the *in vivo* physical interactions by chemical cross-linking. This analysis confirmed that RNase Y does indeed interact with RNase J1, with polynucleotide phosphorylase, with the DEAD-box RNA helicase CshA, and the two glycolytic enzymes enolase and phosphofructokinase (Fig. 34). Whilst the formation of a complex of different endo- and exoribonucleases with an RNA helicase might be intuitive, it is less so for the involvement of the glycolytic enzymes. However, metabolic enzymes are commonly found in RNA-degrading complexes as enolase is also a component of the *E. coli* RNA degradosome (Miczak *et al.*, 1996) and the degradosome of *Caulobacter crescentus* contains aconitase, an RNA-binding enzyme of the tricarboxylic acid cycle (Hardwick *et al.*, 2011). These seemingly unusual connections imply that RNA degradation might be controlled by fluctuations in metabolite concentrations. This hypothesis is supported by the recent finding that the activity of *E. coli* polynucleotide phosphorylase, a component of the RNA degradosome, is controlled by citrate, the first intermediate of the tricarboxylic acid cycle (Nurmohamed *et al.*, 2011). Recently, association of RNase Y with enolase was also reported for *Streptococcus pyogenes* and *Staphylococcus aureus* (Kang *et al.*, 2010; Roux *et al.*, 2011).

The mandatory requirement for RNase Y to have a functional transmembrane domain, and therefore be membrane localized, is intriguing, and may reflect that RNA turnover is somehow compartmentalized in cell. Even though RNase Y is catalytically active without its membrane segment *in vitro*, proper cellular localization is essential *in vivo*. That membrane localization of RNases is physiologically important is an emerging area in RNA biology (see (Evguenieva-Hackenberg *et al.*, 2011) for review). Early studies using membrane fractionation experiments in *E. coli* suggested that RNase E, RNase III and RNase P were associated with the membrane (Miczak *et al.*, 1991). Membrane-localization of RNA-degrading protein complexes was recently also observed in other bacteria and even in archaea (Roppelt *et al.*, 2010). Even though RNase E lacks an obvious transmembrane domain as found in RNase Y, it has been demonstrated that RNase E contains an amphiphatic α -helix which binds to the phospholipid bilayer (Khemici *et al.*, 2008). The importance of the membrane localization of RNase E was demonstrated by the deletion of the membrane binding segment, which compromises growth severely. This phenotype is most likely not due to impaired catalytic activity, but impaired cellular localization. Similarly, RNase Y still exhibits catalytic activity when the transmembrane domain is deleted (Shahbadian *et al.*, 2009), but the consequences *in vivo* are very drastic, as a strain depending only on a copy of RNase Y without the transmembrane segment is not viable. Again, the mandatory need for RNase Y to be membrane located in *Bacillus subtilis* provides additional evidence for the importance of protein compartmentalization in bacteria. The use of GFP technology in *B. subtilis* has revealed that the RNA polymerase is associated primarily with the nucleoid whereas ribosomes occupy the cytoplasmic space outside the nucleoid (Lewis *et al.*, 2000). Therefore bacteria may exhibit a certain level of spatial organization to separate transcription, translation and perhaps also RNA degradation. Consistent with this hypothesis, the GFP-tagging of mRNAs in *E. coli* and *C. crescentus* showed that even mRNAs are not distributed equally throughout the cell (Montero Llopis *et al.*, 2010; Nevo-Dinur *et al.*, 2011). Therefore, despite lacking organelle-like structures, bacteria may organize spatially the synthesis, translation and degradation of messenger RNAs.

The work presented in this study indicates that RNase Y is the central component of the *B. subtilis* RNA degradosome. The hypothesis that disorder – order transitions may play a role in its interactions with its partner proteins paves the way for the structural analysis of this key component of the RNA-degrading machinery in Gram-positive bacteria.

ACKNOWLEDGEMENTS

We wish to thank Jan-Maarten van Dijl for raising antibodies against RNase Y. This work was supported by grants from the Deutsche Forschungsgemeinschaft (SFB860) to J.S. and from the UK BBSRC to R.J.L.

Experimental procedures

Bacterial strains, oligonucleotides and growth conditions - The *B. subtilis* strains were derived from the laboratory strain 168 (*trpC2*) and they are listed in Table 1. *E. coli* DH5 α , BTH101 and BL21 (DE3) (Karimova *et al.*, 1998; Sambrook *et al.*, 1989) were used for cloning experiments, bacterial two-hybrid (B2H) analyses and protein over-production, respectively. *B. subtilis* and *E. coli* were grown in LB medium. LB and SP plates were prepared by addition of 17 g Bacto agar/l (Difco) to LB and SP, respectively (Kunst & Rapoport, 1995; Sambrook *et al.*, 1989).

DNA manipulation - Transformation of *E. coli* and plasmid DNA extraction were performed using standard procedures (Sambrook *et al.*, 1989). All commercially available plasmids, restriction enzymes, T4 DNA ligase and DNA polymerases were used as recommended by the manufacturers. DNA fragments were purified from agarose gels using the Nucleospin Extraction kit (Macherey and Nagel, Germany). All primer sequences are provided as supplementary material. DNA sequences were determined using the dideoxy chain termination method (Sambrook *et al.*, 1989). Chromosomal DNA of *B. subtilis* was isolated as described (Kunst & Rapoport, 1995).

Transformation and phenotypic analysis - Standard procedures were used to transform *E. coli* (Sambrook *et al.*, 1989) and transformants were selected on LB plates containing either ampicillin (100 μ g/ml) or kanamycin (50 μ g/ml). *B. subtilis* was transformed with plasmid DNA according to the two-step protocol (Kunst & Rapoport, 1995). Transformants were selected on SP plates containing erythromycin (2 μ g/ml) plus lincomycin (25 μ g/ml), chloramphenicol (5 μ g/ml) or kanamycin (20 μ g/ml). For colony architecture analysis, bacteria were pre-cultured in LB containing 1% xylose until an OD₆₀₀ of about 1.0 was reached. 10 μ l of this culture were then spotted onto LB/xylose plates and incubated at 22°C for six days.

Plasmid constructions - All plasmids used in this study are listed in the supplementary Table S2. RNase Y variants were expressed in *B. subtilis* under the control of the constitutively active *degQ^{hy}* promoter using the expression vector pBQ200 (Martin-Verstraete *et al.*, 1994). Briefly, the desired *rny* alleles were generated by PCR using the oligonucleotides listed in the supplementary material. The PCR products were digested with *Bam*HI and *Sal*I and cloned into pBQ200 linearised with the same restriction enzymes. The resulting plasmids are listed in Table 2. The chimeric *ezrA-rny* fusion gene was obtained by amplifying the regions encoding the trans-membrane domain of EzrA and RNase Y without the membrane segment, using primer pairs ML32/ML33 and ML34/FR6, respectively. The primers ML33 and ML34 had an overlap allowing fusion of the products in another round of PCR using ML32 and FR6 as amplification primers. The PCR product was then cloned into pBQ200 as described above, and the resulting plasmid was named pGP1352.

To fuse different RNase Y variants to a 3×FLAG tag and allow overexpression in *B. subtilis*, we constructed plasmid pGP1370 that allows multicopy-expression of FLAG-tagged proteins. This plasmid was obtained by amplification of the FLAG-tag encoding region from pGP1331 (Lehnik-Habrink *et al.*, 2010) using the primer pair ML5/ ML6 and insertion of the PCR product into the expression vector pBQ200 (Martin-Verstraete *et al.*, 1994) linearized with HindIII. Next, we amplified the coding sequence of full length RNase Y (FR7/ ML44), RNase Y without the transmembrane helix (FR4+ML44) and the chimeric RNase Y containing the N-terminal domain of EzrA (ML32+ML44). The resulting PCR products as well as plasmid pGP1370 were digested BamHI and SalI to allow subsequent ligation. The resulting plasmids were pGP1363 (full length RNase Y), pGP1364 (RNase Y without transmembrane helix) and pGP1365 (RNase Y with the transmembrane segment of EzrA).

To obtain the plasmids for the B2H analyses, defined regions of *rny* were amplified by PCR using chromosomal DNA of *B. subtilis* 168. The gene specific primers are listed in the supplementals. The PCR products were digested with *Xba*I and *Kpn*I, and the resulting fragments were cloned into each of the four plasmids p25-N, pKNT25, pUT18 and pUT18c (Claessen *et al.*, 2008; Karimova *et al.*, 1998), digested with the same enzymes. The resulting plasmids used for the B2H analyses are listed in Table S2. All plasmid inserts were verified by DNA sequencing.

Construction of a strain that allows controlled depletion of RNase Y - In our previous studies, we noticed that the xylose-controlled expression of RNase Y was not completely

tight in the absence of xylose. To address this problem, we constructed strain GP1092 that encodes an extra copy of the xylose repressor XylR as follows. First, the *xylR* gene was inserted at the ectopic *lacA* site of the *B. subtilis* chromosome by transforming *B. subtilis* 168 with plasmid pGP884 (Gunka, 2011). The resulting strain, GP1091, was then transformed with plasmid pGP774 that places the *rny* gene under the control of the XylR-controlled promoter of the xylose operon (Commichau *et al.*, 2009).

Construction of strains expressing tagged degradosome proteins – To facilitate the detection of the degradosome components by Western blot analysis, we fused RNase J1, RNase J2, PNPase, CshA, PfkA, Eno and YtsJ to a C-terminal triple FLAG tag. For this purpose we used the plasmids pGP1375 (*pfkA*), pGP1376 (*rnjA*), pGP1377 (*pnpA*), and pGP1758 (*ytsJ*) (Lehnik-Habrink *et al.*, 2010; Meyer *et al.*, 2011). Eno and RNase J2 were fused to the FLAG-tag using plasmid pGP1331 (35). Briefly, the corresponding genes *eno* and *rnjB* were amplified with the primer pairs FR86/FR90 and ML173/ML174, respectively, digested with *Bam*HI and *Sal*I and cloned into pGP1331 linearized with the same enzymes. The resulting plasmids were pGP1264 (*eno*) and pGP1851 (*rnjB*). The designations of the resulting strains are listed in Table 1. For primers see Table supplementary material.

To express RNase Y fused to a C-terminal Strep-tag from its native locus we first constructed the cloning vector pGP1389 that allows easy integration of the constructs into the chromosome. For this purpose, the annealed oligonucleotides BD10/BD11 (Herzberg *et al.*, 2007) were inserted into plasmid pUS19 linearized with *Bam*HI and *Hind*III. In the next step, the *rny* gene was amplified using the primer pairs ML97/ML44. The PCR product was cloned between the the *Bam*HI and *Sal*I sites of pGP1389, giving pGP1391. This plasmid was used to construct *B. subtilis* GP1033 expressing the Strep-tagged RNase Y. To avoid interference between the two copies of integrated plasmids that are associated with the Strep- and the FLAG-tagged proteins, we next constructed strain GP1012 that carries the *rny*-strep fusion construct linked to a chloramphenicol resistance gene by transformation with PCR products constructed using oligonucleotides to amplify DNA fragments flanking each target gene and an intervening antibiotic cassette as described previously (Wach, 1996).

In vivo detection of protein-protein interactions - The isolation of protein complexes from *B. subtilis* cells was performed by the SPINE technology (Herzberg *et al.*, 2007). Briefly, growing cultures of *B. subtilis* were treated with formaldehyde (0.6% w/v, 20 min) to facilitate cross-linking of interacting proteins (Herzberg *et al.*, 2007). The Strep-tagged

proteins and their potential interaction partners were then purified from crude extracts using a Streptactin column (IBA, Göttingen, Germany) and desthiobiotin as the eluent. Interacting proteins were identified by Western blot analysis.

Bacterial two-hybrid assay - Primary protein-protein interactions were identified by bacterial two-hybrid (B2H) analysis (Karimova *et al.*, 1998). The B2H system is based on the interaction-mediated reconstruction of *Bordetella pertussis* adenylate cyclase (CyaA) activity in *E. coli*. Functional complementation between two fragments (T18 and T25) of CyaA as a consequence of the interaction between bait and prey molecules results in the synthesis of cAMP, which is monitored by measuring the β -galactosidase activity of the cAMP-CAP-dependent promoter of the *E. coli lac* operon. Plasmids pUT18 and p25N allow the expression of proteins fused to the N-terminus of the T18 and T25 fragments of CyaA, respectively, whereas pUT18C and pKT25 allow the expression of proteins fused to the C-terminus of the T18 and T25 fragments of CyaA (Claessen *et al.*, 2008; Karimova *et al.*, 1998). The plasmids constructed for the B2H assay (see Table S2) were used for co-transformation of *E. coli* BTH101 and the protein-protein interactions were then analyzed by plating the cells on LB plates containing 100 μ g/ml ampicillin, 50 μ g/ml kanamycin, 40 μ g/ml X-Gal (5-bromo-4-chloro-3-indolyl- β -D-galactopyranoside) and 0.5 mM IPTG (isopropyl- β -D-thiogalactopyranoside), respectively. The plates were incubated for a maximum of 36 h at 30° C.

Recombinant protein production - To generate RNase Y constructs for recombinant protein production, coding sequences were amplified by PCR with Phusion High fidelity DNA polymerase (New England Biolabs) and the primers listed in supplementary material using *B. subtilis* 168 genomic DNA as the template. The PCR product encoding residues 25-520 of the RNase Y ORF, designed so as to remove the predicted N-terminal transmembrane helix, was cloned into pET24a by restriction with *NdeI* and *NotI* for the over-expression of an in-frame C-terminal hexa-histidine tagged protein. The RNase Y constructs were transformed into *E. coli* BL21 (DE3) or Rosetta (DE3) for protein over-expression. Cultures were grown in liquid LB medium at 37°C supplemented with kanamycin until the optical density at 600 nm reached 0.6-0.8 at which point over-expression was induced with the addition of IPTG to a final concentration of 0.1 mM and the culture was left overnight at 25°C before harvesting by centrifugation.

RNase Y was purified by immobilized metal affinity chromatography using a His-Trap column (GE Healthcare), equilibrated in 50 mM Tris pH8.0, 20 mM imidazole and eluted with a linear gradient of 20 – 250 mM imidazole. Fractions containing RNase Y were

pooled, concentrated and loaded onto a Superdex 200 gel filtration column, pre-equilibrated in 50 mM Na/HEPES pH 7.0, 500 mM NaCl. To avoid the precipitation of RNase Y in low ionic strength solutions at high protein concentrations, 500 mM NaCl was included in all buffers to stabilize the protein. The final yield of RNase Y was 0.3 mg protein per gram cell paste. The final protein purity was estimated to be greater than 90% by SDS PAGE and its concentration was determined by measuring the absorbance at 280 nm.

Analytical ultracentrifugation - Sedimentation velocity experiments were carried out in a Beckman Coulter XL-I analytical ultracentrifuge (Palo Alto, USA) using an 8-hole AnTi50 rotor, using both absorbance and interference optics. AUC runs were carried out at a rotation speed of 50,000 rpm using a 400 μ l sample volume with protein concentrations ranging from 0.1 to 2 mg/ml. The density and viscosity of buffers was calculated from their composition using the program SEDENTERP (Laue *et al.*, 1992). The velocity data were analyzed with the program SEDFIT using a diffusion deconvoluted continuous sedimentation coefficient distribution $c(s)$ model (Schuck, 2000).

Western blot analysis - For Western blot analysis, *B. subtilis* cell extracts were separated on 12.5% SDS polyacrylamide gels. After electrophoresis, the proteins were transferred to a polyvinylidene difluoride membrane (PVDF, BioRad) by electroblotting. RNase Y and RNase Y-FLAG were detected using antibodies raised against RNase Y (Zweers *et al.*, 2009) and the FLAG-tag (SIGMA), respectively. The primary antibodies were visualised by using anti-rabbit IgG-AP secondary antibodies (Promega) and the CDP* detection system (Roche Diagnostics).

6. Identification of targets of RNase Y in *Bacillus subtilis*

The results described in this chapter were published in:

Lehnik-Habrink, M., Schaffer, M., Mäder, U., Diethmaier, C., Herzberg, C. & Stülke, J. (2011b). RNA processing in *Bacillus subtilis*: identification of targets of the essential RNase Y. *Mol Microbiol.* **4**, 1459-1473

Author's contribution:

The experiments were designed and interpreted by MLH, UM and JS. MLH performed all experiments for the transcriptome analysis (RNA isolation, Western blot analysis). The microanalysis was performed by MS and UM. MLH and CH performed the Northern blot analysis. MLH and CH made all experiments concerning the biofilm formation. CD contributed the expression analysis. MLH and JS wrote the paper.

Abstract

RNA processing and degradation is initiated by endonucleolytic cleavage of the target RNAs. In many bacteria, this activity is performed by RNase E which is not present in *Bacillus subtilis* and other Gram-positive bacteria. Recently, the essential endoribonuclease RNase Y has been discovered in *B. subtilis*. This RNase is involved in the degradation of bulk mRNA suggesting a major role in RNA metabolism. However, only a few targets of RNase Y have been identified so far. In order to assess the global impact of RNase Y, we compared the transcriptomes in response to the expression level of RNase Y. Our results demonstrate that processing by RNase Y results in accumulation of about 550 mRNAs. Some of these targets were substantially stabilized by RNase Y depletion, resulting in half-lives in the range of an hour. Moreover, about 350 mRNAs were less abundant when RNase Y was depleted among them the mRNAs of the operons required for biofilm formation. Interestingly, overexpression of RNase Y was sufficient to induce biofilm formation. The results presented in this work emphasize the importance of RNase Y as the global acting endoribonuclease for *Bacillus subtilis*.

Introduction

The rapid turnover of mRNAs contributes to the ability of bacteria to adapt very quickly to changing environmental conditions. However, this decay has to be regulated. The most important players in this process are RNases. These enzymes can act either as exoribonucleases degrading mRNAs from the ends or as endoribonucleases cleaving inside the molecule. Even though both degradation mechanisms are necessary, the endonucleolytic attack is considered to be rate-limiting in the mRNA turnover process (Carpousis, 2007; Kushner, 2002).

In *Escherichia coli*, the endonucleolytic attack is primarily carried out by the essential endoribonuclease RNase E. The endonucleolytic cleavage by RNase E creates upstream fragments with free 3' ends which are subject to subsequent 3'-to-5' exonucleolytic attack by the polynucleotide phosphorylase PnpA, RNase II and RNase R. The downstream fragments undergo further rounds of RNase E-mediated cleavage and subsequent exonucleolytic degradation (Belasco, 2010). Inactivation of RNase E in temperature-sensitive mutants leads to prolonged half-life time of bulk mRNA, confirming the fundamental impact of this RNase on mRNA turnover (Babitzke & Kushner, 1991). Although no canonical target sequence can be identified, RNase E cleaves single stranded RNA preferentially at A/U rich sequences (Bessarab *et al.*, 1998). Adjacent stem-loop

structures are necessary for the turnover of some target mRNAs (Diwa *et al.*, 2000). RNase E itself has two distinct functional domains. The N-terminal domain comprises the catalytic activity whereas the C-terminal part organizes protein-protein interactions in the formation of the RNA degradosome (Vanzo *et al.*, 1998). This multi-component assembly contains besides RNase E the exoribonuclease PnpA, the RNA helicase RhlB and the glycolytic enzyme enolase, all binding the flexible C-terminus of RNase E (Carpousis, 2007). Such complexes can also be found in other bacteria harbouring RNase E homologs (Ait-Bara & Carpousis, 2010; Hardwick *et al.*, 2011; Marcaida *et al.*, 2006).

In contrast to the Gram-negative proteobacteria, the Gram-positive Firmicutes do not possess RNase E. Therefore, it has remained for a long time enigmatic how RNA processing is initiated. Recent evidence suggests that the newly discovered essential RNase Y performs this activity in *B. subtilis* (Commichau *et al.*, 2009; Shahbadian *et al.*, 2009; Yao & Bechhofer, 2010). Moreover, as RNase E in *E. coli*, RNase Y was suggested to be the central component of the RNA degradosome in *B. subtilis* (Commichau *et al.*, 2009; Lehnik-Habrink *et al.*, 2010). A third similarity between RNase E and RNase Y is their cellular localization. Both proteins are attached to the cell membrane, and are thus thought to tether the degradosomes to the membrane (Khemici *et al.*, 2008; Lehnik-Habrink *et al.*, 2010; Zweers *et al.*, 2009). Once an endonucleolytic cleavage has been done, the RNA fragments can be degraded by exonucleases. In both Gram-positive and Gram-negative bacteria, the polynucleotide phosphorylase PnpA degrades RNA fragments in 3' → 5' direction. In *B. subtilis*, PnpA is the major out of four 3'-to-5' exonucleases (Oussenko *et al.*, 2005). In addition, the RNases J1 and J2 also exhibit exonuclease activity and degrade the RNA fragments from the 5' end (Mathy *et al.*, 2007). Such an activity is not present in proteobacteria such as *E. coli*.

Analyses of RNA stability and processing in *B. subtilis* revealed that the mean half-life of the mRNAs is in the range of 2.5 to 5 min (Even *et al.*, 2005; Hambræus *et al.*, 2003). Depletion of the essential RNase Y results in an increased stability of bulk mRNA (Shahbadian *et al.*, 2009). In addition, depletion of RNase J1 has a minor impact on the global RNA stability (Even *et al.*, 2005; Mäder *et al.*, 2008). The investigation of targets of the exonucleases revealed that only few mRNAs are affected by a mutation in *pnpA*, the gene encoding polynucleotide phosphorylase. Among these targets are the *trp* operon mRNA and the mRNA of the *ygcMNO* proline utilization operon (Deikus *et al.*, 2004). The inactivation of the two J-type RNases results in higher expression of about 300 genes. Moreover, the expression of about 300 other genes is significantly reduced in such a mutant. Interestingly, inactivation of the individual genes for the RNase J1 and J2, *rnjA* and

rnjB, has only little effect on gene expression. This is in good agreement with the observation that the two proteins form a complex *in vivo* (Commichau *et al.*, 2009; Mäder *et al.*, 2008; Mathy *et al.*, 2010). Among the targets of the J-type RNases are the leader sequences of the *trp* operon as well as the *thrS* and *thrZ* mRNAs, the mRNA for the ribosomal protein RpsO, and the 5' end of 16S rRNA (Britton *et al.*, 2007; Deikus *et al.*, 2008; Even *et al.*, 2005; Mäder *et al.*, 2008; Yao & Bechhofer, 2010).

In this study, we performed a transcriptome analysis to investigate the impact of RNase Y in *B. subtilis* on a global scale. We found that this RNase affects the abundance of about 900 transcripts corresponding to more than 20% of all open reading frames. One of the most interesting impacts of RNase Y depletion are the reduced amounts of mRNAs involved in the formation of biofilms. Further investigation of this phenomenon revealed an increased amount and stability of the *sinR* mRNA encoding the master regulator of biofilm formation. Taken together, our study provides experimental support for the hypothesis that RNase Y initiates mRNA degradation in *B. subtilis*.

Results

Expression of RNase Y

Since the expression of RNase Y has never been studied, we first addressed the expression of the corresponding *rny* gene by a reporter fusion. The mRNA for *rny* has a long non-translated leader region (Irnov *et al.*, 2010). To study the expression of RNase Y in more detail, a translational *rny-lacZ* fusion was constructed by cloning the *rny* promoter region upstream of the *lacZ* gene. The resulting strain, GP63, was grown in LB and in CSE minimal medium with glucose. The *lacZ* expression driven from the *rny* promoter was detectable throughout growth suggesting that RNase Y is present both during logarithmic growth and in the stationary phase. Expression was maximal in the mid-logarithmic phase (Fig. 35). Therefore, all following experiments were performed with mid-logarithmic cells.

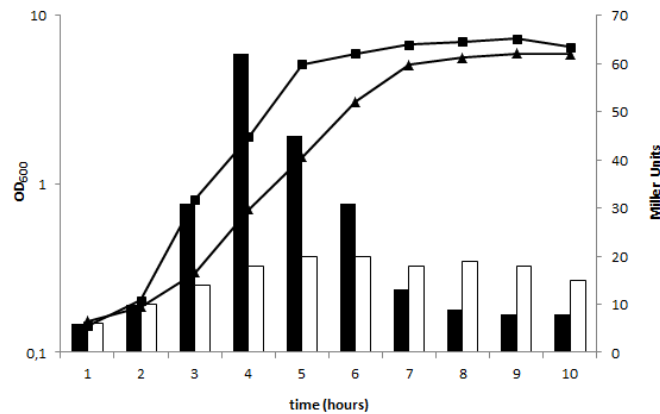


Fig. 35 Expression pattern of the *rny* gene encoding RNase Y. β -galactosidase assays of a translational *P_{rny}-lacZ* fusion were conducted in *B. subtilis* GP63 grown in complex medium (LB, squares, black bars) or in CSE minimal medium supplemented with glucose (0.5%, w/v; triangles, white bars) at 37°C. The expression was determined in Miller units of β -galactosidase. The expression patterns of *P_{rny}-lacZ* were measured through the whole growth curve (log OD₆₀₀).

Establishment of experimental conditions for the depletion of RNase Y

So far, only a few targets of RNase Y have been identified (Commichau *et al.*, 2009; Shahbadian *et al.*, 2009; Yao & Bechhofer, 2010). However, a global role for RNase Y was suggested because of the stabilization of the bulk mRNA in an *rny* depletion mutant (Shahbadian *et al.*, 2009). To study the global function of RNase Y in more detail, we performed microarray analyses with a strain allowing controlled depletion of RNase Y. For this purpose, we used *B. subtilis* GP193 that expresses the *rny* gene under the control of a xylose-inducible promoter. In the absence of xylose, expression of *rny* is repressed and the bacteria are no longer viable (Commichau *et al.*, 2009). However, this might cause problems with the microarray results since the growth rate of the strain decreases upon removal of the inducer xylose. To avoid secondary effects due to the different growth rates of the two cultures to be compared, we characterized the growth and RNase Y amounts and activity of GP193 prior to the microarray experiments. Cells were cultivated and the optical densities of the cultures were recorded. Moreover, mRNA samples were taken and used for the analysis of *gapA* operon mRNA maturation that depends on the presence of functional RNase Y. These data (see supplementary material) allowed us to identify an early time point at which RNase Y was no longer sufficient for the processing of the *gapA* operon mRNA even though the growth rate was still identical to the culture grown in the presence of xylose. To verify the depletion of RNase Y at the chosen time point, we performed a Western blot analysis using antibodies raised against RNase Y. As shown in

Fig. 36, RNase Y was still detectable in cells grown without the inducer xylose; however, the amount of the protein was strongly reduced as compared to the cells grown in presence of xylose. Based on the significantly reduced amount of RNase Y and on the lack of processing of the *gapA* operon mRNA, the chosen time point enabled us to minimize secondary effects due to the different growth rate.

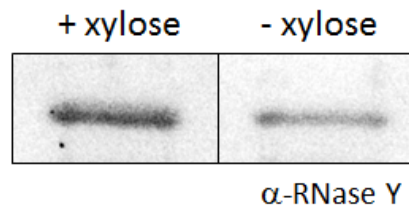


Fig. 36. Assay of RNase Y depletion. Crude extracts were prepared from *B. subtilis* GP193 grown in the presence or absence of the inducer xylose. Samples were harvested at the first sign of ceasing growth. After electrophoresis (12.5% SDS-PAGE) and transfer onto a PVDF membrane, RNase Y was detected by rabbit polyclonal antibodies raised against RNase Y from *B. subtilis*. 5 μ g of protein extract were applied per lane.

The role of RNase Y in global gene expression

Our transcriptome analysis revealed that a total of about 900 mRNAs were affected in abundance by the very stringent growth criteria applied in our experiments. In detail, 550 mRNAs showed significantly increased abundance, whereas 350 mRNAs were reduced in their steady-state levels. A compilation of the respective genes is provided in the supplementary data. This list was created based on a cut-off value of 1.5 that was selected to facilitate comparison to similar studies with *E. coli* RNase E (Lee *et al.*, 2002; Stead *et al.*, 2011). The observation that RNase Y affects the mRNA turnover on such a global scale is in good agreement with the previous report that RNase Y depletion results in stabilization of bulk mRNA (Shahbabian *et al.*, 2009).

To condense the extensive catalogue of 900 affected genes to those that are most severely controlled by RNase Y; we compiled all mRNAs with a factor of control of more than 2.5. The corresponding RNAs (see Table 4) are likely to be major targets of RNase Y. As expected, we found the *cggR-gapA* transcript in this list, which was already shown to be strongly regulated by RNase Y (Commichau *et al.*, 2009). Among the operons with increased mRNA amounts were also the *trp* operon as well as a part of the folate operon (*pabAC*) that are both controlled by a TRAP-dependent RNA switch (see below). The members of the MalR regulon that are required for the uptake and utilization of malate (Tanaka *et al.*, 2003) constitute another set of genes that were overexpressed in the

absence of RNase Y. Among the operons expressed at lower levels in the absence of RNase Y, three SinR-controlled transcription units involved in biofilm formation are most notable. These are the *eps* operon for the biosynthesis of the extracellular matrix polysaccharide (Kearns *et al.*, 2005), the *tapA-sipW-tasA* operon encoding the matrix protein as well as the assembly factor for the TasA amyloid fibers (Kolodkin-Gal *et al.*, 2010; Romero *et al.*, 2010; Romero *et al.*, 2011) and the *slrR* gene. The SlrR protein is an antagonist of SinR and at the same time a transcription repressor of genes involved in autolysis (Chai *et al.*, 2010b). In addition, mRNAs of several genes that are part of the offensive and defensive potential of *B. subtilis* cells were less abundant as a result of RNase Y depletion. These are the *sunT-bdbA-yolJ* operon required for maturation and export of the lantibiotic sublancin (Paik *et al.*, 1998) as well as the *sdpABC* operon required for the cannibalism of siblings at the onset of sporulation (González-Pastor *et al.*, 2003). Moreover, the product of the *ydg* gene controls the activity of the LiaRS two-component system which in turn controls the expression of genes that confer protection of *B. subtilis* against antibiotics (Butcher *et al.*, 2007).

The promoter of the *yndB* gene that is located downstream of *rny* has not been characterized. Therefore, we could not exclude the possibility that the effects observed in the transcriptome analysis were due to polar effects on the expression of *yndB*. To verify the results and to rule out the implication of *yndB*, we constructed strain *B. subtilis* GP1015. In this strain, *yndB* is ectopically expressed from the constitutive *pgk* promoter, and RNase Y can be depleted since its gene is under control of a xylose-controlled promoter. RNA of GP1015 cultivated in minimal medium in the presence or absence of the inducer xylose (resulting in presence or depletion of RNase Y, respectively) was isolated and used for quantitative reverse transcription RT-PCR of several genes that are subject to positive or negative control by RNase Y. The results are in excellent agreement with those obtained in the transcriptome analysis (see supplemental material chapter). These findings thus confirm the microarray study and indicate that *yndB* has no or only a minor impact on the altered mRNA amounts of the twelve selected genes.

Table 4. Effect of RNase Y depletion on the expression of *B. subtilis* genes and operons

Transcription unit ¹	Function ²	Remarks	Fold regulation upon RNase Y depletion
mRNAs with increased amounts upon depletion of RNase Y			
<i>trpEDCFBA-hisC-tyrA-aroE</i>	tryptophan and aromatic amino acid biosynthesis	controlled by TRAP-dependent RNA switch	13.1
<i>yhbIJ-yhcABCDEFGHI</i>	unknown, may be involved in drug resistance and export		7.1
<i>ysbAB</i>	unknown		6.8
<i>yrhG</i>	similar to formate dehydrogenase		5.2
<i>maeA-ywkB</i>	malic enzyme	activated by MalR	4.7
<i>nhaC</i>	Na ⁺ /H ⁺ antiporter		4.5
<i>guaC</i>	GMP reductase		3.5
<i>ydaB</i>	unknown		3.5
<i>maeN</i>	malate transporter	activated by MalR	3.4
<i>cimH</i>	citrate/ malate transporter		3.3
<i>ynfC</i>	unknown		3.3

<i>yrhED</i>	formate dehydrogenase		3.2
<i>yjbC-spx</i>	regulation of stress responses		3.1
<i>yrhF</i>	unknown		3.0
<i>speD</i>	S-adenosylmethionine decarboxylase		3.0
<i>yhfH</i>	unknown		2.9
<i>pabAC</i>	biosynthesis of folate and tryptophan	controlled by TRAP- dependent RNA switch	2.9
<i>yebC</i>	unknown		2.9
<i>yurRQ-frIBONMD</i>	utilisation of sugar amines		2.8
<i>yuxJ</i>	similar to multidrug efflux transporter		2.8
<i>lmrAB</i>	resistance to lincomcin		2.7
<i>yrhH</i>	similar to methyltransferase		2.7
<i>acoABCD</i>	acetoin dehydrogenase		2.7
<i>ribU</i>	riboflavin transporter	controlled by riboswitch (FMN-box)	2.7
<i>pbpA</i>	penicillin-binding protein 2A		2.6
<i>ytdI</i>	NAD kinase		2.6

<i>cggR-gapA</i>	central glycolytic regulator, glyceraldehyde 3-phosphate dehydrogenase		2.5
<i>yhdY</i>	mechanosensitive channel (small conductivity)		2.5
<i>ywcl</i>	unknown		2.5
<i>yflS</i>	malate transporter	activated by MalR	2.5
prophage SP β genes ³	prophage SP β		
<i>yorW</i>			4.4

mRNAs with decreased amounts upon depletion of RNase Y

<i>slrR</i>	transcriptional regulator of biofilm formation and motility	repressed by SinR	0.2
<i>epsA-O</i>	extracellular polysaccharide synthesis	repressed by SinR	0.2
<i>ctaO</i>	minor heme O synthase		0.3
<i>lip</i>	extracellular lipase		0.3
<i>sunT-bdbA-yolJ</i>	maturation and export of sublancin		0.3
<i>yydFGHIJ</i>	control of LiaRS activity		0.3
<i>tapA-sipW-tasA</i>	biofilm formation	repressed by SinR	0.4
<i>dhbACEBF</i>	bacillibactin biosynthesis		0.4

<i>thrZ</i>	minor threonyl tRNA synthetase	controlled by T-box	0.4
<i>yfmG</i>	unknown		0.4
<i>sdpABC</i>	cannibalism of siblings		0.4
<i>wprA</i>	cell wall-associated protein		0.4
<i>yxeKLM</i>	unknown, involved sulphur metabolism		0.4
<i>yxbB</i>	unknown		0.4

¹ Genes with factors ≥ 2.5 are shown in boldface.

² Functional information is based on the *SubtiWiki* database (Lammers *et al.*, 2010).

³ In addition to *yorW*, 29 other SP β prophage genes met the stringency criterium (> 2.5 fold regulation). For details of RNase Y-responsive SP β genes (Lazarevic *et al.*, 1999) see supplementary material.

.

Transcription analysis of mRNAs that are stabilized in the absence of RNase Y

Our microarray analysis undoubtedly showed that RNase Y is a global acting RNase in *B. subtilis*. The very nature of RNase Y as an endoribonuclease suggested that depletion of the enzyme would result in a significant stabilization of the corresponding mRNAs. Therefore, we compared the steady state abundance and the stabilities of a selected set of target mRNAs. For this analysis, we picked the bicistronic operon *yjbC-spx* encoding the transcriptional regulator Spx, the long *yhbIJ-yhcABCDEFGHI* gene cluster encoding proteins of unknown functions and the *gapB-speD* operon encoding the S-adenosylmethionine decarboxylase SpeD.

The Northern blot analysis using a riboprobe directed against *spx* showed signals corresponding to the bicistronic *yjbC-spx* and the monocistronic *spx* mRNA. Half-life time determinations for the monocistronic *spx* mRNA revealed a sixfold stabilization of the transcript in cells depleted for RNase Y (Fig. 37A). The *yhbIJ-yhcABCDEFGHI* gene cluster was investigated using an *yhbI* specific riboprobe. We detected a large mRNA of about 7.9 kb that corresponds to the complete *yhbIJ-yhcABCDEFGHI* operon. This polycistronic mRNA was stabilized tenfold in cells depleted for RNase Y (see Fig. 37B). For the *gapB-speD* operon we only detected a strong signal of about 400 bases that corresponds to a monocistronic *speD* mRNA. The reason is the tight repression of the promoter in front of *gapB* due to the presence of glucose in the medium. Therefore transcription is only driven by the internal SigA-dependent promoter. As shown in Fig. 37C, the half-life of the *speD* mRNA is strongly increased in cells depleted for RNase Y (from 1.4 min to 36 min).

We wondered, whether the strong stabilization of the three mRNAs tested thus far (the *speD* mRNA is stabilized more than 20 fold) was specific for these RNase Y targets or whether it reflects a general phenomenon. Therefore, we selected three additional targets of RNase Y (*guaC*, *ydaB*, *ynfC*) which all are likely to be monocistronic and appear in elevated amounts upon *rny* depletion in the microarray analysis. As for the targets described above these three transcripts showed not only increased amounts but also had prolonged half-life times (see Fig. 37D). In the case of *ynfC* and *ydaB*, the half-lives were increased to 50 and 80 min, respectively, upon RNase Y depletion!

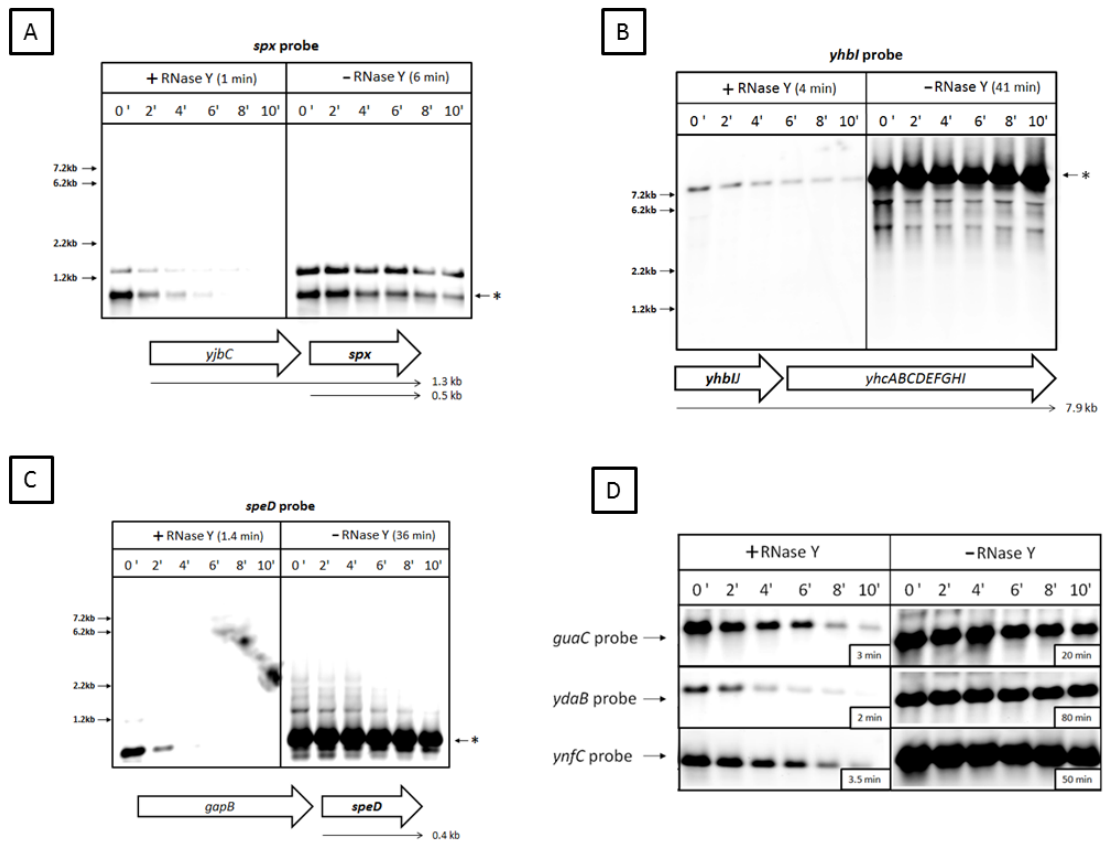


Fig. 37. Effects of RNase Y on the stability of the *spx* (A), *yhbI* (B), *speD* (C) transcripts as well as of the *guaC*, *ydaB* and *ynfC* (D) mRNAs. Total RNA was isolated from a *Pxyl-rny* strain in the presence and absence of xylose. RNA was prepared from cells grown in minimal medium supplemented with 0.5% glucose before (0') and after the addition of rifampicin (2, 4, 6, 8 and 10 min). 5 µg of total RNA was loaded per lane. The time in brackets indicates the half-life of the transcript marked with the asterisk. A schematic illustration of the operon structure is given below each Northern blot. For (D) no illustration is provided, as all transcripts are monocistronic.

Taken together, all Northern blot analyses were in excellent agreement with the transcriptome analysis thus validating the implication of RNase Y in the control of a large set of mRNAs for genes with different physiological functions. The strong stabilization of all tested mRNAs in the cells depleted for RNase Y is remarkable and supports the crucial role of RNase Y in the mRNA turnover of *B. subtilis*.

Effect of RNase Y depletion on the tryptophan operon

The *trp* operon mRNA encoding enzymes for the biosynthesis of tryptophan was the most positively affected target found in the microarray analysis. Furthermore, RNase Y depletion also affected the abundance of the folate operon mRNA. Both operons are

controlled by the RNA-binding protein TRAP. Therefore, we investigated the impact of RNase Y on the tryptophan and folate operons by Northern blot analysis.

First, we focused on the *trp* operon. It was reported that transcription initiated at the *aroH* promoter might extend into the TRAP-controlled genes (Gollnick *et al.*, 2005). Therefore, we used a probe specific for *aroB* to detect the transcripts. However, we only detected an mRNA of 2.8 kb (see Fig. 38A). No read-through into the downstream genes was observed in our experiments. With a probe specific for *trpE*, no signals for the tryptophan operon were observed in the wild type strain 168 as well as in *B. subtilis* GP193 under conditions that allow RNase Y expression. The absence of *trp* mRNA might result from the presence of tryptophan in the medium that causes TRAP-mediated transcription termination. In contrast, strong signals were observed upon depletion of RNase Y (see Fig. 38B). The significant accumulation of the *trp* operon mRNA in the Northern blot confirms the data obtained by transcriptome and qRT-PCR analyses presented above. Two large transcripts were observed with the *trpE* probe in the absence of RNase Y. The smaller signal of about 6 kb corresponds to the hexacistronic *trpEDCFBA*. Since no read-through was observed from the upstream *aroFBH* operon, the larger 9.7 kb transcript most likely corresponds to the nonacistronic *trpEDCFBA hisC tyrA aroE* mRNAs (see Fig. 4 B, D). The idea of read-through into the *hisC tyrA aroE* genes is supported by a Northern blot experiment with a *tyrA*-specific riboprobe. For this probe, a prominent 3.7 kb transcript corresponding to the tricistronic *hisC tyrA aroE* mRNA and the 9.7 kb transcript of the nonacistronic *trpEDCFBA hisC tyrA aroE* mRNA were present in increased amounts upon depletion of RNase Y (see Fig. 38C, D). Moreover, a signal of about 7 kb might correspond to a read-through transcript that originated at the *hisC* promoter.

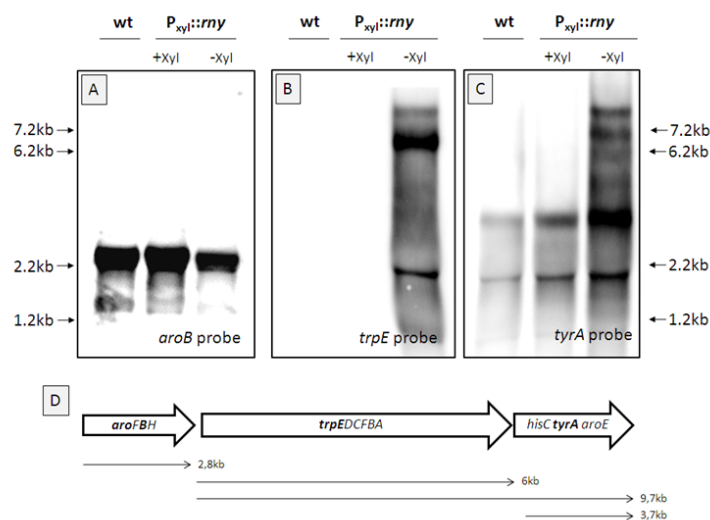


Fig. 38. RNase Y depletion affects the stability of the *trp* super-operon mRNA. Northern blot analyses to test the effect of RNase Y depletion on the expression of different mRNAs species of the aromatic amino biosynthesis super-operon. The *rny* gene was placed under control of a xylose-inducible promoter. The strain *B. subtilis* GP1015 was grown in CSE minimal medium containing 0.5% glucose in the presence (+) and in the absence (-) of xylose. The transcripts were detected with riboprobes specific for *aroB* (A), *trpE* (B), and *tyrA* (C). (D) Schematic illustration of the aromatic amino biosynthesis super-operon.

Under the conditions employed thus far (medium containing tryptophan), we were unable to determine the half-life of the *trp* operon mRNAs in the wild type strain due to their immediate degradation. Therefore we used *B. subtilis* GP1090 that is prototrophic for tryptophan and omitted the amino acid from the medium. As expected, the omission of tryptophan resulted in the induction of the *trp* operon. Unfortunately, we were unable to detect discrete bands needed for half-life determination (see supplementary Figure S2). A *trp* operon mRNA smear was previously observed and suggested to result from degradation or premature termination (Deikus *et al.*, 2004). Even though we were unable to determine the specific half-life, the *trp* mRNA is obviously strongly stabilized upon depletion of RNase Y (see supplementary Figure S2). Similarly, strong stabilization could also be observed for the *pabA* (folate) operon mRNA, the second TRAP controlled mRNA found in the microarray analysis to be positively affected by RNase Y depletion. We determined a 20-fold stabilization of the full-length folate operon transcript in cells depleted for RNase Y (for further details see supplementary Figure S2 in the supplementary chapter).

Effect of RNase Y depletion on the processing of the *thrS* mRNA

RNase Y was originally described as being responsible for the processing of the *gapA* operon mRNA and for the maturation of the *yitJ* S-box leader mRNA (Commichau *et al.*, 2009; Shahbadian *et al.*, 2009). Processing of an mRNA containing a secondary structure at the 5' end was also observed for the T-box of the *thrS* mRNA. While *in vitro* data suggested that RNase J1 is responsible for this processing event, this idea is not supported by *in vivo* data (Condon & Bechhofer, 2011; Even *et al.*, 2005). To address the possible implication of RNase Y in this processing event, we performed Northern blot analyses for the *thrS* gene encoding the major threonyl-tRNA synthetase. For this gene, we observed two transcripts corresponding to the primary non-processed RNA and a shorter mature transcript (Fig. 39). While the larger primary transcript (marked with an asterisk in Fig. 39) disappeared rapidly in the presence of RNase Y (+ xylose), it remained

prominent in the absence of RNase Y (Fig. 39). The mature mRNA was the major transcript in the presence of RNase Y even under steady-state conditions (0 min, Fig. 39); in contrast, the non-processed transcript was dominating in the absence of RNase Y. The half-lives of the primary mRNAs were 1.2 and 3.7 min. Thus, RNase Y is required for the processing of the *thrS* mRNA *in vivo*.

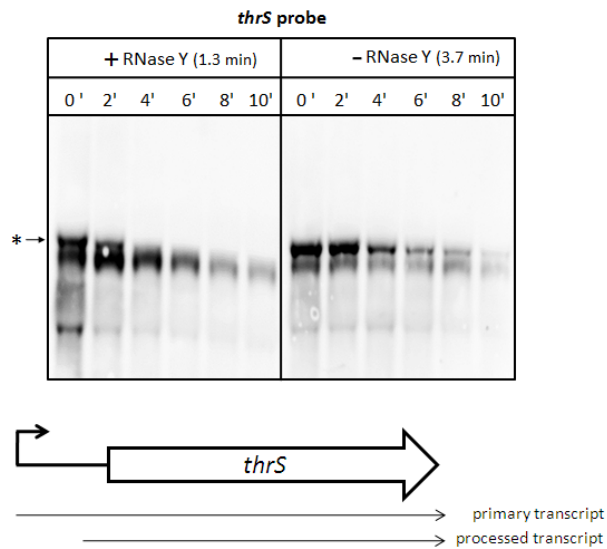


Fig. 39. Influence of RNase Y on the maturation of the *thrS* mRNA. Northern Blot analysis to demonstrate the influence of RNase Y on the processing and stability of the *thrS* mRNA. RNA was isolated from a *Pxyl-rny* strain in the presence and absence of xylose. RNA was prepared from cells grown in minimal media supplemented with 0.5% glucose before (0') and after the addition of rifampicin (2, 4, 6, 8 and 10 min). 5 μ g of total RNA was loaded per lane. A schematic illustration of the primary and processed mRNAs is shown below the Northern blot.

The implication of RNase Y in biofilm formation

Most of the genes involved in biofilm formation exhibited a reduced expression upon RNase Y depletion. As a representative of these genes, we analysed the transcription of the *tapA-sipW-tasA* locus. These genes were suggested to form an operon (Stöver & Driks, 1999); however, no Northern blot analyses have so far been reported. Our data confirm the expression as a three-cistronic operon (represented by two mRNA species of 2.5 and 2.1 kb) (see Fig. 40A), moreover, we detected a minor two-cistronic *tapA-sipW* mRNA of 1.6 kb. Upon depletion of RNase Y, the two smaller transcripts disappeared whereas the intensity of the signal for the largest mRNA was reduced.

Intuitively, one would expect stabilization of specific mRNAs rather than reduced amounts upon depletion of an RNase. To address this issue, we re-consulted the results of

the transcriptome experiments and noticed that the amount of the *sinR* mRNA that encodes the repressor of the biofilm operons was increased upon RNase Y depletion (1.4-fold). To verify the altered *sinR* expression, we again performed Northern blot analyses. Three transcripts were detected with the *sinR* probe, a major monocistronic *sinR* mRNA, and two minor transcripts, a bicistronic *sinIR* mRNA and a tricistronic *yqhG sinIR* mRNA (see Fig. 40B). As visible in Fig. 40B, the amounts of the bicistronic *sinIR* and the monocistronic *sinR* mRNAs were increased upon depletion of RNase Y, and the half-life of the latter, major transcript was increased from 3.5 to 13 min. This increased expression of SinR might result in stronger repression of the biofilm operons, and thus in reduced expression of the biofilm genes without directly affecting the stability of these transcripts.

Since depletion of RNase Y resulted in reduced expression of the two major operons required for biofilm formation, we were interested in the effect of overexpression of RNase Y. To address this problem, we expressed the *rny* gene under the control of a strong promoter in *B. subtilis* 168. The high-level expression of RNase Y in this strain carrying the expression vector pGP1201 was verified by Western blot analysis using antibodies raised against RNase Y (data not shown). As expected, the laboratory strain 168 carrying the empty vector pBQ200 did not form complex colonies. In contrast, the strain expressing large amounts of RNase Y formed complex colonies even in the genetic background of the laboratory strain (see Fig. 40C). Thus, depletion of RNase Y results in reduced amounts of biofilm gene mRNAs whereas overexpression of RNase Y is sufficient to cause biofilm formation.

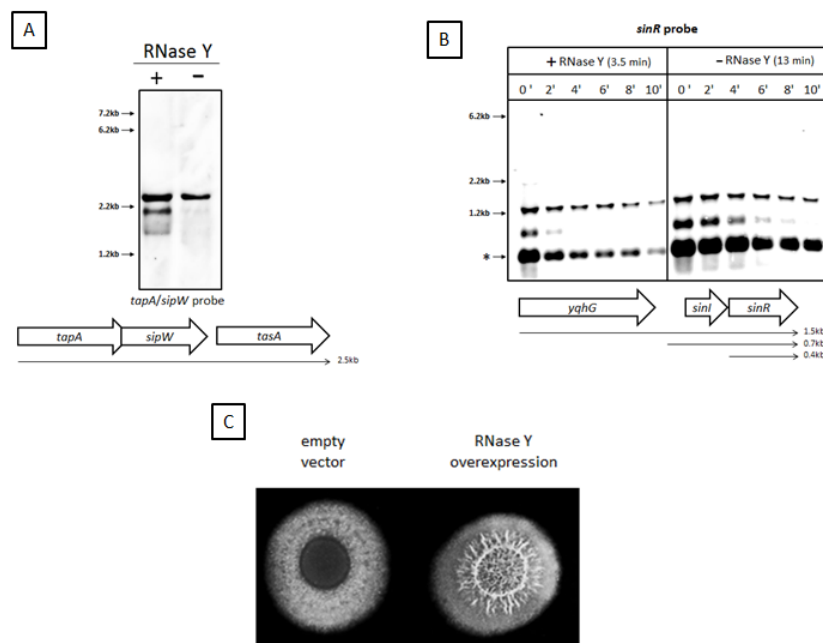


Fig. 40. Implication of RNase Y in biofilm formation. (A) Northern blot analyses to verify the decreased amount of the *tapA* biofilm operon due to RNase Y depletion. The *rny* gene was placed under control of a xylose-inducible promoter. This strain was grown in minimal medium containing 0.5% glucose in the presence (+) and in the absence (-) of xylose. The transcripts were detected with riboprobes specific for *tapA/sipW*. A schematic illustration of the genetic organization of the gene locus is given below the Northern blot. (B) Depletion of RNase Y stabilizes the *sinR* mRNA. Conditions were as described in (A). Rifampicin was added at the indicated time points. Time in brackets shows the half-life time of the transcript marked with the asterisk. (C) RNase Y overexpression leads to increased biofilm formation. Phenotypic characterization of the wild type 168 harbouring the empty expression vector pBQ200 and a *rny* overexpression plasmid (pGP1201). Both colonies were spotted on MSgg agar plates.

Transcription analysis of mRNAs that are less abundant upon depletion of RNase Y

Among the mRNAs that were present in reduced amounts after depletion of RNase Y (see Table 1), we selected the *lip* gene and the *sunT-bdbA-yolJ-bdbB* operon in addition to the biofilm operon *tapA-sipW-tasA* for a more detailed analysis.

As shown in Fig. 41, two transcripts were observed with a probe specific for the *lip* gene encoding an extracellular lipase. The shorter 0.7 kb mRNA corresponds to a monocistronic *lip* transcript whereas the larger 2.4 kb mRNA may represent a bicistronic *lip-yccF* operon. Such an operon including a portion forming an antisense transcript to *yczC* gene has been observed in large-scale transcriptome studies (Mäder, unpublished results). Depletion of RNase Y resulted in a reduced accumulation of both transcripts. The reduced expression was accompanied by a reduced mRNA stability upon RNase depletion (10 min vs. 19 min for the *lip-yccF* mRNA). The amount of the *yccF* gene mRNA was not altered in the transcriptome experiment. This may result from the presence of an additional promoter directly upstream of *yccF* (Mäder, unpublished results).

The *sunT-bdbA-yolJ-bdbB* operon was only weakly expressed under the conditions used in this study. This may be due to the dependence of this operon on activation by YvrHb (Serizawa *et al.*, 2005). However, the expression of the full-length 4.4 kb mRNA as well as of a monocistronic *sunT* transcript was clearly reduced in the absence of RNase Y (see Fig. 41B). Due to the complete absence of this mRNA when RNase Y was depleted, we were unable to determine the RNA stability of this transcript.

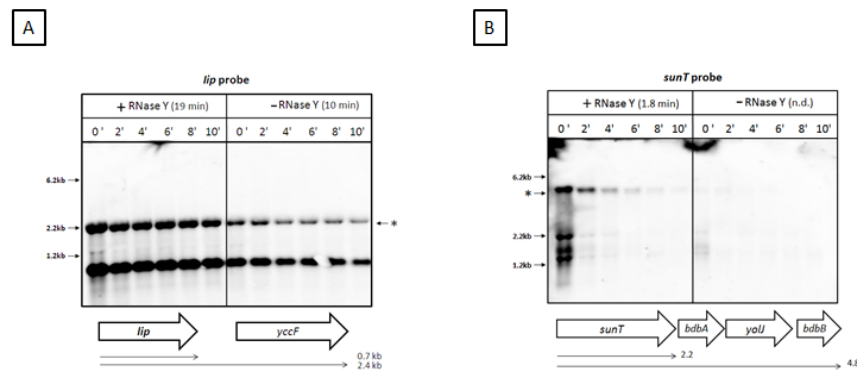


Fig. 41. Effects of RNase Y on the stability of different mRNAs. Stability of the *lip* (A) and *sunT* (B) transcripts isolated from a *Pxyl-rny* strain in the presence and absence of xylose. RNA was prepared from cells grown in minimal media supplemented with 0.5% glucose before (0') and after the addition of rifampicin (2, 4, 6, 8 and 10 min). 5 μ g of total RNA was loaded per lane. Time in brackets indicate the half-life time of the transcript marked with the asterisk (n.d., not detectable). A schematic illustration of the operon structures is shown below the Northern blots.

Discussion

With this study, we establish the role of RNase Y in global control of mRNA stability in *B. subtilis*. Our transcriptome analysis revealed that depletion of RNase Y affects the abundance of about 900 mRNAs. Furthermore, the determination of mRNA half-lives revealed strongly increased stabilities of the selected target mRNAs upon RNase Y depletion (see Fig. 37). To the best of our knowledge, RNase Y is unique in *B. subtilis* with respect to its quantitative and qualitative impact on global mRNA turnover as judged from the number of targets and the impact on stability of individual RNAs. These findings are in very good agreement with the observation that RNase Y is involved in bulk mRNA degradation (Shahbadian *et al.*, 2009). The substantial stabilization of several of the selected mRNA targets from half-lives of less than five minutes to more than 30 minutes as observed for the *spx*, *speD*, or *ydaB* transcripts (see Fig. 37) suggests that the contribution of RNase Y to the turnover of these transcripts is crucial. It is interesting to note that RNase Y shares its major role in bulk mRNA degradation with the *E. coli* RNase E; whereas loss of RNases J1 and J2 results in minor bulk mRNA stabilization (Babitzke & Kushner, 1991; Even *et al.*, 2005).

RNase Y was initially discovered because of its role in the processing of the mRNA of the glycolytic *gapA* operon and the *yitJ* leader mRNA (Commichau *et al.*, 2009; Shahbadian *et al.*, 2009). In this work, we extend the set of mRNAs that require RNase Y for processing: the maturation of the *thrS* mRNA is also dependent on RNase Y. As

observed for the *gapA* operon, the primary transcript accumulates upon depletion of RNase Y (see Fig. 39). The *thrS* mRNA contains a threonine-responsive structure, the T-box at its 5' end. If the concentration of threonine is low, uncharged tRNA^{Thr} binds to the T-box thus causing the formation of an antitermination structure that allows transcription of the complete gene. This antitermination structure is then cleaved to allow the formation of a stem at the very 5' end of the mature RNA. It is well established that the generation of such 5' stem structures by mRNA processing results in a substantial stabilization of their mRNAs and this is also the case for the *thrS* transcript (Condon *et al.*, 1996; Homuth *et al.*, 1999; Ludwig *et al.*, 2001). When transferred to *E. coli*, the *thrS* mRNA is processed by RNase E (Condon *et al.*, 1997). *In vitro* experiments indicated that RNase J1 might be responsible for the cleavage of the *thrS* mRNA (Even *et al.*, 2005), however, this idea is not supported by *in vivo* evidence and the implication of RNase Y in this processing event was discussed (Condon & Bechhofer, 2011; Mäder *et al.*, 2008). Indeed, this work provides the evidence for this hypothesis.

Another interesting result of this study is the observation that two mRNAs that are required for the synthesis of tryptophan biosynthetic enzymes and that are under the control of the RNA-binding protein TRAP, are also more stable in the absence of RNase Y. It has previously been shown that degradation of the leader mRNA of the *trp* operon is necessary to recycle the TRAP protein (Deikus *et al.*, 2004). This degradation process involves both RNase J1 and polynucleotide phosphorylase (Deikus *et al.*, 2008). Here, we provide evidence that RNase Y is an essential component of the degradation of the *trp* operon mRNA. Moreover, our work extends this observation to the *pabAC* mRNA (see Fig. 38). Interestingly, the first gene of this operon is *pabB*, but the termination protein TRAP binds between the *pabB* and *pabA* coding region resulting in control of *pabAC* transcription in response to tryptophan availability (de Saizieu *et al.*, 1997). Depletion of RNase Y strongly affects the *pabA* and *pabC* transcripts but not the promoter-proximal *pabB* mRNA (see Table 1; Fig. S2). This suggests that the RNA switch that is the target of TRAP might also be targeted by RNase Y, and that this processing might also serve to recycle the bound TRAP protein. An effect of RNase Y depletion on TRAP expression and/or activity might provide an alternative explanation for our observations. However, this is highly unlikely since neither the *mtrB* nor the *rtpA* genes encoding TRAP and its antagonist, respectively, are affected by the depletion of RNase Y. Thus, RNase Y seems to play a direct role in the processing of these transcripts.

Among the mRNAs that are present in reduced amounts in the absence of RNase Y are three transcripts that are controlled by the transcription factor SinR. The genes of the

SinR regulon encode all proteins necessary for biofilm formation (Chu *et al.*, 2006). The fact that these mRNAs were less abundant when RNase Y was depleted suggested an indirect effect. This idea is supported by the observation that the mRNA of the *tapA-sipW-tasA* operon is even more stable upon RNase Y depletion even though the amounts of the transcript are reduced (our unpublished results). This prompted us to investigate the stability of the *sinR* mRNA. As shown in Fig. 40, the monocistronic *sinR* mRNA was substantially more stable, thus allowing the production of higher amounts of the SinR repressor protein. This may allow titration of the SinR antagonists SinI and SlrR and ultimately result in stronger repression of the SinR-controlled genes. If depletion of RNase Y results in stronger repression of biofilm genes, one might hypothesize that overexpression of the *rny* gene might lead to higher expression of these genes. Indeed, we observed that the laboratory strain *B. subtilis* 168 was able to form complex colonies when RNase Y was highly expressed. This observation is in excellent support of the idea that RNase Y plays a crucial role in biofilm formation, one of the major lifestyles of *B. subtilis*.

Given the strong impact of RNase Y on mRNA turnover in *B. subtilis*, it is tempting to speculate about the essential nature of the enzyme. Among the about 900 target mRNAs are 43 that code for essential functions (highlighted in the supplementary material). Out of these RNAs, seven exhibit reduced amounts when RNase Y is depleted. The corresponding genes are excellent candidates for being causal for RNase Y essentiality. Interestingly, RNase Y depletion resulted in decreased amounts of three out of the 28 aminoacyl tRNA synthetases, and five additional tRNA synthetases are just 0.1 points below the threshold. Thus, the essential loading of tRNAs might be limited upon *rny* depletion. In addition to the aminoacyl tRNA synthetases, the RNAs for the genes of the *resABCDE* operon were significantly less abundant when RNase Y was depleted. The products of the *resB* and *resC* genes are essential for the viability of *B. subtilis*; they are required for cytochrome c biogenesis (Le Brun *et al.*, 2000). Finally, the mRNA corresponding to the essential *pdhA* gene was present in reduced amounts upon depletion of RNase Y. The product, PdhA, is the alpha subunit of the Enzyme 1 of pyruvate dehydrogenase, the enzyme that links glycolysis to the citric acid cycle.

While our results are compatible with the conclusion, that one or more of the above-mentioned essential targets of RNase Y cause the indispensability of the enzyme, a different explanation is possible and also in agreement with the data presented here: The Northern blot analyses of several RNase Y targets revealed an extreme stabilization of transcripts to more than one hour upon depletion of RNase Y (see Fig. 37). Such a strong stabilization may easily compromise the fine-tuned balance of mRNA synthesis and decay

and in turn interfere with the cell's viability. Actually, it seems quite plausible that the impact of RNase Y on so many targets might impair the physiology of the cell.

With the results presented in this work, it is obvious that RNase Y is a key player in RNA degradation and processing in *B. subtilis*. This is supported by the fact that the *rny* gene is essential. This and previous work suggests that RNase Y might be a functional analog of RNase E in *E. coli*: both RNases are involved in the control of bulk mRNA stability and the accumulating evidence suggests that both prefer AU-rich sequences in the vicinity of double-stranded structures (Bessarab *et al.*, 1998; Commichau *et al.*, 2009; Ludwig *et al.*, 2001; Meinken *et al.*, 2003; Shahbadian *et al.*, 2009). Moreover, both RNases are located at the cytoplasmic membrane (Hunt *et al.*, 2006; Khemici *et al.*, 2008; Lehnik-Habrink *et al.*, 2010; Liou *et al.*, 2001; Zweers *et al.*, 2009). Finally, they are capable of interacting with different exoribonucleases, RNA helicases and glycolytic enzymes, and do thus form the core of RNA degrading complexes (Carpousis, 2007; Commichau *et al.*, 2009; Lehnik-Habrink *et al.*, 2010). The analysis of the interactions of RNase Y and its partners at the molecular level, the identification of precise target sequences/structures, and the elucidation of the essential role of RNase Y will be important tasks for future research.

Acknowledgements

We are grateful to Fabian M. Commichau and Sebastian Hübner for helpful discussions in the initial phase of this project. This work was supported by grants of the Deutsche Forschungsgemeinschaft (SFB860), the Federal Ministry of Education and Research SYSMO network (PtJ-BIO/0315784B and 0315784A) and the Fonds der Chemischen Industrie to J. S..

Experimental procedures

B. subtilis strains and growth conditions - All *B. subtilis* strains used in this work are derived from the laboratory wild type strain 168. *B. subtilis* was grown in LB medium and in CSE minimal medium containing succinate and glutamate/ ammonium as basic sources of carbon and nitrogen, respectively (Wacker *et al.*, 2003). The medium was supplemented with auxotrophic requirements (at 50 mg/l) and glucose as indicated. Plates were prepared by the addition of 17 g Bacto agar/l (Difco) to the liquid medium.

DNA manipulation and transformation - *E. coli* DH5 α (Sambrook *et al.*, 1989) was used for cloning experiments. Transformation of *E. coli* and plasmid DNA extraction were

performed using standard procedures (Sambrook *et al.*, 1989). Restriction enzymes, T4 DNA ligase and DNA polymerases were used as recommended by the manufacturers. DNA fragments were purified from agarose gels using the Nucleospin Extract kit (Macherey and Nagel, Germany). *Phusion* DNA polymerase was used for the polymerase chain reaction as recommended by the manufacturer. All primer sequences are provided in the supplementary chapter. DNA sequences were determined using the dideoxy chain termination method (Sambrook *et al.*, 1989). All plasmid inserts derived from PCR products were verified by DNA sequencing. Chromosomal DNA of *B. subtilis* was isolated as described (Wacker *et al.*, 2003).

Transformation and phenotypic analysis - Standard procedures were used to transform *E. coli* (Sambrook *et al.*, 1989) and transformants were selected on LB plates containing ampicillin (100 µg/ml). *B. subtilis* was transformed with plasmid or chromosomal DNA according to the two-step protocol described previously (Kunst & Rapoport, 1995). Transformants were selected on SP plates containing chloramphenicol (Cm 5 µg/ml), kanamycin (Km 5 µg/ml), spectinomycin (Spc 100 µg/ml), or erythromycin plus lincomycin (Em 1 µg/ml and Lin 10 µg/ml).

In *B. subtilis*, amylase activity was detected after growth on plates containing nutrient broth (7.5 g/l), 17 g Bacto agar/l (Difco) and 5 g hydrolyzed starch/l (Connaught). Starch degradation was detected by sublimating iodine onto the plates.

Quantitative studies of *lacZ* expression in *B. subtilis* were performed as follows: cells were grown in CSE medium supplemented with different carbon and nitrogen sources as indicated. Cells were harvested at OD₆₀₀ of 0.6 to 0.8. β-Galactosidase specific activities were determined with cell extracts obtained by lysozyme treatment as described previously (Kunst & Rapoport, 1995). One unit of β-galactosidase is defined as the amount of enzyme which produces 1 nmol of o-nitrophenol per min at 28° C.

For colony architecture analysis, bacteria were precultured in LB to an OD₆₀₀ of about 0.6. 10 µl of this culture were then spotted onto MSgg medium (Branda *et al.*, 2001) containing 1.5% agar and incubated at room temperature for four days.

Plasmids - Plasmid pAC7 (Weinrauch *et al.*, 1991) was used to construct a translational fusion of the *rny* control region with the *lacZ* gene. For the construction of plasmid pGP459 containing a *rny-lacZ* fusion, the region upstream of *rny* was amplified using the oligonucleotides SHU70/SHU71. The PCR product was digested with *EcoRI* and *BamHI* PCR and cloned into pAC7 linearized with the same enzymes.

Plasmid pGP774 (Commichau *et al.*, 2009) was used to construct strains allowing depletion of RNase Y due to a fusion of the corresponding *rny* gene to a xylose-regulated promoter. Plasmid pGP1354 for the ectopic expression of *ymdB* was obtained by cloning of the *EcoRI/ BamHI* fragment of plasmid pGP1062 (Diethmaier *et al.*, 2011) into pAC7 (Weinrauch *et al.*, 1991).

For high-level expression of RNase Y in *B. subtilis*, we constructed plasmid pGP1201. For this purpose the *rny* gene was amplified with the primers FR6 and FR7 using chromosomal DNA of *B. subtilis* as a template. The PCR product was digested with *BamHI* and *Sall* and cloned into the overexpression vector pBQ200 (Martin-Verstraete *et al.*, 1994). All plasmids used in this study are listed in the supplementary Table S3.

Western blotting - For Western blot analysis, proteins were separated by 12.5% SDS-PAGE and transferred onto polyvinylidene difluoride (PVDF) membranes (Bio-Rad) by electroblotting. Rabbit anti-Rny polyclonal antibodies (1:50,000) (Zweers *et al.*, 2009) served as primary antibodies. They were visualized by using anti-rabbit immunoglobulin G-alkaline phosphatase secondary antibodies (Promega) and the CDP-Star detection system (Roche Diagnostics), as described previously (Commichau *et al.*, 2007).

Northern blot analysis - Preparation of total RNA and Northern blot analysis were carried out as described previously (Ludwig *et al.*, 2001). Digoxigenin (DIG) RNA probes were obtained by *in vitro* transcription with T7 RNA polymerase (Roche Diagnostics) using PCR-generated DNA fragments as templates. The primer pairs used to amplify DNA fragments specific for *aroB*, *cggR*, *gapA*, *lip*, *pabA*, *speD*, *spx*, *sunT*, *trpE*, *tyrA*, *yhbl*, and *tapA/sipW* are listed in the supplementary material chapter. The reverse primers contained a T7 RNA polymerase recognition sequence. *In vitro* RNA labelling, hybridization and signal detection were carried out according to the instructions of the manufacturer (DIG RNA labelling kit and detection chemicals; Roche Diagnostics). The sizes of the transcripts were estimated based on the transcripts of the *gapA* operon. On each gel, a RNA sample from a culture grown in CSE minimal medium containing glucose was separated and analysed with a probe specific for *gapA*. The sizes of the transcripts are 7.2, 6.2, 2.2, and 1.2 kb (Ludwig *et al.*, 2001). RNA stability was analyzed as described previously (Meinken *et al.*, 2003). Briefly, rifampicin was added to logarithmically growing cultures (final concentration 100 µg/ml) and samples were taken at the time points indicated. The quantification was performed using the Image J software v1.42 (Abramoff *et al.*, 2004).

Transcriptome analysis - Briefly, Cy3/ Cy5 labelled cDNA was synthesized from RNA samples obtained from cells expressing RNase Y and cells depleted for RNaseY, respectively, and hybridized competitively to custom-designed 44,000 feature microarrays manufactured by Agilent Technologies. Sample pairs from three independent cultivations were analyzed by using a dye-swap design resulting in a total of six hybridizations.

To deplete the essential RNase Y from strain GP193 (P_{xyI} -*rny*), exponentially growing cells were used to inoculate two cultures in CSE minimal medium to an optical density of 0.1. Of these cultures, one contained xylose whereas the other one was devoid of the inducer to achieve repression of the *rny* gene. Prior to inoculation, the bacteria were washed in CSE medium to avoid the input of xylose from the preculture. At the first sign of reduced growth of the culture without xylose (at around OD_{600} 0.8), the cells of both cultures were immediately harvested for RNA isolation.

Preparation of total RNA was carried out as described previously (Ludwig *et al.*, 2001). For transcriptome analysis, 35 μ g RNA were DNase-treated using the RNase-Free DNase Set (Qiagen) and purified using the RNA Clean-Up and Concentration Micro Kit (Norgen). The quality of the RNA preparations was assessed by means of the Agilent 2100 Bioanalyzer according to the manufacturer's instructions. Synthesis and purification of fluorescently labeled cDNA were carried out according to Charbonnier *et al.* with minor modifications (Charbonnier *et al.*, 2005). In detail, 10 μ g of total RNA were mixed with random primers (Promega) and spike-ins (Two-Color RNA Spike-In Kit, Agilent Technologies). The RNA/primer mixture was incubated at 70 °C for 10 min followed by 5 min incubation on ice. Then, the following reagents were added: 10 μ l of 5x First Strand Buffer (Invitrogen), 5 μ l of 0.1 M DTT (Invitrogen), 0.5 μ l of a dNTP mix (10 mM dATP, dGTP, and dTTP, 2.5 mM dCTP), 1.25 μ l of Cy3-dCTP or Cy5-dCTP (GE Healthcare) and 2 μ l of SuperScript II reverse transcriptase (Invitrogen). The reaction mixture was incubated at 42 °C for 60 min and then heated to 70 °C for 10 min. After 5 min on ice, the RNA was degraded by incubation with 2 units of RNaseH (Invitrogen) at room temperature for 30 min. Labeled cDNA was then purified using the CyScribe GFX Purification Kit (GE Healthcare) and hybridized to the microarray following Agilent's hybridization, washing and scanning protocol (Two-Color Microarray-based Gene Expression Analysis, version 5.5).

Data were extracted and processed using the Feature Extraction software (version 9.5, Agilent Technologies). For each gene on the microarray, the error-weighted average of

the log ratio values of the individual probes was calculated using the Rosetta Resolver software (version 7.2.1, Rosetta Biosoftware). Genes were considered as differentially expressed if the difference in the expression levels between cultures expressing RNase Y and depleted cultures was at least 1.5-fold.

The microarray data have been deposited in NCBI's Gene Expression Omnibus (GEO) database and are accessible through GEO Series accession number no. GSE30430.

Real time quantitative reverse transcription PCR - For RNA isolation, the cells were grown to an OD₆₀₀ of 0.5 – 0.8 and harvested. Preparation of total RNA was carried out as described previously (Ludwig *et al.*, 2001). cDNAs were synthesized using the One-Step RT-PCR kit (BioRad) as described (Rietkötter *et al.*, 2008). qRT-PCR was carried out on the iCycler instrument (BioRad) following the manufacturer's recommended protocol by using the primer pairs listed in Table S3. The *rpsE* and *rpsJ* genes encoding constitutively expressed ribosomal proteins were used as internal controls and were amplified with the primers *rpsE*-RT-*fwd*/*rpsE*-RT-*rev* and *rpsJ*-RT-*fwd*/*rpsJ*-RT-*rev*, respectively. Data analysis and the calculation of expression ratios as fold changes were performed as described (Rietkötter *et al.*, 2008). qRT-PCR experiments were performed in duplicate.

7. The role of YmdB in *Bacillus subtilis*

The results described in this chapter were published in:

Diethmaier, C., Pietack, N., Gunka, K., Wrede, C., **Lehnik-Habrink, M.**, Herzberg, C., Hübner, S. & Stülke, J. (2011). A Novel Factor Controlling Bistability in *Bacillus subtilis*: The YmdB Protein Affects Flagellin Expression and Biofilm Formation. *J Bacteriol.*

Author's contribution:

MLH contributed genetic material (plasmids and primers) used in this publication.

Abstract

Cells of *Bacillus subtilis* can either be motile or sessile, depending on the expression of mutually exclusive sets of genes that are required for flagellum or biofilm formation, respectively. Both activities are coordinated by the master regulator SinR. We have analysed the role of the previously uncharacterized *ymdB* gene for bistable gene expression in *B. subtilis*. We observed a strong overexpression of the *hag* gene encoding flagellin and of other genes of the σ^D -dependent motility regulon in the *ymdB* mutant, whereas the two major operons for biofilm formation, *tapA-sipW-tasA*, and *epsA-O*, were not expressed. As a result, the *ymdB* mutant is unable to form biofilms. An analysis of the individual cells of a population revealed that the *ymdB* mutant no longer exhibited bistable behaviour; instead all cells are short and motile. The inability of the *ymdB* mutant to form biofilms is suppressed by the deletion of the *sinR* gene encoding the master regulator of biofilm formation indicating that SinR-dependent repression of biofilm genes cannot be relieved in a *ymdB* mutant. Our studies demonstrate that lack of expression of SlrR, an antagonist of SinR, is responsible for the observed phenotypes. Overexpression of SlrR suppresses the effects of a *ymdB* mutation.

Introduction

Bacteria can live their lives in very different ways. In the laboratory, they are usually cultured as uniform populations of individual independent cells. However, in natural habitats the formation of aggregates, so-called biofilms, allows them to get better access to nutrients and to protect themselves against harmful substances such as toxins and antibiotics (Abee *et al.*, 2011; Stoodley *et al.*, 2002). Moreover, under difficult conditions of extreme nutrient limitation some bacteria such as the Gram-positive model organism *Bacillus subtilis* undergo a differentiation program and form dormant spores that can survive for decades.

In the last few years, it became obvious that cultivation of uniform single cells produces laboratory artefacts rather than providing meaningful insights into the real physiology of the bacteria. Instead, the formation of all kinds of cell complexes including biofilms seems to be much more representative for the life of bacteria in their natural environments (Kolter, 2010).

For *B. subtilis*, biofilm formation was discovered only a decade ago (Branda *et al.*, 2001). Moreover, it turned out that bacteria in liquid culture are not physiologically identical, but that individual cells can choose one fate or the other. This latter property is

referred to as bistability (Dubnau & Losick, 2006). In liquid cultures of *B. subtilis*, two types of cells can be observed: short motile cells and long non-motile cells. The motility correlates with the expression of the major flagellin, which is present only in the motile cells, but the different morphologies of the two cell types suggest that a larger set of genes is subject to bistable expression and that all these genes are controlled in a coordinate manner. Indeed, both biofilm formation and motility are controlled by a common regulator, the transcription factor SinR (see below).

The formation of flagella, motility and chemotaxis requires a set of genes that is under the control of the alternative RNA polymerase sigma factor, σ^D (Serizawa *et al.*, 2004). The activity of this sigma factor is modulated by a regulatory interaction with its antagonist, FlgM (Bertero *et al.*, 1999). Normally, σ^D is present in low amounts in the cell. Thus, the availability of σ^D is a limiting factor for the expression of the motility regulon and σ^D is thus a major determinant of bistability. The formation of a biofilm involves the synthesis of an extracellular polysaccharide matrix that is produced by the gene products of the *epsA-O* operon (Kearns *et al.*, 2005). Moreover, the amyloid-like protein TasA is a major matrix component (Romero *et al.*, 2010). Both the *epsA-O* and the *tapA-sipW-tasA* operon are controlled by the transcription repressor SinR (Chu *et al.*, 2006). This protein binds its operator sites in the control regions of the biofilm operons in its free form. However, normally SinR is sequestered due to its regulatory interaction with either of its antagonists, SinI or SlrR (Bai *et al.*, 1993; Chai *et al.*, 2009).

Biofilm formation and motility are mutually exclusive lifestyles of *B. subtilis*: biofilm formation would be impossible if the cells were freely moving. Therefore, there are several checks and balances to control the choice. First, one of the proteins expressed in the *eps* operon, EpsE, interacts with the flagellar motor switch protein FliG to prevent the rotation of the flagellum (Blair *et al.*, 2008). In this way, motility is directly inhibited in cells that undergo biofilm formation. Second, SinR does not only control biofilm formation but is also involved in the regulation of motility. In an alternative complex with the transcription factor SlrR, SinR triggers the DNA binding activity of this regulator resulting in repression of autolysis and motility genes (Chai *et al.*, 2009). On the other hand, in complex with SlrR, SinR can no longer repress the biofilm operons. Thus, only one of the two sets of the genes can be expressed in a cell at a given timepoint.

We are interested in RNA degradation in *B. subtilis*. This process involves the exonucleases RNase J1 and J2 and polynucleotide phosphorylase (Condon, 2010; Deikus & Bechhofer, 2009). Recently, the novel essential endoribonuclease RNase Y that is required

for the initial steps of RNA degradation was identified (Commichau *et al.*, 2009; Shahbadian *et al.*, 2009; Yao & Bechhofer, 2010). The *rny* gene encoding RNase Y is clustered in all *Bacillus* species with a previously uncharacterized gene, *ymdB*. Based on the characterization of a homologous protein from *Deinococcus radiodurans*, the YmdB protein is a phosphodiesterase of unknown physiological function (Shin *et al.*, 2008). In the pathogenic firmicute *Listeria monocytogenes*, *ymdB* mutants are defective in hemolysis and exhibit intracellular growth defects (Zemansky *et al.*, 2009). To gain insight into the role of YmdB in *B. subtilis*, we analyzed the phenotypes of an *ymdB* mutant. Our results demonstrate that YmdB is involved in the decision-making for lifestyle selection: the *ymdB* mutant exhibits a severe overexpression of flagellin and the complete σ^D regulon; in contrast, the biofilm operons are not expressed in the mutant. Both phenotypes can be traced back to a lack of SlrR expression. In consequence, there is no SlrR-mediated repression of motility genes, and SlrR does not antagonize SinR, which is thus constitutively repressing the biofilm operons.

Results

Overexpression of flagellin in the *ymdB* mutant

The *B. subtilis ymdB* gene is located downstream of the *rny* gene. While the *rny* gene product was identified as the novel essential RNase Y, no function has been associated with *ymdB* (Commichau *et al.*, 2009; Shahbadian *et al.*, 2009). A Northern blot analysis revealed that *ymdB* is the distal gene of the bicistronic *rny-ymdB* operon (see supplementary material available at the *Jbac* homepage → <http://jb.asm.org/>). In a first attempt to identify possible functions of this gene and its product, we made use of the $\Delta ymdB$ mutant strain GP583. GP583 and the isogenic wild type *B. subtilis* 168 were cultivated in LB medium and the protein patterns of the two strains were compared (Fig. 42). While the general pattern of protein expression was very similar for the two strains, one protein of about 37 kDa was present as an extremely prominent band in the *ymdB* mutant GP583, but not in the wild type strain. This band was excised from the gel and identified by mass spectrometry as the flagellin protein Hag. In order to verify that the protein in the prominent band was indeed flagellin, we constructed a *hag* deletion mutant that was otherwise isogenic to the *ymdB* mutant GP583. The analysis of the proteome of the *hag ymdB* double mutant GP904 revealed that the prominent band was absent (see Fig. 42). This observation unequivocally confirms the identity of the protein overexpressed in the *ymdB* mutant as flagellin. To ensure that the overexpression of flagellin was due

specifically to the deletion of *ymdB* and to exclude the possibility of any indirect effect, we performed a complementation analysis by ectopically expressing the *ymdB* gene under the control of a constitutive promoter. This strain, GP925, is isogenic to the *ymdB* mutant GP583. As shown in Fig. 42, the intense flagellin band did not appear when expression of *ymdB* was restored. Thus, a functional *ymdB* gene is required for proper synthesis of flagellin.

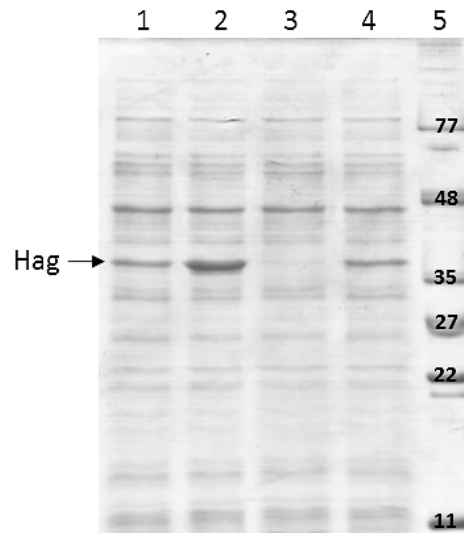


Fig. 42. Accumulation of the flagellin Hag in the *ymdB* deletion strain. The proteome of a *ymdB* mutant strain was compared to the wild type strain. Crude extracts were isolated from *B. subtilis* strains grown in complex medium (LB) at 37°C. Lane 1: 168 (wild type); lane 2: GP583 ($\Delta ymdB$); lane 3: GP904 ($\Delta ymdB \Delta hag$); lane 4: GP925 ($\Delta ymdB$ complementation with pGP1062); lane 5: protein weight marker. 15 μ g crude extract of each culture was loaded on a 12% sodium dodecyl sulfate-polyacrylamide gel. After electrophoresis the gel was stained with Coomassie Brilliant Blue G-250. The flagellin Hag is indicated with an arrow.

To test whether the accumulation of flagellin in the *ymdB* mutant is caused at the level of gene expression, we determined the expression of a transcriptional *hag-lacZ* fusion. For this purpose, the strains GP910 (wild type) and the isogenic *ymdB* mutant GP918 were grown in CSE minimal medium containing 0.5% glucose, and the β -galactosidase activities driven by the *hag* promoter were determined. The *hag* promoter activity resulted in 82 and 1105 units of β -galactosidase in the wild type and the *ymdB* mutant strain, respectively. Thus, YmdB is a novel player involved in the control of flagellin gene expression.

YmdB is required for the formation of complex colony architecture

B. subtilis exhibits “multicellular” behaviour by forming complex colonies and biofilms. These properties have been lost during the domestication of strain 168 (McLoon *et al.*, 2011). Therefore, we analyzed the role of YmdB for complex colony formation using the isogenic strain pair derived from NCIB3610. In good agreement with previous observations (Kearns & Losick, 2005), the wild type strain exhibited complex colony architecture. In contrast, smooth non-structured colonies were detected for the *ymdB* mutant (Fig. 43, see supplementary movies M1 and M2). This phenotype might be an indirect result of the overexpression of flagellin in the *ymdB* mutant. To test this idea, we expressed the *hag* gene under the control of a strong promoter using plasmid pGP1089 and compared the colony morphology to that of the wild type strain carrying the empty vector pBQ200. No difference was observed suggesting that the high expression of flagellin is not the cause for the inability of the *ymdB* mutant to form complex structures (data not shown). Thus, YmdB is essential for the multicellular lifestyle of *B. subtilis*.

Biofilm formation depends on the synthesis of an extracellular polysaccharide and on an amyloid-like fiber protein, TasaA. These functions are encoded by genes of the *epsA-O* and the *tapA-sipW-tasA* operons (Branda *et al.*, 2006; Kearns *et al.*, 2005; Romero *et al.*, 2011). To test whether the loss of the complex colony phenotype is accompanied by altered expression of these genes, we studied the activity of a *tapA-lacZ* fusion in the wild type and the *ymdB* mutant strain. While about 470 units of β -galactosidase were detected in the wild type strain GP993, the promoter was inactive (2 units) in the isogenic *ymdB* mutant GP994. Thus, YmdB is also involved in the control of biofilm gene expression in *B. subtilis*.

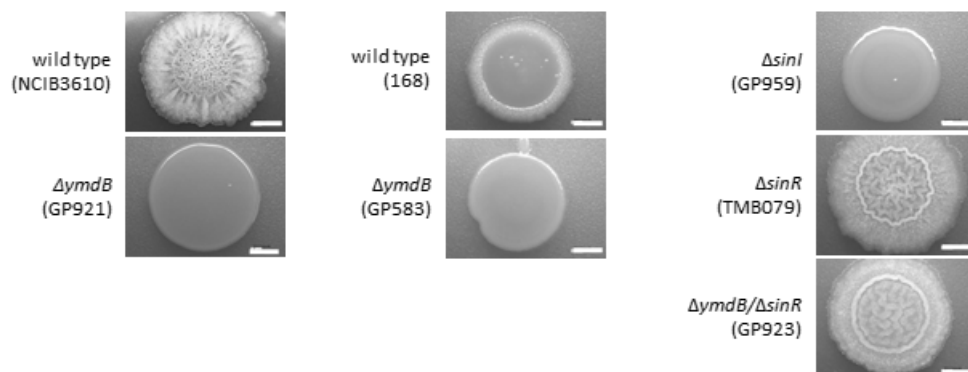


Fig. 43. Effect of a *ymdB* deletion on biofilm formation: SinR is epistatic over YmdB. Colony surface architectures of individual colonies grown on MSgg medium are shown. The colonies were filmed (Stereomicroscope) after incubation for 3 days at 22°C. The indicated wild-type and mutant strains were as

follows: undomesticated wild type (NCIB3610), *ymdB* (GP921 based on NCIB3610), wild type (168), *ymdB* (GP583 based on 168), *sinI* (GP959), *sinR* (TMB079) and *ymdB sinR* (GP923). Scale bar is 250µm.

Single cell expression analysis of motility and biofilm genes

The experiments described above demonstrate that YmdB directly affects the expression of the *hag* and the *tapA* genes. However, the reporter fusion analyses were performed with *B. subtilis* populations rather than with individual cells. It has been shown previously, that *hag* and *tapA* have a bistable expression mode, *i. e.* they are transcribed only in a subset of the cells in a population (Kearns & Losick, 2005; Lopez *et al.*, 2010). Thus, YmdB might affect the bistable expression of *hag* and *tapA*. To address this issue, we made use of a strain that carries transcriptional fusions of the *hag* and *tapA* promoters to the promoterless *cfp* and *yfp* genes, respectively. In the strains harbouring these fusions, the blue and yellow fluorescence reflects the activities of the *hag* and *tapA* promoters, respectively (Fig. 44). In the wild type strain GP845, we observed two cell types, short and long cells. As reported previously (Kearns & Losick, 2005), the short cells exhibited a blue bright fluorescence due to the activity of the *hag* promoter whereas the long cells had a yellow fluorescence indicative of *tapA* expression. Notably, the activity of the two promoters was mutually exclusive. The deletion of *ymdB* in the isogenic strain GP847 completely abolished both the appearance of different cell morphologies and the bistable gene expression: all *ymdB* mutant cells were short, and all showed a bright blue fluorescence suggesting that they express the *hag* gene, but not the *tapA* gene (see Fig. 44). Thus, YmdB is required for the differentiation of *B. subtilis* populations into two distinct cell types.

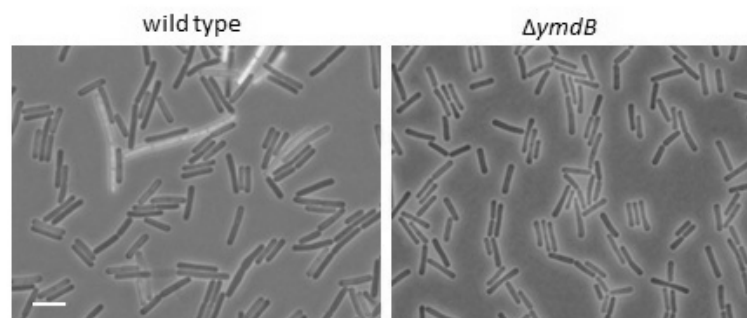


Fig. 44. YmdB affects the bistable expression of motility and biofilm genes. Fluorescence microscopy of cells harboring both P_{hag} -*cfp* and either P_{tapA} -*yfp* fusion in the wild type strain (GP845) and the isogenic *ymdB* mutant (GP847). Cells were observed using fluorescence microscopy. P_{hag} -CFP was false colored in blue (dark colored) and P_{tapA} -YFP in yellow (light colored). Cells of GP845 (wild type) and GP847 ($\Delta ymdB$) were grown in LB and prepared for microscopy in the logarithmic phase of growth. Scale bar is 5 µm.

Implication of YmdB in the expression of the Sigma D regulon

Recently, it was demonstrated that the bistable expression of *hag* is due to the limited activity of the sigma factor, σ^D (Cozy & Kearns, 2010). The lack of bistable *hag* expression in the *ymdB* mutant suggests that YmdB might be implicated in the control of σ^D activity. Therefore, we analyzed the effect of the *ymdB* mutation on the expression of several σ^D -dependent genes by real time quantitative reverse transcription PCR (qRT-PCR). This analysis confirmed the high-level expression of the *hag* gene in the *ymdB* mutant (see Fig. 45). As expected, other σ^D -dependent genes such as *cheV* and *motA* were also more strongly expressed in the *ymdB* mutant (20- and 25-fold overexpression, respectively, see Fig. 45). Moreover, the expression of the *fla-che* operon that includes the *sigD* gene encoding σ^D was also strongly increased in the *ymdB* mutant. The expression of the first gene of the operon, *flgB*, was 7.5-times elevated in the *ymdB* mutant, and *sigD* expression was increased by a factor of 14 (see Fig. 45). To exclude any non-specificity of our assay system, we used the *ptsH* gene that is expressed under all conditions as a control. Transcription of this gene was not significantly affected by the deletion of *ymdB*. Thus, the deletion of YmdB results in an increased expression of the complete σ^D regulon.

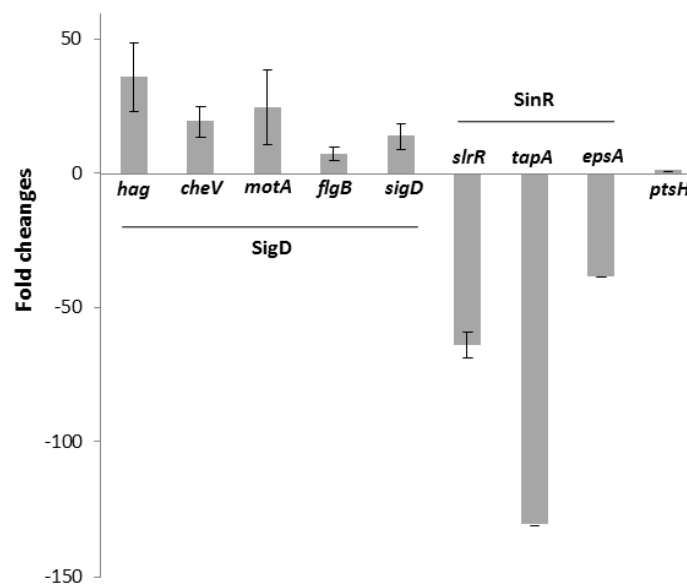


Fig. 45. Effect of a *ymdB* deletion on the expression of genes involved in motility and biofilm formation. Fold changes in the expression of SigD-dependent motility genes (*hag*, *cheV*, *motA*, *flgB*, *sigD*) and SinR-dependent biofilm genes (*slrR*, *tapA*, *epsA*) in a $\Delta ymdB$ mutant relative to the wild type strain (168) are shown. RNA was purified from each strain and quantitative RT-PCR was performed using primer sets specific for the indicated genes. The gene *ptsH* was used as a control. Errors bars indicate the standard deviation.

Impact of YmdB on the expression of genes required for biofilm formation

As shown above, YmdB is not only involved in controlling the expression of the σ^D regulon, it is also required for biofilm formation and for *tapA* expression (see Fig. 43, Fig. 44). To test role of YmdB in the expression of biofilm genes, we performed qRT-PCR analyses with RNA isolated from the wild type strain *B. subtilis* 168 and its isogenic $\Delta ymdB$ derivative GP583. Again, the constitutively expressed *ptsH* gene served as a control. As described above, the amount of the *ptsH* mRNA was not affected by the *ymdB* allele. The expression of both operons involved in biofilm formation (*tapA-sipW-tasA* and *epsA-O*) was strongly affected by the deletion of *ymdB*: The expression of the promoter-proximal genes of these operons, *tapA* and *epsA*, was reduced about 130- and 40-fold, respectively, upon inactivation of *ymdB* (see Fig. 45). Thus, YmdB is required for the expression of the biofilm genes, and the strong reduction of their expression is the likely cause of the inability of the *ymdB* mutant to form a biofilm.

The *hag* core promoter is the target for YmdB-dependent regulation

The results presented above show that YmdB controls the expression of *hag* and the other genes of the σ^D regulon. This control could be exerted at the level of transcription initiation or at the level of transcript stability. The localization of the *ymdB* gene in an operon with the RNase Y-encoding *rny* gene was suggestive of the latter hypothesis. Therefore, the stability of the *hag* transcript in the wild type and *ymdB* mutant strains was compared. For this purpose, the strains were grown in LB medium, and RNA synthesis was stopped by the addition of rifampicin. The amounts of *hag*-specific mRNA were then probed by Northern blot analysis. As reported previously (Horsburgh *et al.*, 2001), we observed a single mRNA species that corresponds to a monocistronic *hag* mRNA. Moreover, this experiment confirmed the strongly increased expression of the *hag* gene in the *ymdB* mutant GP583. The analysis of the stability of the *hag* mRNA revealed a half-life of about 19 min and 32 min in the wild type strain 168 and the *ymdB* mutant GP583, respectively (data not shown). These observations suggest that YmdB has a minor effect on the stability of the *hag* mRNA.

The experiments described above indicate that YmdB may act both at the level of transcription initiation and transcript stability. In order to determine the site of control by YmdB in the *hag* promoter region more precisely, we constructed a series of *hag-lacZ*

fusions with deletions in the 3' or 5' part of the promoter fragment and determined the promoter activities of the remaining fragments by assaying the resulting β -galactosidase activities in isogenic wild type and *ymdB* mutant strains. As shown in Fig. 46A, all *hag-lacZ* translational fusions used in this study responded to the deletion of *ymdB* by a higher promoter activity. This was the case even if the promoter fragment did not contain any DNA upstream of the core promoter (see GP908 vs. GP916, Fig. 46A). Usually, positively acting transcription factors bind their DNA targets upstream of the promoter. Thus, YmdB might control *hag* expression in a different way. To exclude the implication of the non-translated mRNA leader in YmdB-dependent expression, we constructed another set of transcriptional *hag-lacZ* fusions with consecutive deletions of the leader region. Again, all constructs exhibited an strongly increased expression in the *ymdB* mutant background even if the promoter fragment was deleted up to the transcription start point (see GP 912 vs. GP920, Fig. 46B). Taken together, these results indicate that YmdB exerts its regulatory effect via the core promoter rather than by binding a target sequence upstream or downstream of the promoter. Thus, it is most likely that σ^D activity is enhanced in the *ymdB* mutant.

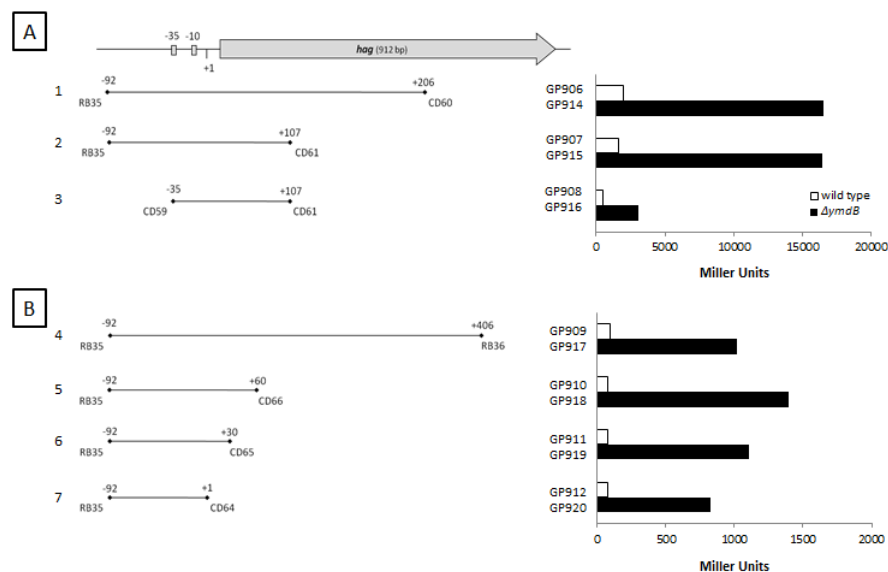


Fig. 46. YmdB affects *hag* expression via the core promoter. A deletion analysis of the *hag* promoter is shown. The region upstream of *hag* gene containing the *hag* promoter region is mapped (top panel). The block arrow represents the *hag* ORF. Bars represent DNA fragments (with their corresponding primer sets) translationally (A) or transcriptionally (B) fused to a *lacZ* reporter (left panel). Cells containing the fusions P_1 -*lacZ* (GP906, GP914), P_2 -*lacZ* (GP907, GP915), P_3 -*lacZ* (GP908, GP916), P_4 -*lacZ* (GP909, GP917), P_5 -*lacZ* (GP910, GP918), P_6 -*lacZ* (GP911, GP919) and P_7 -*lacZ* (GP912, GP920) were used for a β -galactosidase assay (right panel). The β -galactosidase activities are expressed in Miller Units.

YmdB controls σ^D accumulation

The activity of σ^D is controlled by a regulatory interaction with the anti-sigma factor FlgM. An increased σ^D activity may therefore result from a high-level expression of σ^D that titrates FlgM or from an impaired interaction between σ^D and FlgM that results in higher levels of σ^D available for transcription initiation. To distinguish between these possibilities, we tested both the cellular amounts of the σ^D protein and possible protein-protein interactions between σ^D , FlgM and YmdB. The amounts of the σ^D protein in the wild type strain and in an isogenic *ymdB* mutant were compared using a *sigD* allele that fuses a triple FLAG-tag to the C-terminus of σ^D . These strains were grown in LB medium and the presence of SigD-FLAG was tested by Western blot analysis. As shown in Fig. 47, the cellular amount of the σ^D protein was increased about twofold in the *ymdB* mutant GP950 as compared to the isogenic wild type GP948. Protein-protein interactions were studied using a bacterial two-hybrid system. As reported previously (Bertero *et al.*, 1999), σ^D and FlgM showed an interaction in this assay. In contrast, YmdB did not interact with SigD or with FlgM (data not shown). These data suggest that the higher expression of σ^D is the reason for the increased σ^D activity and the resulting elevated expression of the σ^D regulon in the *ymdB* mutant.

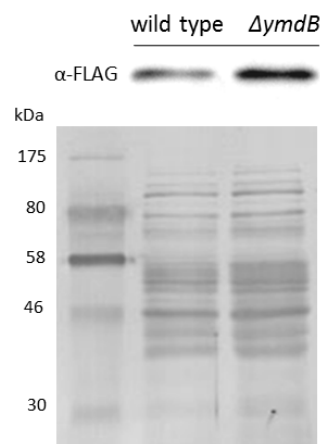


Fig. 47. The cellular amount of SigD is increased in a *ymdB* mutant. Crude extracts were isolated from the *B. subtilis* strains GP948 (*sigD*-FLAG, wild type) and GP950 (*sigD*-FLAG, $\Delta ymdB$) grown in complex medium (LB) at 37°C. 5 μ g crude extract of each culture was loaded on a 12% sodium dodecyl sulfate-polyacrylamide gel. After electrophoresis and blotting onto a polyvinylidene difluoride membrane, the FLAG-tag was detected using rabbit polyclonal antibodies. All cultures were harvested in the stationary phase. As a loading control, the membrane was stained with Coomassie Brilliant Blue G-250.

YmdB controls the activity of SinR

The strongly reduced expression of both biofilm operons suggests that YmdB exerts a general regulatory effect rather than controlling each operon individually. The expression of both operons is repressed by the SinR transcription factor, and induction occurs upon interaction of SinR with its anti-repressor, SinI (Lewis *et al.*, 1998). To test whether YmdB interferes with SinI/SinR signalling, we compared the biofilm formation of *ymdB*, *sinI* and *sinR* mutants. As shown in Fig. 43, the wild type strain 168 formed colonies with little complexity. The *ymdB* mutant GP583 formed absolutely smooth colonies. This is in good agreement with the lack of biofilm formation observed in the genetic background of the non-domesticated strain NCIB3610 (see Fig. 43, see supplementary movies M1 and M2). Similarly, the *sinI* mutant formed smooth colonies. In contrast and in good agreement with previously published observations (Kearns *et al.*, 2005), the *sinR* mutant formed complex colonies (see supplementary movies M3 and M4 available at the *Jbac* homepage → <http://jb.asm.org/>). To test whether YmdB is involved in this signalling pathway, we constructed the *ymdB sinR* double mutant GP923 and tested its ability to form structurally complex colonies. As shown in Fig. 43, the phenotype of this double mutant was very similar to that of the *sinR* mutant TMB079. Thus, the effect of YmdB on biofilm formation is only detectable in the presence of the functional SinR repressor. This suggests that YmdB is involved in the control of SinR activity, and more specifically, that the deletion of *ymdB* results in permanent transcription repression by SinR.

The results reported above show that YmdB acts like an antagonist of SinR activity, and indeed, the phenotype of the *ymdB* mutant with respect to biofilm formation is identical to that of the mutant strain GP959 that lacks the anti-repressor SinI (see Fig. 43). Thus, YmdB might control the regulatory interaction between SinI and SinR or directly inactivate SinR. To distinguish between these two possibilities, we tested possible interactions of YmdB with SinI and SinR as well as their interaction in a *ymdB* mutant. The possible interactions between SinI, SinR, and YmdB were studied using the bacterial two-hybrid system. In good agreement with previous reports (Lewis *et al.*, 1998), we observed an interaction between SinI and SinR, whereas YmdB did not interact with either of the two proteins (data not shown). Additionally, we tested the *in vivo* interaction between SinI and SinR in the wild type strain and a *ymdB* mutant by co-purification of Strep-tagged SinR with interaction partners from strains that express FLAG-tagged SinI. The two proteins were co-purified irrespective of the status of the *ymdB* gene (data not shown). These results exclude the possibility that YmdB interferes with the regulatory protein-protein

interaction between SinI and SinR and suggest that the altered activity of SinR in the *ymdB* mutant is brought about by a different mechanism.

Reduced SlrR expression is responsible for the phenotypes of the *ymdB* mutant

Both biofilm operons are under the control of SinR, and the evidence presented above demonstrates that YmdB is involved in the control of SinR activity in a SinI-independent manner. Therefore, we considered the possibility that additional factors related to SinR might be affected by the *ymdB* mutation. Indeed, the expression of the *slrR* gene is repressed by SinR, and the SlrR protein in turn controls the activity of SinR and acts as a direct regulator of motility genes (Chai *et al.*, 2010a; Chai *et al.*, 2010b; Kobayashi, 2008). Thus, we compared the expression of the *slrR* gene in the wild type strain 168 and its isogenic *ymdB* mutant GP583 by qRT-PCR analysis. As shown in Fig. 45, the deletion of *ymdB* resulted in a strong (about 65-fold) reduction of *slrR* expression. To gain insight into the expression of *slrR*, we performed a Northern blot analysis using a probe specific for *slrR*. We detected a signal at a size of 2000 nucleotides that corresponds to a *slrR-pnbA* operon (see Fig. 48). The *pnbA* gene encodes a para-nitrobenzyl esterase of unknown physiological function (Ribitsch *et al.*, 2011; Zock *et al.*, 1994). The *slrR-pnbA* transcript was not detectable in the *ymdB* mutant thus confirming the qRT-PCR analysis. This result is in excellent agreement with the idea that the complete SinR regulon is constitutively repressed in the *ymdB* mutant.

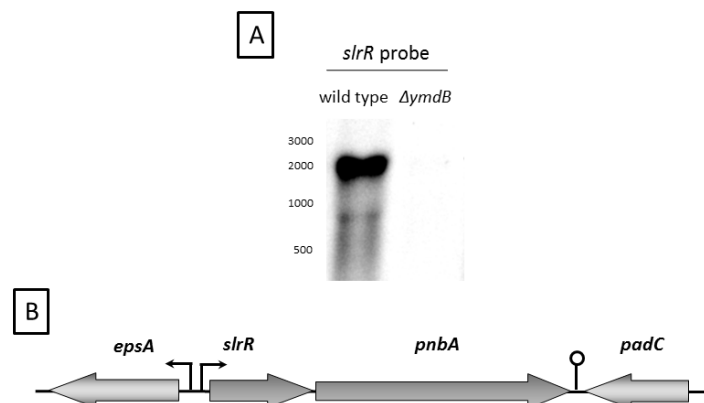


Fig. 48. YmdB affects the expression of the *slrR* mRNA. (A) Northern blot analyses to test the effect of YmdB on the expression of the *slrR* mRNA. The strains *B. subtilis* 168 (wild type) and GP583 (*ymdB* mutant) were grown in CSE minimal medium containing 0.5% glucose. The cells were harvested in the exponential phase of growth. The transcripts were detected with riboprobes specific for *slrR*. (B) Schematic illustration of the *slrR-pnbA* operon.

However, the experiments described above did not allow us to conclude whether the reduced *slrR* expression is just another result of the deletion of the *ymdB* gene, or whether there is a causal relation between *slrR* expression in the mutant and the other phenotypes observed. To address this problem, we constructed a strain that allows expression of the *slrR* gene under the control of the xylose operon promoter. In this strain, GP975, the *slrR* gene is expressed if xylose is added to the medium. First, we determined the colony architecture of the *ymdB* mutant in the absence or presence of xylose, i.e. with or without an expressed *slrR* gene. As shown in Fig. 49, the wild type strain NCIB3610 showed a complex colony architecture that was completely lost when *ymdB* was deleted (GP921). The same result was obtained with GP975 in the absence of xylose, i. e. when *slrR* was not expressed. In contrast, induction of *slrR* expression in GP975 suppressed the phenotype of the *ymdB* mutation suggesting that indeed the weak expression of *slrR* was responsible for the lack of complex colony architecture in the *ymdB* mutant.

If the weak expression of *slrR* were responsible for all effects of the *ymdB* mutation, one would expect that the expression levels of the affected motility and biofilm genes in the *ymdB* mutant would be reversed upon expression of *slrR*. This hypothesis was addressed by comparing the expression levels of the corresponding genes in the isogenic strains GP972 and GP973. In both strains the *ymdB* gene was deleted, and in addition the *slrR* gene was expressed from a xylose-controlled promoter in GP973. As in the previous experiments, we used the *ptsH* gene as the control, and expression of this gene was not affected by *slrR* expression (see Fig. 49). As shown in Fig. 49, the expression of the *hag* gene was essentially abolished upon overexpression of SlrR. This is in perfect agreement with the established role of SlrR as a transcription repressor of *hag* and other motility genes (Chai *et al.*, 2010a). Similarly, expression of the *sigD* gene was also reduced when *slrR* was expressed. The effect was different when the biofilm operons were analysed. While the *ymdB* mutation resulted in loss of expression of the *tapA-sipW-tasA* and *epsA-O* operons (see above, Fig. 45), the expression of *slrR* in the *ymdB* mutant restored the expression of both operons (see Fig. 49). This observation is in good agreement with the suppression of the *ymdB* mutant phenotype with respect to colony architecture upon *slrR* overexpression.

The reversal of the effects of the *ymdB* mutation upon *slrR* overexpression was also tested for the *hag-yfp* fusion. As shown in Fig. 49C, overexpression of *slrR* resulted in loss of fluorescence indicating that the *hag* promoter was not active when SlrR was

overexpressed. This result fits very well with the data from the qRT-PCR analysis of *hag* expression.

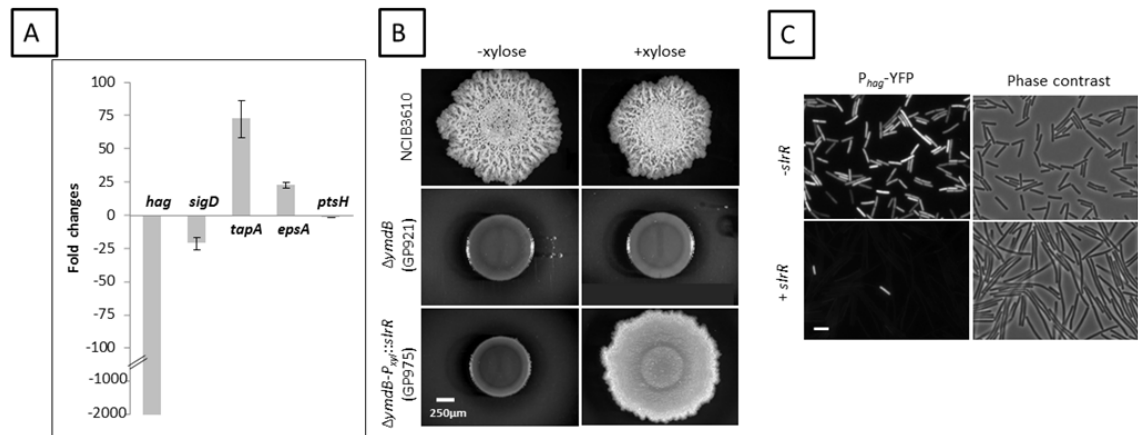


Fig. 49. The defective expression of motility and biofilm genes in the *ymdB* mutant can be restored by *slrR* overexpression. (A) Fold changes in expression of *hag*, *sigD*, *tapA* and *epsA* were investigated in the $\Delta ymdB$ mutant (GP973) with and without induction of *slrR*. In the strain GP973 the *slrR* gene was placed under control of a xylose-inducible promoter. The strains were grown in CSE minimal medium containing 0.5% glucose in the presence or absence of xylose. RNA was purified from each strain and quantitative RT-PCR was performed using primer sets specific to the indicated genes. *ptsH* was used as a control. Errors bars are the standard deviation of two replicates. (B) Colony surface architectures of individual colonies grown on MSgg medium with and without xylose are shown. The colonies were filmed (Stereomicroscope) after incubation for 4 days at 22°C. The indicated wild type and mutant strains were as follows: wild type (NCIB3610), *ymdB* (GP921), and $\Delta ymdB$ $P_{xyl}::slrR$ (GP975). Scale bar is 250 μ m. (C) Fluorescence microscopy of cells (GP976) harboring a P_{hag} -yfp fusion and an inducible *slrR*-expression. Cells of GP976 ($\Delta ymdB$) were grown in LB with and without xylose and prepared for microscopy in the logarithmic phase of growth. Cells were observed using fluorescence microscopy. P_{hag} -YFP was false colored in yellow. Live cells are shown on the right. Scale bar is 5 μ m.

In conclusion, the defective expression of *slrR* in the *ymdB* mutant is responsible for the changes in gene expression of motility and biofilm genes when the *ymdB* gene is deleted.

Discussion

During logarithmic growth, the cells of a *B. subtilis* population choose one out of two alternative ways of life: one portion of a culture forms small motile cells whereas the other cells are long and may consequently form multicellular structures such as biofilms and pellicles on solid surfaces and in liquid medium, respectively. These different cellular fates result from the expression of distinct sets of genes: the short motile cells express flagellin and the other proteins of the large motility regulon controlled by σ^D , whereas the

longer cells seem to express genes involved in biofilm formation (Lopez *et al.*, 2010). The work presented here demonstrates that the YmdB protein is implicated in this choice: Cells that are devoid of an active YmdB protein have no choice but expressing the σ^D regulon. In contrast, biofilm formation is defective in such cells due to the lack of expression of the *epsA-O* and *tapA-sipW-tasA* operons. Thus, YmdB is a novel component of the regulatory machinery that determines bistable gene expression and the ultimate fate of the individual cells.

The SinR transcription factor is the master regulator for bistable gene expression in *B. subtilis*: On one hand, SinR represses the expression of the genes required for the synthesis of the biofilm matrix. On the other hand, the gene for an additional transcription factor, SlrR, is repressed by SinR. SlrR, in turn, is a repressor of σ^D -dependent genes for autolysis and motility, including the *hag* gene (Chai *et al.*, 2010b). The activity of SinR is controlled by regulatory interactions with its cognate anti-repressor SinI and with SlrR (Chai *et al.*, 2010b; Lewis *et al.*, 1998). Moreover, expression of the *sinIR* operon encoding SinR and its antagonist is activated by the master regulator of sporulation initiation, Spo0A, in its phosphorylated form. Spo0A itself is phosphorylated only in a fraction of the population (Chastanet *et al.*, 2010; de Jong *et al.*, 2010). Thus, bistability conferred by Spo0A may influence motility and biofilm formation via the expression and activity of SinR.

Bistable gene expression may be affected by any mutation that interferes with the expression, accumulation and/or activity of the regulators that control the transcription of the bistable target genes. Recently, it has been shown, that increased expression of the *sigD* gene results in the accumulation of active σ^D . This may result from the inability of the anti-sigma factor FlgM to inactivate the increased amounts of the sigma factor due to the shift in the stoichiometry between the two proteins. As a consequence, expression of the σ^D regulon including the *hag* gene encoding flagellin no longer exhibits bistability, but occurs in all cells of the population (Cozy & Kearns, 2010; Veening & Kuipers, 2010). The higher amount of σ^D in the *ymdB* mutant may also explain the increased expression of the σ^D regulon and the expression of flagellin in all cells of the population (see Figs. 44, 45, 47).

The data presented in this study demonstrate that YmdB affects the expression of both the σ^D and SinR regulons by controlling the expression of SlrR, a bifunctional transcription repressor of motility genes and an antagonistic interaction partner of SinR. As a member of the SinR regulon, the *slrR* gene is poorly expressed in the *ymdB* mutant,

and establishing a causal relation is a problem similar to that of the hen and the egg. However, the overexpression of SlrR in the *ymdB* mutant strain restored the expression of biofilm genes and resulted in decreased expression of the members of the σ^D regulon. Moreover, overexpression of SlrR allowed the *ymdB* mutant to form complex colonies. Thus, overexpression of *slrR* suppresses all known phenotypes of the *ymdB* mutant strain. This suggests that YmdB and SlrR are part of one signalling chain that ultimately controls the expression of motility and biofilm genes in an antagonistic manner. Based on our results, YmdB might sense some signal(s) and transducer this information to the expression and/or activity of SlrR which in turn might repress the expression of motility genes and release active SinR to repress biofilm formation. The antagonistic interactions of SlrR with SlrA and SinR as well as of SinR with SinI and SlrR have been intensively studied (Chai *et al.*, 2009; Kobayashi, 2008; Lewis *et al.*, 1998), however, the nature of input signals that control these interactions are largely unknown. This work establishes YmdB as the most upstream factor in the signalling pathway for motility and biofilm formation.

The key question that remains open is related to the molecular mechanism that mediates this control. Based on its similarity to a phosphodiesterase from *D. radiodurans* (Shin *et al.*, 2008), YmdB may have the same biochemical activity. It is well established that phosphodiesterases play a crucial role in many signalling processes. In *E. coli*, the cyclic AMP phosphodiesterase CpdA degrades cAMP and is thus a player in carbon catabolite repression (Imamura *et al.*, 1996). On the other hand, all RNases are also phosphodiesterases that participate in gene regulation. The elucidation of the activity of YmdB at the molecular level and the link of this activity to the control of *slrR* expression will be the subject of further work.

Acknowledgements

Dörte Becher (University of Greifswald) is acknowledged for the identification of the Hag band by mass spectrometry. Ricarda Banse, Stefan Wicht, Boris Görke are acknowledged for the help with some experiments. We are grateful to Paola Bisicchia, Sina Jordan, Oscar Kuipers, Fabian Commichau, Daniel López, and Thorsten Mascher for the gift of strains and plasmids. This work was supported by grants of the Deutsche Forschungsgemeinschaft (SFB860) and the Fonds der Chemischen Industrie to J. S..

Experimental procedures

B. subtilis strains and growth conditions - All *B. subtilis* strains used in this work are derived from the laboratory wild type strain 168 or the non-domesticated strain NCIB3610. Mutations were transferred to the NCIB3610 background using SPP1 mediated generalized transduction (Yasbin & Young, 1974). All strains are listed in Table 1. *B. subtilis* was grown in LB medium or in CSE minimal medium containing succinate and glutamate/ ammonium as basic sources of carbon and nitrogen, respectively (Wacker et al., 2003). The medium was supplemented with auxotrophic requirements (at 50 mg/l) and glucose as indicated. SP, MSgg and CSE plates were prepared by the addition of 17 g Bacto agar/l (Difco) to SP (8 g of nutrient broth per liter-1 mM MgSO₄-13 mM KCl, supplemented after sterilization with 2.5 μM FeSO₄, 500 μM CaCl₂, and 10 μM MnCl₂), MSgg medium (Branda et al., 2001) or CSE medium, respectively.

Assays of complex colony formation. - For colony architecture analysis, bacteria were precultured in LB until an OD₆₀₀ of 0.6 to 0.8. The culture (1.5 ml) was then pelleted and resuspended in 100 μl of the sterile supernatant. 10 μl of this cell suspension were then spotted onto minimal MSgg medium (Branda et al., 2001) containing 1.5% agar and incubated at 22°C for three to five days.

DNA manipulation and transformation - *E. coli* DH5α (Sambrook et al., 1989) was used for cloning experiments. Plasmid DNA extraction was performed using standard procedures (Sambrook et al., 1989). Restriction enzymes, T4 DNA ligase and DNA polymerases were used as recommended by the manufacturers. DNA fragments were purified from agarose gels using the QIAquick PCR purification kit (Qiagen, Germany). Phusion DNA polymerase was used for the polymerase chain reaction as recommended by the manufacturer. All primer sequences are provided as supplementary material. DNA sequences were determined using the dideoxy chain termination method (Sambrook et al., 1989). All plasmid inserts derived from PCR products were verified by DNA sequencing. Chromosomal DNA of *B. subtilis* was isolated as described (Wacker et al., 2003).

Transformation and phenotypic analysis - Standard procedures were used to transform *E. coli* (Sambrook et al., 1989) and transformants were selected on LB plates containing ampicillin (100 μg/ml). *B. subtilis* was transformed with plasmid or chromosomal DNA according to the two-step protocol described previously (Kunst & Rapoport, 1995). Transformants were selected on SP plates containing chloramphenicol (Cm 5 μg/ml), kanamycin (Km 10 μg/ml), spectinomycin (Spc 100 μg/ml), tetracyclin (10 μg/ml), or erythromycin plus lincomycin (Em 1 μg/ml and Lin 10 μg/ml).

In *B. subtilis*, amylase activity was detected after growth on plates containing nutrient broth (7.5 g/l), 17 g Bacto agar/l (Difco) and 5 g hydrolyzed starch/l (Connaught). Starch degradation was detected by sublimating iodine onto the plates.

Quantitative studies of lacZ expression in *B. subtilis* were performed as follows: cells were grown in LB medium. Cells were harvested throughout growth. β -Galactosidase specific activities were determined with cell extracts obtained by lysozyme treatment as described previously (Kunst & Rapoport, 1995). One unit of β -galactosidase is defined as the amount of enzyme which produces 1 nmol of o-nitrophenol per min at 28° C.

Plasmids - Plasmids pAC6 (Stülke et al., 1997) and pAC7 (Weinrauch et al., 1991) were used to construct transcriptional and translational fusions, respectively, of the hag or tapA control regions with the lacZ gene. The hag promoter region was amplified using the primer pairs shown in Fig. 46, and the PCR products were digested with EcoRI and BamHI and cloned into pAC6 and pAC7 linearized with the same enzymes. The resulting plasmids (see Table 1, Table S2 for details) were linearized with PstI and used to transform *B. subtilis* 168 or GP583. The tapA promoter region was amplified using the primer pair CD226/CD233, and the PCR product was digested with EcoRI and BamHI and cloned into pAC6 linearized with the same enzymes. The resulting plasmid pGP1926 was linearized with PstI and used to transform *B. subtilis* 168 or GP583.

To express a plasmid-borne hag gene in *B. subtilis*, we constructed plasmid pGP1089. For this purpose the hag gene was amplified with the primers CD172 and CD173 using chromosomal DNA of *B. subtilis* as a template. The PCR product was digested with BamHI and Sall and cloned into the overexpression vector pBQ200 (Martin-Verstraete et al., 1994).

Construction of deletion and complementation strains - Deletion of the ymdB and hag genes was achieved by transformation with PCR products constructed using oligonucleotides to amplify DNA fragments flanking the target genes and intervening antibiotic resistance cassettes (Guerout-Fleury et al., 1995) as described previously (Wach, 1996).

In order to allow ectopic expression of ymdB, we constructed *B. subtilis* GP925. In this strain, ymdB is expressed in the amyE locus under the control of the constitutive pgk promoter (Ludwig et al., 2001). Strain GP925 was obtained by transformation of *B. subtilis* GP583 with plasmid pGP1062. This plasmid was obtained as follows: The promoter of the pgk gene and the ymdB gene were amplified using the primer pairs HL51/CD94 and CD95/CD93, and digested with EcoRI/ HindIII and HindIII/ BamHI, respectively. These

fragments were used in a three-arm ligation with pAC6 (Stülke et al., 1997) linearized with EcoRI and BamHI. The resulting plasmid was pGP1062.

Regulated expression of slrR - To allow the controlled expression of the slrR gene, we placed this gene behind a xylose-regulated promoter and integrated this cassette into the lacA gene in the *B. subtilis* chromosome. First, the origin of replication and bla resistance gene were amplified from plasmid pUC19 (Sambrook et al., 1989) using the primer pair KG50/ KG51. This fragment was ligated to the flanking regions of the *B. subtilis* lacA gene (amplified with KG54/ KG55 and KG56/ KG57). The resulting plasmid was pGP882. Next, the *B. subtilis* region containing the xylR gene and the xylA promoter as well as the aphA3 kanamycin resistance gene from pDG780 (Guerout-Fleury et al., 1995) were amplified (KG58/ KG59 and KG46/ KG47, respectively) and cloned between the BamHI and SmaI sites of pGP882. With the oligonucleotide KG59, the translation initiation signals of the strongly expressed gapA gene were attached downstream of the xylA promoter. The resulting plasmid was pGP884. Then, the DNA region corresponding to the C-terminal fragment of the improved yellow fluorescent protein from plasmid pIYFP (Veening et al., 2004) was amplified using the primer pair KG60/ KG61. With KG60, a multiple cloning region encompassing XbaI, BamHI, KpnI, and EcoRI sites was added. The fragment was cloned between the BamHI and Sall sites of pGP884 to give pGP888. Finally, the promoterless slrR gene was amplified using the primer pair CD157/ML266 and cloned into pGP888. The resulting plasmid pGP1888 was linearized with Scal and used to transform *B. subtilis* GP583.

Analysis of protein expression - To monitor the expression patterns of σ^D , this protein was fused to a triple FLAG-tag at its C-terminus. The sigD gene is the penultimate gene of the fla-che operon. To avoid any polar effect on the downstream swrB gene, plasmid pGP1087 was designed that allows Campbell-type integration of the plasmid and expression of downstream genes under the control of an IPTG-inducible pSPAC promoter. This plasmid was obtained as follows: The triple FLAG-tag was amplified from plasmid pGP1331 (Lehnik-Habrink et al., 2010) using the primer pair CD133/ CD134, digested with XmaIII and inserted into XmaIII-linearized pMUTIN-FLAG (Kaltwasser et al., 2002). Next, the 3'-end of the sigD gene was amplified using the oligonucleotides CD129/ CD130 and cloned into pGP1087 using the HindIII and ClaI restriction sites. The resulting plasmid was pGP1085 (*sigD*-3×FLAG).

Real time quantitative reverse transcription PCR - For RNA isolation, the cells were grown in CSE minimal medium containing 0.5% (w/v) glucose to an OD₆₀₀ of 0.5 – 0.8

and harvested. Preparation of total RNA was carried out as described previously (35). cDNAs were synthesized using the One-Step RT-PCR kit (BioRad) as described (Rietkötter et al., 2008). qRT-PCR was carried out on the iCycler instrument (BioRad) following the manufacturer's recommended protocol by using the primers indicated in the supplementary material. The *rpsE* and *rpsJ* genes encoding constitutively expressed ribosomal proteins were used as internal controls. Data analysis and the calculation of expression ratios as fold changes were performed as described (Rietkötter et al., 2008). qRT-PCR experiments were performed in duplicate.

Northern blot analyses - Preparation of total RNA and Northern blot analysis were carried out as described previously (Ludwig et al., 2001). Digoxigenin (DIG) RNA probes were obtained by in vitro transcription with T7 RNA polymerase (Roche Diagnostics) using PCR-generated DNA fragments as templates. The primer pairs used to amplify DNA fragments specific for *rny*, *ymdB*, *hag*, and *slrR* are listed in the supplementary material. The reverse primer contained a T7 RNA polymerase recognition sequence. In vitro RNA labelling, hybridization and signal detection were carried out according to the instructions of the manufacturer (DIG RNA labelling kit and detection chemicals; Roche Diagnostics). RNA stability was analyzed as described previously (38). Briefly, rifampicin was added to logarithmically growing cultures (final concentration 100 µg/ml) and samples were taken at the time points indicated. The quantification was performed using the Image J software v1.42 (Abramoff et al., 2004).

Western blotting - For Western blot analysis, proteins were separated by 12.5% or 15% SDS-PAGE and transferred onto polyvinylidene difluoride (PVDF) membranes (BioRad) by electroblotting. Rabbit anti-FLAG polyclonal antibodies (Sigma-Aldrich; 1:10 000) served as primary antibodies. The antibodies were visualized by using anti-rabbit immunoglobulin alkaline phosphatase secondary antibodies (Promega) and the CDP-Star detection system (Roche Diagnostics), as described previously (Commichau et al., 2007).

In vivo detection of protein-protein interactions - The isolation of protein complexes from *B. subtilis* cells was performed by the SPINE technology (Herzberg et al., 2007). Briefly, growing cultures of *B. subtilis* were treated with formaldehyde (0.6% w/v, 20 min) to facilitate cross-linking of interacting proteins (Herzberg et al., 2007). The Strep-tagged proteins and their potential interaction partners were then purified from crude extracts using a Streptactin column (IBA, Göttingen, Germany) and desthiobiotin as the eluent. Interacting proteins were identified by Western blot analysis.

The strain GP946 expressing SinI-FLAG was obtained as follows: First, we constructed plasmid pGP1370 that allows multicopy-expression of FLAG-tagged proteins. This plasmid was obtained by amplification of the FLAG-tag encoding region from pGP1331 (Lehnik-Habrink et al., 2010) using the primer pair ML5/ ML6 and insertion of the PCR product into the expression vector pBQ200 (Martin-Verstraete et al., 1994) linearized with HindIII. Next, we amplified *sinI* and the upstream *yqhG* gene using the primer pair CD147/ CD148. The PCR product was cloned between the BamHI and Sall sites of pGP1370 giving pGP1084. Finally, strain GP946 was constructed by transformation with a PCR product obtained using oligonucleotides to amplify DNA fragments covering the *yqhG-sinI-FLAG* and *tasA* regions as well as an intervening kanamycin resistance cassette (Guerout-Fleury et al., 1995; Wach, 1996). To allow complementation of *sinR* that is deleted in GP946, we constructed plasmid pGP1083 that expressed SinR fused to a N-terminal Strep-tag. This plasmid was obtained by cloning of the *sinR* gene (amplified using the oligonucleotides CD137/ CD138) between the BamHI and Sall sites of pGP380 (Herzberg et al., 2007).

B2H assay - Primary protein-protein interactions were studied by bacterial two-hybrid (B2H) analysis. The B2H system is based on the interaction-mediated reconstruction of adenylate cyclase (*CyaA*) activity from *Bordetella pertussis* in *E. coli* (Karimova et al., 1998). Briefly, proteins suspected to interact physically were fused with separated domains of the adenylate cyclase as described previously (Lehnik-Habrink et al., 2010). DNA fragments corresponding to the *ymdB*, *sigD*, *flgM*, *sinI*, and *sinR* genes were obtained by PCR (for primers, see supplementary material). The PCR products were digested with KpnI and XbaI and cloned into the vectors of the two-hybrid system that had been linearized with the same enzymes. The resulting plasmids (see supplementary Table S2) were used for cotransformations of *E. coli* BTH101 and the protein-protein interactions were then analyzed by plating the cells on LB plates containing ampicillin (100 µg/ml), kanamycin (50 µg/ml), X-Gal (40 µg/ml) (5-bromo-4-chloro-3-indolyl-β-D-galactopyranoside) and IPTG (0.5 mM) (isopropyl-β-D-thiogalactopyranoside), respectively. The plates were incubated for a maximum of 48 h at 30°C.

Microscopy - For fluorescence microscopy cells were grown in LB medium to an OD₆₀₀ of 0.7 - 1.0, harvested and resuspended in phosphate buffered saline (pH 7.5; 50 mM). Fluorescence images were obtained with the Axioskop 40 FL fluorescence microscope, equipped with digital camera AxioCam MRm and AxioVision Rel 4.8 software for image processing (Carl Zeiss, Göttingen, Germany) and Neofluar series objective at 100x primary magnification. The applied filter sets were YFP HC-Filterset (BP: 500/24, FT

520, LP 542/27; AHF Analysentechnik, Tübingen, Germany) for YFP detection and filter set 47 (BP: 436/20, FT 455, LP: 480/40; Carl Zeiss) for CFP visualization. All images were taken at the same exposure time. The overlays of fluorescent and phase-contrast images were prepared for presentation with Adobe Photoshop Elements 8.0 (Adobe Systems, San Jose, USA).

Time-lapse microscopy of colony formation was performed with the Stemi 2000-C equipped with the AxioVision software including the multidimensional acquisition module and the AxioCam ICc1 (Carl Zeiss). Images were taken every 15 min over a time period of 72 h at room temperature. Relative time stamps were added the images following the format HH:MM:SS:MS. The scale bar in the movies corresponds to 0.5 cm.

8. Discussion

8.1. RNase Y: the missing endoribonuclease of *Bacillus subtilis*

The degradation of mRNAs is a fundamental process in every organism. This step is essential for recycling nucleotides and adds an additional layer in the overall process of gene expression. In addition, rapid turnover leading to short half-lives of transcripts permits a quick adaptation to changing environmental conditions especially in prokaryotes. Due to the assumption of conserved mechanisms of mRNA degradation among bacteria, much effort was spent focusing on mRNA decay in *E. coli* in the past, whereas research on Gram positive organisms like *B. subtilis* has remained minor. Nevertheless recent findings strongly suggest fundamental differences between both bacteria.

In the general model for *E. coli* the rate-limiting step in the process of mRNA degradation is conducted by the endoribonuclease RNase E which initiates the decay by cleaving within the body of the transcript. This cleavage produces an upstream fragment that is subject to 3'-5' degradation by exoribonucleases like RNase II and PnpA and a downstream fragment that is further subject to new rounds of RNase E cleavage (Kushner, 2002). With the availability of the complete genome sequence of *B. subtilis* it became apparent that there have to be substantial differences between the two organisms. This is due to the fact that no homologs for the major players of mRNA turnover of *E. coli* exist in *B. subtilis* (Kunst *et al.*, 1997). Especially the absence of an RNase E homolog was surprising.

The apparent lack of a global acting endoribonuclease in *B. subtilis* made it difficult to predict a model for mRNA degradation as it was very unlikely that only 3'-5' exonucleolytic decay exists (Condon, 2003). Furthermore a number of cases in *B. subtilis* were already known in which endonucleolytic cleavages occurred but the involved endonucleolytically-acting RNase remained unknown (Condon *et al.*, 1997; Homuth *et al.*, 1999; Ludwig *et al.*, 2001). It took several years (after the publication of the *B. subtilis* genome and therefore the possibility to do alignment studies) until the first more globally acting endoribonucleases named RNase J1 and J2 were discovered (Even *et al.*, 2005). Subsequent transcriptome analysis revealed that the deletion of either one RNase had only a slight effect on mRNA turnover whereas a double mutant affected the abundance of hundreds of mRNAs (Mäder *et al.*, 2008). However, the impact of both RNases on global mRNA half-life was surprisingly minor, suggesting that the two enzymes may not be

involved in initiating the global mRNA decay (Even *et al.*, 2005). Therefore it was possible that another, yet undiscovered, endoribonuclease could be present in *B. subtilis*.

Investigations of the unknown protein YmdA already pointed to an endoribonuclease-like function. This essential protein was found in a study searching for interaction partners of the glycolytic enzymes (Commichau *et al.*, 2009). Here, YmdA interacted with the glycolytic enzymes enolase and phosphoglycerate kinase. Further analysis demonstrated that YmdA is involved in the processing of the *gapA* operon, suggesting that this unknown essential protein is a factor involved in RNA processing. Therefore YmdA was subsequently renamed Rny (Commichau *et al.*, 2009). The actual verification that YmdA/Rny is indeed an RNase was brought already in the same year. *In vitro* experiments demonstrated that Rny initiates the turnover of S-adenosylmethionine-dependent riboswitches. Therefore Rny was further renamed RNase Y. Most importantly in terms of global mRNA degradation was the discovery that depletion of RNase Y resulted in a significant stabilization of bulk mRNA (Shahbadian *et al.*, 2009). Note, the only RNase in *E. coli* being able to slow mRNA degradation on a global scale is RNase E (Babitzke & Kushner, 1991), indicating a certain analogy in the function of both proteins in terms of their roles in mRNA decay.

Global impact of RNase Y on the transcriptome of *B. subtilis*

Even though it was shown that RNase Y affected global mRNA half-lives significantly, only a few targets of the endoribonuclease were known. These targets were the SAM-dependent riboswitches like the leader mRNA of *yitJ* (Shahbadian *et al.*, 2009), the mRNA of the ribosomal protein RpsO (Yao & Bechhofer, 2010) and the mRNA of the *gapA* operon (Commichau *et al.*, 2009). Using a global microarray-based approach we were able to confirm all three mentioned mRNAs as targets of RNase Y. We further identified more than 900 mRNAs that were affected in their abundance upon RNase Y depletion (Lehnik-Habrink *et al.*, 2011b). The impressive number of affected mRNAs is in good agreement with the idea of RNase Y being the globally acting endoribonuclease in *B. subtilis*. As mentioned before, the only other known RNase having such a strong impact on the transcriptome of a bacterium is RNase E of *E. coli*. In the terms of scope, RNase Y depletion resulted in changed abundances of 20% of the approximately 4.200 open reading frames in *B. subtilis*. Even though RNase E in *E. coli* affects 40%-60% of total mRNA (depending on the study), the genetic system used to carry out the experiments in *B. subtilis* and *E. coli* were rather different (Lee *et al.*, 2002; Stead *et al.*, 2011). In *E. coli* the

deletion of *rne* was facilitated by an overexpression of RNase G. Therefore RNase E was completely absent in the strains. In our system, RNase Y was depleted from the cells until growth had ceased. Nevertheless, Western blot analysis demonstrated significant residual amounts of RNase Y in cells at the time point of RNA isolation (Lehnik-Habrink *et al.*, 2011b). It seems plausible that total depletion of RNase Y would affect more targets in the cell and also lead to increased fold changes. However, this would be achieved at the price of a large number of false-positives that merely show up due to the change in growth rate (Klumpp *et al.*, 2009). Therefore we decided to apply rather stringent growth criteria in our study to impede the number of false positives even though this may lead in some cases to underestimation of the impact of RNase Y on certain transcripts.

In addition of the large number of mRNAs affected in abundance we also revealed an extraordinary stabilization of several transcripts by RNase Y depletion. Some of the selected targets exhibited half lives of less than five minutes under wild type conditions and were substantially stabilized to half lives over 30 min upon RNase Y depletion (see *ynfC*, *yhbJ*, *speD*). Especially the stabilization of the *ydaB* transcript from two minutes to 80 min was remarkable (Lehnik-Habrink *et al.*, 2011b). These findings are in very good agreement with the observation that RNase Y depletion leads to significant slow down of pace of global mRNA turnover (Shahbadian *et al.*, 2009). The large number of targets and the strong stabilizing impact on individual mRNAs makes RNase Y a unique enzyme in *B. subtilis* with respect to its influence in terms of quality and quantity. RNase Y shares its property of global influence on RNA stability with RNase E of *E. coli*, whereas loss of RNase J1 and J2 only had minor impacts on the bulk mRNA stability (Babitzke & Kushner, 1991; Even *et al.*, 2005; Shahbadian *et al.*, 2009).

Impact of RNase Y on individual transcripts

Our microarray analysis revealed the existence of about 550 mRNAs exhibiting increased abundance. The most strongly affected target upon RNase Y depletion was the *trp* operon (Lehnik-Habrink *et al.*, 2011b). This operon encodes almost all proteins needed for the biosynthesis of tryptophan from chorismate. Northern blot analysis revealed for the first time a distinct single transcript of the operon, suggesting a crucial contribution of RNase Y to the turnover of the mRNA. This operon is also under the control of the RNA-binding protein TRAP. Under conditions of high tryptophan concentration TRAP binds to the leader sequence of the mRNA and in turn facilitates the formation of a transcriptional terminator. To recycle TRAP for ongoing termination, the leader sequence

has to be degraded to release the protein from the mRNA (Deikus *et al.*, 2004). It was previously shown that two other RNases are also involved in the turnover of the *trp* mRNA, RNase J1 and the polynucleotide phosphorylase (Deikus *et al.*, 2008). Therefore RNase Y, RNase J1 and PnpA influence the abundance of one and the same mRNA, the *trp* transcript. Nevertheless the impact of RNase Y is most severely as deletion or depletion of the other two RNases did not result in the appearance of a distinct full length transcript in Northern blot analysis (Deikus *et al.*, 2004; Lehnik-Habrink *et al.*, 2011b). As mentioned before, almost all proteins needed for the biosynthesis of tryptophan are encoded in the *trp* operon. The first reaction in the pathway from chorismate to tryptophan is the formation of anthranilate. This step is catalyzed by an enzymatic complex consisting of TrpE and PabA. PabA is the only protein not encoded in the *trp* operon but in the *pab* operon. Interestingly, this operon is also affected by RNase Y depletion. The operon contains the genes *pabB*, *pabA* and *pabC*. Between the *pabB* and *pabA* coding region is also a TRAP binding site resulting in the control of *pabAC* transcription in response to tryptophan availability (de Saizieu *et al.*, 1997). Remarkably, RNase Y depletion leads to increased amounts of *pabA* and *pabC*, but the promoter-proximal *pabB* mRNA remained unaffected. This result suggests that this TRAP-dependent RNA switch might also be a target for RNase Y.

In a very recent publication the influence of RNase J1 and RNase Y on the *trp* leader mRNA was investigated (Deikus & Bechhofer, 2011). It was hypothesized that due to equal half lives of the *trp* leader mRNA in cells depleted of J1 or Y the effects of RNase Y depletion may be more indirect. Even though this is possible for the degradation of this leader mRNA the full length transcript is much more affected by RNase Y as demonstrated in our Northern blot experiments. Furthermore, the mRNAs that were affected in abundance in our RNase Y depletion experiments were quite different to the microarray results of RNase J1 (Lehnik-Habrink *et al.*, 2011b; Mäder *et al.*, 2008).

Another mRNA being subjected to an endonucleolytic processing event is the *gapA* mRNA (Ludwig *et al.*, 2001). The bicistronic *gapA* transcript encodes the regulatory protein CggR and glycolytic enzyme glyceraldehyde 3-phosphate dehydrogenase. Due to their unequal function both proteins can be found in very different amounts in the cell, even though they are located on the same mRNA (the cell contains 100x more GapA than CggR) (Meinken *et al.*, 2003). One of the factors contributing to this unequal expression is the processing of the mRNA where both genes are located on. Here, processing divides the mRNA resulting in the formation of an unstable *cggR* and a stable *gapA* mRNA (Ludwig *et al.*, 2001). The processing event leads to the formation of a 5' stem at the beginning of the

mature *gapA* transcript which contributes to the increased stability of this mRNA. Even though the underlying mechanism was known for quite a while the endoribonuclease responsible for the cleavage has remained unknown. Our Northern blot analysis clearly demonstrated that RNase Y is responsible for this processing event. The significant stabilization of the full length transcript upon depletion of RNase Y demonstrates that the enzyme cleaves the transcript and therefore contributes to the different stabilities of the mRNAs (Commichau *et al.*, 2009).

As mentioned before our global microarray analysis revealed that RNase Y depletion resulted in altered abundances of over 900 mRNAs. From these mRNAs about one third (350 mRNAs) exhibited decreased amounts. Using Northern blot analysis we were able to elucidate two mechanisms how decreased abundance can result from RNase Y depletion (Lehnik-Habrink *et al.*, 2011b).

The very nature of RNase Y as an RNA cleaving enzyme would suggest primarily the appearance of mRNAs with increased amounts. Therefore it is quite likely that the majority of the transcripts with lower abundances are somehow indirectly regulated by RNase Y depletion. One major group of these mRNAs with decreased abundances are transcripts encoding proteins important for the formation of biofilms. All three of the affected biofilm operons are under the repression of the master regulator SinR. Northern blot analysis of one of the operons (the *tapA-sipW-tasA* operon) revealed that even though the transcript itself was stabilized the overall amount of the mRNA was decreased. As this clearly pointed in a direction of indirect regulation, we performed Northern blot analysis with the master regulator (and repressor) SinR. The analysis revealed that the monocistronic *sinR* mRNA was clearly stabilized probably leading to higher amounts of the repressor (Lehnik-Habrink *et al.*, 2011b). It is quite likely that higher SinR amounts suppress the effect of its antagonists SinI and SlrR by titration and eventually lead to even stronger repression of the operons. As RNase Y depletion gave higher repression of the biofilm operons we expected that increasing the amounts of RNase Y should result in lower repression and therefore lead to increased biofilm formation. Indeed, RNase Y overexpression resulted in the formation of complex colony architecture in the background of the wild type strain 168 (Lehnik-Habrink *et al.*, 2011b). These findings are in support of the idea that RNase Y is one factor influencing the formation of biofilms. To conclude, we were able to trace back the effect of RNase Y depletion leading to decreased amounts of transcripts encoding proteins involved in biofilm formation. We predict that the strong stabilization of the mRNA of the master regulator/repressor SinR results in stronger repression of its targets.

However, decreased amounts of mRNAs do not always have to be indirect effects of RNase Y depletion. Also direct targets can be negatively affected in terms of abundance by the lack of the endoribonuclease. One example is the *thrS* mRNA. As a global acting endoribonuclease, RNase Y functions not only as an initiator of RNA degradation but also fine tunes mRNAs abundances in response to nutrient availability. Our Northern blot analysis revealed that RNase Y is responsible for the maturation of the *thrS* transcript. The *thrS* mRNA encodes the major threonyl-tRNA synthetase and contains a long 5' untranslated region upstream of the structural gene. Here, a threonine-responsive structure is located, the so called T-box. Under low threonine concentration, uncharged tRNA^{Thr} binds the T-box causing the formation of an antiterminator structure so that transcription can proceed further into the structural gene. This antiterminator structure is subsequently cleaved by a so far unknown endoribonuclease leading to the formation of a stem at the very 5' end of the mature mRNA. In general, the formation of such a stem-loop structure at the 5' end results in a significant stabilization of the transcript which is also the case for *thrS* (Condon *et al.*, 1996; Homuth *et al.*, 1999; Ludwig *et al.*, 2001). Even though *in vitro* experiments suggested that RNase J1 might be responsible for the cleavage of the *thrS* mRNA (Even *et al.*, 2005), our *in vivo* results strongly point to RNase Y as the endoribonuclease being involved in this processing event. In summary, with this Northern blot analysis we were able demonstrate that RNase Y is responsible for the maturation of the *thrS* mRNA *in vivo* (Lehnik-Habrink *et al.*, 2011b). Interestingly, the *thrS* mRNA is one of the mRNAs exhibiting lower overall abundance upon RNase Y depletion. It is very likely that the effect of decreased amounts of the *thrS* mRNA is the result of the missing stem at the 5' end of the full length transcript, which protects the mRNA from further degradation. Therefore even though RNase Y depletion leads to the accumulation of the full length mRNA, this unprocessed transcript is more unstable compared to the mature form and in turn leads to decreased amounts of the mRNA. This example shows how a direct target of RNase Y can appear in decreased amounts upon RNase Y depletion in our microarray analysis.

8.2. Re-finishing the structure of RNase Y

Since its first discovery RNase Y was annotated to contain a transmembrane domain at its amino terminal end, a KH domain for RNA binding and a HD domain for its catalytic activity, both located in the middle of the protein (Commichau *et al.*, 2009; Hunt *et al.*, 2006; Shahbadian *et al.*, 2009). With the help of various biochemical and

bioinformatics tools we were able to re-fine the domain organization of the enzyme. We demonstrated that RNase Y contains a coiled-coil domain and demonstrated that this domain is important for the oligomerization of the protein (Lehnik-Habrink *et al.*, 2011a). The finding that coiled-coil domains are involved in the formation of oligomers was already shown for several other proteins (Duman & Löwe, 2010; Ghigo & Beckwith, 2000). Interestingly, our biochemical data demonstrated that RNase Y is a disordered protein in solution. The investigation of such unfolded proteins is a rather new field in protein research (Dyson & Wright, 2005). This is due to the fact that classic biochemical methods are strongly biased towards the characterization of folded proteins as unfolded proteins are very sensitive to protease dependent degradation for example in the process of purification. Moreover, crystallization of such unfolded proteins is rather difficult. These disordered regions within proteins play an important role in direct protein-protein interactions. They open the possibility to evolve microdomains (small domains involved in protein interactions) without the structural and thermodynamic constraints of protein folding and stability. Therefore high specificity, but low affinity interactions can arise where the free energy of the interaction is used for protein folding (Lehnik-Habrink *et al.*, 2011a). A nice example of this paradigm is the C-terminus of RNase E, which is also natively unstructured. This part of the protein is important for direct protein-protein interactions. Here, the formation of microdomains provides the interaction specificity for the other proteins of the RNA degradosome. Furthermore, new regulatory properties of the degradosome can arise rapidly, because partners that modify its function could be recruited by quickly evolving microdomains (Marcaida *et al.*, 2006).

Our new domain annotation was further the basis for investigations dealing with the impact of these domains to the functions of the protein *in vivo* and their implication for the interaction with other proteins of the RNA degradosome. We were able to demonstrate that the first (the transmembrane) and the last domain (the conserved C-terminal part) are essential for the protein to function properly in the cell. It was somehow surprising to see that the proper membrane localization of RNase Y is essential for *B. subtilis*. Re-localization of RNase Y by fusing an unrelated transmembrane domain was successful, suggesting that the major function of this part of the protein is to tether the enzyme to the membrane. The fact that RNase Y must be located at a certain site in the cell is in agreement with accumulating observations that mRNA degradation is spatially organized in the bacterial cell. In *E. coli* several RNases can also be found the membrane fraction of the cell (Miczak *et al.*, 1991). The membrane association of RNase E was verified by electron microscopy experiments, too (Liou *et al.*, 2001). Further experiments identified a

distinct membrane binding domain (an amphipathic alpha-helix) being important for its proper localization. The deletion of this segment resulted in impaired growth behavior (Khemici *et al.*, 2008). But not only RNases can be spatially organized. With the availability of more sensitive fluorescence methods it becomes evident that also mRNAs are molecules that are not evenly distributed throughout the cell. A study conducted in *E. coli* demonstrated that several mRNAs are associated to the inner cytoplasmic membrane of the cell. Furthermore it was shown that cis-acting sequences within the transmembrane-coding sequence of the membrane proteins were necessary and sufficient for mRNA targeting to the membrane (Nevo-Dinur *et al.*, 2011). Another publication dealing with *C. crescentus* and *E. coli* demonstrated that several mRNAs display limited dispersion from their site of transcription. In contrast to *E. coli*, the RNase E homolog in *C. crescentus* appears associated with the DNA and not with the inner membrane of the cell. Even though a lot of work has yet to be done in the field of spatial organization of mRNA decay, our finding that proper membrane localization of RNase Y is essential for the *B. subtilis* emphasizes the prediction that this field will provide some promising new discoveries.

8.3. The RNA degradosome of *B. subtilis*

mRNA degradation can be carried out either by single enzymes or by protein complexes. Such protein complexes devoted to RNA degradation are called exosomes in eukaryotes and archea or degradosomes in bacteria. In *E. coli* the major endoribonuclease RNase E not only initiates the decay of mRNAs but also provides the binding sites for the exoribonuclease PnpA, the DEAD-box RNA helicase RhlB and the glycolytic enzyme enolase. All four proteins together form the core of the RNA degradosome in *E. coli* (Carpousis, 2007). Such RNase E dependent degradosomes can be found in many bacteria like *Caulobacter crescentus*, *Pseudoalteromonas haloplanktis* and *Vibrio angustum* (Ait-Bara & Carpousis, 2010; Erce *et al.*, 2010; Hardwick *et al.*, 2011). Even though these protein complexes were discovered in an increasing number of bacteria, their existence in Gram positive bacteria not containing RNase E was long unknown. Only in the recent years a number of publications accumulated strongly suggesting the existence of such a complex independently of the presence of RNase E. First evidences for this kind of complex in *B. subtilis* was derived from pull down experiments using glycolytic enzymes as bait proteins revealing interactions with RNase Y as well as RNase J1. A further bacterial two hybrid screen demonstrated direct interaction between: the glycolytic enzymes enolase and phosphofructokinase, the RNases polynucleotide phosphorylase, RNase J1/J2 and the

endoribonuclease RNase Y (at this time called Rny). The only RNase that was able to contact all proteins (except RNase J2, which most likely only loosely associates to the complex via RNase J1) was RNase Y (Commichau *et al.*, 2009). This model of the degradosome was re-fined by the identification of the DEAD-box RNA helicase CshA as the central helicase of the complex due to its unique ability to interact with RNase Y (see Fig. 50) (Lehnik-Habrink *et al.*, 2010). Later on, all interactions predicted by the two hybrid assay concerning RNase Y were confirmed *in vivo* (Lehnik-Habrink *et al.*, 2011a). The idea of such a protein complex in *B. subtilis* was challenged by the fact that these interactions were not seen in a yeast two hybrid screen conducted by others (Mathy *et al.*, 2010). However this yeast two hybrid screen also failed to detect self-interactions of the RNases J1 and J2, which was suggested by our bacterial two hybrid approach (Commichau *et al.*, 2009). Furthermore, self-interaction of J1 and J2 is very likely as RNase J1 crystallized as a dimer and in *in vitro* experiments J1 only functions properly in its dimeric form (Li de la Sierra-Gallay *et al.*, 2008; Newman *et al.*, 2011).

In agreement with the idea of an RNase E independent degradosome in Gram positive bacteria, a growing number of publications reports interactions of RNase Y reminiscent of the postulated RNA degradosome of *B. subtilis*. In the related organisms *Staphylococcus aureus*, interactions between RNase Y and CshA, enolase and phosphofructokinase were demonstrated. In addition it was shown that RNase J1 interacted with the exoribonuclease PnpA (Roux *et al.*, 2011). Furthermore, the RNase Y homolog in *Streptococcus pyogenes* also interacts with the glycolytic enzyme enolase (Kang *et al.*, 2010).

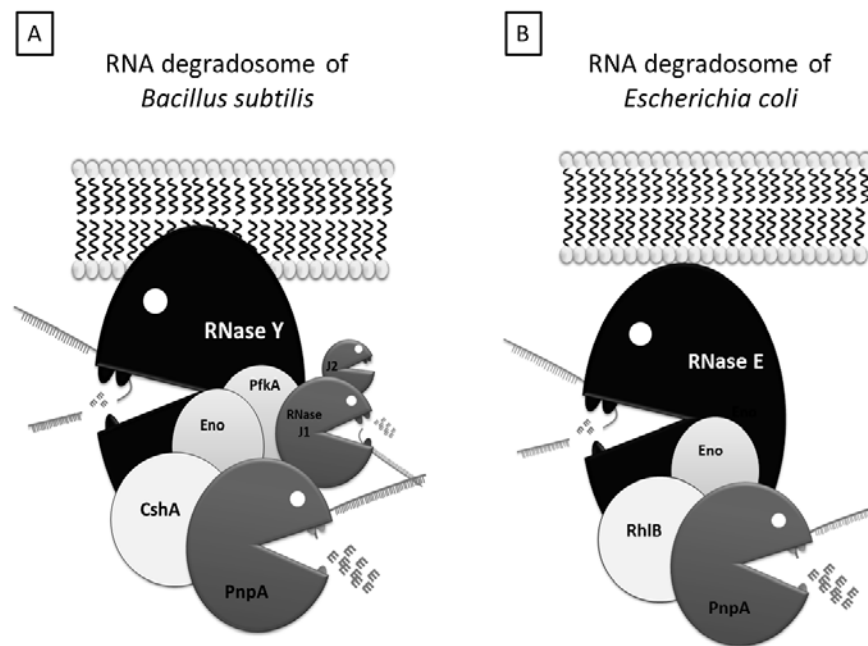


Fig. 50. Comparison of the RNA degradosomes of *B. subtilis* and *E. coli*. (A) The membrane-bound RNase Y coordinates the RNA degradosome of *B. subtilis*. This protein can bind the two glycolytic enzymes enolase (Eno) and phosphofruktokinase (PfkA), the DEAD-box RNA helicase CshA and the two RNases polynucleotide phosphorylase (PnpA) and RNase J1. RNase J2 is only loosely associated via RNase J1. (B) The membrane-attached RNase E sequesters the RNA degradosome of *E. coli* to the inner cytoplasmic membrane. RNase E contains the binding sites for the glycolytic enzyme enolase (Eno), the DEAD-box RNA helicase RhlB and the RNase polynucleotide phosphorylase (PnpA).

8.4. mRNA degradation in *B. subtilis*

Our microarray analysis establishes the role of RNase Y as the global RNase in the mRNA decay of *B. subtilis*. We demonstrated that under the stringent growth criteria used in our experimental setup over 900 mRNAs were significantly affected. In addition, Northern blot analysis revealed a remarkable stabilization of individual transcript up to the range of hours (Lehnik-Habrink *et al.*, 2011b). But how does RNase Y fit into the overall process of mRNA decay in *B. subtilis*?

8.5. Which is the chief-endoribonuclease, RNase J1 vs RNase Y?

As mentioned earlier, no exact model for RNA degradation in *B. subtilis* was predicted due to a high uncertainty of the accomplishment of this process. This uncertainty was nurtured by that fact that the general model derived from *E. coli* with RNase E as the central endoribonuclease initiating the mRNA turnover could not be

assigned to *B. subtilis* because no functional equivalent of the enzyme was known. Therefore the discovery of the ribonucleases RNase J1/J2 and RNase Y as novel endoribonucleases was very welcome (Even *et al.*, 2005; Shahbadian *et al.*, 2009). As in *E. coli* the initial endonucleolytic cleavage by RNase E represents the rate-limiting step in mRNA decay, the question arises which of the two novel RNases is responsible for this important step in the overall process of mRNA degradation in *B. subtilis*?

As all bacteria exhibited an all or nothing paradigm of mRNA decay, the first initial cleavage is the rate limiting step in the overall process. Suppressing this first step should result in the stabilization of mRNAs on a global scale. Judging both RNases by their impact on total mRNA turnover RNase Y is clearly more important. Depleting the enzyme from the cells leads to a significant reduction of total mRNA decay and therefore results in a remarkable stabilization of bulk mRNA (Shahbadian *et al.*, 2009). Our Northern blot analysis, determining half-lives of individual targets strongly supports this idea as we observed extraordinary stabilization of several mRNAs upon RNase Y depletion (Lehnik-Habrink *et al.*, 2011b). In contrast to RNase Y, the stabilizing effect of the J-type RNases was only minor. The deletion of RNase J2 had no effect on bulk mRNA turnover at all. Even the combined depletion and deletion of J1 and J2 resulted only in a very weak reduction of pace of bulk mRNA decay (Even *et al.*, 2005). These results indicate that RNase Y is the enzyme performing the first initial cut in the overall mRNA decay process in *B. subtilis*.

Our global transcriptome analysis is in very good agreement with this idea. We found that over 900 mRNAs were affected by the depletion of RNase Y. About two third of them exhibited increased amounts (Lehnik-Habrink *et al.*, 2011b). In contrast, the loss of the individual J-RNases had almost no effect on the transcriptome of *B. subtilis*. The combined depletion and deletion of the both, J1 and J2, resulted in 600 mRNAs exhibiting changed abundances. Nevertheless this number should be handled with care, as the same number of mRNAs showed increased as well as decreased amounts (Mäder *et al.*, 2008). This fact is somehow inconsistent with the idea of an endoribonuclease initiating the global mRNA turnover in *B. subtilis*. Furthermore, a significant number of mRNAs found in elevated amounts can be assigned to large regulons, where the regulators itself is affected, too. For example, 61 members of the SigD regulon are positively affected by RNase J1/J2 depletion/deletion, but the regulator itself is also 2.5 fold increased in amount (Mäder *et al.*, 2008). The only global regulator found in our microarray analysis being affected at least 2.5 fold was Spx (Lehnik-Habrink *et al.*, 2011b). Nevertheless even overexpression does not alter the amount of Spx in the cell, as Spx is under stringent posttranslational

control by Clp proteases (Nakano *et al.*, 2002). Therefore indirect effects on the transcriptome due to the increased abundance of the *spx* mRNA are very unlikely.

One difficulty of the microarray analysis arises from the fact that RNase Y as well as RNase J1 are essential enzymes. Therefore conditional mutants were used in both studies allowing the controlled depletion of the RNases. Using this kind of genetic system demands high attention for the choice of the timepoints of RNA isolation. Harvesting the cells too early would result in unchanged mRNA degradation due to high residual amounts of the RNase. Therefore sufficient depletion of the RNase is necessary. Nevertheless, prolonged depletion of the enzyme also affects the growth speed of the two cultures to be compared, as the function of the enzyme is essential for the cells to survive. A difference in the growth rate of the cells is quite problematic as it has a significant impact on the transcriptome itself (Klumpp *et al.*, 2009). Therefore we took care to isolate RNA from cells exhibiting exactly the same growth rate. It is therefore difficult to interpret some of the microarray results for RNase J1/J2 because the strains used in this study fall short with respect to their growth abilities, as they exhibit quite different growth rates (45 min vs 81 min doubling time) (Mäder *et al.*, 2008). A consequence of this drawback could be for example the appearance of 30 mRNAs encoding ribosomal proteins found to be negatively affected. This set of mRNAs is probably more tightly controlled by the growth rate than by the depletion/deletion of J1/J2, resulting in an overestimation of the impact of the double mutation of the J-type RNases (Paul *et al.*, 2004). Even though we are certain that the results of the transcriptome analysis are surely done with care, their origin, meaning the genetic system of deleting and depleting the RNases is somewhat troubling. Interpreting the transcriptome results of the RNase J1 study is even more complicated regarding the fact that RNase J1 exhibits a second catalytic activity. In addition to the endonucleolytic activity, RNase J1 also has a 5'-3' exonucleolytic activity making the enzyme unique in the bacterial world (the exonucleolytic activity of RNase J2 is extremely limited (Mathy *et al.*, 2010)). Nevertheless, considering that RNase J1 comprise both activities; it is not known which of the activities is responsible for the changed mRNA abundances found in the microarrays.

Besides the experiments of global mRNA stabilization and microarray analysis arguing for a model in which RNase Y is the endoribonuclease responsible for the initiation of mRNA decay, there are also *in vitro* data that support the notion that RNase J1 is more a 5'-3' exoribonuclease. In a very informative review of C. Condon about the endonucleolytic and exonucleolytic activities of RNase J1 it is stated that *in vitro* assays for the endoribonuclease activity of RNase J1/J2 "require very high concentrations of the

enzyme, often in orders of magnitude excess over the substrate and lower concentrations of the enzyme were inefficient” (Condon, 2010). This fact is further supported by the finding that high amounts of RNase J1 can be used to determine the three dimensional structure of an unknown RNA molecule as the enzyme cleaves under these conditions almost any nucleotide that is present in a single-stranded conformation (Daou-Chabo & Condon, 2009). Perhaps this property of RNase J1 exhibited at high enzyme concentrations *in vitro* explains the conflicting findings that RNase J1/J2 cleaves the *thrS* leader RNA *in vitro* but no differences in the amount of the *thrS* mRNA were found in microarray analysis revealing *in vivo* targets (Even *et al.*, 2005; Mäder *et al.*, 2008). In agreement with this idea, we found that *in vivo* RNase Y is responsible for processing the *thrS* leader RNA (Lehnik-Habrink *et al.*, 2011b). Nevertheless it is possible that both RNases are implicated in the turnover of the target, although no *in vivo* evidence for an implication of RNase J1 is available. One more fact arguing against RNase J1 to be the major mRNA decay initiating endoribonuclease is that homologs of RNase J found in archaea exclusively possess the 5'-3' exonucleolytic activity (Clouet-d'Orval *et al.*, 2010; Hasenöhrl *et al.*, 2011).

In summary, it can be concluded that RNase Y is the major endoribonuclease initiating mRNA decay in *B. subtilis*. Therefore only RNase Y can stabilize global mRNAs so sustainable. In contrast, RNase J1/J2 only stabilizes mRNAs on a global scale to a minor extent. Furthermore a number of facts argue for the notion that the enzyme is more a 5'-3' exoribonuclease than an endoribonuclease, still making it very important and indispensable for the overall process of mRNA decay in *B. subtilis*.

8.6. A model for the mRNA degradation in *B. subtilis*.

A similarity in the mRNA decay of *B. subtilis* and *E. coli* is the fact of an “all nor none” pattern found in Northern blot analysis of both bacteria, meaning that in most cases only full length transcripts can be observed but no decay intermediates. This pattern suggests that mRNA decay is first order, and depends on an initial step that is rate-limiting (Bechhofer, 2009). In *E. coli* this first decay-initiating step is conducted by RNase E. In *B. subtilis* the recently discovered enzyme RNase Y is likely to be the functional equivalent, as stated above. Therefore the ability of reducing the pace of global mRNA turnover is only unique to these two enzymes.

In the current model RNase Y initiates the mRNA decay by performing the first endoribonucleolytic cleavage within the body of the transcript. This cleavage produces new entry sites for exoribonucleases. In contrast to *E. coli*, *B. subtilis* is able to degrade the two resulting fragments in both directions due to the presence of the unique 5'-3' enzymatic activity of RNase J1. Therefore it can be postulated that after the initial cut of RNase Y the downstream fragment is subject to 5'-3' exonucleolytic decay by RNase J1 whereas the upstream fragment is subject to 3'-5' exonucleolytic degradation of ribonucleases like PnpA or RNase R (see Fig 51A). This general paradigm of transcript turnover was already verified for the degradation of the *rpoS* mRNA (Yao & Bechhofer, 2010), the turnover of the *yitJ* leader mRNA (Shahbabian *et al.*, 2009) and the degradation of the *infC* mRNA (Bruscella *et al.*, 2011).

Interestingly, this model also favors the existence of an RNA degradosome. In this complex RNase Y binds to RNase J1 and PnpA (see Fig. 50). The binding of the two exoribonucleases to RNase Y would be beneficial for the process of mRNA decay as RNase Y escort RNase J1 and PnpA to their site of action; the new entry sites generated by the endonucleolytic cleavage of the enzyme (see Fig 51A).

Besides this major route of mRNA decay, initiated by RNase Y, a number of transcripts were degraded in an RNase J1 dependent manner. First, due to its unique 5'-3' exonucleolytic activity RNase J1 is able to degrade mRNAs from their 5'-end. This specific pathway was revealed for the decay of the bicistronic *yhxA-glpP* mRNA (Richards *et al.*, 2011). In addition it was demonstrated that 5'-3' degradation from the native 5' end of this transcript depends strongly on the phosphorylation status of the mRNA. While a monophosphorylated mRNA is degraded rapidly, the presence of a triphosphate at the 5' end impedes the exonucleolytic activity of RNase J1 significantly (Richards *et al.*, 2011)(see Fig 51B).

As RNase J1 has the unique ability of an endo- and exonucleolytic activity a second possibility of RNase J1 dependent mRNA degradation exists, starting with an endonucleolytic cleavage of the enzyme. In this case RNase J1 initiates the degradation of the transcripts by a first cut within the body of the transcripts. Subsequently RNase J1 can "switch" its activity and use the newly generated (monophosphorylated) 5' end to degrade in 5'-3' direction. As suggested for RNase Y dependent degradation, 3'-5' directed decay can be performed by PnpA or other 3'-5' exonucleases (see Fig 51B). The structural basis of the dual activity of RNase J1 was elucidated in detail just recently (Dorléans *et al.*, 2011; Newman *et al.*, 2011).

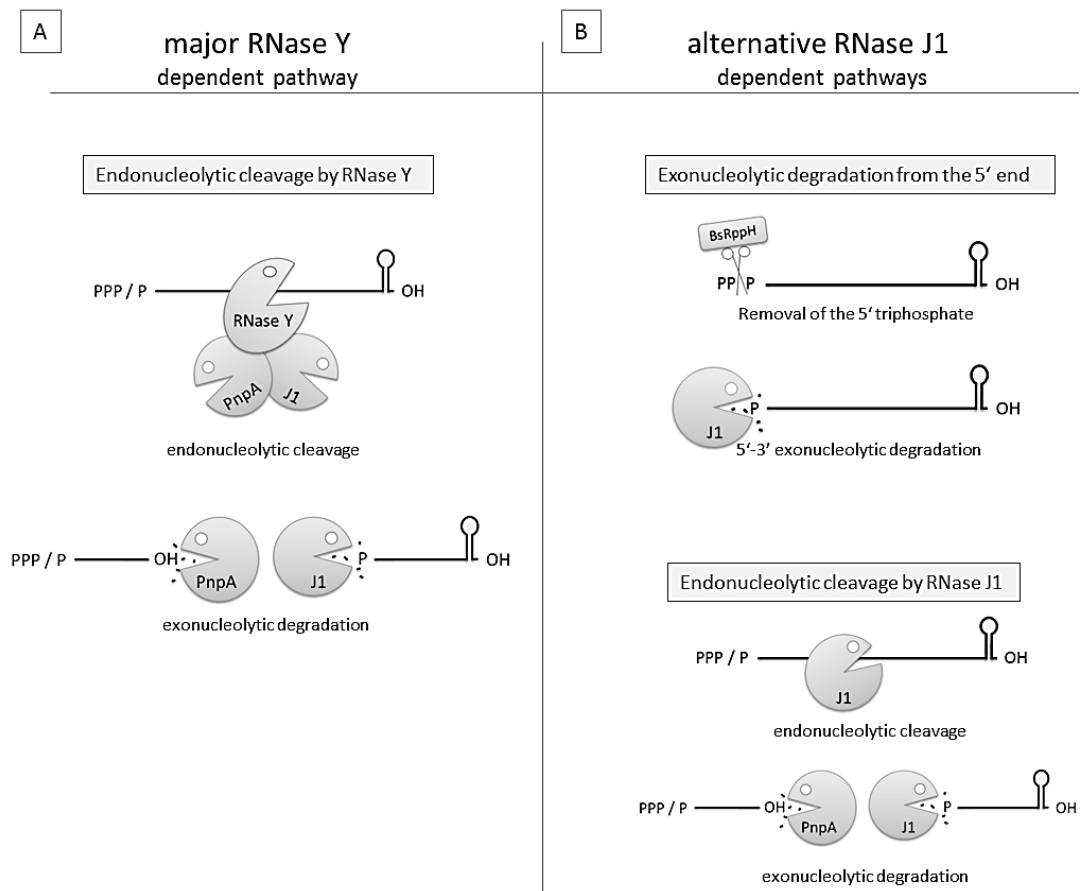


Fig 51. mRNA degradation in *B. subtilis*. The decay of mRNAs can occur via different pathways in *B. subtilis*. (A) As pointed out in the text the major pathway includes the endonucleolytic cleavage of RNase Y. Further degradation of the fragments is carried out by RNase J1 in 5'-3' direction and by PnpA or other 3'-5' exonucleases in the opposite direction. As RNase Y is able to bind RNase J1, PnpA and other proteins to form the RNA degradosome, the constitution of the complex can support the overall mRNA decay because RNase Y escorts the exonucleases to the newly generated entry sites. This turnover process was verified for the *rpsO* mRNA, the leader mRNA of *yitJ* and the *infC* mRNA. Nevertheless, alternative pathways involving RNase J1 may exist (B). First, due to its unique 5'-3' exonucleolytic activity, RNase J1 is capable of simply degrading its substrate from the 5' start. As this activity prefers monophosphorylated transcripts, the conversion of the triphosphate to a monophosphate may be an important step for this mode of action. In *B. subtilis* BsRppH exhibits this activity to a certain extent. So far this pathway was only verified for the *yhxA-glpP* transcript. Second, the dual activity of RNase J1 also opens the possibility of initiating mRNA degradation by endonucleolytic cleavage. Further degradation in both directions can proceed by RNase J1 and 3'-5' dependent exonucleases like PnpA. The occurrence of this kind of degradation was demonstrated for the *trp* leader mRNA.

Consequences of the model

The model shown in Fig. 51 reveals similarities as well as fundamental differences in the general turnover of mRNAs in *B. subtilis* and *E. coli*. While the decay is initiated by an endoribonuclease in both organisms, the fate of the resulting cleavage products is different. The model of *E. coli* predicts sequential RNase E cleavages due to the fact that subsequent exonucleolytic degradation can only occur from the newly generated 3' ends. In contrast to *E. coli*, *B. subtilis* contains 5'-3' exoribonuclease activity (RNase J1) making new rounds of RNase Y cleavage unnecessary (Mathy *et al.*, 2007). Nevertheless further endonucleolytic cleavages by RNase Y are likely. Another consequence of the model is the hypothesis that RNase J1 is most likely essential due to its unique 5' exonucleolytic activity. While none of the many 3'-5' exonucleases are essential, as they probably can complement the loss of another, RNase J1 is the only enzyme in *B. subtilis* exhibiting a significant 5'-3' exonuclease activity (the exonucleolytic activity of RNase J2 is very poor (Mathy *et al.*, 2010)). Therefore the essentiality of the enzyme is most likely conferred by its unique 5'-3' exonucleolytic activity.

The role of the 5' status of the transcript

General models of mRNA decay usually start with endoribonucleolytic cleavage of the transcript. However, recent evidence suggested a non-nucleolytic step prior to this cleavage (Celesnik *et al.*, 2007). In *E. coli* it was found that the RNA pyrophosphorylase RppH can convert 5' triphosphate ends to monophosphates (Celesnik *et al.*, 2007). These monophosphorylated ends are the preferred substrates for endoribonucleases like RNase E or RNase Y *in vitro* (Mackie, 1998; Shahbadian *et al.*, 2009). For RppH it was shown that deletion of the enzyme resulted in the stabilization of several transcripts suggesting that the modification of the 5' end significantly influences the decay of those transcripts. However, strains harboring deletions in *rppH* are viable and microarray analysis revealed that less than 10% of the overall transcripts are affected in abundance (Deana *et al.*, 2008). It is therefore possible that other enzymes besides RppH exhibit pyrophosphorylase activity thus masking the importance of this enzyme. It should be noted that besides this focus on the phosphorylation status of the 5' end an alternative model called "direct entry" was proposed. This model suggests cleavage by RNase E irrespectively of the phosphorylation status of the 5' end of the mRNA (Baker & Mackie, 2003; Kime *et al.*, 2010). It is conceivable that both pathways exist in parallel in the *E. coli* cell. In a very recent publication this activity was also found in *B. subtilis* (Richards *et al.*,

2011). The protein BsRppH/YtkD also possesses a pyrophosphorylase activity. In contrast to *E. coli*, this activity primarily resulted in the stabilization of the tested transcript by the suppression of the 5'-3' exonucleolytic decay by RNase J1. In agreement, the turnover of *trp* leader mRNA which is dependent on RNase J1 endonucleolytic cleavage occurred irrespective phosphorylation status of the 5' end (Deikus & Bechhofer, 2011). Interestingly, a very recent report demonstrates that RNase Y dependent endonucleolytic decay also occurred independently of the presence of a mono-, or triphosphate at the 5' end of the *ermC* mRNA (Yao *et al.*, 2011). The finding of such a pyrophosphorylase activity in *B. subtilis* is very intriguing, however, its significance for the overall mRNA decay remains to be demonstrated.

8.7. CshA: A versatile RNA helicase of *B. subtilis*

Identification of CshA as the major RNA helicase in the RNA degradosome of *B. subtilis*

The first evidence for an RNA degradosome in *B. subtilis* was received from an interaction study of the glycolytic enzymes. In this study the initial model without an DEAD-box RNA helicase was postulated (Commichau *et al.*, 2009). However, the interaction of these enzymes with RNases in general and in such multiprotein complexes in particular is very well established (Carpousis, 2007; Lin-Chao *et al.*, 2007; Liou *et al.*, 2002). Therefore we re-addressed this question and cloned all known RNA helicase genes of *B. subtilis* into the vectors of the bacterial two hybrid system and tested the resulting constructs for their interaction abilities with enzymes of the RNA degradosome. While the RNA helicase YfmL did not interact with any protein, DeaD and CshB were capable of interacting with several of the proteins of the complex. However, the only enzyme that displayed clear interactions with all proteins of the degradosome was CshA. Furthermore CshA was the only DEAD-box RNA helicase that was able to interact with RNase Y, a key enzyme of the complex (Lehnik-Habrink *et al.*, 2010). The finding that more than one RNA helicase has the ability to interact with the complex is in agreement with results for *E. coli* showing that other RNA helicases besides RhlB (the resident RNA helicase) can interact with the degradosome under certain conditions. It was demonstrated that the RNA helicase CsdA binds to the complex at low temperatures. Further experiments revealed that CsdA was also able to take over certain functions of RhlB (Prud'homme-Généreux *et al.*, 2004). The reason for this backup can be the fact that under conditions of cold shock, where the formation of secondary structures on mRNAs is thermodynamically favored, the

additional availability of multiple DEAD-box RNA helicases ensures continuous RNA degradation even under conditions that normally would impede mRNA decay.

As mentioned, the DEAD-box RNA helicase CshA was the only RNA helicase that was able of interacting with RNase Y, a central protein of the complex. To elucidate the contributions of the different domains to this property we made several truncations of the enzyme. We revealed that a CshA variant devoid of the first RecA-like domain (the N-terminus of the enzyme) is still able to interact with all partner proteins except PfkA (Lehnik-Habrink *et al.*, 2010). In agreement, the functional homolog in the *E. coli* RNA degradosome RhlB also interacts via its C-terminal part with RNase E (Liou *et al.*, 2002). To further pinpoint the site of RNase Y interaction specificity, we created a hybrid product comprising the two RecA-like domains of CshB (which do not bind RNase Y) and the C-terminal domain of CshA. The exchange of this C-terminal part enabled the hybrid CshB to interact with RNase Y, indicating that the C-terminus confers the interaction specificity of CshA to RNase Y (Lehnik-Habrink *et al.*, 2010). The importance of the C-terminal extensions of DEAD-box RNA helicases is well known, for example the RNA helicase DeaD/YxiN is able to bind its substrate the 23S RNA via this domain (Kossen *et al.*, 2002). Whether the C-terminal domain of CshA is only necessary for the interaction specificity to RNase Y, or this part also confers RNA specificity remains to be elucidated.

The physiological role of CshA in *B. subtilis*

To get further insight into the role of CshA in the physiology of *B. subtilis* we constructed a mutant strain devoid of *cshA*. This strain grew indistinguishable to the wild type strain at 37°C but exhibited a clear growth defect at lower temperatures. At 20°C no growth was observed for the mutant strain on LB agar plates. This defect in growth at reduced temperatures was accompanied by a change in the morphology, exhibiting long wrinkled cells which most likely have a defect in cell separation. Due to its participation in the RNA degradosome CshA can be considered as the functional homolog of RhlB in *E. coli*. However, deletion of *rhlB* did not alter the growth behavior of *E. coli* at lower temperatures or compromises the shape of the bacteria (Iost & Dreyfus, 2006). Interestingly, blast analysis of CshA against the genome of *E. coli* revealed that the closest homolog is the RNA helicase CsdA (remember that CshA is an RNA helicase of *B. subtilis* whereas CsdA is present in *E. coli*). This RNA helicase was also shown to bind to the degradosome at low temperatures (Prud'homme-Généreux *et al.*, 2004). While *rhlB* deletion results in no obvious phenotype, mutations in the *csdA* gene leads to cold

sensitivity, just as observed for *csH*A deletions in *B. subtilis* (Iost & Dreyfus, 2006). The implication of RNA helicases for growth at lower temperatures results from the fact that secondary structures in RNA molecules are thermodynamically favored at decreased temperatures. DEAD-box RNA helicases can help to unwind these undesired mRNA structures that can otherwise be deleterious for the organism (Phadtare & Severinov, 2010). Another class of proteins helping the cell to overcome this burden are the so called “cold shock proteins” (El-Sharoud & Graumann, 2007). It was already shown in *B. subtilis* that the RNA helicase CshB interacts with the cold shock protein B (CspB) most likely to rescue misfolded mRNAs (Hunger *et al.*, 2006). To test whether CshA is able of interacting with cold shock proteins too, we performed bacterial two hybrid analysis with the RNA helicase and the three cold shock proteins encoded in the genome of *B. subtilis*. This analysis revealed a strong interaction of CshA with CspD, suggesting that both proteins work in conjunction to ensure proper translation initiation and mRNA folding. The finding that CshA is involved in the process of growth at low temperature resembles more the properties of the *E. coli* RNA helicase CsdA than RhlB.

Another difference between CshA of *B. subtilis* and RhlB of *E. coli* is the implication of both RNA helicases in the biogenesis of ribosomes. The deletion of *rhlB* in *E. coli* did not affect the biogenesis of the ribosomes at all (Iost & Dreyfus, 2006). Our pull down experiments and further two hybrid studies revealed interactions of CshA with RplA and RplC in *B. subtilis*. Subsequent analysis of the ribosomes by saccharose gradients centrifugation revealed an aberrant ribosomal profile. Both experiments together suggest that CshA is implicated in the biogenesis of the 50S subunit of the ribosome. In this process, CshA binds to its target (the large subunit) via the ribosomal proteins RplA and RplC. A connection between impeded ribosome formation and interaction with ribosomal proteins was already shown for the RNA helicase SrmB of *E. coli*. Here, the deletion of *srmB* leads also to a deficit of free 50S subunits (Charollais *et al.*, 2003). In contrast to CshA of *B. subtilis*, SrmB of *E. coli* was shown to bind the ribosomal proteins RplD and L24. In addition, it was demonstrated that SrmB interacts with the 23S rRNA (Trubetskoy *et al.*, 2009). Whether CshA is also able to bind ribosomal RNA will be an interesting issue for future experiments.

As CshA is part of an RNA degrading complex, deletion of the RNA helicase should result in altered mRNA turnover. To confirm this idea, we performed microarray analysis to assess the impact of the loss of *csH*A on the transcriptome of *B. subtilis*. In total more than 200 mRNAs were affected by the deletion of *csH*A, suggesting a significant impact of the enzyme on the mRNA turnover. As RNA helicases contain no inherent RNA cleaving

activity their influences on the abundance of the mRNAs have to be indirect. However, DEAD-box proteins can affect the stability of certain transcripts by making them more or less amenable for the degradation by RNases. For example, during the late acclimatization phase of cold shock in *E. coli*, PnpA is needed to degrade the mRNAs of cold shock proteins, that otherwise would be deleterious for the cell during further growth. In addition, deletion of the RNA helicase CsdA also leads to stabilization of mRNAs of cold shock proteins. Both proteins, PnpA and CsdA, interact with each other suggesting that they work in conjunction to degrade the mRNAs of these proteins (Liou *et al.*, 2002; Yamanaka & Inouye, 2001). In agreement with this example we revealed an overlap of more than 30% of the targets of RNase Y and mRNAs that were affected by the deletion of *csmA* (Lehnik-Habrink *et al.*, 2011b). Furthermore in previous experiments we demonstrated that CshA is able to interact with further RNases suggesting that some of the transcripts altered in abundance by *csmA* deletion are degraded in conjunction with RNase J1 and PnpA (Lehnik-Habrink *et al.*, 2010). The elucidation of the interplay between RNases and RNA helicases will be an interesting task for further experiments as we found that a number of targets were regulated in opposite directions in the microarray analyses of RNase Y and CshA. In addition, it would be interesting to see the impact of the loss of *csmA* on the transcriptome at lower temperatures. As stated before under these conditions the formation of secondary structures is favored, making RNA helicases crucial for the adaptation process to these conditions (Phadtare & Severinov, 2010). Therefore it is very likely that the impact of a *csmA* deletion is much more drastic at low temperatures. This idea is supported by our finding that the deletion of *csmA* results in a severe growth defect at reduced temperatures.

Concluding the results, we were able to demonstrate a significant impact of CshA on the transcriptome of *B. subtilis* supporting the idea of its participation in the RNA degradosome. We further demonstrated that loss of *csmA* resulted in a cold-sensitive phenotype. In agreement with these results, we found that CshA is able to interact with the cold shock protein CspD. Furthermore CshA interacted *in vivo* with ribosomal proteins and deletion of the RNA helicase impeded the biogenesis of the 50S subunit of the ribosome. Therefore we conclude that the RNA helicase CshA has multiple roles in the physiology of *B. subtilis*.

Outlook

In this work, we established the role of RNase Y as the major mRNA decay initiating endoribonuclease of *B. subtilis*. Furthermore we demonstrated that the enzyme is a central member of the RNA degradosome. The identification of “targets of the RNA degradosome” will be an interesting task for future experiments. Therefore microarray analyses, conducted under identical conditions (e.g. medium, growth phase), for RNase J and PnpA would probably reveal transcripts that are degraded by the concerted interplay of the three RNases.

Another member of the RNA degradosome is the RNA helicase CshA. Our experiments revealed that the RNA helicase has multiple roles in the physiology of *B. subtilis*. For future studies it would be interesting to dissect whether the growth defect of a *cshA* mutant at reduced temperatures is caused by the interference with the biogenesis of ribosomes or is due to its implication in mRNA decay.

9. References

- Abee, T., Kovacs, A. T., Kuipers, O. P. & van der Veen, S. (2011).** Biofilm formation and dispersal in Gram-positive bacteria. *Current opinion in biotechnology* **22**, 172-179.
- Abramoff, M. D., Magelhaes, P. J. & Ram, S. J. (2004).** Image processing with ImageJ. *Biophotonics Int* **11**, 36-42.
- Ait-Bara, S. & Carpousis, A. J. (2010).** Characterization of the RNA degradosome of *Pseudoalteromonas haloplanktis*: conservation of the RNase E-RhlB interaction in the gammaproteobacteria. *J Bacteriol* **192**, 5413-5423.
- Amar, P., Legent, G., Thellier, M., Ripoll, C., Bernot, G. & other authors (2008).** A stochastic automaton shows how enzyme assemblies may contribute to metabolic efficiency. *BMC Syst Biol* **2**, 27.
- An, S., Kumar, R., Sheets, E. D. & Benkovic, S. J. (2008).** Reversible compartmentalization of *de novo* purine biosynthetic complexes in living cells. *Science* **320**, 103-106.
- Anantharaman, V., Koonin, E. V. & Aravind, L. (2002).** Comparative genomics and evolution of proteins involved in RNA metabolism. *Nucleic Acids Res* **30**, 1427-1464.
- Ando, Y. & Nakamura, K. (2006).** *Bacillus subtilis* DEAD protein YdbR possesses ATPase, RNA binding, and RNA unwinding activities. *Biosci Biotechnol Biochem* **70**, 1606-1615.
- Aravind, L. & Koonin, E. V. (1998).** The HD domain defines a new superfamily of metal-dependent phosphohydrolases. *Trends Biochem Sci* **23**, 469-472.
- Aregger, R. & Klostermeier, D. (2009).** The DEAD box helicase YxiN maintains a closed conformation during ATP hydrolysis. *Biochemistry* **48**, 10679-10681.
- Arraiano, C. M., Andrade, J. M., Domingues, S., Guinote, I. B., Malecki, M. & other authors (2010).** The critical role of RNA processing and degradation in the control of gene expression. *FEMS Microbiol Rev* **34**, 883-923.
- Baba, T., Ara, T., Hasegawa, M., Takai, Y., Okumura, Y. & other authors (2006).** Construction of *Escherichia coli* K-12 in-frame, single-gene knockout mutants: the Keio collection. *Mol Syst Biol* **2**, 2006 0008.

- Babitzke, P. & Kushner, S. R. (1991).** The Ams (altered mRNA stability) protein and ribonuclease E are encoded by the same structural gene of *Escherichia coli*. *Proc Natl Acad Sci U S A* **88**, 1-5.
- Bai, U., Mandic-Mulec, I. & Smith, I. (1993).** SinI modulates the activity of SinR, a developmental switch protein of *Bacillus subtilis*, by protein-protein interaction. *Genes Dev* **7**, 139-148.
- Baker, K. E. & Mackie, G. A. (2003).** Ectopic RNase E sites promote bypass of 5'-end-dependent mRNA decay in *Escherichia coli*. *Mol Microbiol* **47**, 75-88.
- Bechhofer, D. H. (2009).** Messenger RNA decay and maturation in *Bacillus subtilis*. *Prog Mol Biol Transl Sci* **85**, 231-273.
- Beckering, C. L., Steil, L., Weber, M. H., Völker, U. & Marahiel, M. A. (2002).** Genomewide transcriptional analysis of the cold shock response in *Bacillus subtilis*. *J Bacteriol* **184**, 6395-6402.
- Belasco, J. G. (2010).** All things must pass: contrasts and commonalities in eukaryotic and bacterial mRNA decay. *Nat Rev Mol Cell Biol* **11**, 467-478.
- Bernstein, J. A., Lin, P. H., Cohen, S. N. & Lin-Chao, S. (2004).** Global analysis of *Escherichia coli* RNA degradosome function using DNA microarrays. *Proc Natl Acad Sci U S A* **101**, 2758-2763.
- Bertero, M. G., Gonzales, B., Tarricone, C., Ceciliani, F. & Galizzi, A. (1999).** Overproduction and characterization of the *Bacillus subtilis* anti-sigma factor FlgM. *J Biol Chem* **274**, 12103-12107.
- Bessarab, D. A., Kaberdin, V. R., Wei, C. L., Liou, G. G. & Lin-Chao, S. (1998).** RNA components of *Escherichia coli* degradosome: evidence for rRNA decay. *Proc Natl Acad Sci U S A* **95**, 3157-3161.
- Blair, K. M., Turner, L., Winkelman, J. T., Berg, H. C. & Kearns, D. B. (2008).** A molecular clutch disables flagella in the *Bacillus subtilis* biofilm. *Science* **320**, 1636-1638.
- Blum, H., Beier, H. & Gross, H. J. (1987).** Improved silver staining of plant proteins, RNA and DNA in polyacrylamide gels. *Electrophoresis* **8**, 93-99.
- Branda, S. S., González-Pastor, J. E., Ben-Yehuda, S., Losick, R. & Kolter, R. (2001).** Fruiting body formation by *Bacillus subtilis*. *Proc Natl Acad Sci U S A* **98**, 11621-11626.

Branda, S. S., Chu, F., Kearns, D. B., Losick, R. & Kolter, R. (2006). A major protein component of the *Bacillus subtilis* biofilm matrix. *Mol Microbiol* **59**, 1229-1238.

Brandi, A., Spurio, R., Gualerzi, C. O. & Pon, C. L. (1999). Massive presence of the *Escherichia coli* 'major cold-shock protein' CspA under non-stress conditions. *EMBO J* **18**, 1653-1659.

Britton, R. A., Wen, T., Schaefer, L., Pellegrini, O., Uicker, W. C. & other authors (2007). Maturation of the 5' end of *Bacillus subtilis* 16S rRNA by the essential ribonuclease YkqC/RNase J1. *Mol Microbiol* **63**, 127-138.

Bruscella, P., Shahbadian, K., Laalami, S. & Putzer, H. (2011). RNase Y is responsible for uncoupling the expression of translation factor IF3 from that of the ribosomal proteins L35 and L20 in *Bacillus subtilis*. *Mol Microbiol*.

Budde, I., Steil, L., Scharf, C., Volker, U. & Bremer, E. (2006). Adaptation of *Bacillus subtilis* to growth at low temperature: a combined transcriptomic and proteomic appraisal. *Microbiology* **152**, 831-853.

Bumann, D. (2008). Has nature already identified all useful antibacterial targets? *Curr Opin Microbiol* **11**, 387-392.

Butcher, B. G., Lin, Y. P. & Helmann, J. D. (2007). The *yvdFGHIJ* operon of *Bacillus subtilis* encodes a peptide that induces the LiaRS two-component system. *J Bacteriol* **189**, 8616-8625.

Büttner, K., Wenig, K. & Hopfner, K. P. (2006). The exosome: a macromolecular cage for controlled RNA degradation. *Mol Microbiol* **61**, 1372-1379.

Callaghan, A. J., Grossmann, J. G., Redko, Y. U., Ilag, L. L., Moncrieffe, M. C. & other authors (2003). Quaternary structure and catalytic activity of the *Escherichia coli* ribonuclease E amino-terminal catalytic domain. *Biochemistry* **42**, 13848-13855.

Callaghan, A. J., Aurikko, J. P., Ilag, L. L., Gunter Grossmann, J., Chandran, V. & other authors (2004). Studies of the RNA degradosome-organizing domain of the *Escherichia coli* ribonuclease RNase E. *J Mol Biol* **340**, 965-979.

Callaghan, A. J., Marcaida, M. J., Stead, J. A., McDowall, K. J., Scott, W. G. & Luisi, B. F. (2005). Structure of *Escherichia coli* RNase E catalytic domain and implications for RNA turnover. *Nature* **437**, 1187-1191.

Campanella, M. E., Chu, H. & Low, P. S. (2005). Assembly and regulation of a glycolytic enzyme complex on the human erythrocyte membrane. *Proc Natl Acad Sci U S A* **102**, 2402-2407.

- Campanella, M. E., Chu, H., Wandersee, N. J., Peters, L. L., Mohandas, N. & other authors (2008).** Characterization of glycolytic enzyme interactions with murine erythrocyte membranes in wild-type and membrane protein knockout mice. *Blood* **112**, 3900-3906.
- Canback, B., Andersson, S. G. & Kurland, C. G. (2002).** The global phylogeny of glycolytic enzymes. *Proc Natl Acad Sci U S A* **99**, 6097-6102.
- Carpousis, A. J. (2007).** The RNA degradosome of *Escherichia coli*: an mRNA-degrading machine assembled on RNase E. *Annu Rev Microbiol* **61**, 71-87.
- Carpousis, A. J., Luisi, B. F. & McDowall, K. J. (2009).** Endonucleolytic initiation of mRNA decay in *Escherichia coli*. *Prog Mol Biol Transl Sci* **85**, 91-135.
- Carzaniga, T., Briani, F., Zangrossi, S., Merlino, G., Marchi, P. & Deho, G. (2009).** Autogenous regulation of *Escherichia coli* polynucleotide phosphorylase expression revisited. *J Bacteriol* **191**, 1738-1748.
- Celesnik, H., Deana, A. & Belasco, J. G. (2007).** Initiation of RNA decay in *Escherichia coli* by 5' pyrophosphate removal. *Mol Cell* **27**, 79-90.
- Chai, Y., Kolter, R. & Losick, R. (2009).** Paralogous antirepressors acting on the master regulator for biofilm formation in *Bacillus subtilis*. *Mol Microbiol* **74**, 876-887.
- Chai, Y., Kolter, R. & Losick, R. (2010a).** Reversal of an epigenetic switch governing cell chaining in *Bacillus subtilis* by protein instability. *Mol Microbiol* **78**, 218-229.
- Chai, Y., Norman, T., Kolter, R. & Losick, R. (2010b).** An epigenetic switch governing daughter cell separation in *Bacillus subtilis*. *Genes Dev* **24**, 754-765.
- Chandran, V. & Luisi, B. F. (2006).** Recognition of enolase in the *Escherichia coli* RNA degradosome. *J Mol Biol* **358**, 8-15.
- Chandran, V., Poljak, L., Vanzo, N. F., Leroy, A., Miguel, R. N. & other authors (2007).** Recognition and cooperation between the ATP-dependent RNA helicase RhlB and ribonuclease RNase E. *J Mol Biol* **367**, 113-132.
- Chaney, S. G. & Boyer, P. D. (1972).** Incorporation of water oxygens into intracellular nucleotides and RNA. II. Predominantly hydrolytic RNA turnover in *Escherichia coli*. *J Mol Biol* **64**, 581-591.
- Charbonnier, Y., Gettler, B., Francois, P., Bento, M., Renzoni, A. & other authors (2005).** A generic approach for the design of whole-genome oligoarrays, validated for genotyping,

deletion mapping and gene expression analysis on *Staphylococcus aureus*. *BMC Genomics* **6**, 95.

Charollais, J., Pflieger, D., Vinh, J., Dreyfus, M. & Iost, I. (2003). The DEAD-box RNA helicase SrmB is involved in the assembly of 50S ribosomal subunits in *Escherichia coli*. *Mol Microbiol* **48**, 1253-1265.

Charollais, J., Dreyfus, M. & Iost, I. (2004). CsdA, a cold-shock RNA helicase from *Escherichia coli*, is involved in the biogenesis of 50S ribosomal subunit. *Nucleic Acids Res* **32**, 2751-2759.

Chastanet, A., Vitkup, D., Yuan, G. C., Norman, T. M., Liu, J. S. & Losick, R. M. (2010). Broadly heterogeneous activation of the master regulator for sporulation in *Bacillus subtilis*. *Proc Natl Acad Sci U S A* **107**, 8486-8491.

Cheng, Z. F., Zuo, Y., Li, Z., Rudd, K. E. & Deutscher, M. P. (1998). The *vacB* gene required for virulence in *Shigella flexneri* and *Escherichia coli* encodes the exoribonuclease RNase R. *J Biol Chem* **273**, 14077-14080.

Chu, F., Kearns, D. B., Branda, S. S., Kolter, R. & Losick, R. (2006). Targets of the master regulator of biofilm formation in *Bacillus subtilis*. *Mol Microbiol* **59**, 1216-1228.

Claessen, D., Emmins, R., Hamoen, L. W., Daniel, R. A., Errington, J. & Edwards, D. H. (2008). Control of the cell elongation-division cycle by shuttling of PBP1 protein in *Bacillus subtilis*. *Mol Microbiol* **68**, 1029-1046.

Clouet-d'Orval, B., Rinaldi, D., Quentin, Y. & Carpousis, A. J. (2010). Euryarchaeal beta-CASP proteins with homology to bacterial RNase J have 5'- to 3'-exoribonuclease activity. *J Biol Chem* **285**, 17574-17583.

Commichau, F. M., Herzberg, C., Tripal, P., Valerius, O. & Stülke, J. (2007). A regulatory protein-protein interaction governs glutamate biosynthesis in *Bacillus subtilis*: the glutamate dehydrogenase RocG moonlights in controlling the transcription factor GltC. *Mol Microbiol* **65**, 642-654.

Commichau, F. M. & Stülke, J. (2008). Trigger enzymes: bifunctional proteins active in metabolism and in controlling gene expression. *Mol Microbiol* **67**, 692-702.

Commichau, F. M., Rothe, F. M., Herzberg, C., Wagner, E., Hellwig, D. & other authors (2009). Novel activities of glycolytic enzymes in *Bacillus subtilis*: interactions with essential proteins involved in mRNA processing. *Mol Cell Proteomics* **8**, 1350-1360.

Condon, C., Putzer, H. & Grunberg-Manago, M. (1996). Processing of the leader mRNA plays a major role in the induction of *thrS* expression following threonine starvation in *Bacillus subtilis*. *Proc Natl Acad Sci U S A* **93**, 6992-6997.

Condon, C., Putzer, H., Luo, D. & Grunberg-Manago, M. (1997). Processing of the *Bacillus subtilis thrS* leader mRNA is RNase E-dependent in *Escherichia coli*. *J Mol Biol* **268**, 235-242.

Condon, C. & Putzer, H. (2002). The phylogenetic distribution of bacterial ribonucleases. *Nucleic Acids Res* **30**, 5339-5346.

Condon, C. (2003). RNA processing and degradation in *Bacillus subtilis*. *Microbiol Mol Biol Rev* **67**, 157-174, table of contents.

Condon, C. (2010). What is the role of RNase J in mRNA turnover? *RNA Biol* **7**, 316-321.

Condon, C. & Bechhofer, D. H. (2011). Regulated RNA stability in the Gram positives. *Curr Opin Microbiol* **14**, 148-154.

Cordin, O., Banroques, J., Tanner, N. K. & Linder, P. (2006). The DEAD-box protein family of RNA helicases. *Gene* **367**, 17-37.

Cornish-Bowden, A. & Cardenas, M. L. (1993). Channelling can affect concentrations of metabolic intermediates at constant net flux: artefact or reality? *Eur J Biochem* **213**, 87-92.

Cozy, L. M. & Kearns, D. B. (2010). Gene position in a long operon governs motility development in *Bacillus subtilis*. *Mol Microbiol* **76**, 273-285.

Crick, F. (1970). Central dogma of molecular biology. *Nature* **227**, 561-563.

Dandekar, T., Schuster, S., Snel, B., Huynen, M. & Bork, P. (1999). Pathway alignment: application to the comparative analysis of glycolytic enzymes. *Biochem J* **343 Pt 1**, 115-124.

Daou-Chabo, R. & Condon, C. (2009). RNase J1 endonuclease activity as a probe of RNA secondary structure. *RNA* **15**, 1417-1425.

de Jong, I. G., Veening, J. W. & Kuipers, O. P. (2010). Heterochronic phosphorelay gene expression as a source of heterogeneity in *Bacillus subtilis* spore formation. *J Bacteriol* **192**, 2053-2067.

de Saizieu, A., Vankan, P., Vockler, C. & van Loon, A. P. (1997). The *trp* RNA-binding attenuation protein (TRAP) regulates the steady-state levels of transcripts of the *Bacillus subtilis* folate operon. *Microbiology* **143** (Pt 3), 979-989.

Deana, A., Celesnik, H. & Belasco, J. G. (2008). The bacterial enzyme RppH triggers messenger RNA degradation by 5' pyrophosphate removal. *Nature* **451**, 355-358.

Decker, B. L. & Wickner, W. T. (2006). Enolase activates homotypic vacuole fusion and protein transport to the vacuole in yeast. *J Biol Chem* **281**, 14523-14528.

Deikus, G., Babitzke, P. & Bechhofer, D. H. (2004). Recycling of a regulatory protein by degradation of the RNA to which it binds. *Proc Natl Acad Sci U S A* **101**, 2747-2751.

Deikus, G., Condon, C. & Bechhofer, D. H. (2008). Role of *Bacillus subtilis* RNase J1 endonuclease and 5'-exonuclease activities in *trp* leader RNA turnover. *J Biol Chem* **283**, 17158-17167.

Deikus, G. & Bechhofer, D. H. (2009). *Bacillus subtilis trp* Leader RNA: RNase J1 endonuclease cleavage specificity and PNPase processing. *J Biol Chem* **284**, 26394-26401.

Deikus, G. & Bechhofer, D. H. (2011). 5'-end-independent RNase J1 endonucleolytic cleavage of a *Bacillus subtilis* model RNA. *JBC*.

Delumeau, O., Lecoite, F., Muntel, J., Guillot, A., Guedon, E. & other authors (2011). The dynamic protein partnership of RNA polymerase in *Bacillus subtilis*. *Proteomics* **11**, 2992-3001.

Deutscher, J., Francke, C. & Postma, P. W. (2006). How phosphotransferase system-related protein phosphorylation regulates carbohydrate metabolism in bacteria. *Microbiol Mol Biol Rev* **70**, 939-1031.

Deutscher, M. P. & Reuven, N. B. (1991). Enzymatic basis for hydrolytic versus phosphorolytic mRNA degradation in *Escherichia coli* and *Bacillus subtilis*. *Proc Natl Acad Sci U S A* **88**, 3277-3280.

Diethmaier, C., Pietack, N., Gunka, K., Wrede, C., Lehnik-Habrink, M. & other authors (2011). A Novel Factor Controlling Bistability in *Bacillus subtilis*: The YmdB Protein Affects Flagellin Expression and Biofilm Formation. *J Bacteriol*.

Diwa, A., Bricker, A. L., Jain, C. & Belasco, J. G. (2000). An evolutionarily conserved RNA stem-loop functions as a sensor that directs feedback regulation of RNase E gene expression. *Genes Dev* **14**, 1249-1260.

Donovan, W. P. & Kushner, S. R. (1986). Polynucleotide phosphorylase and ribonuclease II are required for cell viability and mRNA turnover in *Escherichia coli* K-12. *Proc Natl Acad Sci U S A* **83**, 120-124.

Dorléans, A., Li de la Sierra-Gallay, I., Piton, J., Zig, L., Gilet, L. & other authors (2011). Molecular Basis for the Recognition and Cleavage of RNA by the Bifunctional 5'-3' Exo/Endoribonuclease RNase J. *Structure* **19**, 1252-1261.

Dubnau, D. & Losick, R. (2006). Bistability in bacteria. *Mol Microbiol* **61**, 564-572.

Duffy, J. J., Chaney, S. G. & Boyer, P. D. (1972). Incorporation of water oxygens into intracellular nucleotides and RNA. I. Predominantly non-hydrolytic RNA turnover in *Bacillus subtilis*. *J Mol Biol* **64**, 565-579.

Duman, R. E. & Löwe, J. (2010). Crystal structures of *Bacillus subtilis* Lon protease. *J Mol Biol* **401**, 653-670.

Dunker, A. K., Lawson, J. D., Brown, C. J., Williams, R. M., Romero, P. & other authors (2001). Intrinsically disordered protein. *J Mol Graph Model* **19**, 26-59.

Dyson, H. J. & Wright, P. E. (2005). Intrinsically unstructured proteins and their functions. *Nat Rev Mol Cell Biol* **6**, 197-208.

El-Sharoud, W. M. & Graumann, P. L. (2007). Cold shock proteins aid coupling of transcription and translation in bacteria. *Science progress* **90**, 15-27.

Entelis, N., Brandina, I., Kamenski, P., Krasheninnikov, I. A., Martin, R. P. & Tarassov, I. (2006). A glycolytic enzyme, enolase, is recruited as a cofactor of tRNA targeting toward mitochondria in *Saccharomyces cerevisiae*. *Genes Dev* **20**, 1609-1620.

Erce, M. A., Low, J. K. & Wilkins, M. R. (2010). Analysis of the RNA degradosome complex in *Vibrio angustum* S14. *FEBS J* **277**, 5161-5173.

Erlandsen, H., Abola, E. E. & Stevens, R. C. (2000). Combining structural genomics and enzymology: completing the picture in metabolic pathways and enzyme active sites. *Curr Opin Struct Biol* **10**, 719-730.

Even, S., Pellegrini, O., Zig, L., Labas, V., Vinh, J. & other authors (2005). Ribonucleases J1 and J2: two novel endoribonucleases in *B.subtilis* with functional homology to E.coli RNase E. *Nucleic Acids Res* **33**, 2141-2152.

Evguenieva-Hackenberg, E., Schiltz, E. & Klug, G. (2002). Dehydrogenases from all three domains of life cleave RNA. *J Biol Chem* **277**, 46145-46150.

Evguenieva-Hackenberg, E., Walter, P., Hochleitner, E., Lottspeich, F. & Klug, G. (2003). An exosome-like complex in *Sulfolobus solfataricus*. *EMBO Rep* **4**, 889-893.

Evguenieva-Hackenberg, E. & Klug, G. (2009). RNA degradation in Archaea and Gram-negative bacteria different from *Escherichia coli*. *Prog Mol Biol Transl Sci* **85**, 275-317.

Evguenieva-Hackenberg, E., Roppelt, V., Lassek, C. & Klug, G. (2011). Subcellular localization of RNA degrading proteins and protein complexes in prokaryotes. *RNA Biol* **8**, 49-54.

Eymann, C., Dreisbach, A., Albrecht, D., Bernhardt, J., Becher, D. & other authors (2004). A comprehensive proteome map of growing *Bacillus subtilis* cells. *Proteomics* **4**, 2849-2876.

Faires, N., Tobisch, S., Bachem, S., Martin-Verstraete, I., Hecker, M. & Stülke, J. (1999). The catabolite control protein CcpA controls ammonium assimilation in *Bacillus subtilis*. *J Mol Microbiol Biotechnol* **1**, 141-148.

Fairman, M. E., Maroney, P. A., Wang, W., Bowers, H. A., Gollnick, P. & other authors (2004). Protein displacement by DEXH/D "RNA helicases" without duplex unwinding. *Science* **304**, 730-734.

Fioulaine, S., Morera, S., Poncet, S., Mijakovic, I., Galinier, A. & other authors (2002). X-ray structure of a bifunctional protein kinase in complex with its protein substrate HPr. *Proc Natl Acad Sci U S A* **99**, 13437-13441.

Fillinger, S., Boschi-Muller, S., Azza, S., Dervyn, E., Branlant, G. & Aymerich, S. (2000). Two glyceraldehyde-3-phosphate dehydrogenases with opposite physiological roles in a nonphotosynthetic bacterium. *J Biol Chem* **275**, 14031-14037.

Fong, J. H., Shoemaker, B. A., Garbuzynskiy, S. O., Lobanov, M. Y., Galzitskaya, O. V. & Panchenko, A. R. (2009). Intrinsic disorder in protein interactions: insights from a comprehensive structural analysis. *PLoS Comput Biol* **5**, e1000316.

Forchhammer, K. (2008). P(II) signal transducers: novel functional and structural insights. *Trends in microbiology* **16**, 65-72.

French, C. T., Lao, P., Loraine, A. E., Matthews, B. T., Yu, H. & Dybvig, K. (2008). Large-scale transposon mutagenesis of *Mycoplasma pulmonis*. *Mol Microbiol* **69**, 67-76.

Gancedo, C. & Flores, C. L. (2008). Moonlighting proteins in yeasts. *Microbiol Mol Biol Rev* **72**, 197-210, table of contents.

Ghigo, J. M. & Beckwith, J. (2000). Cell division in *Escherichia coli*: role of FtsL domains in septal localization, function, and oligomerization. *J Bacteriol* **182**, 116-129.

Ghora, B. K. & Apirion, D. (1978). Structural analysis and in vitro processing to p5 rRNA of a 9S RNA molecule isolated from an *rne* mutant of *E. coli*. *Cell* **15**, 1055-1066.

Ghosh, S. & Deutscher, M. P. (1999). Oligoribonuclease is an essential component of the mRNA decay pathway. *Proc Natl Acad Sci U S A* **96**, 4372-4377.

Gollnick, P., Babitzke, P., Antson, A. & Yanofsky, C. (2005). Complexity in regulation of tryptophan biosynthesis in *Bacillus subtilis*. *Annu Rev Genet* **39**, 47-68.

González-Pastor, J. E., Hobbs, E. C. & Losick, R. (2003). Cannibalism by sporulating bacteria. *Science* **301**, 510-513.

Gorbalenya, A. E. & Koonin, E. V. (1993). Helicases: amino acid sequence comparisons and structure-function relationships. *Curr Opin Struct Biol* **3**, 419-429.

Green, N. J., Grundy, F. J. & Henkin, T. M. (2010). The T box mechanism: tRNA as a regulatory molecule. *FEBS Lett* **584**, 318-324.

Grigoryan, G. & Keating, A. E. (2008). Structural specificity in coiled-coil interactions. *Curr Opin Struct Biol* **18**, 477-483.

Groicher, K. H., Firek, B. A., Fujimoto, D. F. & Bayles, K. W. (2000). The *Staphylococcus aureus* IrgAB operon modulates murein hydrolase activity and penicillin tolerance. *J Bacteriol* **182**, 1794-1801.

Guerout-Fleury, A. M., Shazand, K., Frandsen, N. & Stragier, P. (1995). Antibiotic-resistance cassettes for *Bacillus subtilis*. *Gene* **167**, 335-336.

Gunka, K. (2011). Der Einfluss der Glutamatdehydrogenasen auf die Verknüpfung des Kohlenstoff- und Stickstoffwechsels in *Bacillus subtilis*. *Ph. D. thesis*. University of Göttingen.

Hahne, H., Wolff, S., Hecker, M. & Becher, D. (2008). From complementarity to comprehensiveness--targeting the membrane proteome of growing *Bacillus subtilis* by divergent approaches. *Proteomics* **8**, 4123-4136.

- Hambraeus, G., von Wachenfeldt, C. & Hederstedt, L. (2003).** Genome-wide survey of mRNA half-lives in *Bacillus subtilis* identifies extremely stable mRNAs. *Mol Genet Genomics* **269**, 706-714.
- Hardwick, S. W., Chan, V. S., Broadhurst, R. W. & Luisi, B. F. (2011).** An RNA degradosome assembly in *Caulobacter crescentus*. *Nucleic Acids Res* **39**, 1449-1459.
- Hartung, S. & Hopfner, K. P. (2009).** Lessons from structural and biochemical studies on the archaeal exosome. *Biochem Soc Trans* **37**, 83-87.
- Hasenöhr, D., Konrat, R. & Bläsi, U. (2011).** Identification of an RNase J ortholog in *Sulfolobus solfataricus*: implications for 5'-to-3' directional decay and 5'-end protection of mRNA in Crenarchaeota. *RNA* **17**, 99-107.
- Hecker, M. & Völker, U. (1998).** Non-specific, general and multiple stress resistance of growth-restricted *Bacillus subtilis* cells by the expression of the sigmaB regulon. *Mol Microbiol* **29**, 1129-1136.
- Hecker, M. (2003).** A proteomic view of cell physiology of *Bacillus subtilis*--bringing the genome sequence to life. *Adv Biochem Eng Biotechnol* **83**, 57-92.
- Hecker, M., Pane-Farre, J. & Völker, U. (2007).** SigB-dependent general stress response in *Bacillus subtilis* and related gram-positive bacteria. *Annu Rev Microbiol* **61**, 215-236.
- Heidrich, N., Chinali, A., Gerth, U. & Brantl, S. (2006).** The small untranslated RNA SR1 from the *Bacillus subtilis* genome is involved in the regulation of arginine catabolism. *Mol Microbiol* **62**, 520-536.
- Herzberg, C., Weidinger, L. A., Dörrbecker, B., Hübner, S., Stülke, J. & Commichau, F. M. (2007).** SPINE: a method for the rapid detection and analysis of protein-protein interactions *in vivo*. *Proteomics* **7**, 4032-4035.
- Homuth, G., Mogk, A. & Schumann, W. (1999).** Post-transcriptional regulation of the *Bacillus subtilis* *dnaK* operon. *Mol Microbiol* **32**, 1183-1197.
- Horsburgh, M. J., Thackray, P. D. & Moir, A. (2001).** Transcriptional responses during outgrowth of *Bacillus subtilis* endospores. *Microbiology* **147**, 2933-2941.
- Hunger, K., Beckering, C. L., Wiegeshoff, F., Graumann, P. L. & Marahiel, M. A. (2006).** Cold-induced putative DEAD box RNA helicases CshA and CshB are essential for cold adaptation and interact with cold shock protein B in *Bacillus subtilis*. *J Bacteriol* **188**, 240-248.

Hunt, A., Rawlins, J. P., Thomaides, H. B. & Errington, J. (2006). Functional analysis of 11 putative essential genes in *Bacillus subtilis*. *Microbiology* **152**, 2895-2907.

Imamura, R., Yamanaka, K., Ogura, T., Hiraga, S., Fujita, N. & other authors (1996). Identification of the *cpdA* gene encoding cyclic 3',5'-adenosine monophosphate phosphodiesterase in *Escherichia coli*. *J Biol Chem* **271**, 25423-25429.

Iost, I. & Dreyfus, M. (2006). DEAD-box RNA helicases in *Escherichia coli*. *Nucleic Acids Res* **34**, 4189-4197.

Ishida, T. & Kinoshita, K. (2008). Prediction of disordered regions in proteins based on the meta approach. *Bioinformatics* **24**, 1344-1348.

Islam, M. M., Wallin, R., Wynn, R. M., Conway, M., Fujii, H. & other authors (2007). A novel branched-chain amino acid metabolon. Protein-protein interactions in a supramolecular complex. *J Biol Chem* **282**, 11893-11903.

Jäger, S., Fuhrmann, O., Heck, C., Hebermehl, M., Schiltz, E. & other authors (2001). An mRNA degrading complex in *Rhodobacter capsulatus*. *Nucleic Acids Res* **29**, 4581-4588.

Jain, C. (2002). Degradation of mRNA in *Escherichia coli*. *IUBMB Life* **54**, 315-321.

Jain, C. (2008). The *E. coli* RhlE RNA helicase regulates the function of related RNA helicases during ribosome assembly. *RNA* **14**, 381-389.

Jannièrè, L., Canceill, D., Suski, C., Kanga, S., Dalmais, B. & other authors (2007). Genetic evidence for a link between glycolysis and DNA replication. *PLoS One* **2**, e447.

Jeffery, C. J. (1999). Moonlighting proteins. *Trends Biochem Sci* **24**, 8-11.

Jones, P. G. & Inouye, M. (1994). The cold-shock response--a hot topic. *Mol Microbiol* **11**, 811-818.

Jones, P. G., Mitta, M., Kim, Y., Jiang, W. & Inouye, M. (1996). Cold shock induces a major ribosomal-associated protein that unwinds double-stranded RNA in *Escherichia coli*. *Proc Natl Acad Sci U S A* **93**, 76-80.

Kaberdin, V. R., Miczak, A., Jakobsen, J. S., Lin-Chao, S., McDowall, K. J. & von Gabain, A. (1998). The endoribonucleolytic N-terminal half of *Escherichia coli* RNase E is evolutionarily conserved in *Synechocystis sp.* and other bacteria but not the C-terminal half, which is sufficient for degradosome assembly. *Proc Natl Acad Sci U S A* **95**, 11637-11642.

Kaberdin, V. R., Singh, D. & Lin-Chao, S. (2011). Composition and conservation of the mRNA-degrading machinery in bacteria. *J Biomed Sci* **18**, 23.

Kaltwasser, M., Wiegert, T. & Schumann, W. (2002). Construction and application of epitope- and green fluorescent protein-tagging integration vectors for *Bacillus subtilis*. *Appl Environ Microbiol* **68**, 2624-2628.

Kandror, O. & Goldberg, A. L. (1997). Trigger factor is induced upon cold shock and enhances viability of *Escherichia coli* at low temperatures. *Proc Natl Acad Sci U S A* **94**, 4978-4981.

Kang, S. O., Caparon, M. G. & Cho, K. H. (2010). Virulence gene regulation by CvfA, a putative RNase: the CvfA-enolase complex in *Streptococcus pyogenes* links nutritional stress, growth-phase control, and virulence gene expression. *Infect Immun* **78**, 2754-2767.

Karimova, G., Pidoux, J., Ullmann, A. & Ladant, D. (1998). A bacterial two-hybrid system based on a reconstituted signal transduction pathway. *Proc Natl Acad Sci U S A* **95**, 5752-5756.

Karow, A. R. & Klostermeier, D. (2009). A conformational change in the helicase core is necessary but not sufficient for RNA unwinding by the DEAD box helicase YxiN. *Nucleic Acids Res* **37**, 4464-4471.

Kearns, D. B., Chu, F., Branda, S. S., Kolter, R. & Losick, R. (2005). A master regulator for biofilm formation by *Bacillus subtilis*. *Mol Microbiol* **55**, 739-749.

Kearns, D. B. & Losick, R. (2005). Cell population heterogeneity during growth of *Bacillus subtilis*. *Genes Dev* **19**, 3083-3094.

Khemici, V. & Carpousis, A. J. (2004). The RNA degradosome and poly(A) polymerase of *Escherichia coli* are required in vivo for the degradation of small mRNA decay intermediates containing REP-stabilizers. *Mol Microbiol* **51**, 777-790.

Khemici, V., Poljak, L., Luisi, B. F. & Carpousis, A. J. (2008). The RNase E of *Escherichia coli* is a membrane-binding protein. *Mol Microbiol* **70**, 799-813.

Kim, J. W. & Dang, C. V. (2005). Multifaceted roles of glycolytic enzymes. *Trends Biochem Sci* **30**, 142-150.

Kime, L., Jourdan, S. S., Stead, J. A., Hidalgo-Sastre, A. & McDowall, K. J. (2010). Rapid cleavage of RNA by RNase E in the absence of 5' monophosphate stimulation. *Mol Microbiol* **76**, 590-604.

- Klostermeier, D. & Rudolph, M. G. (2009).** A novel dimerization motif in the C-terminal domain of the *Thermus thermophilus* DEAD box helicase Hera confers substantial flexibility. *Nucleic Acids Res* **37**, 421-430.
- Klumpp, S., Zhang, Z. & Hwa, T. (2009).** Growth rate-dependent global effects on gene expression in bacteria. *Cell* **139**, 1366-1375.
- Ko, J. H., Han, K., Kim, Y., Sim, S., Kim, K. S. & other authors (2008).** Dual function of RNase E for control of M1 RNA biosynthesis in *Escherichia coli*. *Biochemistry* **47**, 762-770.
- Kobayashi, K., Ehrlich, S. D., Albertini, A., Amati, G., Andersen, K. K. & other authors (2003).** Essential *Bacillus subtilis* genes. *Proc Natl Acad Sci U S A* **100**, 4678-4683.
- Kobayashi, K. (2008).** SlrR/SlrA controls the initiation of biofilm formation in *Bacillus subtilis*. *Mol Microbiol* **69**, 1399-1410.
- Kolodkin-Gal, I., Romero, D., Cao, S., Clardy, J., Kolter, R. & Losick, R. (2010).** D-amino acids trigger biofilm disassembly. *Science* **328**, 627-629.
- Kolter, R. (2010).** Biofilms in lab and nature: a molecular geneticist's voyage to microbial ecology. *International microbiology : the official journal of the Spanish Society for Microbiology* **13**, 1-7.
- Kossen, K. & Uhlenbeck, O. C. (1999).** Cloning and biochemical characterization of *Bacillus subtilis* YxiN, a DEAD protein specifically activated by 23S rRNA: delineation of a novel sub-family of bacterial DEAD proteins. *Nucleic Acids Res* **27**, 3811-3820.
- Kossen, K., Karginov, F. V. & Uhlenbeck, O. C. (2002).** The carboxy-terminal domain of the DExDH protein YxiN is sufficient to confer specificity for 23S rRNA. *J Mol Biol* **324**, 625-636.
- Kunst, F. & Rapoport, G. (1995).** Salt stress is an environmental signal affecting degradative enzyme synthesis in *Bacillus subtilis*. *J Bacteriol* **177**, 2403-2407.
- Kunst, F., Ogasawara, N., Moszer, I., Albertini, A. M., Alloni, G. & other authors (1997).** The complete genome sequence of the gram-positive bacterium *Bacillus subtilis*. *Nature* **390**, 249-256.
- Kushner, S. R. (2002).** mRNA decay in *Escherichia coli* comes of age. *J Bacteriol* **184**, 4658-4665; discussion 4657.

Laue, T., Shah, B., Ridgeway, T. & Pelletier, S. (1992). *Computer-aided interpretation of analytical sedimentation data for proteins* (Harding, S., Rowe, A. & Horton, J., Eds.), The Royal Society of Chemistry.

Le Brun, N. E., Bengtsson, J. & Hederstedt, L. (2000). Genes required for cytochrome c synthesis in *Bacillus subtilis*. *Mol Microbiol* **36**, 638-650.

Lee, K., Bernstein, J. A. & Cohen, S. N. (2002). RNase G complementation of rne null mutation identifies functional interrelationships with RNase E in *Escherichia coli*. *Mol Microbiol* **43**, 1445-1456.

Lee, K. & Cohen, S. N. (2003). A *Streptomyces coelicolor* functional orthologue of *Escherichia coli* RNase E shows shuffling of catalytic and PNPase-binding domains. *Mol Microbiol* **48**, 349-360.

Lehnik-Habrink, M., Pförtner, H., Rempeters, L., Pietack, N., Herzberg, C. & Stülke, J. (2010). The RNA degradosome in *Bacillus subtilis*: identification of CshA as the major RNA helicase in the multiprotein complex. *Mol Microbiol* **77**, 958-971.

Lehnik-Habrink, M., Newman, J., Rothe, F. M., Solovyova, A. S., Rodrigues, C. & other authors (2011a). RNase Y in *Bacillus subtilis*: a Natively Disordered Protein That Is the Functional Equivalent of RNase E from *Escherichia coli*. *J Bacteriol* **193**, 5431-5441.

Lehnik-Habrink, M., Schaffer, M., Mäder, U., Diethmaier, C., Herzberg, C. & Stülke, J. (2011b). RNA processing in *Bacillus subtilis*: identification of targets of the essential RNase Y. *Mol Microbiol* **81**, 1459-1473.

Levin, P. A., Kurtser, I. G. & Grossman, A. D. (1999). Identification and characterization of a negative regulator of FtsZ ring formation in *Bacillus subtilis*. *Proc Natl Acad Sci U S A* **96**, 9642-9647.

Lewis, P. J., Thaker, S. D. & Errington, J. (2000). Compartmentalization of transcription and translation in *Bacillus subtilis*. *EMBO J* **19**, 710-718.

Lewis, R. J., Brannigan, J. A., Offen, W. A., Smith, I. & Wilkinson, A. J. (1998). An evolutionary link between sporulation and prophage induction in the structure of a repressor:anti-repressor complex. *J Mol Biol* **283**, 907-912.

Li de la Sierra-Gallay, I., Zig, L., Jamalli, A. & Putzer, H. (2008). Structural insights into the dual activity of RNase J. *Nat Struct Mol Biol* **15**, 206-212.

- Li, Z., Pandit, S. & Deutscher, M. P. (1999).** RNase G (CafA protein) and RNase E are both required for the 5' maturation of 16S ribosomal RNA. *EMBO J* **18**, 2878-2885.
- Lin-Chao, S., Wei, C. L. & Lin, Y. T. (1999).** RNase E is required for the maturation of *ssrA* RNA and normal *ssrA* RNA peptide-tagging activity. *Proc Natl Acad Sci U S A* **96**, 12406-12411.
- Lin-Chao, S., Chiou, N. T. & Schuster, G. (2007).** The PNPase, exosome and RNA helicases as the building components of evolutionarily-conserved RNA degradation machines. *J Biomed Sci* **14**, 523-532.
- Lin, P. H. & Lin-Chao, S. (2005).** RhlB helicase rather than enolase is the beta-subunit of the *Escherichia coli* polynucleotide phosphorylase (PNPase)-exoribonucleolytic complex. *Proc Natl Acad Sci U S A* **102**, 16590-16595.
- Linder, P., Gasteiger, E. & Bairoch, A. (2000).** A comprehensive web resource on RNA helicases from the baker's yeast *Saccharomyces cerevisiae*. *Yeast* **16**, 507-509.
- Liou, G. G., Jane, W. N., Cohen, S. N., Lin, N. S. & Lin-Chao, S. (2001).** RNA degradosomes exist *in vivo* in *Escherichia coli* as multicomponent complexes associated with the cytoplasmic membrane via the N-terminal region of ribonuclease E. *Proc Natl Acad Sci U S A* **98**, 63-68.
- Liou, G. G., Chang, H. Y., Lin, C. S. & Lin-Chao, S. (2002).** DEAD box RhlB RNA helicase physically associates with exoribonuclease PNPase to degrade double-stranded RNA independent of the degradosome-assembling region of RNase E. *J Biol Chem* **277**, 41157-41162.
- Liu, Q., Greimann, J. C. & Lima, C. D. (2006).** Reconstitution, activities, and structure of the eukaryotic RNA exosome. *Cell* **127**, 1223-1237.
- Lopez, D., Vlamakis, H. & Kolter, R. (2010).** Biofilms. *Cold Spring Harbor perspectives in biology* **2**, a000398.
- Ludwig, H., Homuth, G., Schmalisch, M., Dyka, F. M., Hecker, M. & Stülke, J. (2001).** Transcription of glycolytic genes and operons in *Bacillus subtilis*: evidence for the presence of multiple levels of control of the *gapA* operon. *Mol Microbiol* **41**, 409-422.
- Lupas, A., Van Dyke, M. & Stock, J. (1991).** Predicting coiled coils from protein sequences. *Science* **252**, 1162-1164.
- Mackie, G. A. (1998).** Ribonuclease E is a 5'-end-dependent endonuclease. *Nature* **395**, 720-723.

Mäder, U., Zig, L., Kretschmer, J., Homuth, G. & Putzer, H. (2008). mRNA processing by RNases J1 and J2 affects *Bacillus subtilis* gene expression on a global scale. *Mol Microbiol* **70**, 183-196.

Marcaida, M. J., DePristo, M. A., Chandran, V., Carpousis, A. J. & Luisi, B. F. (2006). The RNA degradosome: life in the fast lane of adaptive molecular evolution. *Trends Biochem Sci* **31**, 359-365.

Martin-Verstraete, I., Débarbouillé, M., Klier, A. & Rapoport, G. (1994). Interactions of wild-type and truncated LevR of *Bacillus subtilis* with the upstream activating sequence of the levanase operon. *J Mol Biol* **241**, 178-192.

Mathy, N., Benard, L., Pellegrini, O., Daou, R., Wen, T. & Condon, C. (2007). 5'-to-3' exoribonuclease activity in bacteria: role of RNase J1 in rRNA maturation and 5' stability of mRNA. *Cell* **129**, 681-692.

Mathy, N., Hebert, A., Mervelet, P., Benard, L., Dorleans, A. & other authors (2010). *Bacillus subtilis* ribonucleases J1 and J2 form a complex with altered enzyme behaviour. *Mol Microbiol* **75**, 489-498.

McDowall, K. J., Kaberdin, V. R., Wu, S. W., Cohen, S. N. & Lin-Chao, S. (1995). Site-specific RNase E cleavage of oligonucleotides and inhibition by stem-loops. *Nature* **374**, 287-290.

McLoon, A. L., Guttenplan, S. B., Kearns, D. B., Kolter, R. & Losick, R. (2011). Tracing the domestication of a biofilm-forming bacterium. *J Bacteriol* **193**, 2027-2034.

Meinken, C., Blencke, H. M., Ludwig, H. & Stülke, J. (2003). Expression of the glycolytic *gapA* operon in *Bacillus subtilis*: differential syntheses of proteins encoded by the operon. *Microbiology* **149**, 751-761.

Meyer, F. M., Gerwig, J., Hammer, E., Herzberg, C., Commichau, F. M. & other authors (2011). Physical interactions between tricarboxylic acid cycle enzymes in *Bacillus subtilis*: evidence for a metabolon. *Metab Eng* **13**, 18-27.

Michels, P. A., Bringaud, F., Herman, M. & Hannaert, V. (2006). Metabolic functions of glycosomes in trypanosomatids. *Biochim Biophys Acta* **1763**, 1463-1477.

Miczak, A., Srivastava, R. A. & Apirion, D. (1991). Location of the RNA-processing enzymes RNase III, RNase E and RNase P in the *Escherichia coli* cell. *Mol Microbiol* **5**, 1801-1810.

Miczak, A., Kaberdin, V. R., Wei, C. L. & Lin-Chao, S. (1996). Proteins associated with RNase E in a multicomponent ribonucleolytic complex. *Proc Natl Acad Sci U S A* **93**, 3865-3869.

Miller, C. M., Baumberg, S. & Stockley, P. G. (1997). Operator interactions by the *Bacillus subtilis* arginine repressor/activator, AhrC: novel positioning and DNA-mediated assembly of a transcriptional activator at catabolic sites. *Mol Microbiol* **26**, 37-48.

Misra, T. K. & Apirion, D. (1979). RNase E, an RNA processing enzyme from *Escherichia coli*. *J Biol Chem* **254**, 11154-11159.

Mitchell, P., Petfalski, E., Shevchenko, A., Mann, M. & Tollervey, D. (1997). The exosome: a conserved eukaryotic RNA processing complex containing multiple 3'→5' exoribonucleases. *Cell* **91**, 457-466.

Mitra, S., Hue, K. & Bechhofer, D. H. (1996). In vitro processing activity of *Bacillus subtilis* polynucleotide phosphorylase. *Mol Microbiol* **19**, 329-342.

Mogk, A., Homuth, G., Scholz, C., Kim, L., Schmid, F. X. & Schumann, W. (1997). The GroE chaperonin machine is a major modulator of the CIRCE heat shock regulon of *Bacillus subtilis*. *EMBO J* **16**, 4579-4590.

Mohanty, B. K. & Kushner, S. R. (2000). Polynucleotide phosphorylase functions both as a 3' right-arrow 5' exonuclease and a poly(A) polymerase in *Escherichia coli*. *Proc Natl Acad Sci U S A* **97**, 11966-11971.

Montero Llopis, P., Jackson, A. F., Sliusarenko, O., Surovtsev, I., Heinritz, J. & other authors (2010). Spatial organization of the flow of genetic information in bacteria. *Nature* **466**, 77-81.

Morita, T., Kawamoto, H., Mizota, T., Inada, T. & Aiba, H. (2004). Enolase in the RNA degradosome plays a crucial role in the rapid decay of glucose transporter mRNA in the response to phosphosugar stress in *Escherichia coli*. *Mol Microbiol* **54**, 1063-1075.

Nakano, S., Zheng, G., Nakano, M. M. & Zuber, P. (2002). Multiple pathways of Spx (YjdB) proteolysis in *Bacillus subtilis*. *J Bacteriol* **184**, 3664-3670.

Nevo-Dinur, K., Nussbaum-Shochat, A., Ben-Yehuda, S. & Amster-Choder, O. (2011). Translation-independent localization of mRNA in *E. coli*. *Science* **331**, 1081-1084.

Newman, J., Hewitt, L., Rodrigues, C., Solovyova, A. S., Harwood, C. R. & Lewis, R. J. (2011). Unusual, dual endo- and exo-nuclease activity in the degradosome explained by crystal structure analysis of RNase J1. *Structure*.

Niyogi, S. K. & Datta, A. K. (1975). A novel oligoribonuclease of *Escherichia coli*. I. Isolation and properties. *J Biol Chem* **250**, 7307-7312.

Nurmohamed, S., Vincent, H. A., Titman, C. M., Chandran, V., Pears, M. R. & other authors (2011). Polynucleotide phosphorylase activity may be modulated by metabolites in *Escherichia coli*. *J Biol Chem* **286**, 14315-14323.

Oussenko, I. A., Abe, T., Ujiie, H., Muto, A. & Bechhofer, D. H. (2005). Participation of 3'-to-5' exoribonucleases in the turnover of *Bacillus subtilis* mRNA. *J Bacteriol* **187**, 2758-2767.

Ow, M. C. & Kushner, S. R. (2002). Initiation of tRNA maturation by RNase E is essential for cell viability in *E. coli*. *Genes Dev* **16**, 1102-1115.

Paik, S. H., Chakicherla, A. & Hansen, J. N. (1998). Identification and characterization of the structural and transporter genes for, and the chemical and biological properties of, sublancin 168, a novel lantibiotic produced by *Bacillus subtilis* 168. *J Biol Chem* **273**, 23134-23142.

Pandiani, F., Brillard, J., Bornard, I., Michaud, C., Chamot, S. & other authors (2010). Differential involvement of the five RNA helicases in adaptation of *Bacillus cereus* ATCC 14579 to low growth temperatures. *Appl Environ Microbiol* **76**, 6692-6697.

Pandiani, F., Chamot, S., Brillard, J., Carlin, F., Nguyen-The, C. & Broussolle, V. (2011). Role of the five RNA helicases in adaptive response of *Bacillus cereus* ATCC 14579 cells to temperature, pH and oxidative stress. *Appl Environ Microbiol*.

Paul, B. J., Ross, W., Gaal, T. & Gourse, R. L. (2004). rRNA transcription in *Escherichia coli*. *Annu Rev Genet* **38**, 749-770.

Payne, D. J., Gwynn, M. N., Holmes, D. J. & Pompliano, D. L. (2007). Drugs for bad bugs: confronting the challenges of antibacterial discovery. *Nat Rev Drug Discov* **6**, 29-40.

Persson, L. O. & Johansson, G. (1989). Studies of protein-protein interaction using countercurrent distribution in aqueous two-phase systems. Partition behaviour of six Calvin-cycle enzymes from a crude spinach (*Spinacia oleracea*) chloroplast extract. *Biochem J* **259**, 863-870.

Phadtare, S. & Severinov, K. (2010). RNA remodeling and gene regulation by cold shock proteins. *RNA Biol* **7**, 788-795.

Piggot, P. J. & Hilbert, D. W. (2004). Sporulation of *Bacillus subtilis*. *Curr Opin Microbiol* **7**, 579-586.

Prud'homme-Généreux, A., Beran, R. K., Iost, I., Ramey, C. S., Mackie, G. A. & Simons, R. W. (2004). Physical and functional interactions among RNase E, polynucleotide phosphorylase and

the cold-shock protein, CsdA: evidence for a 'cold shock degradosome'. *Mol Microbiol* **54**, 1409-1421.

Purusharth, R. I., Klein, F., Sulthana, S., Jäger, S., Jagannadham, M. V. & other authors (2005). Exoribonuclease R interacts with endoribonuclease E and an RNA helicase in the psychrotrophic bacterium *Pseudomonas syringae* Lz4W. *J Biol Chem* **280**, 14572-14578.

Putzer, H., Gendron, N. & Grunberg-Manago, M. (1992). Co-ordinate expression of the two threonyl-tRNA synthetase genes in *Bacillus subtilis*: control by transcriptional antitermination involving a conserved regulatory sequence. *EMBO J* **11**, 3117-3127.

Py, B., Causton, H., Mudd, E. A. & Higgins, C. F. (1994). A protein complex mediating mRNA degradation in *Escherichia coli*. *Mol Microbiol* **14**, 717-729.

Rasmussen, S., Nielsen, H. B. & Jarmer, H. (2009). The transcriptionally active regions in the genome of *Bacillus subtilis*. *Mol Microbiol* **73**, 1043-1057.

Rauhut, R. & Klug, G. (1999). mRNA degradation in bacteria. *FEMS Microbiol Rev* **23**, 353-370.

Resch, A., Vecerek, B., Palavra, K. & Blasi, U. (2010). Requirement of the CsdA DEAD-box helicase for low temperature riboregulation of *rpoS* mRNA. *RNA Biol* **7**, 796-802.

Ribitsch, D., Heumann, S., Trotscha, E., Herrero Acero, E., Greimel, K. & other authors (2011). Hydrolysis of polyethyleneterephthalate by p-nitrobenzylesterase from *Bacillus subtilis*. *Biotechnology progress*.

Richards, J., Liu, Q., Pellegrini, O., Celesnik, H., Yao, S. & other authors (2011). An RNA pyrophosphohydrolase triggers 5' -exonucleolytic degradation of mRNA in *Bacillus subtilis* Moll Cell.

Rietkötter, E., Hoyer, D. & Mascher, T. (2008). Bacitracin sensing in *Bacillus subtilis*. *Mol Microbiol* **68**, 768-785.

Rigden, M. D., Baier, C., Ramirez-Arcos, S., Liao, M., Wang, M. & Dillon, J. A. (2008). Identification of the coiled-coil domains of *Enterococcus faecalis* DivIVA that mediate oligomerization and their importance for biological function. *J Biochem* **144**, 63-76.

Rocak, S. & Linder, P. (2004). DEAD-box proteins: the driving forces behind RNA metabolism. *Nat Rev Mol Cell Biol* **5**, 232-241.

Romero, D., Aguilar, C., Losick, R. & Kolter, R. (2010). Amyloid fibers provide structural integrity to *Bacillus subtilis* biofilms. *Proc Natl Acad Sci U S A* **107**, 2230-2234.

Romero, D., Vlamakis, H., Losick, R. & Kolter, R. (2011). An accessory protein required for anchoring and assembly of amyloid fibres in *B. subtilis* biofilms. *Mol Microbiol* **80**, 1155-1168.

Roppelt, V., Hobel, C. F., Albers, S. V., Lassek, C., Schwarz, H. & other authors (2010). The archaeal exosome localizes to the membrane. *FEBS Lett* **584**, 2791-2795.

Roux, C. M., Demuth, J. P. & Dunman, P. M. (2011). Characterization of components of the *Staphylococcus aureus* messenger RNA degradosome holoenzyme-like complex. *J Bacteriol.*

Sambrook, J., Fritsch, E. F. & Maniatis, T. (1989). *Molecular Cloning: A Laboratory Manual*. 2nd edn. Cold Spring Harbor, NY: Cold Spring Harbor Laboratory.

Schirmer, F., Ehrt, S. & Hillen, W. (1997). Expression, inducer spectrum, domain structure, and function of MopR, the regulator of phenol degradation in *Acinetobacter calcoaceticus* NCIB8250. *J Bacteriol* **179**, 1329-1336.

Schöbel, S., Zellmeier, S., Schumann, W. & Wiegert, T. (2004). The *Bacillus subtilis* sigmaW anti-sigma factor RsiW is degraded by intramembrane proteolysis through YluC. *Mol Microbiol* **52**, 1091-1105.

Schuck, P. (2000). Size-distribution analysis of macromolecules by sedimentation velocity ultracentrifugation and lamm equation modeling. *Biophys J* **78**, 1606-1619.

Sengoku, T., Nureki, O., Nakamura, A., Kobayashi, S. & Yokoyama, S. (2006). Structural basis for RNA unwinding by the DEAD-box protein *Drosophila* Vasa. *Cell* **125**, 287-300.

Serizawa, M., Yamamoto, H., Yamaguchi, H., Fujita, Y., Kobayashi, K. & other authors (2004). Systematic analysis of SigD-regulated genes in *Bacillus subtilis* by DNA microarray and Northern blotting analyses. *Gene* **329**, 125-136.

Serizawa, M., Kodama, K., Yamamoto, H., Kobayashi, K., Ogasawara, N. & Sekiguchi, J. (2005). Functional analysis of the YvrGHb two-component system of *Bacillus subtilis*: identification of the regulated genes by DNA microarray and northern blot analyses. *Biosci Biotechnol Biochem* **69**, 2155-2169.

Shahbadian, K., Jamalli, A., Zig, L. & Putzer, H. (2009). RNase Y, a novel endoribonuclease, initiates riboswitch turnover in *Bacillus subtilis*. *EMBO J* **28**, 3523-3533.

Shi, Z., Yang, W. Z., Lin-Chao, S., Chak, K. F. & Yuan, H. S. (2008). Crystal structure of *Escherichia coli* PNPase: central channel residues are involved in processive RNA degradation. *RNA* **14**, 2361-2371.

Shin, D. H., Proudfoot, M., Lim, H. J., Choi, I. K., Yokota, H. & other authors (2008). Structural and enzymatic characterization of DR1281: A calcineurin-like phosphoesterase from *Deinococcus radiodurans*. *Proteins* **70**, 1000-1009.

Siebers, B. & Schönheit, P. (2005). Unusual pathways and enzymes of central carbohydrate metabolism in Archaea. *Curr Opin Microbiol* **8**, 695-705.

Silverman, E., Edwalds-Gilbert, G. & Lin, R. J. (2003). DEXD/H-box proteins and their partners: helping RNA helicases unwind. *Gene* **312**, 1-16.

Stead, M. B., Marshburn, S., Mohanty, B. K., Mitra, J., Castillo, L. P. & other authors (2011). Analysis of *Escherichia coli* RNase E and RNase III activity *in vivo* using tiling microarrays. *Nucleic Acids Res* **39**, 3188-3203.

Stickney, L. M., Hankins, J. S., Miao, X. & Mackie, G. A. (2005). Function of the conserved S1 and KH domains in polynucleotide phosphorylase. *J Bacteriol* **187**, 7214-7221.

Stoodley, P., Sauer, K., Davies, D. G. & Costerton, J. W. (2002). Biofilms as complex differentiated communities. *Annu Rev Microbiol* **56**, 187-209.

Stöver, A. G. & Driks, A. (1999). Regulation of synthesis of the *Bacillus subtilis* transition-phase, spore-associated antibacterial protein TasA. *J Bacteriol* **181**, 5476-5481.

Stülke, J., Martin-Verstraete, I., Zagorec, M., Rose, M., Klier, A. & Rapoport, G. (1997). Induction of the *Bacillus subtilis* *ptsGHI* operon by glucose is controlled by a novel antiterminator, GlcT. *Mol Microbiol* **25**, 65-78.

Stülke, J. & Hillen, W. (2000). Regulation of carbon catabolism in *Bacillus* species. *Annu Rev Microbiol* **54**, 849-880.

Suzuki, N., Okai, N., Nonaka, H., Tsuge, Y., Inui, M. & Yukawa, H. (2006). High-throughput transposon mutagenesis of *Corynebacterium glutamicum* and construction of a single-gene disruptant mutant library. *Appl Environ Microbiol* **72**, 3750-3755.

Symmons, M. F., Jones, G. H. & Luisi, B. F. (2000). A duplicated fold is the structural basis for polynucleotide phosphorylase catalytic activity, processivity, and regulation. *Structure* **8**, 1215-1226.

Taghbalout, A. & Yang, Q. (2010). Self-assembly of the bacterial cytoskeleton-associated RNA helicase B protein into polymeric filamentous structures. *J Bacteriol* **192**, 3222-3226.

Tanaka, K., Kobayashi, K. & Ogasawara, N. (2003). The *Bacillus subtilis* YufLM two-component system regulates the expression of the malate transporters MaeN (YufR) and YfIS, and is essential for utilization of malate in minimal medium. *Microbiology* **149**, 2317-2329.

Tanner, N. K. & Linder, P. (2001). DExD/H box RNA helicases: from generic motors to specific dissociation functions. *Mol Cell* **8**, 251-262.

Theissen, B., Karow, A. R., Köhler, J., Gubaev, A. & Klostermeier, D. (2008). Cooperative binding of ATP and RNA induces a closed conformation in a DEAD box RNA helicase. *Proc Natl Acad Sci U S A* **105**, 548-553.

Thiele, T., Steil, L., Gebhard, S., Scharf, C., Hammer, E. & other authors (2007). Profiling of alterations in platelet proteins during storage of platelet concentrates. *Transfusion* **47**, 1221-1233.

Thomaides, H. B., Davison, E. J., Burston, L., Johnson, H., Brown, D. R. & other authors (2007). Essential bacterial functions encoded by gene pairs. *J Bacteriol* **189**, 591-602.

Tjalsma, H., Antelmann, H., Jongbloed, J. D., Braun, P. G., Darmon, E. & other authors (2004). Proteomics of protein secretion by *Bacillus subtilis*: separating the "secrets" of the secretome. *Microbiol Mol Biol Rev* **68**, 207-233.

Tjalsma, H. & van Dijk, J. M. (2005). Proteomics-based consensus prediction of protein retention in a bacterial membrane. *Proteomics* **5**, 4472-4482.

Tomecki, R., Drazkowska, K. & Dziembowski, A. (2010). Mechanisms of RNA degradation by the eukaryotic exosome. *Chembiochem* **11**, 938-945.

Trubetskoy, D., Proux, F., Allemand, F., Dreyfus, M. & Iost, I. (2009). SrmB, a DEAD-box helicase involved in *Escherichia coli* ribosome assembly, is specifically targeted to 23S rRNA *in vivo*. *Nucleic Acids Res* **37**, 6540-6549.

Tuckerman, J. R., Gonzalez, G. & Gilles-Gonzalez, M. A. (2011). Cyclic di-GMP activation of polynucleotide phosphorylase signal-dependent RNA processing. *J Mol Biol* **407**, 633-639.

Uversky, V. N., Gillespie, J. R. & Fink, A. L. (2000). Why are "natively unfolded" proteins unstructured under physiologic conditions? *Proteins* **41**, 415-427.

Vanzo, N. F., Li, Y. S., Py, B., Blum, E., Higgins, C. F. & other authors (1998). Ribonuclease E organizes the protein interactions in the *Escherichia coli* RNA degradosome. *Genes Dev* **12**, 2770-2781.

- Veening, J. W., Smits, W. K., Hamoen, L. W., Jongbloed, J. D. & Kuipers, O. P. (2004).** Visualization of differential gene expression by improved cyan fluorescent protein and yellow fluorescent protein production in *Bacillus subtilis*. *Appl Environ Microbiol* **70**, 6809-6815.
- Veening, J. W. & Kuipers, O. P. (2010).** Gene position within a long transcript as a determinant for stochastic switching in bacteria. *Mol Microbiol* **76**, 269-272.
- Wach, A. (1996).** PCR-synthesis of marker cassettes with long flanking homology regions for gene disruptions in *S. cerevisiae*. *Yeast* **12**, 259-265.
- Wacker, I., Ludwig, H., Reif, I., Blencke, H. M., Detsch, C. & Stülke, J. (2003).** The regulatory link between carbon and nitrogen metabolism in *Bacillus subtilis*: regulation of the *gltAB* operon by the catabolite control protein CcpA. *Microbiology* **149**, 3001-3009.
- Wang, S., Hu, Y., Overgaard, M. T., Karginov, F. V., Uhlenbeck, O. C. & McKay, D. B. (2006).** The domain of the *Bacillus subtilis* DEAD-box helicase YxiN that is responsible for specific binding of 23S rRNA has an RNA recognition motif fold. *RNA* **12**, 959-967.
- Wang, W. & Bechhofer, D. H. (1996).** Properties of a *Bacillus subtilis* polynucleotide phosphorylase deletion strain. *J Bacteriol* **178**, 2375-2382.
- Weinrauch, Y., Msadek, T., Kunst, F. & Dubnau, D. (1991).** Sequence and properties of *comQ*, a new competence regulatory gene of *Bacillus subtilis*. *J Bacteriol* **173**, 5685-5693.
- Welch, G. R. & Easterby, J. S. (1994).** Metabolic channeling versus free diffusion: transition-time analysis. *Trends Biochem Sci* **19**, 193-197.
- Wu, J., Jiang, Z., Liu, M., Gong, X., Wu, S. & other authors (2009).** Polynucleotide phosphorylase protects *Escherichia coli* against oxidative stress. *Biochemistry* **48**, 2012-2020.
- Xu, F. & Cohen, S. N. (1995).** RNA degradation in *Escherichia coli* regulated by 3' adenylation and 5' phosphorylation. *Nature* **374**, 180-183.
- Xue, B., Dunbrack, R. L., Williams, R. W., Dunker, A. K. & Uversky, V. N. (2010).** PONDR-FIT: a meta-predictor of intrinsically disordered amino acids. *Biochim Biophys Acta* **1804**, 996-1010.
- Yamanaka, K. & Inouye, M. (2001).** Selective mRNA degradation by polynucleotide phosphorylase in cold shock adaptation in *Escherichia coli*. *J Bacteriol* **183**, 2808-2816.
- Yao, S., Blaustein, J. B. & Bechhofer, D. H. (2007).** Processing of *Bacillus subtilis* small cytoplasmic RNA: evidence for an additional endonuclease cleavage site. *Nucleic Acids Res* **35**, 4464-4473.

- Yao, S. & Bechhofer, D. H. (2010).** Initiation of decay of *Bacillus subtilis rpsO* mRNA by endoribonuclease RNase Y. *J Bacteriol* **192**, 3279-3286.
- Yao, S., Richards, J., Belasco, J. G. & Bechhofer, D. H. (2011).** Decay of a model mRNA in *Bacillus subtilis* by a combination of RNase J1 5' exonuclease and RNase Y endonuclease activities. *J Bacteriol*.
- Yasbin, R. E. & Young, F. E. (1974).** Transduction in *Bacillus subtilis* by bacteriophage SPP1. *J Virol* **14**, 1343-1348.
- Zemansky, J., Kline, B. C., Woodward, J. J., Leber, J. H., Marquis, H. & Portnoy, D. A. (2009).** Development of a mariner-based transposon and identification of *Listeria monocytogenes* determinants, including the peptidyl-prolyl isomerase PrsA2, that contribute to its hemolytic phenotype. *J Bacteriol* **191**, 3950-3964.
- Zock, J., Cantwell, C., Swartling, J., Hodges, R., Pohl, T. & other authors (1994).** The *Bacillus subtilis pnbA* gene encoding p-nitrobenzyl esterase: cloning, sequence and high-level expression in *Escherichia coli*. *Gene* **151**, 37-43.
- Zweers, J. C., Wiegert, T. & van Dijk, J. M. (2009).** Stress-responsive systems set specific limits to the overproduction of membrane proteins in *Bacillus subtilis*. *Appl Environ Microbiol* **75**, 7356-7364.

10. Appendix

10.1. Oligonucleotides

Oligonucleotides were purchased from either Sigma Aldrich (Munich, Germany) or Eurofins MWG Operon (Ebersber, Germany). Underlined are restriction site and T7 Polymerase recognition sites.

Name	Sequence (5' → 3')	Description
CD47	5'-GGGTGAAAATACAATATACTCCGTCAC	LFH-PCR <i>ymdB</i> (up-fragment fwd)
CD48	5'-CCTATCACCTCAAATGGTTCGCTGTGTTTTG TTCCTCCCTGAATATGTTG	LFH-PCR <i>ymdB</i> (up-fragment rev)
CD49	5'-CGAGCGCCTACGAGGAATTTGTATCGCAAG CAAACCAACAGCCGCAAACG	LFH-PCR <i>ymdB</i> (down-fragment fwd)
CD50	5'-GTTTTTGCTGTTGTTTCGCCAGGCG	LFH-PCR <i>ymdB</i> (down-fragment rev)
CD51	5'-GAATTAACCACAATATTGCAGCGC	Riboprobe <i>hag</i> fwd
CD52	5'- <u>CTAATACGACTCACTATAGGGAGAGGCTGT</u> TGGTTTGCTTGAGCAAG	Riboprobe <i>hag</i> rev
CD59	5'-AAAGAATTCGTATTAACAAAATCAGAGACA ATCCG	Amplification of <i>hag</i> promoter region (EcoRI)
CD60	5'-AAAGGATCCAGACCTCTGATTTGTCCTCTCA TTTT	Amplification of <i>hag</i> promoter region (BamHI)
CD61	5'-AAAGGATCCTTGTGGTTAATTCTCATTGTT TTGTTCC	Amplification of <i>hag</i> promoter region (BamHI)
CD64	5'-AAAGGATCCCATCATTAATATCGGATTGTC TC	Amplification of <i>hag</i> promoter region (BamHI)
CD65	5'-AAAGGATCCGGCTGAGTCTTTTGCGCCTCC	Amplification of <i>hag</i> promoter region (BamHI)
CD66	5'-AAAGGATCCGGCACGTCCTTGTGCCCTTAT	Amplification of <i>hag</i> promoter region (BamHI)
CD68	5'-ATGAGAATTAACCACAATATTGCAGC	RT-PCR <i>hag</i> fwd
CD69	5'-TTCAGAGATCGCAAGACCTG	RT-PCR <i>hag</i> rev
CD70	5'-AATTGTGAAGTTTGGCGTGGG	RT-PCR <i>cheV</i> fwd

CD71	5'-ACAGGGAGGATTTCTCCTCT	RT-PCR <i>cheV</i> rev
CD72	5'-CTTCGTTAATCGGTATTATTCTTGC	RT-PCR <i>motA</i> fwd
CD73	5'-TTGTTGGGAACGCAATAACGAC	RT-PCR <i>motA</i> rev
CD74	5'-CTTGAAAATGCCTTGAGCAGAG	RT-PCR <i>flgB</i> fwd
CD75	5'-TGTTTTTTATCGCTTCAAGACGCG	RT-PCR <i>flgB</i> rev
CD76	5'-CTGCAGATTCTGGAATCCATG	RT-PCR <i>ptsH</i> fwd
CD77	5'-CGCCTTTAGCGATACCTAAAG	RT-PCR <i>ptsH</i> rev
CD78	5'-AAATCTAGAGATGCAATCCTTGAATTATGA AG	Amplification of <i>sigD</i> (XbaI)
CD79	5'-AAAGGTACCCGTTGTATCACTTTTTCCAGCA G	Amplification of <i>sigD</i> (KpnI)
CD80	5'-AAATCTAGAGATGAAAATCAATCAATTTGG AACAC	Amplification of <i>flgM</i> (XbaI)
CD81	5'-AAAGGTACCCGTTGCTTTTTATAAAAATTA ATCATAT	Amplification of <i>flgM</i> (KpnI)
CD82	5'-CCTTGAATTATGAAGATCAGGTGC	RT-PCR <i>sigD</i> fwd
CD83	5'-CTTTATGCACTGATTTCCGGCAG	RT-PCR <i>sigD</i> rev
CD86	5'-CGCCGCACATGGAAAAGGCCT	Riboprobe <i>ymdB</i> fwd
CD87	5'- <u>CTAATACGACTCACTATAGGGAGACCC</u> CAG TATACCGTCATACGGG	Riboprobe <i>ymdB</i> rev
CD88	5'-CATCGGACGGGAAGGGCGTAAC	Riboprobe <i>rny</i> fwd
CD89	5'- <u>CTAATACGACTCACTATAGGGAGAGTC</u> GCA AGCTCTACCCGATCT	Riboprobe <i>rny</i> rev
CD93	5'-AAAGGATCCCTCACTATTCAAAGAACATGTG ATCATCG	Rev primer <i>ymdB</i> (BamHI)
CD94	5'-CGAAGCTTGCAAGAAGGACTTTTGCG	Amplification of <i>pgk</i> promoter region with HL51 (HindIII)
CD95	5'-AAAAAGCTTTTGATAGGACGGCAAGGAATT TTCAAGAAG	Fwd primer <i>ymdB</i> (HindIII)
CD129	5'-AAAAAGCTTCTGTCAATTGATGAAAAGCTC C	Amplification of <i>sigD</i> (HindIII)
CD130	5'-AAAATCGATTTGTATCACTTTTTCCAGCAG ATTC	Amplification of <i>sigD</i> (ClaI)
CD133	5'-ATACGGCCGGATTATAAGGATCATGATGGT	Amplification of 3×FLAG (XmaI)

	GATTATAAGGATCATG	
CD134	5'-ATACGGCCGTTATCACTTGTCTGCATCGTCT TTGTAGTCGATATC	Amplification of 3×FLAG (XmaI)
CD137	5'-AAAGGATCCTTGATTGGCCAGCGTATTTAAA CAATACC	Amplification of <i>sinR</i> (BamHI) fwd
CD138	5'-AAAGTCGACTTACTACTCCTCTTTTTGGGAT TTTCTCC	Amplification of <i>sinR</i> (Sall) rev
CD139	5'-GGCATTGGCGCGAGAAGACAG	Fwd primer <i>yqhG</i>
CD144	5'-CCTATCACCTCAAATGGTTCGCTGTTATCAC TTGTCGTCATCGTCTTTGTAGTCGATATC	Rev primer <i>yqhG</i>
CD141	5'-CGAGCGCTACGAGGAATTTGTATCGCCGGG GTATCGAAAAACAATTTTCGTG	Fwd primer <i>tasA</i>
CD142	5'-CTTCAGTTGTAAACCTGGCAACAGG	Rev primer <i>tasA</i>
CD147	5'-AAAGGATCCGGCATTGGCGCGAGAAGACAG	Amplification of <i>sinI/yqhG</i> (BamHI)
CD148	5'-AAAGTCGACGAAAGGATTTACGGTATGACT TCTGGC	Amplification of <i>sinI/yqhG</i> (Sall)
CD153	5'-AAATCTAGAGTTGATTGGCCAGCGTATTAA ACAATACC	Amplification of <i>sinR</i> (XbaI)
CD154	5'-AAAGGTACCCGCTCCTCTTTTTGGGATTTTC TCCATTTT	Amplification of <i>sinR</i> (KpnI)
CD155	5'-AAATCTAGAGATGAAGAATGCAAACAAGA GCACTTTGA	Amplification of <i>sinI</i> (XbaI)
CD156	5'-AAAGGTACCCGAAAGGATTTACGGTATGA CTTCTGG	Amplification of <i>sinI</i> (KpnI)
CD226	5'-AAAGAATTCCTCAGAGTTAAATGGTATTGC TTCACT	Amplification of <i>tapA</i> (EcoRI)
CD172	5'-AAAGGATCCCATATTCAGGGAGGAACAAAA CAATGAG	Amplification of <i>hag</i> (BamHI)
CD173	5'-AAAGTCGACCTATTAACGTAATAATTGAAG TACGTTTTGCGGC	Amplification of <i>hag</i> (Sall)
CD182	5'-TTGGAAGAATTATCCGTTTGTACCGT	Riboprobe <i>slrR</i> fwd
CD183	5'-CTAATACGACTCACTATAGGGAGAGGATTT GACTTCATGGACAGACAA	Riboprobe <i>slrR</i> rev
CD226	5'-AAAGAATTCCTCAGAGTTAAATGGTATTGC	Amplification of <i>tapA</i> (EcoRI)

	TTCACT	
CD233	5'-AAAGGATCCGGATGTAAACACTGTAACCT GATATGACAA	Amplification of <i>tapA</i> (BamHI)
cggfor	5'-CGAAGAAGCCTGTCTGC	Riboprobe <i>cggR</i> fwd
cggrev	5'-CTAATACGACTCACTATAGGGAGACGGTAA GTGCCTGAAGC	Riboprobe <i>cggR</i> rev
DH13	5'-AAAGGATCCATGACCCCAATTATGATGGTT CTC	Amplification of <i>rny</i> (BamHI)
DH14	5'-AAAGTCGACCTATTATTTTGCATACTCTACG GCTCG	Amplification of <i>rny</i> (Sall)
EW1	5'-AAAGGATCCATGAAACGAATAGGGGTATTA ACGAGCGG	Amplification of <i>pfkA</i> (BamHI)
EW2	5'-TTTGTGCGACTCATTAGATAGACAGTTCTTTT GAAAGCTGATACATGTTTTG	Amplification of <i>pfkA</i> (Sall)
EW3	5'-AAAGGATCCATGCCTTTAGTTTCTATGACG GAAATGTTGAATAC	Amplification of <i>fbaA</i> (BamHI)
EW4	5'-TTTGTGCGACTCATTAAGCTTGGTTTGAAGA ACCAAATTCACGC	Amplification of <i>fbaA</i> (Sall)
EW5	5'-AAAGGATCCATGAGAAAACCAATTATCGCC GGTAACTGG	Amplification of <i>tpiA</i> (BamHI)
EW6	5'-TTTGTGCGACTCATTACTCATATTGACCTTCC TCCAATAATTGAACGAATG	Amplification of <i>tpiA</i> (Sall)
EW7	5'-AAAGGATCCATGGCAGTAAAAGTCGGTATT AACGGTTTTTGGT	Amplification of <i>gapA</i> (BamHI)
EW8	5'-TTTGTGCGACTCATTAAAGACCTTTTTTTTGGC ATGTAAGCTGCAAGGTC	Amplification of <i>gapA</i> (Sall)
EW9	5'-AAAGGATCCATGAATAAAAAAACTCTCAAA GACATCGACGTAAAAGGC	Amplification of <i>pgk</i> (BamHI)
EW10	5'-TTTGTGCGACTCATTATTTATCGTTCAGTGCA GCTACCCCTGGAA	Amplification of <i>pgk</i> (Sall)
EW11	5'-AAAGGATCCATGAGTAAAAAACCAGCTGCA CTCATATTCTTG	Amplification of <i>pgm</i> (BamHI)
EW12	5'-TTTGTGCGACTCATTATTTTTGAATTAAGA TGTTCCCTGTCATTTCTTTTCGGTTTTTC	Amplification of <i>pgm</i> (Sall)
EW13	5'-AAAGGATCCATGCCATACATTGTTGATGTT	Amplification of <i>eno</i> (BamHI)

	TATGCACGCGAAG	
EW14	5'-TTT <u>GTCTGACT</u> CATTACTTGTTTAAGTTGTA GAAAGAGTTGATACCGTGG	Amplification of <i>eno</i> (Sall)
FC126	5'AAATCTAGAGATGAATAAAAAAACTCTCAAA GACATCGACGTAAAAGG	Amplification of <i>pgk</i> (XbaI)
FC127	5'TTTGGTACCGTTTATCGTTCAGTGCAGCTA CCCCTGG	Amplification of <i>pgk</i> (KpnI)
FC128	5'AAATCTAGAGATGCCATACATTGTTGATGTT TATGCACGCG	Amplification of <i>eno</i> (XbaI)
FC129	5'TTTGGTACCGCTTGTTTAAGTTGTAGAAAG AGTTGATACCGTG	Amplification of <i>eno</i> (KpnI)
FC130	5'- AAATCTAGAGATGACCCCAATTATGATGGT TCTCATCTCC	Amplification of <i>rny</i> (XbaI)
FC131	5'- TTTGGTACCGTTTTGCATACTCTACGGCT CGAGTCTC	Amplification of <i>rny</i> (KpnI)
FC132	5'- AAATCTAGAGATGAGAATTTTATTTATCGG AGATGTTGTCGGTTC	Amplification of <i>ymdB</i> (XbaI)
FC133	5'- TTTGGTACCGTTCAAAGAACATGTGATCA TCGTTGATTAATAACG	Amplification of <i>ymdB</i> (KpnI)
FC134	5'- AAATCTAGAGATGGGACAAGAAAAACATGT CTTTACCATAGATTG	Amplification of <i>pnpA</i> (XbaI)
FC135	5'- TTTGGTACCGAGATTGTTGTTCTTCTTTT TCTTTCTTTCACGGAGCACCGC	Amplification of <i>pnpA</i> (KpnI)
FC136	5'- AAATCTAGAGATGAGAAAACCAATTATCGC CGGTAACCTGG	Amplification of <i>tpiA</i> (XbaI)
FC137	5'- TTTGGTACCGCTCATATTGACCTTCCTCCA ATAATTGAACG	Amplification of <i>tpiA</i> (KpnI)
FC138	5'- AAATCTAGAGATGGCAGTAAAAGTCGGTAT TAACGGTTTTGG	Amplification of <i>gapA</i> (XbaI)
FC139	5'- TTTGGTACCGAAGACCTTTTTTTGCGATG TAAGCTGCAAGG	Amplification of <i>gapA</i> (KpnI)
FC140	5'- AAATCTAGAGATGAGTAAAAACCAGCTGC ACTCATCATTCTTG	Amplification of <i>pgm</i> (XbaI)
FC141	5'- TTTGGTACCGTTTTTTGAATTAAAGATGTT CCTGTCATTTCTTTCCG	Amplification of <i>pgm</i> (KpnI)

FC142	5'- AAATCTAGAGATGCCTTTAGTTTCTATGAC GGAAATGTTGAATAC	Amplification of <i>fbaA</i> (XbaI)
FC143	5'- TTTGGTACCCGAGCTTGGTTTGAAGAACCA AATTCACGCATTTTAC	Amplification of <i>fbaA</i> (KpnI)
FC144	5'- AAATCTAGAGATGAAACGAATAGGGGTATT AACGAGCGG	Amplification of <i>pfkA</i> (XbaI)
FC145	5'- TTTGGTACCCGGATAGACAGTTCTTTTGAA AGCTGATACATGTTTTG	Amplification of <i>pfkA</i> (KpnI)
FC154	5'- AAATCTAGAGATGACGCATGTACGCTTGA CTACTC	Amplification of <i>pgi</i> (XbaI)
FC155	5'- TTTGGTACCCGATCTTCCAGACGTTTTTCA AGCTCTGC	Amplification of <i>pgi</i> (KpnI)
FC156	5'- AAATCTAGAGATGAGAAAACTAAAATTGT TTGTACCATCGGTCC	Amplification of <i>pyk</i> (XbaI)
FC157	5'- TTTGGTACCCGAAGAACGCTCGCACGGCCT TGATAG	Amplification of <i>pyk</i> (KpnI)
FR1	5'- TTTGGTACCCGACGAATATAGTCATCGACC TCGCGG	Rev primer <i>rny</i> (anneals to KH domain) (KpnI)
FR2	5'- TTTGGTACCCGCGTGTGTTTCGGCAACGGGT CCG	Rev primer <i>rny</i> (anneals to CC domain) (KpnI)
FR4	5'-AAAGGATCCCTCACTTATTTAAAGGAGGAA ACAATCATGGCGGGCGCACGCGGTGCAGCC	Fwd primer <i>rny</i> (RBS) (BamHI) (anneals to CC domain)
FR5	5'-AAAGGATCCCTCACTTATTTAAAGGAGGAA ACAATCATGCAGCGCTGCGCAGCGGACCAC	Fwd primer <i>rny</i> (RBS) (BamHI) (anneals to KH domain)
FR6	5'-TTTGTCGACTTATTATTTTGCATACTCTACG GCTCGAGTCTC	Rev primer <i>rny</i> (Sall)
FR7	5'-AAAGGATCCCTCACTTATTTAAAGGAGGAA ACAATCATGACCCCAATTATGATGGTTCTCAT CTCC	Fwd primer <i>rny</i> (BamHI) (RBS)
FR8	5'- AAATCTAGAGGTATCAGTTGTCAATCTTCC AAATGATGAGATG	Fwd primer <i>rny</i> (XbaI) (anneals to KH domain)
FR11	5'- AAATCTAGAGATGAAATTTGTAAAAAATG ATCAGACTGC	Amplification of <i>rnjA</i> (XbaI)
FR12	5'- TTTGGTACCCGAACCTCCATAATGATCGGC AG	Amplification of <i>rnjA</i> (KpnI)

FR19	5'- ATGAAAAAGAAAAATACAGAAAACGTTAG AATTATCGCC	Amplification of <i>rnjB</i> (XbaI)
FR20	5'- TTTGGTACCCGTA CTT CCATAATAATTGGG ATGATCATCGGTTTAC	Amplification of <i>rnjB</i> (KpnI)
FR22	5'- AAATCTAGAGATGTCAAAACACTCACATTA TAAAGATAAAAAAAGTTCTAT	Amplification of <i>rnc</i> (XbaI)
FR23	5'- TTTGGTACCCGTTGTTTCGTATGGTGTTTT TGCAATTTAGCTAAAGC	Amplification of <i>rnc</i> (KpnI)
FR24	5'- TTTGTCGACTTATTAACGAATATAGTCATC GACCTCGCGG	Rev primer <i>rny</i> (Sall) (anneals to end of HD domain)
FR86	5'- TTTGTCGACCTTGTTAAGTTGTAGAAAGA GTTGATACCGTGG	Amplification of 5' end of <i>eno</i> (Sall)
FR90	5'- AAAGGATCCCGCTTCAAACAATCGTTGAAG C	Amplification of 5' end of <i>eno</i> (BamHI)
gapAfor	5'- GTAACGTATTCCGCGCAG	Riboprobe <i>gapA</i> fwd
gapAreverse	5'- <u>CTAATACGACTCACTATAGGGAGAGCTGCA</u> AGGTCAACAACG	Riboprobe <i>gapA</i> rev
HL51	5'- CGGAATTCACGAAAGCGGCTACTCTAAC	Amplification of <i>pgk</i> promoter region with CD94 (EcoRI)
HP3	5'-AAATCTAGAGGTGGTAAATCACGACATTAC TGAAACAGCAATTAG	Amplification of <i>csH</i> A (XbaI)
HP4	5'-TTTGGTACCCGGTAAGATTTTTTCTGGCGTC TGTCACCTG	Amplification of <i>csH</i> A (KpnI)
HP5	5'-AAATCTAGAGATGAGTCATTTTAAAACTA TCAAATCAGTCATGACAT	Amplification of <i>deaD</i> (XbaI)
HP6	5'-TTTGGTACCCGTTTATTCGCTTTATTCACCT TCAGCTGTTTCC	Amplification of <i>deaD</i> (KpnI)
HP7	5'-AAATCTAGAGATGAAAGAAACGAAATTTGA ACTTTATGAATTGAAACCAT	Amplification of <i>csH</i> B (XbaI)
HP8	5'-TTTGGTACCCGCTTCTTTTCTTAGATTGGT TTCTTCTCTGTTTTTCTTG	Amplification of <i>csH</i> B (KpnI)
HP9	5'-AAATCTAGAGATGACGCAAACCTGGCCATT TTTACATAATGCAC	Amplification of <i>yfmL</i> (XbaI)
HP10	5'TTTGGTACCCGTTTCGTCTTCAGTTTTCCGCC	Amplification of <i>yfmL</i> (KpnI)

	TGCATAC	Lehnik-Habrink et al. 2010
HP11	5'-AAAGGATCCATGGGACAAGAAAAACATGTC TTTACCATAGATTG	Amplification of <i>pnpA</i> (BamHI)
HP12	5'-TTTGTCTGACTTATTAAGATTGTTGTTCTTCT TTTTCTTTCTCTTCACGGAG	Amplification of <i>pnpA</i> (Sall)
HP23	5`AAAGGTACCCGAACCGTCATTTCTTTTCGCTT TTACTTTTACGTGTT	Rev primer of <i>csHA</i> (anneals to end of 1 st catalytic domain)
HP24	5`AAAGGTACCCGAGTAACCTGTTGCTGACCTT CTAACGCTT	Rev primer of <i>csHA</i> (anneals to end of 2 nd catalytic domain)
HP25	5`AAATCTAGAGATGAAGTAAAGCGAAAGAA ATGACGGTTTCTAACATTC	Fwd primer of <i>csHA</i> (anneals to start of 2 nd catalytic domain)
HP26	5`AAATCTAGAGATGTTGAACGTCTTCGCACAA CAATCAGTAAAAAC	Fwd primer of <i>csHA</i> (anneals to start of C-terminal domain)
KG42	5'- GAAACGGCAAACGTTCTGG	RT-PCR <i>rpsJ</i> fwd
KG43	5'- GTGTTGGGTTCACAAATGTCG	RT-PCR <i>rpsJ</i> rev
KG44	5'- GCGTCGTATTGACCCAAGC	RT-PCR <i>rpsE</i> fwd
KG45	5'- TACCAGTACCGAATCCTACG	RT-PCR <i>rpsE</i> rev
KG46	5`AAGAATTCGATAAACCCAGCGAACCATTTG	Construction of pGP888 (EcoRI)
KG47	5`TTTCCCGGGATCGATACAAATTCCTCGTAGG C	Construction of pGP888 (SmaI)
KG50	5`TTTATCGATGCGGCCGCAATGGTTTCTTAGA CGTCAGGTG	Construction of pGP888 (NotI, ClaI)
KG51	5`AAAGAATTCGCTGTTTCCTGTGTGAAATTGT TAT	Construction of pGP888 (EcoRI)
KG54	5`AAAATCGATCGTCGGTCTATTCAATTTAGTG AAT	Construction of pGP888 (ClaI)
KG55	5`TTTGTCTGACGGATCCAGCTGATGGCATCGAC ATGCTT	Construction of pGP888 (Sall, BamHI)
KG56	5`AAAGTCTGACCCCGGCACCATATAAACTGCT GATCGTC	Construction of pGP888 (Sall, SmaI)
KG57	5`TTTCAATTGATCATACGGGTGATTCCAGATG	Construction of pGP888 (MfeI)

KG58	5'AAAAGATCTATCTTACATTGTAATCATGTCC AGAAAATGATC	Construction of pGP888 (BglII)
KG59	5'TTTCAATTGCCCGGGTTCGACGGATCCATGA TTGTTTCCTCCTTTCAGATGCATTTTATTTTCAT ATAGTAAGTAC	Construction of pGP888 (BamHI, Sall, SmaI, MfeI)
KG60	5'AAAAGATCTTCTAGAGGATCCGGTACCGAAT TCAGGTGGATCAGGCTCGGGATCTGGTTCAAT GGCCGACAAGGAGAAGAACG	Construction of pGP888 (BglII, XbaI, BamHI, KpnI, EcoRI)
KG61	5'TTTGTCGACTTATCACTTGTACAGCTCGTCC ATGCC	Construction of pGP888 (Sall)
LR1	5'- GAGTGCTAAAAAAGTGTACGGGTTTTTAACAC	L. Rempeters, masters thesis
LR2	5'- CTAATACGACTCACTATAGGGAGAATGGTG AACGAGTTCGTTATTGTTCTGC	L. Rempeters, masters thesis
LR11	5'-GGCCACAGCAAAAAGTAAATCGTGAGG	L. Rempeters, masters thesis
LR12	5'- CTAATACGACTCACTATAGGGAGATCTCCT CTGCCAGCTCGTCTGC	L. Rempeters, masters thesis
ML1	5'-CAGAACGCGATCCTGCTAA	RT-PCR <i>gapA</i> fwd
ML2	5'-CTTCGTTAGCAGGAGCAGA	RT-PCR <i>gapA</i> rev
ML3	5'-CGCGAGCTTTTGTGTGTC	RT-PCR <i>cggR</i> fwd
ML4	5'-TGAATAGGCGCCTTGTGAC	RT-PCR <i>cggR</i> rev
ML5	5'-ATAAAGCTTGATTATAAGGATCATGATGGT GATTATAAGGATCATG	Amplification 3xFLAG fwd (HindIII)
ML6	5'-ATAAAGCTTTTATCACTTGTGTCATCGTCT TTGTAGTCCGATATC	Amplification 3xFLAG rev (HindIII)
ML7	5'- AAATCTAGAGTGAGCAAGGGCGAGGAGCTG	Amplification of <i>yfp</i> fwd (w/o ATG) (XbaI)
ML8	5'- AAAGGATCCTTACTTGTACAGCTCGTCCAT GCCGA	Amplification of <i>yfp</i> fwd (BamHI)
ML9	5'- AAATCTAGATCCTCCTTTAAATAAGTGAGA GATATTTATATTGAG	Amplification of <i>cggR</i> (XbaI)
ML10	TTTGGTACCCGTTGCGACGGCTGTTCAATAAT GAA	Amplification of <i>ykoW</i> rev (KpnI) (B2H)
ML11	5'- ACAGTCGACGTAAGATTTTTTCTGGCGTCT GTCACCTG	Amplification of <i>cshA</i> rev (w/o stopp codon) (Sall)

ML12	5'- ACAGGATCCCTGGCTGAAGCTCTGAACCTT CG	Amplification of <i>csbA</i> rev (BamHI)
ML13	5'- ACAGTCGACCTTTCTTTTCTTAGATTGGTT TCTTCTCTGTTTTTTC	Amplification of <i>csbB</i> rev (w/o stopp codon) (Sall)
ML14	5'- ACAGGATCCGGATCTGCAAATGCTTGTGTT CTCAGC	Amplification of <i>csbB</i> rev (BamHI)
ML15	5'- GAGCCGCAAAGAAGTTATTAAGGGATGAAC AATCCCTCAATATAAATATCTCTCACTTATTT AAAGGAG	Mutagenesis of <i>cggR</i> Stopp codon to CAA
ML16	TTTGGTACCCGTTTTTTGTTTTGGTCGTCGTTT ACTTCTTC	Amplification of <i>dnaK</i> rev (KpnI) (B2H)
ML17	TTTGGTACCCGCTTATTGATTAATGCCTTAAC TCGATTC	Amplification of <i>tkf</i> rev (KpnI) (B2H)
ML18	TTTGGTACCCGTTTTACGTTAAAAGTTGAAGA GTCTACTTTGAC	Amplification of <i>rplA</i> rev (KpnI) (B2H)
ML19	TTTGGTACCCGTGCAAGCACCTCCTCTACTTTT TC	Amplification of <i>rplD</i> rev (KpnI) (B2H)
ML20	5'- GTTTCTTTCTGCTGATTCATACAAGA	RT-PCR <i>trpE</i> fwd
ML21	5'- TCAAATTTTTGTGATAAAACACCCTGG	RT-PCR <i>trpE</i> rev
ML22	5'- GCTTATGCACGGGAAAACC	RT-PCR <i>trpG</i> fwd
ML23	5'- TTCGTTTGTGCTGTTACTGTAAAACA	RT-PCR <i>trpG</i> rev
ML24	5'-CAGCAGTGAAAATGAATCAGAAATAATC	RT-PCR <i>epsA</i> fwd
ML25	5'-TCTGATAATATATGTACGCCTTGAC	RT-PCR <i>epsA</i> rev
ML26	5'-GAGGAACATGGGCAGCAT	RT-PCR <i>tasA</i> fwd
ML27	5'-CAAATTGGAAATCCTTTGTCAACTTATC	RT-PCR <i>tasA</i> rev
ML28	5'- GCTGATCAGGACAGCAAATC	Riboprobe <i>trpE</i> fwd
ML29	TTTGGTACCCGTTTAGATTTAACAGCACTTTT AACAGTGATTAAG	Amplification of <i>rplC</i> rev (KpnI)
ML30	5'-TTTGGTACCCGTGCACCGCGTGCGCCCGCAA T	Amplification of TM-domain of RNase Y rev (KpnI) (B2H)
ML31	5'- AAATCTAGAGAAAACCATTGCCGAAGCGAA AATTGCC	Amplification of cc-domain of RNase Y fwd (XbaI) (B2H)
ML32	5'- AAAGGATCCCTCACTTATTTAAAGGAGGAA ACAATCATGGAGTTTGTCAATTGGATTATTAAT TG	Fwd primer <i>ezrA</i> (BamHI) (including RBS for pBQ200)

ML33	5'- GCTTCGGCAATGGTTTTACGCCTGAAAAAG TAGCCTGCC	Rev primer <i>EzrA</i> TM-domain
ML34	5'- CGTAAAACCATTTGCCGAAGC	Fwd primer <i>rny</i> (binds at base 73)
ML35	5'- AAATCTAGAGCGTATGGTTGCGCTTCGTAA ATTTAAAGAAGG	Fwd Primer <i>csH</i> A (binds within the 2nd domain) (XbaI) (B2H)
ML36	5'- GAACAAACAACAAAACGCAAATGGACC	Fwd primer <i>csH</i> A (binds end of 2nd domain)
ML37	5'- GGTCCATTTTGCCTTTTGTGTTTGTTC GTCTTACTAATGCATCCTCATCAG	Rev primer <i>csH</i> B (binds end 2nd domain overlaps to ML36)
ML38	5'- GGTCCATTTTGCCTTTTGTGTTTGTTC TGTCGGCTAAAACCGTTTTTC	Rev-Primer <i>deA</i> D (binds end 2nd domain overlaps to ML36)
ML39	5'- GGTCCATTTTGCCTTTTGTGTTTGTTC ATTTTGTCCACAAGGCTCAGCAC	Rev-Primer <i>yfm</i> L (binds end 2nd domain overlaps to ML36)
ML40	5'- ACAGGATCCATATAAGCCTCACTTTACCAT TATTAATGGTG	Amplification of 5' end of <i>ymd</i> B fwd (BamHI)
ML41	5'- ACAGTCCGACTTCAAAGAACATGTGATCATC GTTGATTAATAACG	Amplification of 5' end of <i>ymd</i> B rev (SalI)
ML42	5'- CGAGCGCTACGAGGAATTTGTATCGGAAA TTACAGACACGCTTGCAC	LFH-PCR <i>rnj</i> A-Strep (down-fragment) fwd
ML43	5'- CTGTTGCTGAAGACAGCAAAG	LFH-PCR <i>rnj</i> A-Strep (down-fragment) rev
ML44	5'- TTTGTCGACTTTTGCATACTCTACGGCTCG AGTCTC	Amplification of <i>rny</i> rev (w/o stopp codon) (SalI)
ML45	5'- TTTGTCGACACGAATATAGTCATCGACCTC GCGG	Amplification of TM,CC,KH-domain of RNase Y rev (w/o Stopp codon) (SalI)
ML46	5'- AAATCTAGAGATGGAGTTTGTTCATTGGATT ATTAATTGTAC	Amplification of TM-domain of <i>Ezr</i> A fwd (XbaI) (B2H)
ML47	5'- GAAGAATCTGCTTACACATACATCG	LFH-PCR <i>rny</i> (up-fragment fwd)
ML48	5'- CCTATCACCTCAAATGGTTGCTGCGAGTA GAATCAGCAAATGGAGATGA	LFH-PCR <i>rny</i> (up-fragment rev)
ML49	5'- CCGAGCGCTACGAGGAATTTGTATCGCAA TTAATGATCTTGAGGCTCATCG	LFH-PCR <i>rny</i> (down-fragment fwd)
ML50	5'- GGACTGGAAGGTTTCGTTTTGAATC	LFH-PCR <i>rny</i> (down-fragment

		rev)
ML51	5'- GAAAGGACGTATCATCGATCGGGAAGGGCG TAAC	Fwd primer for mutation of GXXG motif of RNase Y
ML52	5'- GTTACGCCCTTCCCGATCGATGATACGTCTT TTC	Rev primer for mutation of GXXG motif of RNase Y
ML53	5'- TTTGTCGACCGTTGTTTCGGCAACGTGGTC CG	Rev primer of TM,CC-domain of RNase Y (w/o Stopp codon) (SalI)
ML54	5'- TGGAATCGGCTATCGAAATTGG	LFH-PCR <i>rnjA</i> -Strep (up- fragment) fwd
ML55	5'-ACAGTCGACAGCGGATATGTCAGCTTTGAT TTTTTCAAC	Rev primer <i>ezrA</i> (w/o Stopp codon) (SalI)
ML56	5'-ACAGTCGACGATAGACAGTTCTTTTCAAAG CTGATACA	Amplification of 5' end of <i>pfkA</i> rev (SalI)
ML57	5'- ACAGGATCCGTGGAGACGGTTCCTATATGG	Amplification of 5' end of <i>pfkA</i> fwd (BamHI)
ML58	5'-ACAGTCGACAACCTCCATAATGATCGGCAG G	Amplification of 5' end of <i>rnjA</i> rev (SalI)
ML59	5'- ACAGGATCCCGAACAATCAACCAGCTGTAT CG	Amplification of 5' end of <i>rnjA</i> fwd (BamHI)
ML60	5'-GCTAAGCAAGCTGGCAATG	Riboprobe and RT-PCR <i>yhbI</i> fwd primer
ML61	5'-TCTTCCCCCTCTTCGGTTA	RT-PCR <i>yhbI</i> rev
ML62	5'- <u>CTAATACGACTCACTATAGGGAGACCAAAA</u> ATAAACCCGCCATTAGC	Riboprobe <i>yhbI</i> rev
ML63	5'-CATTCACAGAGGAAATTGTAAGAAATG	RT-PCR <i>maeA</i> fwd
ML64	5'-GGCTTCCTGTTGCAATAAGC	RT-PCR <i>maeA</i> rev
ML65	5'- <u>CTAATACGACTCACTATAGGGAGACCTCCGT</u> ATGTCTCTCTCGGTGTTGG	Riboprobe <i>trpE</i> rev
ML66	5'-CAACTCAGCAAAGGGCTTG	RT-PCR <i>ribU</i> fwd
ML67	5'-GCTGTTTTTATAGCGCTGT	RT-PCR <i>ribU</i> rev
ML68	5'-ACGTCGACAGTAACAGGATC	RT-PCR <i>yhdY</i> fwd
ML69	5'-CGTAATCTGGCGTTTGGTCA	RT-PCR <i>yhdY</i> rev
ML70	5'-GATCGTTTTTGTGATTTTATTGACTTCC	RT-PCR <i>sunT</i> fwd
ML71	5'-ACCATACTTATGAATATTAAGTGATTGTG	RT-PCR <i>sunT</i> rev

	ATTAAA	
ML72	5'-TTGTAGTTATTGAACCACATACACAAAG	RT-PCR <i>yorW</i> fwd
ML73	5'-CTGCTGGAAAGATATCAATTAGACTA	RT-PCR <i>yorW</i> rev
ML74	5'-AAAGAAGCGGCTGGTTCCG	RT-PCR <i>thrZ</i> fwd
ML75	5'-CACCTGCAAGCCTTCTTG	RT-PCR <i>thrZ</i> rev
ML76	5'-GGATAAAAAGAGAAGGAAGAGTTCA	RT-PCR <i>sdpA</i> fwd
ML77	5'-CTTCATTTTTTATAACCTTAATAGGCTTTAT TTG	RT-PCR <i>sdpA</i> rev
ML78	5'-CGCGCATATTATCGGAGAG	RT-PCR <i>ldh</i> fwd
ML79	5'-GCGTTTTTCACATCATCTACAATTTG	RT-PCR <i>ldh</i> rev
ML80	5'-GCTGCGAAATATGGTCATGG	RT-PCR <i>epsA</i> fwd
ML81	5'-ACATCAGGAACGGAGCCTAA	RT-PCR <i>epsA</i> rev
ML82	5'-CAGAAACAATGATGTATGAAAAATCAGC	RT-PCR <i>slrR</i> fwd
ML83	5'-GGTAAGAGGCAGTTTCAGG	RT-PCR <i>slrR</i> rev
ML84	5'-CTAATGGGTGCTTTAGTTGAAGA	Cat check up-fragment (sequencing of up-fragment)
ML85	5'-CTCTATTCAGGAATTGTCAGATAG	Cat check down-fragment (sequencing of down- fragment)
ML86	5'-TGCTTACAATTTTCCGATGATACAAG	RT-PCR <i>yqxM</i> fwd
ML87	5'-ATCTGATATGTGCAAATCACTTTGATC	RT-PCR <i>yqxM</i> rev
ML88	5'- <u>CTAATACGACTCACTATAGGGAGAGGAAGC</u> TGAAAACCTGTGTATTG	Riboprobe <i>yqxM/sipW</i> rev
ML89	5'-CCTATCACCTCAAATGGTTCGCTGTTATCAC TTGTCGTCATCGTCTTTGTAG	Primer anneals to 3' end of FLAG tag and 5' start of kan overhangs used in LFH-PCRs
ML91	5'-ACAG <u>TCGAC</u> AGATTGTTGTTCTTCTTTTTCT TTCTCTTAC	Amplification of 5' end of <i>pnpA</i> rev (SalI)
ML92	5'-ACAGGATCCGCTCGGAGATATGGACTTTAA AG	Amplification of 5' end of <i>pnpA</i> fwd (BamHI)
ML93	5'-ACAGGATCCCGGATGAAATGCTGAACATGG	Primer for <i>cshA</i> -Strep (anneals to base 530)
ML94	5'-CCTATCACCTCAAATGGTTCGCTGAGCTATT ATCATTTTTCGAACTGCGG	Primer anneals to 3' end of Strep tag and 5' start of kan overhangs used in LFH-PCRs

ML95	5'-CGAGCGCCTACGAGGAATTTGTATCGGATC GATTCAGAGCCCAAACATG	LFH-PCR <i>csH</i> A-Strep (down- fragment) fwd
ML96	5'-CAGCTTCAAGCCGTTCTTCATCA	LFH-PCR <i>csH</i> A-Strep (down- fragment) rev
ML97	5'-ACAGGATCCGTCGATGACTATATTCGTGAG ATG	Amplification of 5' end of <i>rny</i> fwd (BamHI)
ML98	5'-GGAATTGACCTGATTATTGATGATAC	RT-PCR <i>rny</i> fwd
ML99	5'-TTTTTCAACCATTTCTTCAATCCGTG	RT-PCR <i>rny</i> rev
ML100	5'-AACCACACATGGGACAAAAAGAAAT	RT-PCR <i>ymdB</i> fwd
ML101	5'-CTGCAAATTAATGACTGCTAGTTCTT	RT-PCR <i>ymdB</i> rev
ML102	5'-TTTTGTCTGACTTCAACACCTTCGTAGGACTC AGAAATTC	Rev Primer for TM+CC+KH+HD of RNase Y (w/o Stopp Codon)
ML103	5'-CTCTTGCCAGTCACGTTAC	spc check up-fragment (sequencing of up-fragment)
ML104	5'-TCTTGGAGAGAATATTGAATGGAC	spc check down-fragment (sequencing of down- fragment)
ML105	5'-ACGCAATGACAGCATCACAATCG	Riboprobe <i>pabA/pabC</i> fwd
ML106	5'-CTAATACGACTCACTATAGGGAGACCTTTTC TCCAGAAGACATTAGATATGA	Riboprobe <i>pabA/pabC</i> rev
ML107	5'-GCTTCATAGAGTAATTCTGTAAAGG	kan check up-fragment (sequencing of up-fragment)
ML108	5'-GACATCTAATCTTTTCTGAAGTACATCC	kan check down-fragment (sequencing of down- fragment)
ML109	5'-GTCTAGTGTGTTAGACTTTATGAAATC	mls check up-fragment (sequencing of up-fragment)
ML110	5'-CTTTAATAATTCATCAACATCTACACC	mls check down-fragment (sequencing of down- fragment)
ML111	5'- ACAGTCTGACTGACTTGGTTGACTTTCTAAG CTC	Amplification of 5' end of <i>ccpA</i> rev (SalI)
ML112	5'- ACAGGATCCGAATTTAAGCGTTCTCCAGTG C	Amplification of 5' end of <i>ccpA</i> fwd (BamHI)
ML113	5'-AAATCTAGAGACGACATTTGAGGTTGGCGT	Fwd primer HD domain of

	TCATGG	RNase Y (XbaI) (B2H)
ML114	5'-TTTGGTACCCGTTCAACACCTTCGTAGGACT CAGAAATTTTC	Rev primer HD domain of RNase Y (KpnI) (B2H)
ML115	5'-AAATCTAGAGGTCGTGATTAACAGTATTGC ATCACACCACG	Fwd primer CT domain of RNase Y (XbaI) (B2H)
ML116	5'-TTTTGTCGACTTATTATTCAACACCTTCGTA GGACTCAGAAATTTTC	Rev primer TM-HD domain of RNase Y (SalI)
ML117	5'-AAAGGATCCATTTCAGTCTCCTGAGCTTGCG ATC	Fwd primer <i>csxA</i> -Strep up- fragment
ML118	5'-ACAGTCGACAATTTCGTCTATCCCAATGGCG AT	Amplification of 5' end of <i>katE</i> rev (SalI)
ML119	5'-ACAGGATCCAGAAATCGCCAAAGGAGTAGG	Amplification of 5' end of <i>katE</i> fwd (BamHI)
ML120	5'-CTCAAGCTTTTAGTAAGATTTTTTCTGGCG TCTGTC	Rev primer <i>csxA</i> (HindIII)
ML121	5'-GACACTGCATGTTCAAACCTGC	Riboprobe <i>aroB</i> fwd
ML122	5'-CTAATACGACTCACTATAGGGAGACCATTT GTTTCAGCCAGCTCT	Riboprobe <i>aroB</i> rev
ML123	5'-GAATCAAATGAAAGATACAATATTGCTCG	Riboprobe <i>tyrA</i> fwd
ML124	5'-CTAATACGACTCACTATAGGGAGAGTCATC AGACTGAAAACCTGATCC	Riboprobe <i>tyrA</i> rev
ML127	5'-ACAGTCGACTTTCGTCTTCAGTTTCCGCCT	Amplification of 5' end of <i>yfmL</i> rev (SalI)
ML128	5'-ACAGGATCCGAGCATCGCGAAACGATGAAG	Amplification of 5' end of <i>yfmL</i> fwd (BamHI)
ML129	5'-CCTATCACCTCAAATGGTTCGCTGCTCCTTC TAATTGCTGTTTCAGTAAT	LFH-PCR <i>csxA</i> (up-fragment rev)
ML130	5'-ATGCATACAGCTGCCAGAC	LFH-PCR <i>csxA</i> (up-fragment fwd)
ML131	5'-CGAGCGCTACGAGGAATTTGTATCGCCTAT GACAAAAAGCGTTCAAACG	LFH-PCR <i>csxA</i> (down-fragment fwd)
ML132	5'-CGTATTCATTGTTTGAATCCGATCAA	LFH-PCR <i>csxA</i> (down-fragment rev)
ML133	5'-AGGCGAAGCTTGAAATCATAAACG	Sequencing primer for <i>csxA</i> up- fragment

ML134	5'-CTGCTGTTTCAATTTGCAGCTTC	Sequencing primer for <i>csnA</i> down-fragment
ML135	5'-CTATCCTAACTGACTCAATTAACAACCT	RT-PCR <i>rpsO</i> fwd
ML136	5'-CACGGTAACGAGTTACGTC	RT-PCR <i>rpsO</i> rev
ML137	5'- CCTTTATGAGGTGAAGGTGAC	LFH-PCR <i>dead</i> (up-fragment fwd)
ML138	5'- CCTATCACCTCAAATGGTTCGCTGCCAATG CTCGTAAAATGTCATGA	LFH-PCR <i>dead</i> (up-fragment rev)
ML139	5'- CGAGCGCTACGAGGAATTTGTATCGGTAG GAACGATTGCCAAAATTGAC	LFH-PCR <i>dead</i> (down-fragment fwd)
ML140	5'- GACTATTCCAGTGTCTGTATCG	LFH-PCR <i>dead</i> (down-fragment rev)
ML141	5'- GCTGGTGTGAAGAGTGATG	Sequencing primer for <i>dead</i> up- fragment
ML142	5'- TTGGCTTAGGATACATTGGAAGC	Sequencing primer for <i>dead</i> down-fragment
ML143	5'- <u>CTAATACGACTCACTATAGGGAGACCAACCC</u> ATAGGATAATTATTGTAAAAGAG	Riboprobe <i>sunT</i> fwd
ML144	5'- CAGTTTAATAGTCATGATTGTGGACTAG	Riboprobe <i>sunT</i> rev
ML145	5'- <u>CTAATACGACTCACTATAGGGAGACTTCTTT</u> AATCAGGCTGTTGACTTG	Riboprobe <i>lip</i> rev
ML146	5'- CAATTTTGATGCTGTCTGTTACATCG	Riboprobe <i>lip</i> fwd
ML147	5'- GGAAGCGGTATCGGTGAT	RT-PCR <i>rnjA</i> fwd
ML148	5'- GTACACAAATCCTCTGGAAATCAAAT	RT-PCR <i>rnjA</i> rev
ML149	5'- AAAAGCTCATTCAAAAATCGCTGAAG	RT-PCR <i>rnjB</i> fwd
ML150	5'- CCTAAACCATCAATTAATAATTTGCCGT	RT-PCR <i>rnjB</i> rev
ML151	5'- <u>ACAGTCGACTT</u> CGAGTTCAAGCTGGACGTTT	Amplification of 5' end of <i>hfq</i> rev (SalI)
ML152	5'- <u>ACAGGATCCAACCGATTAATATTCAGGATC</u> AGTTTTTG	Amplification of 5' end of <i>hfq</i> fwd (BamHI)
ML154	5'- <u>ACAGGATCCATGAAATTTGTAAAAAATGAT</u> CAGACTGCTG	Fwd primer <i>rnjA</i> (BamHI)
ML155	5'- <u>AAAGGATCCCTCACTTATTTAAAGGAGGAA</u> ACAATCATGAAATTTGTAAAAAATGATCAGAC TGCTG	Fwd primer <i>rnjA</i> with RBS (BamHI)

ML157	5'-AAATCTAGAGATGGGATTCGGTATTTGGTC AATGC	Amplification of <i>ykoW</i> fwd (XbaI) (B2H)
ML158	5'-TTTGGTACCCGTTATTGCGACGGCTGTTCAA TAATGAA	Amplification of <i>ykoW</i> fwd (KpnI) (B2H)
ML159	5'-AAATCTAGAGGTGAGTAAAGTTATCGGAAT CGAC	Amplification of <i>dnaK</i> fwd (XbaI)
ML160	5'-TTTGGTACCCGTTATTTTTGTTTTGGTCGT CGTTACTTCTTC	Amplification of <i>dnaK</i> fwd (KpnI) (with Stopp codon)
ML161	5'-AAATCTAGAGATGAAACCGATTAATATTC GGATCAG	Amplification of <i>hfq</i> fwd (XbaI)
ML162	5'-TTTGGTACCCGCTATTTCGAGTTCAAGCTGGA CGTTT	Amplification of <i>hfq</i> fwd (KpnI) (with Stopp codon)
ML163	5'-AAATCTAGAGATGGATACAATTGAAAAGAA ATCAGTTGC	Amplification of <i>tkf</i> fwd (XbaI)
ML164	5'-TTTGGTACCCGTTACTTATTGATTAATGCCT TAACTCGATTC	Amplification of <i>tkf</i> fwd (KpnI) (with Stopp codon)
ML165	5'-AAATCTAGAGATGGCTAAAAAAGGTAAAA GTACGTTG	Amplification of <i>rplA</i> fwd (XbaI)
ML166	5'-TTTGGTACCCGTTATTTTACGTTAAAAGTT GAAGAGTCTACTTTGAC	Amplification of <i>rplA</i> fwd (KpnI) (with Stopp codon)
ML167	5'-AAATCTAGAGATGCCAAAAGTAGCATTATA CAACCAAACG	Amplification of <i>rplD</i> fwd (XbaI)
ML168	5'-TTTGGTACCCGTTATGCAAGCACCTCCTCTA CTTTTTTC	Amplification of <i>rplD</i> fwd (KpnI) (with Stopp codon)
ML169	5'-AAATCTAGAGATGACCAAAGGAATCTTAGG AAGAAAAATTGG	Amplification of <i>rplC</i> fwd (XbaI)
ML170	5'-TTTGGTACCCGTTATTTAGATTTAACAGCAC TTTTAACAGTGATTAAG	Amplification of <i>rplC</i> fwd (KpnI) (with Stopp codon)
ML171	5'-TTTGGTACCGAGCAAACGACATTTGAGGTT G	Fwd primer <i>rny</i> (anneals to base 900) (KpnI)
ML172	5'-TTTGGTACCCTGGCTGAAGCTCTGAACCTTC G	Fwd primer <i>csH</i> A (anneals to base 900) (KpnI)
ML173	5'-ACAGTCGACTACTTCCATAATAATTGGGAT GATCATCG	Amplification of 5' end of <i>hfq</i> rev (Sall)
ML174	5'-ACAGGATCCCTCATTACTCTAAAACAGTA	Amplification of 5' end of <i>hfq</i>

	GATCTTC	fwd (BamHI)
ML175	5'-CATTTTCGGTTGTCCTCCAATAC	Sequencing primer for <i>csbB</i> up-fragment
ML176	5'- ATTATAGCCAATCTCACTTAAGATATCAAA G	LFH-PCR <i>csbB</i> (up-fragment fwd)
ML177	5'- CCTATCACCTCAAATGGTTCGCTGGCATCT ATAATAAATGGTTTCAATTCATAAAGTTC	LFH-PCR <i>csbB</i> (up-fragment rev)
ML178	5'- CGAGCGCCTACGAGGAATTTGTATCGGAAA TTGCTCATCGTCTCGTG	LFH-PCR <i>csbB</i> (down-fragment fwd)
ML179	5'- GCATTTCAATCTCAAAACGGTATGG	LFH-PCR <i>csbB</i> (down-fragment rev)
ML180	5'- GCTCAAACAGTTAATGAACTATTCAAAC	Sequencing primer for <i>csbB</i> down-fragment
ML181	5'-ACAGTCGACTTTTATTCGCTTTATTCACCTTC AGCTG	Amplification of 5' end of <i>deadD</i> rev (SalI)
ML182	5'-ACAGGATCCGAATTGGATGACTTGGGATAT CC	Amplification of 5' end of <i>deadD</i> fwd (BamHI)
ML183	5'- GCTCGATCATATCCATCTTATCG	Sequencing primer for <i>yfmL</i> up-fragment
ML184	5'- CTGCTGCTGCTTTTTGTAGG	LFH-PCR <i>yfmL</i> (up-fragment fwd)
ML185	5'- CCTATCACCTCAAATGGTTCGCTGCCAATT CTCTTGATAAATGATTGTGC	LFH-PCR <i>yfmL</i> (up-fragment rev)
ML186	5'- CGAGCGCCTACGAGGAATTTGTATCGGTGA CAAATTTGGAGGAATCTAAGC	LFH-PCR <i>yfmL</i> (down-fragment fwd)
ML187	5'- GGTGATGAATCTGCTCAATGAATTTG	LFH-PCR <i>yfmL</i> (down-fragment rev)
ML188	5'- CAATTACAAAACAGCGGATGATATCC	Sequencing primer for <i>yfmL</i> down-fragment
ML189	5'- CTCAGCATGCATGACTGG	Sequencing primer <i>ykoW</i> (anneals to base 750)
ML190	5'- ATGGTTACACTATACACATCACCAAGC	Riboprobe <i>spx</i> fwd
ML191	5'- <u>CTAATACGACTCACTATAGGGAGAGTTTGC</u> CAAACGCTGTGCTTC	Riboprobe <i>spx</i> rev
ML192	5'- ATGGAACAATGGGGCGTCAC	Riboprobe <i>speD</i> fwd

ML193	5'- <u>CTAATACGACTCACTATAGGGAGATAGTAC</u> TTTCGCTTGCGCCTGTTTAA	Riboprobe <i>speD</i> rev
ML194	5'- TTATCACTTGTTCGTCATCGTCTTTGTA	Rev primer <i>rny</i> -Strep
ML195	5'- GACTACAAAGACGATGACGACAAGTGATAA AGTGATGCGCTAAGCATCACTTTATTTTTTTTG AC	Fwd primer <i>ymdB</i> with Strep overhang
ML196	5'- CCTATCACCTCAAATGGTTCGCTGTTCTGC TCCCCCTTAGTTTTACAATG	Rev primer <i>ymdB</i> with kan overhang
ML197	5'- CGAGCGCTACGAGGAATTTGTATCGAACG GCATATATTACTGATGTGGGAATG	Fwd primer <i>spoVS</i> with kan overhang
ML198	5'- <u>ACAGTCGACCTCCGATTATAGCAGTATTGG</u> TACACA	Rev primer <i>spoVS</i> (Sall)
ML199	5'- <u>ACAGGATCCCGAAACAACGGTATCAGTTGT</u> CAATC	Fwd primer <i>rny</i>
ML200	5'- CACTTTTACACTGCTGACATTCTCTC	Sequencing primer <i>spoVS</i>
ML201	5'- AATTAATCGTATGGGATTTGAAGAAGC	Riboprobe <i>cshA</i> fwd
ML202	5'- CTAATACGACTCACTATAGGGAGACAAGTG TAGGCTCCTTCATG	Riboprobe <i>cshA</i> rev
ML203	5'- TGGAAAGACTCACGCTTATTTACTG	Riboprobe <i>cshB</i> fwd
ML204	5'- CTAATACGACTCACTATAGGGAGACGAGAC GATGAGCAATTCATC	Riboprobe <i>cshB</i> rev
ML205	5'- GAACGAAAGGATCTTGTTCGTC	Riboprobe <i>deaD</i> fwd
ML206	5'- CTAATACGACTCACTATAGGGAGACTTCCT TGCCACTTCCTCTTGA	Riboprobe <i>deaD</i> rev
ML207	5'- GAAAGGATGTCATTGCAGAATCG	Riboprobe <i>yfmL</i> fwd
ML208	5'- CTAATACGACTCACTATAGGGAGACTTCAC TCAGCTCAACACCAAG	Riboprobe <i>yfmL</i> rev
ML209	5'-AAAT <u>CTAGAGATGGCAATTACTCAAGAGCG</u> TAAAAACC	Amplification of <i>rpoS</i> fwd (XbaI)
ML210	5'-TTT <u>GGTACCCGTCGACGTAAGCCTAGTTTGT</u> TAATTAATC	Amplification of <i>rpoS</i> rev (KpnI)
ML211	5'-AAAT <u>CTAGAGATGAATAAGGATCAATCAAA</u> AATCCGCAG	Amplification of <i>rex</i> fwd (XbaI)
ML212	5'-TTT <u>GGTACCCGTTTCGATTTCTCTAAA</u> ACTG AATAATGCTTC	Amplification of <i>rex</i> rev (KpnI)

ML213	5'- AAAGGATCCCTCACTTATTTAAAGGAGGAA ACAATCTTGAAAAAGAAAAATACAGAAAACGT TAGAATTATCG	Fwd primer <i>rnjB</i> (BamHI) (with RBS)
ML214	5'- ATGATCTTCGTGCCCGTGCGTTAAAAAGAT TG	Primer for mutation <i>rnjB</i> → <i>rnjA</i>
ML215	5'- ACGCACGGGCACGAAGATCATATCGGCGGC GTTTTTACTTATTAACAAGCTGTCC	Primer for mutation <i>rnjB</i> → <i>rnjA</i>
ML216	5'- ACAGTCGACTTATACTTCCATAATAATTGG GATGATCATC	Rev primer <i>rnjB</i> (SalI)
ML217	5'- TTTGTGCTTGATGCCGGCCTTATGTTTCCA GAAAACGAAATGCTCGGTATTG	CCR Primer 1 <i>rnjB</i> → <i>rnjA</i>
ML218	5'- CTGCTTAAACCAAATATTTGATTCCTGTA CATGGCGAATACAGAATGCAAAAAGCTCATTC	CCR Primer 2 <i>rnjB</i> → <i>rnjA</i>
ML219	5'- CGTCAAGGCAATCTTTTTAACGCACGGGCA CGAAGATCATATCGGCGGCGTTTTTTACTTAT TAAAC	CCR Primer 3 <i>rnjB</i> → <i>rnjA</i>
ML220	5'-ATAAAGCTTATGAGTAAAGGAGAAGAACTT TTCACTG	Amplification of <i>gfp</i> fwd (HindIII)
ML221	5'-ATAAAGCTTTTATTTGTATAGTTCATCCAT GCCATGTG	Amplification of <i>gfp</i> rev (HindIII)
ML222	5'-ATAAAGCTTATGGTGAGCAAGGGCGAG	Amplification of <i>yfp</i> fwd (HindIII)
ML223	5'-ATAAAGCTTTTACTTGTACAGCTCGTCCATG C	Amplification of <i>yfp</i> rev (HindIII)
ML224	5'- TGATTCACTCATATGAAAACCATTGCCGAA GCGAAAATTGCG	Fwd primer <i>rny</i> (w/o TM- domain) (NdeI)
ML225	5'- CTCGAGGCTCTTCCGCATTTTGCATACTCT ACGGCT	Rev primer <i>rny</i> (SapI)
ML226	5'- CTATTGCCGATCTTGCGGATC	Sequencing primer for <i>rnjB</i>
ML227	5'- AAATCTAGAGATGTCTGTAAAATGGGAAAA ACAAGAAGGCAACG	Amplification of <i>tig</i> fwd (XbaI)
ML228	5'- TTTGGTACCCGACGGTTTTCTACAAGAAAA TCAATTGCTTTGCGAAC	Amplification of <i>tigrev</i> (KpnI)
ML229	5'- AAATCTAGAGATGTTAGAAGGTAAAGTAA AATGGTTCAACTC	Amplification of <i>cspB</i> fwd (XbaI)

ML230	5'- <u>TTTGGTACCCGCGCTTCTTTAGTAACGTTA</u> GCAGC	Amplification of <i>cspB</i> rev (KpnI)
ML231	5'- <u>AAATCTAGAGATGGAACAAGGTACAGTTAA</u> ATGGTTTAATGC	Amplification of <i>cspC</i> fwd (XbaI)
ML232	5'- <u>TTTGGTACCCGAGCTTTTTGAACGTTAGCA</u> GCTTGAG	Amplification of <i>cspC</i> rev (KpnI)
ML233	5'- <u>AAATCTAGAGATGCAAAACGGTAAAGTAAA</u> ATGGTTCAACAAC	Amplification of <i>cspD</i> fwd (XbaI)
ML234	5'- <u>TTTGGTACCCGGAGTTTTACAACATTAGAA</u> GCTTGAGGTC	Amplification of <i>cspD</i> rev (KpnI)
ML235	5'- CGTCTATTTTTGGAGAATACAAGAGATTCT GC	Riboprobe <i>ctaO</i> fwd
ML236	5'- <u>CTAATACGACTCACTATAGGGAGAGATCAG</u> AAACATCATAAATGAATCGATCATCATGATG	Riboprobe <i>ctaO</i> rev
ML237	5'- CGTATTTGATTACGAAGATATTCAGCTAAT TCCTG	Riboprobe <i>guaC</i> fwd
ML238	5'- <u>CTAATACGACTCACTATAGGGAGACCATTA</u> AAAATGGAATTCTTCACAATCACATAATCC	Riboprobe <i>guaC</i> rev
ML239	5'- GGATTGGGGTATTATTATAAAAATATTCAG TAATATTAAGG	Riboprobe <i>ynfC</i> fwd
ML240	5'- <u>CTAATACGACTCACTATAGGGAGACATAAT</u> CGGGTGATGTTGAACATGAAGTTTG	Riboprobe <i>ynfC</i> rev
ML241	5'- TGCATGACATGCCGAATAGCGAAGAAATAG	Riboprobe <i>ydaB</i> fwd
ML242	5'- <u>CTAATACGACTCACTATAGGGAGAGAGGAT</u> CTTCCACTTTGACTTTAACACCTG	Riboprobe <i>ydaB</i> rev
ML243	5'- AGTTGTGGTCAGCATGCTGAGCAGC	Riboprobe <i>ribU</i> fwd
ML244	5'- <u>CTAATACGACTCACTATAGGGAGAGGATAT</u> GTGCACTTCGCTGCTGCTCAAT	Riboprobe <i>ribU</i> rev
ML245	5'- GAAAAGAAACGTTTGAAGAAGAAATTAACC AGAGTG	Riboprobe <i>yebC</i> fwd
ML246	5'- <u>CTAATACGACTCACTATAGGGAGAGGAATC</u> AACGACGCCGTAATATATTCAGAAATAA	Riboprobe <i>yebC</i> rev
ML247	5'- GAGAGCTTCAAACACACATGCAATTGCAAA CG	Riboprobe <i>cimH</i> fwd
ML248	5'- <u>CTAATACGACTCACTATAGGGAGACAGAAT</u>	Riboprobe <i>cimH</i> rev

	CGTGATAATATTGCTGAGGTAAAAAGCG	
ML249	5'- <u>CTAATACGACTCACTATAGGGAGATTTTTT</u> TTCGCTTTTCATTTCTCCGTACGCGGTTGA	Riboprobe <i>mtrB</i> rev
ML250	5'- ATGAACCAAAAGCATTCAAGTGATTTTGTC GTCA	Riboprobe <i>mtrB</i> fwd
ML251	5'- TTGATTGGCCAGCGTATTAACAATACCGT AAAG	Riboprobe <i>sinR</i> fwd
ML252	5'- <u>CTAATACGACTCACTATAGGGAGACTCCTC</u> TTTTTGGGATTTTCTCCATTTTTGA	Riboprobe <i>sinR</i> rev
ML253	5'- ATGGGTATGAAAAGAAATTGAGTTTAGG AGTTGC	Riboprobe <i>tasA</i> fwd
ML254	5'- <u>CTAATACGACTCACTATAGGGAGACTCGCT</u> ATGCGCTTTTTCATTTTCTTTCACGTAAC	Riboprobe <i>tasA</i> rev
ML255	5'- <u>TTTGGTACCCGTTATTAGTAAGATTTTTTC</u> TGGCGTCTGTCACCTG	Rev primer <i>csxA</i> (KpnI)
ML256	5'- <u>AAAGGTACCCGTTATTAAGTAACCTGTTGC</u> TGACCTTCTAACGCTT	Rev primer <i>csxA</i> (only catalytic core) (KpnI)
ML257	5'- ATGTTTCGATTGTTTCACAATCAGCAAAAG GCGAAG	Riboprobe <i>yqxM</i> fwd
ML258	5'- <u>CTAATACGACTCACTATAGGGAGAGTGTTG</u> TTTCATTCTCCTTTTTGACGTCCGAC	Riboprobe <i>yqxM</i> rev
ML259	5'- CGTGATCATCTTTACTCTTATTATTGTGCT GACAC	Riboprobe <i>sipW</i> fwd
ML260	5'- <u>CTAATACGACTCACTATAGGGAGAGTAGAC</u> ATGGTGCTGTCCTTTGTATCTGTTTCCAAGG	Riboprobe <i>sipW</i> rev
ML261	5'- CATTTCTGATGGAGCAGTCAAGGAGTTTG	Riboprobe <i>thrS</i> fwd
ML262	5'- <u>CTAATACGACTCACTATAGGGAGACAGTGT</u> CCTGATGTTTCATACAGCTCTTTGC	Riboprobe <i>thrS</i> rev
ML263	5'- <u>TTTGGTACCCGTTACTACTTTCTTTTCTTA</u> GATTGGTTTCTTCTCTGTTTTTTC	Rev primer <i>csxB</i> (KpnI)
ML264	5'- TTTGGTACCCGTTATTTATTCGCTTTATTC ACCTCAGCTGTTTCC	Rev primer <i>deaD</i> (KpnI)
M265	5'- TTTGGTACCCGTTATTTGCTTTCAGTTTT CCGCCTGCATAC	Rev primer <i>yfmL</i> (KpnI)
ML266	5'- <u>TTTGGTACCCGTTATCATCTTCCCTTTGTTT</u>	Rev primer <i>slrR</i> (KpnI)

	TTAAAAAGGATTTGACTTCATG	
ML267	5'- AAAGGATCCCTCACTTATTTAAAGGAGGAA ACAATCATGATTGGAAGAATTATCCGTTTGTA CCGTA AAAAG	Amplification of <i>slrR</i> fwd (BamHI) (with RBS)
ML268	5'- TTTTGTGCGACTTATCATCTTCCCTTTGTTTT TAAAAAGGATTTGACTTCATGG	Amplification of <i>slrR</i> rev (SalI)
ML269	5'- GAAGAAAAGCTAAAACAGCTGGAACAAGAA GCTTTAG	Riboprobe <i>pheS</i> fwd
ML270	5'- CTAATACGACTCACTATAGGGAGAGTTTAA ACTGCGAAATAAATCTGACATCGTTTGTATAG AAG	Riboprobe <i>pheS</i> rev
ML271	5'- TTGCAAAGACAGGTGTTAATCGGTGACG	Riboprobe <i>yitJ</i> fwd
ML272	5'- CTAATACGACTCACTATAGGGAGAGCTTCT TTTAATTCAGCAGCAGCGGAC	Riboprobe <i>yitJ</i> rev
ML273	5'- TTTGGTACCCGTTATTTTGCATACTCTACG GCTCGAGTCTC	Rev primer <i>rny</i> (KpnI)
ML274	5'- TTTGGTACCCGTTACTATTCAAAGAACATG TGATCATCGTTGATTA AAAATACG	Rev primer <i>yndB</i> (KpnI)
ML275	5'- CAGGAATATCCGAAAGGCATCACAATCAAA G	Riboprobe <i>thrZ</i> fwd
ML276	5'- CTAATACGACTCACTATAGGGAGAGAATAC AGGCTGTTTTTAAAGATGAGCATGTGG	Riboprobe <i>thrZ</i> rev
ML277	5'- GCGATAGACCGTCATTATTTATCAGATTAT CC	Sequencing primer for <i>sfp</i> fwd
ML278	5'- AGCATCTCCGCCTGTACACTAAAACAAAG	Sequencing primer for <i>sfp</i> rev
ML279	5'- CAGGTGTTATATAAAGAATGTGTGCGAACC	Sequencing primer for <i>epsC</i> fwd
ML280	5'- GATTGTGTCCATTAAGGCACATGCTTAT G	Sequencing primer for <i>epsC</i> rev
ML281	5'- AACAGACACTATCTCTCACCGCCTCAAG	Sequencing primer for <i>swrAA</i> fwd
ML282	5'- TTGCAAGTTGCCTAGTCTTTGTTTACTTCA TACAA	Sequencing primer for <i>swrAA</i> rev
ML283	5'- TGCTTTTGTAAATGTTTCGTAATGAATCTG TCG	Sequencing primer for <i>degQ</i> promoter region fwd
ML284	5'- CTTATAGTTTGTATATCAGACTGTTCCGGCT	Sequencing primer for <i>degQ</i>

	G	promoter region rev
ML285	5'-TTTTGTCGACTTCAACACCTTCGTAGGACTC AGAAATTTTC	Rev primer RNase Y HD domain
ML286	5'-GAAAGTTTGTTCGGAAACACTCATGCAG	Riboprobe <i>trpB</i> fwd
ML287	5'-CTAATACGACTCACTATAGGGAGACCTGAT AAACAGACGAGAATGAGTTGACC	Riboprobe <i>trpB</i> rev
ML288	5'-ATCCAGTTCCTGAGGTTTCGATTGAACTG	Riboprobe <i>trpA</i> fwd
ML289	5'-CTAATACGACTCACTATAGGGAGAGTACAA GCCGCTAAACGCCATTGCATAAT	Riboprobe <i>trpA</i> rev
NP56	5'-GCGTTCATGGCCTCCACCCAGATCTCATC	LFH-PCR <i>ymdB</i> (up-fragment fwd)
NP58	5'-CCTATCACCTCAAATGGTTCGCTGGCCCGGT GAACCGACAACATCTCCG	LFH-PCR <i>ymdB</i> (up-fragment rev)
NP59	5'-CCGAGCGCCTACGAGGAATTTGTATCGGAC ATTGACGATCAAACGAAAAAAG	LFH-PCR <i>ymdB</i> (down- fragment fwd)
NP60	5'-GCAGACACATACTCTCCCACTTTTACACT GCTGACAT	LFH-PCR <i>ymdB</i> (down- fragment rev)
NP64	5'-AGCAGGAAGCCATCCGTTATTTTCAGCAATT TGCGG	Sequencing of <i>pnpA</i> up- fragment
NP65	5'-GAATGGTACAAACGGATTCGGAGCGAGCGG AA	LFH-PCR <i>pnpA</i> (up-fragment fwd)
NP66	5'-CCTATCACCTCAAATGGTTCGCTGTAAAGA CATGTTTTTCTTGTCCCAT	LFH-PCR <i>pnpA</i> (up-fragment rev)
NP67	5'-CCGAGCGCCTACGAGGAATTTGTATCGGAT AAACAAGGACGAGTGAATTTAT	LFH-PCR <i>pnpA</i> (down-fragment fwd)
NP68	5'-GTTCATTAGTCTTGTCGAGCTGCTCGGAAA TTCTTCC	LFH-PCR <i>pnpA</i> (down-fragment rev)
NP69	5'-GAGCGAACCACTTTGGCTTAACGCCGATCG	Sequencing of <i>pnpA</i> down- fragment
RB35	5'-CATGAATTCTTGCGATGTGATCTCCGCATTA TCCTCACAAAAAAGTG	Amplification of <i>hag</i> promoter region (EcoRI)
RB36	5'-ACGGGATCCACTTTGTCCTGAGTTCCAGTGT TTCCAGCTTG	Amplification of <i>hag</i> promoter region (BamHI)

10.2. Plasmids

Name	Relevant characteristics	Restriction sites	Reference
pGP87	pGP380- <i>pfkA</i>	BamHI/SalI	Commichau <i>et al.</i> , 2009
pGP88	pGP380- <i>fbaA</i>	BamHI/SalI	Commichau <i>et al.</i> , 2009
pGP89	pGP380- <i>tpiA</i>	BamHI/SalI	Commichau <i>et al.</i> , 2009
pGP90	pGP380- <i>gapA</i>	BamHI/SalI	Commichau <i>et al.</i> , 2009
pGP91	pGP380- <i>pgk</i>	BamHI/SalI	Commichau <i>et al.</i> , 2009
pGP92	pGP380- <i>pgm</i>	BamHI/SalI	Commichau <i>et al.</i> , 2009
pGP93	pGP380- <i>eno</i>	BamHI/SalI	Commichau <i>et al.</i> , 2009
pGP124	pWH884- <i>glcT</i>		Lengbein <i>et al.</i> , 2004
pGP380	N-terminal Strep-tag fusion proteins of <i>B. subtilis</i>		Herzberg <i>et al.</i> , 2007
pGP382	C-terminal Strep-tag fusion proteins of <i>B. subtilis</i>		Herzberg <i>et al.</i> , 2007
pGP459	pAC7- <i>rny</i>	EcoRI/BamHI	Lehnik-Habrink <i>et al.</i> , 2011b
pGP774	pX2- <i>rny</i>	BamHI	Commichau <i>et al.</i> , 2009
pGP775	pGP380- <i>rny</i>	BamHI/SalI	Lehnik-Habrink <i>et al.</i> 2010
pGP882	origin of pUC19, <i>bla</i> resistance gene, and regions flanking the <i>B. subtilis lacA</i> gene		Diethmaier <i>et al.</i> , 2011
pGP884	pGP882 containing a <i>aphA3</i> resistance gene, the <i>xylA</i> promoter and the <i>xylR</i> repressor gene		Diethmaier <i>et al.</i> , 2011
pGP888	pGP884 containing C-YFP Allows overexpression of genes by the P _{xyl} -promoter, integrates into <i>lacA</i> site		Diethmaier <i>et al.</i> , 2011
pGP968	pUT18- <i>pgk</i>	XbaI/KpnI	Commichau <i>et al.</i> , 2009
pGP969	pUT18C- <i>pgk</i>	XbaI/KpnI	Commichau <i>et al.</i> , 2009
pGP970	p25-N- <i>pgk</i>	XbaI/KpnI	Commichau <i>et al.</i> , 2009
pGP971	pKT25- <i>pgk</i>	XbaI/KpnI	Commichau <i>et al.</i> , 2009
pGP972	pUT18- <i>eno</i>	XbaI/KpnI	Commichau <i>et al.</i> , 2009
pGP973	pUT18C- <i>eno</i>	XbaI/KpnI	Commichau <i>et al.</i> , 2009
pGP974	p25-N- <i>eno</i>	XbaI/KpnI	Commichau <i>et al.</i> , 2009

pGP975	pKT25- <i>eno</i>	XbaI/KpnI	Commichau <i>et al.</i> , 2009
pGP976	pUT18- <i>rny</i>	XbaI/KpnI	Commichau <i>et al.</i> , 2009
pGP977	pUT18C- <i>rny</i>	XbaI/KpnI	Commichau <i>et al.</i> , 2009
pGP978	p25-N- <i>rny</i>	XbaI/KpnI	Commichau <i>et al.</i> , 2009
pGP979	pKT25- <i>rny</i>	XbaI/KpnI	Commichau <i>et al.</i> , 2009
pGP980	pUT18- <i>ymdB</i>	XbaI/KpnI	Diethmaier <i>et al.</i> , 2011
pGP981	pUT18C- <i>ymdB</i>	XbaI/KpnI	Diethmaier <i>et al.</i> , 2011
pGP982	p25-N- <i>ymdB</i>	XbaI/KpnI	Diethmaier <i>et al.</i> , 2011
pGP983	pKT25- <i>ymdB</i>	XbaI/KpnI	Diethmaier <i>et al.</i> , 2011
pGP984	pUT18- <i>pnpA</i>	XbaI/KpnI	Commichau <i>et al.</i> , 2009
pGP985	pUT18C- <i>pnpA</i>	XbaI/KpnI	Commichau <i>et al.</i> , 2009
pGP986	p25-N- <i>pnpA</i>	XbaI/KpnI	Commichau <i>et al.</i> , 2009
pGP987	pKT25- <i>pnpA</i>	XbaI/KpnI	Commichau <i>et al.</i> , 2009
pGP988	pUT18- <i>tpiA</i>	XbaI/KpnI	Commichau <i>et al.</i> , 2009
pGP989	pUT18C- <i>tpiA</i>	XbaI/KpnI	Commichau <i>et al.</i> , 2009
pGP990	p25-N- <i>tpiA</i>	XbaI/KpnI	Commichau <i>et al.</i> , 2009
pGP991	pKT25- <i>tpiA</i>	XbaI/KpnI	Commichau <i>et al.</i> , 2009
pGP992	pUT18- <i>gapA</i>	XbaI/KpnI	Commichau <i>et al.</i> , 2009
pGP993	pUT18C- <i>gapA</i>	XbaI/KpnI	Commichau <i>et al.</i> , 2009
pGP994	p25-N- <i>gapA</i>	XbaI/KpnI	Commichau <i>et al.</i> , 2009
pGP995	pKT25- <i>gapA</i>	XbaI/KpnI	Commichau <i>et al.</i> , 2009
pGP996	pUT18- <i>pgm</i>	XbaI/KpnI	Commichau <i>et al.</i> , 2009
pGP997	pUT18C- <i>pgm</i>	XbaI/KpnI	Commichau <i>et al.</i> , 2009
pGP998	p25-N- <i>pgm</i>	XbaI/KpnI	Commichau <i>et al.</i> , 2009
pGP999	pKT25- <i>pgm</i>	XbaI/KpnI	Commichau <i>et al.</i> , 2009
pGP1032	pAC7- <i>hag1</i>	EcoRI/BamHI	Diethmaier <i>et al.</i> , 2011
pGP1033	pAC7- <i>hag2</i>	EcoRI/BamHI	Diethmaier <i>et al.</i> , 2011
pGP1034	pAC7- <i>hag3</i>	EcoRI/BamHI	Diethmaier <i>et al.</i> , 2011
pGP1035	pAC6- <i>hag4</i>	EcoRI/BamHI	Diethmaier <i>et al.</i> , 2011
pGP1036	pAC6- <i>hag5</i>	EcoRI/BamHI	Diethmaier <i>et al.</i> , 2011
pGP1037	pAC6- <i>hag6</i>	EcoRI/BamHI	Diethmaier <i>et al.</i> , 2011
pGP1038	pAC6- <i>hag7</i>	EcoRI/BamHI	Diethmaier <i>et al.</i> , 2011
pGP1050	pKT25- <i>sigD</i>	XbaI/KpnI	Diethmaier <i>et al.</i> , 2011
pGP1051	p25-N- <i>sigD</i>	XbaI/KpnI	Diethmaier <i>et al.</i> , 2011
pGP1052	pUT18- <i>sigD</i>	XbaI/KpnI	Diethmaier <i>et al.</i> , 2011

pGP1053	pUT18C- <i>sigD</i>	XbaI/KpnI	Diethmaier <i>et al.</i> , 2011
pGP1054	pKT25- <i>flgM</i>	XbaI/KpnI	Diethmaier <i>et al.</i> , 2011
pGP1055	p25-N- <i>flgM</i>	XbaI/KpnI	Diethmaier <i>et al.</i> , 2011
pGP1056	pUT18- <i>flgM</i>	XbaI/KpnI	Diethmaier <i>et al.</i> , 2011
pGP1057	pUT18C- <i>flgM</i>	XbaI/KpnI	Diethmaier <i>et al.</i> , 2011
pGP1062	pAC6-P _{pgk} - <i>ymdB</i>	EcoRI/BamHI	Diethmaier <i>et al.</i> , 2011
pGP1083	pGP380- <i>sinR</i>	BamHI/SalI	Diethmaier <i>et al.</i> , 2011
	pGP1370- <i>yqhG-sinI</i> - 3xFLAG	BamHI/SalI	Diethmaier <i>et al.</i> , 2011
pGP1084			
pGP1085	pGP1087- <i>sigD</i> -3xFLAG	HindIII/ClaI	Diethmaier <i>et al.</i> , 2011
pGP1087	pMUTIN-3xFLAG	XmaI	Diethmaier <i>et al.</i> , 2011
pGP1089	pBQ200- <i>hag</i>	BamHI/SalI	Diethmaier <i>et al.</i> , 2011
pGP1090	pUT18- <i>sinR</i>	XbaI/KpnI	Diethmaier <i>et al.</i> , 2011
pGP1091	pUT18C- <i>sinR</i>	XbaI/KpnI	Diethmaier <i>et al.</i> , 2011
pGP1092	pKT25- <i>sinR</i>	XbaI/KpnI	Diethmaier <i>et al.</i> , 2011
pGP1093	p25-N- <i>sinR</i>	XbaI/KpnI	Diethmaier <i>et al.</i> , 2011
pGP1094	pUT18- <i>sinI</i>	XbaI/KpnI	Diethmaier <i>et al.</i> , 2011
pGP1095	pUT18C- <i>sinI</i>	XbaI/KpnI	Diethmaier <i>et al.</i> , 2011
pGP1096	pKT25- <i>sinI</i>	XbaI/KpnI	Diethmaier <i>et al.</i> , 2011
pGP1097	p25-N- <i>sinI</i>	XbaI/KpnI	Diethmaier <i>et al.</i> , 2011
pGP1103	pUT18- <i>fbaA</i>	XbaI/KpnI	Commichau <i>et al.</i> , 2009
pGP1104	pUT18C- <i>fbaA</i>	XbaI/KpnI	Commichau <i>et al.</i> , 2009
pGP1105	p25-N- <i>fbaA</i>	XbaI/KpnI	Commichau <i>et al.</i> , 2009
pGP1106	pKT25- <i>fbaA</i>	XbaI/KpnI	Commichau <i>et al.</i> , 2009
pGP1107	pUT18- <i>pfkA</i>	XbaI/KpnI	Commichau <i>et al.</i> , 2009
pGP1108	pUT18C- <i>pfkA</i>	XbaI/KpnI	Commichau <i>et al.</i> , 2009
pGP1109	p25-N- <i>pfkA</i>	XbaI/KpnI	Commichau <i>et al.</i> , 2009
pGP1110	pKT25- <i>pfkA</i>	XbaI/KpnI	Commichau <i>et al.</i> , 2009
pGP1111	pUT18- <i>pgi</i>	XbaI/KpnI	Commichau <i>et al.</i> , 2009
pGP1112	pUT18C- <i>pgi</i>	XbaI/KpnI	Commichau <i>et al.</i> , 2009
pGP1113	p25-N- <i>pgi</i>	XbaI/KpnI	Commichau <i>et al.</i> , 2009
pGP1114	pKT25- <i>pgi</i>	XbaI/KpnI	Commichau <i>et al.</i> , 2009
pGP1115	pUT18- <i>pyk</i>	XbaI/KpnI	Commichau <i>et al.</i> , 2009
pGP1116	pUT18C- <i>pyk</i>	XbaI/KpnI	Commichau <i>et al.</i> , 2009
pGP1117	p25-N- <i>pyk</i>	XbaI/KpnI	Commichau <i>et al.</i> , 2009

pGP1118	pKT25- <i>pyk</i>	XbaI/KpnI	Commichau <i>et al.</i> , 2009
pGP1201	pBQ200- <i>rny</i>	BamHI/HindIII	Lehnik-Habrink <i>et al.</i> , 2011a
pGP1202	pBQ200- <i>rny</i> truncation (CC-KH-HD-CT)	XbaI/KpnI	Lehnik-Habrink <i>et al.</i> , 2011a
pGP1203	pBQ200- <i>rny</i> truncation (KH-HD-CT)	XbaI/KpnI	Lehnik-Habrink <i>et al.</i> , 2011a
pGP1206	pUT18- <i>rny</i> truncation (TM-CC-KH)	XbaI/KpnI	Lehnik-Habrink <i>et al.</i> , 2011a
	pUT18- <i>rny</i> truncation (KH-HD-CT)	XbaI/KpnI	Lehnik-Habrink <i>et al.</i> , 2011a
pGP1211			
pGP1215	pUT18- <i>rny</i> (KH-domain)	XbaI/KpnI	Lehnik-Habrink <i>et al.</i> , 2011a
pGP1221	p25N- <i>rny</i> (KH-domain)	XbaI/KpnI	Lehnik-Habrink <i>et al.</i> , 2011a
pGP1222	pUT18- <i>rnjA</i>	XbaI/KpnI	Commichau <i>et al.</i> , 2009
pGP1223	pUT18C- <i>rnjA</i>	XbaI/KpnI	Commichau <i>et al.</i> , 2009
pGP1224	p25-N- <i>rnjA</i>	XbaI/KpnI	Commichau <i>et al.</i> , 2009
pGP1225	pKT25- <i>rnjA</i>	XbaI/KpnI	Commichau <i>et al.</i> , 2009
pGP1232	pUT18- <i>rnjB</i>	XbaI/KpnI	Commichau <i>et al.</i> , 2009
pGP1233	pUT18C- <i>rnjB</i>	XbaI/KpnI	Commichau <i>et al.</i> , 2009
pGP1234	p25-N- <i>rnjB</i>	XbaI/KpnI	Commichau <i>et al.</i> , 2009
pGP1235	pKT25- <i>rnjB</i>	XbaI/KpnI	Commichau <i>et al.</i> , 2009
pGP1236	pUT18- <i>rnc</i>	XbaI/KpnI	Commichau <i>et al.</i> , 2009
pGP1237	pUT18C- <i>rnc</i>	XbaI/KpnI	Commichau <i>et al.</i> , 2009
pGP1238	p25-N- <i>rnc</i>	XbaI/KpnI	Commichau <i>et al.</i> , 2009
pGP1239	pKT25- <i>rnc</i>	XbaI/KpnI	Commichau <i>et al.</i> , 2009
pGP1242	pBQ200- <i>rny</i> truncation (TM-CC-KH)	XbaI/KpnI	Lehnik-Habrink <i>et al.</i> , 2011a
pGP1264	pGP1331- <i>eno</i>	BamHI/Sall	Lehnik-Habrink <i>et al.</i> , 2011a
pGP1331	pUS19-3xFLAG	HindIII	Lehnik-Habrink <i>et al.</i> 2010
pGP1332	pGP1331- <i>cskB</i>	BamHI/Sall	Lehnik-Habrink <i>et al.</i> 2010
pGP1333	pGP1331- <i>csmA</i>	BamHI/Sall	Lehnik-Habrink <i>et al.</i> 2010
pGP1334	pUT18- <i>rplA</i>	XbaI/KpnI	This study
pGP1335	pUT18C- <i>rplA</i>	XbaI/KpnI	This study
pGP1336	p25N- <i>rplA</i>	XbaI/KpnI	This study
pGP1337	pKT25- <i>rplA</i>	XbaI/KpnI	This study
pGP1338	pUT18- <i>rplC</i>	XbaI/KpnI	This study

pGP1339	pUT18C- <i>rplC</i>	XbaI/KpnI	This study
pGP1340	p25N- <i>rplC</i>	XbaI/KpnI	This study
pGP1341	pKT25- <i>rplC</i>	XbaI/KpnI	This study
pGP1342	pGP380- <i>pnpA</i>	BamHI/Sall	Lehnik-Habrink <i>et al.</i> 2010
pGP1343	pUT18- <i>rny</i> (TM-domain)	XbaI/KpnI	Lehnik-Habrink <i>et al.</i> , 2011a
pGP1344	p25N- <i>rny</i> (TM-domain)	XbaI/KpnI	Lehnik-Habrink <i>et al.</i> , 2011a
pGP1345	pGP1331- <i>deaD</i>	BamHI/Sall	This study
pGP1346	pGP1331- <i>yfmL</i>	BamHI/Sall	This study
pGP1347	pUT18- <i>rny</i> (CC-domain)	XbaI/KpnI	Lehnik-Habrink <i>et al.</i> , 2011a
pGP1348	p25N- <i>rny</i> (CC-domain)	XbaI/KpnI	Lehnik-Habrink <i>et al.</i> , 2011a
pGP1349	pUT18- <i>rny</i> truncation (CC-KH-HD-CT)	XbaI/KpnI	Lehnik-Habrink <i>et al.</i> , 2011a
pGP1350	p25N- <i>rny</i> truncation (CC-KH-HD-CT)	XbaI/KpnI	This study
pGP1351	pBQ200- <i>rny</i> truncation (TM-CC-KH-HD)	BamHI/Sall	This study
pGP1352	pBQ200- <i>rny</i> (TM _{ezrA} -CC- KH-HD-CT)	BamHI/Sall	Lehnik-Habrink <i>et al.</i> , 2011a
pGP1353	pUT18- <i>cshA</i> (half of 2CD + CTD)	XbaI/KpnI	This study
pGP1354	pAC7-P _{pgk} - <i>ymdB</i>	EcoRI/BamHI	Lehnik-Habrink <i>et al.</i> , 2011a
pGP1355	pUT18- <i>cshB</i> _{<i>cshA</i>} (1 st /2 nd CD of CshB+ CTD of CshA)	XbaI/KpnI	This study
pGP1356	p25N- <i>cshB</i> _{<i>cshA</i>} (1 st /2 nd CD of CshB+ CTD of CshA)	XbaI/KpnI	Lehnik-Habrink <i>et al.</i> 2010
pGP1357	pUT18- <i>deaD</i> _{<i>cshA</i>} (1 st /2 nd CD of DeaD + CTD of CshA)	XbaI/KpnI	This study
pGP1358	p25N- <i>deaD</i> _{<i>cshA</i>} (1 st /2 nd CD of DeaD + CTD of CshA)	XbaI/KpnI	This study
pGP1359	pUT18C- <i>deaD</i> _{<i>cshA</i>} (1 st /2 nd CD of DeaD + CTD)	XbaI/KpnI	This study

	of CshA)		
pGP1360	pKT25- <i>deaD</i> _{<i>cshA</i>} (1 st /2 nd CD of DeaD + CTD of CshA)	XbaI/KpnI	This study
pGP1361	pUT18- <i>yfmL</i> _{<i>cshA</i>} (1 st /2 nd CD of DeaD + CTD of CshA)	XbaI/KpnI	This study
pGP1362	p25N- <i>yfmL</i> _{<i>cshA</i>} (1 st /2 nd CD of DeaD + CTD of CshA)	XbaI/KpnI	This study
pGP1363	pGP1370- <i>rny</i>	HindIII	Lehnik-Habrink <i>et al.</i> , 2011a
pGP1364	pGP1370- <i>rny</i> truncation (CC-KH-HD-CT)	BamHI/SalI	Lehnik-Habrink <i>et al.</i> , 2011a
pGP1365	pGP1370- <i>rny</i> truncation (TM _{<i>ezrA</i>} -CC-KH-HD-CT)	BamHI/SalI	Lehnik-Habrink <i>et al.</i> , 2011a
pGP1366	pGP1370- <i>rny</i> truncation (TM-CC-KH)	BamHI/SalI	This study
pGP1367	pUT18- <i>rny</i> _{<i>ezrA</i>} (TM _{<i>ezrA</i>} -CC-KH-HD-CT)	XbaI/KpnI	This study
pGP1368	pSG1187- <i>rny</i>	KpnI/SalI	This study
pGP1369	pSG1187- <i>cshA</i>	KpnI/SalI	This study
pGP1370	pBQ200-3×FLAG	BamHI/SalI	Lehnik-Habrink <i>et al.</i> , 2011a
pGP1371	pGP1389- <i>deaD</i>	BamHI/SalI	This study
pGP1372	pGP1370- <i>rny</i> truncation (TM-CC-KH-HD)	BamHI/SalI	This study
pGP1373	pGP1370- <i>rny</i> truncation (KH-HD-CT)	BamHI/SalI	This study
pGP1374	pGP1331- <i>ymdB</i>	BamHI/SalI	This study
pGP1375	pGP1331- <i>pfkA</i>	BamHI/SalI	Lehnik-Habrink <i>et al.</i> 2010
pGP1376	pGP1331- <i>rnjA</i>	BamHI/SalI	Lehnik-Habrink <i>et al.</i> 2010
pGP1377	pGP1331- <i>pnpA</i>	BamHI/SalI	Lehnik-Habrink <i>et al.</i> 2010
pGP1378	pGP1331- <i>hfq</i>	BamHI/SalI	This study
pGP1379	pGP1389- <i>cshA</i>		This study
pGP1380	pBQ200- <i>rny</i> truncation (TM-CC-KH-HD)	BamHI/SalI	Lehnik-Habrink <i>et al.</i> , 2011a

pGP1381	pUT18- <i>rny</i> (HD-domain)	XbaI/KpnI	Lehnik-Habrink <i>et al.</i> , 2011a
pGP1382	p25N- <i>rny</i> (HD-domain)	XbaI/KpnI	Lehnik-Habrink <i>et al.</i> , 2011a
pGP1383	pUT18- <i>rny</i> (CT-domain)	XbaI/KpnI	Lehnik-Habrink <i>et al.</i> , 2011a
pGP1384	p25N- <i>rny</i> (CT-domain)	XbaI/KpnI	Lehnik-Habrink <i>et al.</i> , 2011a
pGP1385	pUT18- <i>rny</i> truncation (TM-CC-KH-HD)	XbaI/KpnI	Lehnik-Habrink <i>et al.</i> , 2011a
pGP1386	pWH844- <i>csHA</i>	BamHI/HindIII	Lehnik-Habrink <i>et al.</i> 2010
pGP1387	pGP382- <i>csHA</i>	BamHI/SalI	Lehnik-Habrink <i>et al.</i> 2010
pGP1388	pGP1331- <i>rny</i>	BamHI/SalI	Lehnik-Habrink <i>et al.</i> 2010
pGP1389	pUS19-StrepTag	PstI/HindIII	Lehnik-Habrink <i>et al.</i> , 2011a
pGP1390	pGP1389- <i>pnpA</i>	BamHI/SalI	This study
pGP1391	pGP1389- <i>rny</i>	BamHI/SalI	This study
pGP1392	pGP1389- <i>rnjA</i>	BamHI/SalI	This study
pGP1393	p25N- <i>rny</i> truncation (TM-CC-KH-HD)	XbaI/KpnI	This study
pGP1394	pGP382- <i>rnjA</i>	BamHI/SalI	This study
pGP1395	pUT18- <i>rplD</i>	XbaI/KpnI	This study
pGP1396	pUT18C- <i>rplD</i>	XbaI/KpnI	This study
pGP1397	p25N- <i>rplD</i>	XbaI/KpnI	This study
pGP1398	pKT25- <i>rplD</i>	XbaI/KpnI	This study
pGP1600	pUT18C- <i>csHA</i>	XbaI/KpnI	Lehnik-Habrink <i>et al.</i> 2010
pGP1601	pUT18- <i>csHA</i>	XbaI/KpnI	Lehnik-Habrink <i>et al.</i> 2010
pGP1602	p25-N- <i>csHA</i>	XbaI/KpnI	Lehnik-Habrink <i>et al.</i> 2010
pGP1603	pKT25- <i>csHA</i>	XbaI/KpnI	Lehnik-Habrink <i>et al.</i> 2010
pGP1604	pUT18C- <i>csHA</i> ₁ (only 1 st CD)	XbaI/KpnI	Lehnik-Habrink <i>et al.</i> 2010
pGP1605	pUT18- <i>csHA</i> ₁ (only 1 st CD)	XbaI/KpnI	Lehnik-Habrink <i>et al.</i> 2010
pGP1606	p25-N- <i>csHA</i> ₁ (only 1 st CD)	XbaI/KpnI	Lehnik-Habrink <i>et al.</i> 2010
pGP1607	pKT25- <i>csHA</i> ₁ (only 1 st CD)	XbaI/KpnI	Lehnik-Habrink <i>et al.</i> 2010
pGP1608	pUT18C- <i>csHA</i> ₂ (only 2 nd CD)	XbaI/KpnI	Lehnik-Habrink <i>et al.</i> 2010
pGP1609	pUT18- <i>csHA</i> ₂ (only 2 nd CD)	XbaI/KpnI	Lehnik-Habrink <i>et al.</i> 2010
pGP1610	p25-N- <i>csHA</i> ₂ (only 2 nd CD)	XbaI/KpnI	Lehnik-Habrink <i>et al.</i> 2010
pGP1611	pKT25- <i>csHA</i> ₂ (only 2 nd CD)	XbaI/KpnI	Lehnik-Habrink <i>et al.</i> 2010
pGP1612	pUT18C- <i>csHA</i> _{CTD} (only	XbaI/KpnI	Lehnik-Habrink <i>et al.</i> 2010

	CTD)		
pGP1613	pUT18- <i>csHA</i> _{CTD} (only CTD)	XbaI/KpnI	Lehnik-Habrink <i>et al.</i> 2010
pGP1614	p25-N- <i>csHA</i> _{CTD} (only CTD)	XbaI/KpnI	Lehnik-Habrink <i>et al.</i> 2010
pGP1615	pKT25- <i>csHA</i> _{CTD} (only CTD)	XbaI/KpnI	Lehnik-Habrink <i>et al.</i> 2010
pGP1616	pUT18C- <i>csHA</i> ₁₊₂ (1 st and 2 nd CD)	XbaI/KpnI	Lehnik-Habrink <i>et al.</i> 2010
pGP1617	pUT18- <i>csHA</i> ₁₊₂ (1 st and 2 nd CD)	XbaI/KpnI	Lehnik-Habrink <i>et al.</i> 2010
pGP1618	p25-N- <i>csHA</i> ₁₊₂ (1 st and 2 nd CD)	XbaI/KpnI	Lehnik-Habrink <i>et al.</i> 2010
pGP1619	pKT25- <i>csHA</i> ₁₊₂ (1 st and 2 nd CD)	XbaI/KpnI	Lehnik-Habrink <i>et al.</i> 2010
pGP1620	pUT18C- <i>csHA</i> _{2+CTD} (2 nd and CTD)	XbaI/KpnI	Lehnik-Habrink <i>et al.</i> 2010
pGP1621	pUT18- <i>csHA</i> _{2+CTD} (2 nd and CTD)	XbaI/KpnI	Lehnik-Habrink <i>et al.</i> 2010
pGP1622	p25-N- <i>csHA</i> _{2+CTD} (2 nd and CTD)	XbaI/KpnI	Lehnik-Habrink <i>et al.</i> 2010
pGP1623	pKT25- <i>csHA</i> _{2+CTD} (2 nd and CTD)	XbaI/KpnI	Lehnik-Habrink <i>et al.</i> 2010
pGP1624	pUT18C- <i>csHB</i>	XbaI/KpnI	Lehnik-Habrink <i>et al.</i> 2010
pGP1625	pUT18- <i>csHB</i>	XbaI/KpnI	Lehnik-Habrink <i>et al.</i> 2010
pGP1626	p25-N- <i>csHB</i>	XbaI/KpnI	Lehnik-Habrink <i>et al.</i> 2010
pGP1627	pKT25- <i>csHB</i>	XbaI/KpnI	Lehnik-Habrink <i>et al.</i> 2010
pGP1628	pUT18C- <i>deaD</i>	XbaI/KpnI	Lehnik-Habrink <i>et al.</i> 2010
pGP1629	pUT18- <i>deaD</i>	XbaI/KpnI	Lehnik-Habrink <i>et al.</i> 2010
pGP1630	p25-N- <i>deaD</i>	XbaI/KpnI	Lehnik-Habrink <i>et al.</i> 2010
pGP1631	pKT25- <i>deaD</i>	XbaI/KpnI	Lehnik-Habrink <i>et al.</i> 2010
pGP1632	pUT18C- <i>yfmL</i>	XbaI/KpnI	Lehnik-Habrink <i>et al.</i> 2010
pGP1633	pUT18- <i>yfmL</i>	XbaI/KpnI	Lehnik-Habrink <i>et al.</i> 2010
pGP1634	p25-N- <i>yfmL</i>	XbaI/KpnI	Lehnik-Habrink <i>et al.</i> 2010
pGP1635	pKT25- <i>yfmL</i>	XbaI/KpnI	Lehnik-Habrink <i>et al.</i> 2010
pGP1785	pGP1331- <i>ytsJ</i>	BamHI/SalI	Lehnik-Habrink <i>et al.</i> 2010
pGP1851	pGP1331- <i>rnjB</i>	BamHI/SalI	Lehnik-Habrink <i>et al.</i> , 2011a
pGP1852	pGP382- <i>rny</i>	BamHI/SalI	This study

pGP1853	pUT18- <i>tkl</i>	XbaI/KpnI	This study
pGP1854	pUT18C- <i>tkl</i>	XbaI/KpnI	This study
pGP1855	p25N- <i>tkl</i>	XbaI/KpnI	This study
pGP1856	pKT25- <i>hfq</i>	XbaI/KpnI	This study
pGP1861	pUT18- <i>hfq</i>	XbaI/KpnI	This study
pGP1862	pUT18C- <i>hfq</i>	XbaI/KpnI	This study
pGP1863	p25N- <i>hfq</i>	XbaI/KpnI	This study
pGP1864	pKT25- <i>ykoW</i>	XbaI/KpnI	This study
pGP1865	pUT18- <i>ykoW</i>	XbaI/KpnI	This study
pGP1866	pUT18C- <i>ykoW</i>	XbaI/KpnI	This study
pGP1867	p25N- <i>ykoW</i>	XbaI/KpnI	This study
pGP1868	pKT25- <i>tkl</i>	XbaI/KpnI	This study
pGP1869	pGP1389- <i>cskB</i>	BamHI/SalI	This study
pGP1870	pUS19- <i>gfp</i>	HindIII	D. Tödter, bachelor thesis
pGP1871	pUS19- <i>yfp</i>	HindIII	D. Tödter, bachelor thesis
pGP1872	pGP1870- <i>csmA</i>	BamHI/SalI	D. Tödter, bachelor thesis
pGP1873	pGP1871- <i>yfmL</i>	BamHI/SalI	D. Tödter, bachelor thesis
pGP1874	pKT25- <i>cspB</i>	XbaI/KpnI	D. Tödter, bachelor thesis
pGP1875	pUT18- <i>cspB</i>	XbaI/KpnI	D. Tödter, bachelor thesis
pGP1876	pUT18C- <i>cspB</i>	XbaI/KpnI	D. Tödter, bachelor thesis
pGP1877	p25N- <i>cspB</i>	XbaI/KpnI	D. Tödter, bachelor thesis
pGP1878	pKT25- <i>cspC</i>	XbaI/KpnI	D. Tödter, bachelor thesis
pGP1879	pUT18- <i>cspC</i>	XbaI/KpnI	D. Tödter, bachelor thesis
pGP1880	pUT18C- <i>cspC</i>	XbaI/KpnI	D. Tödter, bachelor thesis
pGP1881	p25N- <i>cspC</i>	XbaI/KpnI	D. Tödter, bachelor thesis
pGP1882	pKT25- <i>cspD</i>	XbaI/KpnI	D. Tödter, bachelor thesis
pGP1883	pUT18- <i>cspD</i>	XbaI/KpnI	D. Tödter, bachelor thesis
pGP1884	pUT18C- <i>cspD</i>	XbaI/KpnI	D. Tödter, bachelor thesis
pGP1885	p25N- <i>cspD</i>	XbaI/KpnI	D. Tödter, bachelor thesis
pGP1886	pGP888- <i>csmA</i>	XbaI/KpnI	D. Tödter, bachelor thesis
pGP1887	pGP888- <i>csmA</i> (w/o CTD)	XbaI/KpnI	D. Tödter, bachelor thesis
pGP1888	pGP888- <i>slrR</i>	KpnI/XbaI	Diethmaier <i>et al.</i> , 2011
pGP1926	pAC6- <i>tapA</i>	EcoRI/BamHI	Diethmaier <i>et al.</i> , 2011
pIYFP	template for <i>yfp</i> gene		Veening <i>et al.</i> , 2004
pUC19	cloning vector		Yanisch-Perron, <i>et al.</i> , 1985

pDG780	template for kanamycin resistance (<i>aphA3</i> gene)	Guérout-Fleury <i>et al.</i> , 1995
pMUTIN-FLAG	Construction of C-terminally FLAG tagged proteins	Kaltwasser <i>et al.</i> , 2002
pAC6	Vector for construction of transcriptional <i>lacZ</i> fusions in <i>B. subtilis</i> , integrates into <i>amyE</i> site	Stülke <i>et al.</i> , 1997
pAC7	Vector for construction of translational <i>lacZ</i> fusions in <i>B. subtilis</i> , integrates into <i>amyE</i> site	Weinrauch <i>et al.</i> , 1991
pBQ200		Martin-Verstaete <i>et al.</i> , 1994
pUT18	<i>P_{lac}-mcs-cyaA bla</i>	Karimova <i>et al.</i> , 1998
pUT18C	<i>P_{lac}-cyaA-mcs bla</i>	Karimova <i>et al.</i> , 1998
pUT18C::zip	<i>P_{lac}-cyaA-zip bla</i>	Karimova <i>et al.</i> , 1998
p25-N	<i>P_{lac}-mcs-cyaA kan</i>	Claessen <i>et al.</i> , 2008
pKT25	<i>P_{lac}-cyaA-mcs kan</i>	Karimova <i>et al.</i> , 1998
pKT25::zip	<i>P_{lac}-cyaA-zip kan</i>	Karimova <i>et al.</i> , 1998
pAL-FLAG- <i>rsiW</i>		Schöbel <i>et al.</i> , 2004
pUS19		Benson <i>et al.</i> , 1993
pWH844	Expression of proteins carrying a His tag at their N-terminus in <i>E. coli</i>	Schirmer <i>et al.</i> , 1997

10.3. Strains

B. subtilis strains used in this study

Strain	Genotype	Reference / Construction
168	<i>trpC2</i>	
BP494	<i>trpC2 bglS::(hag-cfp aphA3)</i>	Paola Bisicchia
BP496	<i>trpC2 amyE::(hag-yfp cat)</i>	Paola Bisicchia
CB40	<i>trpC2 pheA cshB::ermC</i>	Hunger <i>et al.</i> , 2006
DL714	<i>lacA:: p(tapA-yfp ermC)</i> in CU1065 (based on 168)	Daniel Lopez
DS91	NCIB 3610 <i>sinI::spc</i>	Keans <i>et al.</i> , 2005
GP63	<i>trpC2 amyE::(rny-lacZ aphA3)</i>	Lehnik-Habrink <i>et al.</i> , 2011b
GP193	<i>trpC2 ΩymdA::pGP774 (p_{xyIA}-ymdA cat)</i>	Commichau <i>et al.</i> , 2009
GP391	auxotrophic strain	Schilling <i>et al.</i> , 2007
GP583	<i>trpC2 ΔymdB::spc</i>	Diethmaier <i>et al.</i> , 2011
GP584	<i>trpC2 ΔpnpA::aphA3</i>	Lehnik-Habrink <i>et al.</i> , 2010
GP845	<i>trpC2 bglS::(hag-cfp aphA3) lacA:: p(tapA-yfp ermC)</i>	Diethmaier <i>et al.</i> , 2011
GP847	<i>trpC2 bglS::(hag-cfp aphA3) lacA:: p(tapA-yfp ermC) ΔymdB::spc</i>	Diethmaier <i>et al.</i> , 2011
GP902	<i>trpC2 Δhag::tet</i>	Diethmaier <i>et al.</i> , 2011
GP904	<i>trpC2 ΔymdB::spc Δhag::tet</i>	Diethmaier <i>et al.</i> , 2011
GP906	<i>trpC2 amyE::(hag1-lacZ aphA3)</i>	Diethmaier <i>et al.</i> , 2011
GP907	<i>trpC2 amyE::(hag2-lacZ aphA3)</i>	Diethmaier <i>et al.</i> , 2011
GP908	<i>trpC2 amyE::(hag3-lacZ aphA3)</i>	Diethmaier <i>et al.</i> , 2011
GP909	<i>trpC2 amyE::(hag4-lacZ cat)</i>	Diethmaier <i>et al.</i> , 2011
GP910	<i>trpC2 amyE::(hag5-lacZ cat)</i>	Diethmaier <i>et al.</i> , 2011
GP911	<i>trpC2 amyE::(hag6-lacZ cat)</i>	Diethmaier <i>et al.</i> , 2011
GP912	<i>trpC2 amyE::(hag7-lacZ cat)</i>	Diethmaier <i>et al.</i> , 2011
GP914	<i>trpC2 amyE::(hag1-lacZ aphA3) ΔymdB::spc</i>	Diethmaier <i>et al.</i> , 2011
GP915	<i>trpC2 amyE::(hag2-lacZ aphA3) ΔymdB::spc</i>	Diethmaier <i>et al.</i> , 2011
GP916	<i>trpC2 amyE::(hag3-lacZ aphA3) ΔymdB::spc</i>	Diethmaier <i>et al.</i> , 2011
GP917	<i>trpC2 amyE::(hag4-lacZ cat) ΔymdB::spc</i>	Diethmaier <i>et al.</i> , 2011
GP918	<i>trpC2 amyE::(hag5-lacZ cat) ΔymdB::spc</i>	Diethmaier <i>et al.</i> , 2011

GP919	<i>trpC2 amyE::(hag6-lacZ cat) ΔymdB::spc</i>	Diethmaier <i>et al.</i> , 2011
GP920	<i>trpC2 amyE::(hag7-lacZ cat) ΔymdB::spc</i>	Diethmaier <i>et al.</i> , 2011
GP921	<i>ΔymdB::spc</i>	Diethmaier <i>et al.</i> , 2011
GP922	<i>trpC2 ΔymdB::cat</i>	Diethmaier <i>et al.</i> , 2011
GP923	<i>trpC2 ΔymdB::cat ΔsinR::spc</i>	Diethmaier <i>et al.</i> , 2011
GP925	<i>trpC2 ΔymdB::spc amyE::(p_{pgk}-ymdB cat)</i>	Diethmaier <i>et al.</i> , 2011
GP946	<i>trpC2 sinI-3xFLAG ΔsinR::aphA3</i>	Diethmaier <i>et al.</i> , 2011
GP947	<i>trpC2 sinI-3xFLAG ΔsinR::aphA3 ΔymdB::spc</i>	Diethmaier <i>et al.</i> , 2011
GP948	<i>trpC2 sigD-3xFLAG ermC</i>	Diethmaier <i>et al.</i> , 2011
GP950	<i>trpC2 ΔymdB::spc sigD-3xFLAG ermC</i>	Diethmaier <i>et al.</i> , 2011
GP953	<i>trpC2 amyE::(hag-yfp cat) ΔymdB::spc</i>	Diethmaier <i>et al.</i> , 2011
GP959	<i>trpC2 ΔsinI::spc</i>	Diethmaier <i>et al.</i> , 2011
GP972	<i>trpC2 ΔymdB::spc lacA::(p_{xyI} C-yfp aphA3)□</i>	Diethmaier <i>et al.</i> , 2011
GP973	<i>trpC2 ΔymdB::spc lacA::(p_{xyI} slrR aphA3)</i>	Diethmaier <i>et al.</i> , 2011
GP975	<i>lacA::(p_{xyI} slrR aphA3) ΔymdB::spc</i>	Diethmaier <i>et al.</i> , 2011
GP976	<i>trpC2 amyE::(hag-yfp cat) lacA::(p_{xyI} slrR aphA3) ΔymdB::spc</i>	Diethmaier <i>et al.</i> , 2011
GP993	<i>trpC2 amyE::(tapA-lacZ cat)</i>	Diethmaier <i>et al.</i> , 2011
GP994	<i>trpC2 amyE::(tapA-lacZ cat) ΔymdB::spc</i>	Diethmaier <i>et al.</i> , 2011
GP1001	<i>trpC2 rnjB-3×FLAG</i>	pGP1851 → 168
GP1002	<i>trpC2 pnpA-Strep::cat</i>	LFH → 168
GP1003	<i>trpC2 pnpA-Strep cshA-3×FLAG</i>	pGP1333 → GP1002
GP1004	<i>trpC2 pnpA-Strep pfkA-3×FLAG</i>	pGP1375 → GP1002
GP1005	<i>trpC2 pnpA-Strep rnjA-3×FLAG</i>	pGP1376 → GP1002
GP1006	<i>trpC2 pnpA-Strep rny-3×FLAG</i>	pGP1388 → GP1002
GP1007	<i>trpC2 pnpA-Strep ytsJ-3×FLAG</i>	pGP1758 → GP1002
GP1008	<i>trpC2 pnpA-Strep rnjB-3×FLAG</i>	pGP1851 → GP1002
GP1009	<i>trpC2 pnpA-Strep eno-3×FLAG</i>	pGP1264 → GP1002
GP1010	<i>trpC2 cshA-3xFLAG spc</i>	Lehnik-Habrink <i>et al.</i> , 2010
GP1011	<i>trpC2 cshB-3xFLAG spc</i>	Lehnik-Habrink <i>et al.</i> , 2010
GP1012	<i>trpC2 rny-Strep ΔymdB::cat</i>	Lehnik-Habrink <i>et al.</i> , 2011a
GP1013	<i>trpC2 rny-Strep ΔymdB::cat amyE::pGP1354 (P_{pgk}::ymdB)</i>	Lehnik-Habrink <i>et al.</i> , 2011a

GP1014	<i>trpC2 amyE::(p_{pgk}-y_{mdB} aphA3)</i>	Lehnik-Habrink <i>et al.</i> , 2011b
GP1015	<i>trpC2 Ω_{rny}::pGP774(P_{xyIA}-rny cat)</i> <i>amyE::(p_{pgk}-y_{mdB} aphA3)</i>	Lehnik-Habrink <i>et al.</i> , 2011b
GP1016	<i>trpC2 rny-Strep Δy_{mdB}::cat</i> <i>amyE::pGP1354 (P_{pgk}::y_{mdB}) pnpA-3×FLAG</i>	Lehnik-Habrink <i>et al.</i> , 2011a
GP1017	<i>trpC2 ΔpnpA::aphA3 cshA-3×FLAG spc</i>	Lehnik-Habrink <i>et al.</i> , 2010
GP1018	<i>trpC2 y_{mdB}-3×FLAG spc</i>	pGP1374 → 168
GP1019	<i>trpC2 pfkA-3×FLAG spc</i>	pGP1375 → 168
GP1020	<i>trpC2 rnjA-3×FLAG spc</i>	pGP1376 → 168
GP1021	<i>trpC2 pnpA-3×FLAG spc</i>	pGP1377 → 168
GP1022	<i>trpC2 rny-Strep Δy_{mdB}::cat</i> <i>amyE::pGP1354 (P_{pgk}::y_{mdB}) cshA-3×FLAG</i>	Lehnik-Habrink <i>et al.</i> , 2011a
GP1023	<i>trpC2 rny-Strep Δy_{mdB}::cat</i> <i>amyE::pGP1354 (P_{pgk}::y_{mdB}) pfkA-3×FLAG</i>	Lehnik-Habrink <i>et al.</i> , 2011a
GP1024	<i>trpC2 rny-Strep Δy_{mdB}::cat</i> <i>amyE::pGP1354 (P_{pgk}::y_{mdB}) rnjA-3×FLAG</i>	Lehnik-Habrink <i>et al.</i> , 2011a
GP1025	<i>trpC2 rny-Strep Δy_{mdB}::cat</i> <i>amyE::pGP1354 (P_{pgk}::y_{mdB}) ytsJ-3×FLAG</i>	Lehnik-Habrink <i>et al.</i> , 2011a
GP1026	<i>trpC2 cshA-Strep aphA3</i>	Lehnik-Habrink <i>et al.</i> , 2010
GP1027	<i>trpC2 cshA-Strep aphA3 pfkA-3×FLAG spc</i>	Lehnik-Habrink <i>et al.</i> , 2010
GP1028	<i>trpC2 cshA-Strep aphA3 rnjA-3×FLAG spc</i>	Lehnik-Habrink <i>et al.</i> , 2010
GP1029	<i>trpC2 cshA-Strep aphA3 pnpA-3×FLAG spc</i>	Lehnik-Habrink <i>et al.</i> , 2010
GP1031	<i>trpC2 cshA-Strep aphA3 rny-3×FLAG spc</i>	Lehnik-Habrink <i>et al.</i> , 2010
GP1032	<i>trpC2 cshA-Strep aphA3 ytsJ-3×FLAG spc</i>	Lehnik-Habrink <i>et al.</i> , 2010
GP1033	<i>trpC2 rny-Strep spc</i>	Lehnik-Habrink <i>et al.</i> , 2011a
GP1034	<i>trpC2 rnjA-Strep spc</i>	pGP1391 → 168
GP1035	<i>trpC2 ΔcshA ::aphA3</i>	LFH → 168
GP1038	<i>trpC2 pnpA-Strep</i>	pGP1390 → 168
GP1039	<i>trpC2 rny-Strep Δy_{mdB}::cat</i> <i>amyE::pGP1354 (P_{pgk}::y_{mdB}) rnjB-3×FLAG</i>	Lehnik-Habrink <i>et al.</i> , 2011a
GP1040	<i>trpC2 rny-Strep Δy_{mdB}::cat</i> <i>amyE::pGP1354 (P_{pgk}::y_{mdB}) eno-3×FLAG</i>	Lehnik-Habrink <i>et al.</i> , 2011a
GP1042	<i>trpC2 rnjA-Strep::cat</i>	LFH
GP1043	<i>trpC2 rnjA -Strep cshA-3×FLAG</i>	pGP1333 → GP1042
GP1044	<i>trpC2 rnjA -Strep pfkA-3×FLAG</i>	pGP1375 → GP1042

GP1045	<i>trpC2 rnjA</i> -Strep <i>pnpA</i> -3×FLAG	pGP1376 → GP1042
GP1046	<i>trpC2 rnjA</i> -Strep <i>rny</i> -3×FLAG	pGP1388 → GP1042
GP1047	<i>trpC2 rnjA</i> -Strep <i>ytsJ</i> -3×FLAG	pGP1758 → GP1042
GP1048	<i>trpC2 rnjA</i> -Strep <i>rnjB</i> -3×FLAG	pGP1851 → GP1042
GP1049	<i>trpC2 rnjA</i> -Strep <i>eno</i> -3×FLAG	pGP1264 → GP1042
GP1050	<i>trpC2 rny</i> -Strep Δ <i>ymdB</i> :: <i>cat</i> <i>amyE</i> ::pGP1354 (<i>P_{pgk}</i> :: <i>ymdB</i> -3×FLAG)	pGP1374 → GP1013
GP1051	<i>trpC2</i> Δ <i>cshB</i> :: <i>cm</i>	LFH → 168
GP1052	<i>trpC2</i> Δ <i>deaD</i> :: <i>tet</i>	chrDNA → 168
GP1053	<i>trpC2</i> Δ <i>yfmL</i> :: <i>mls</i>	LFH → 168
GP1056	<i>trpC2</i> Δ <i>deaD</i> :: <i>tet</i> Δ <i>yfmL</i> :: <i>mls</i>	chrDNA GP1053 → GP1052
GP1057	<i>trpC2</i> Δ <i>deaD</i> :: <i>tet</i> Δ <i>cshB</i> :: <i>cm</i>	chrDNA GP1051 → GP1052
GP1058	<i>trpC2</i> Δ <i>deaD</i> :: <i>tet</i> Δ <i>cshA</i> :: <i>aphA3</i>	chrDNA GP1035 → GP1052
GP1059	<i>trpC2</i> Δ <i>deaD</i> :: <i>tet</i> Δ <i>cshA</i> :: <i>aphA3</i> Δ <i>cshB</i> :: <i>cm</i>	chrDNA GP1034 → GP1057
GP1060	<i>trpC2</i> Δ <i>deaD</i> :: <i>tet</i> Δ <i>yfmL</i> :: <i>mls</i> Δ <i>cshB</i> :: <i>cm</i>	chrDNA GP1051 → GP1056
GP1061	<i>trpC2</i> Δ <i>cshA</i> :: <i>aphA3</i> Δ <i>cshB</i> :: <i>cm</i>	chrDNA GP1051 → GP1035
GP1062	<i>trpC2</i> Δ <i>cshB</i> :: <i>cm</i> , Δ <i>yfmL</i> :: <i>mls</i>	chrDNA GP1053 → GP1051
GP1063	<i>trpC2</i> Δ <i>deaD</i> :: <i>tet</i> Δ <i>cshA</i> :: <i>aphA3</i> Δ <i>cshB</i> :: <i>cm</i> Δ <i>yfmL</i> :: <i>mls</i>	chrDNA GP1053 → GP1059
GP1064	<i>trpC2 cshB</i> -Strep <i>spc</i>	pGP1869 → 168
GP1065	<i>trpC2 deaD</i> -Strep <i>spc</i>	pGP1371 → 168
GP1066	<i>trpC2 yfmL</i> -FLAG <i>spc</i>	pGP1346 → 168
GP1067	<i>trpC2 hfq</i> -FLAG <i>spc</i>	pGP1378 → 168
GP1068	<i>trpC2 deaD</i> -FLAG	pGP1345 → 168
GP1069	<i>trpC2 yfmL</i> -Strep	pGP1380 → 168
GP1070	<i>cshA</i> -Strep <i>trpC2</i> +	GP1026 → GP391
GP1071	<i>deaD</i> -Strep <i>trpC2</i> +	pGP1371 → GP391
GP1072	<i>cshB</i> -Strep <i>trpC2</i> +	pGP1869 → GP391
GP1073	<i>yfmL</i> -Strep <i>trpC2</i> +	pGP1380 → GP391
GP1074	<i>trpC2 cshA</i> -FLAG <i>tet</i>	LFH → 168
GP1075	<i>trpC2 J1</i> -FLAG <i>kan</i>	LFH → 168
GP1076	<i>trpC2 pnpA</i> -FLAG <i>erm</i>	LFH → 168
GP1077	<i>trpC2 rny</i> -Strep Δ <i>ymdB</i> :: <i>cat</i> <i>cshA</i> -FLAG <i>tet</i>	GP1074 → GP1012
GP1078	<i>trpC2 rny</i> -Strep Δ <i>ymdB</i> :: <i>cat</i> <i>cshA</i> -FLAG <i>tet</i>	GP1075 → GP1077

	<i>J1-FLAG kan</i>	
GP1079	<i>trpC2 rny-Strep ΔymdB ::cat cshA-FLAG tet</i> <i>J1-FLAG kan eno-FLAG spc</i>	pGP1264 → GP1078
GP1080	<i>trpC2 rny-Strep ΔymdB ::cat cshA-FLAG tet</i> <i>J1-FLAG kan eno-FLAG spc pnpA-FLAG erm</i>	GP1076 → GP1079
GP1081	<i>trpC2cshA-gfp spc</i>	pGP1872 → 168
GP1082	<i>trpC2yfmL-yfp spc</i>	pGP1873 → 168
GP1083	<i>trpC2 ΔcshA::cat</i>	LFH → 168
GP1084	<i>trpC2 ΔcshA::cat lacA::cshA aphA3</i>	pGP1886 → GP1083
GP1085	<i>trpC2 ΔcshA::cat lacA::cshA-CTD aphA3</i>	pGP1887 → GP1083
GP1089	<i>amyE::(p_{pgk}-ymdB aphA3)</i>	Lehnik-Habrink <i>et al.</i> , 2011b
GP1090	□ <i>rny::pGP774(P_{xyIA}-rny cat) amyE::(p_{pgk}-ymdB aphA3)</i>	Lehnik-Habrink <i>et al.</i> , 2011b
GP1091	<i>trpC2 lacA::xylR aphA3</i>	Lehnik-Habrink <i>et al.</i> , 2011a
GP1092	<i>trpC2 lacA::xylR aphA3</i> <i>ΩymdA::pGP774(P_{xyIA}-rny cat)</i>	Lehnik-Habrink <i>et al.</i> , 2011a
GP1173	<i>trpC2 lacA::(p_{xyl} C-yfp aphA3)□</i>	Diethmaier <i>et al.</i> , 2011
NCIB3610	non-domesticated wild type	Laboratory collection
TMB079	<i>trpC2 ΔsinR::spc</i>	Jordan <i>et al.</i> , 2007

E. coli used in this study.

Strain	Genotype	Reference / Construction
BL21 (DE)	<i>F⁻ ompT gal dcm lon hsdS_B(r_B⁻ m_B⁻) λ(DE3)</i> <i>pLysS(cm^R)</i>	Sambrook <i>et al.</i> , 1989
BTH101	<i>F⁻ cya-99 araD139 galE15 galK16 rpsL1</i> <i>(Str^r) hsdR2 mcrA1 mcrB1</i>	Karimova <i>et al.</i> , 2005
DH5α	<i>F⁻ endA1 glnV44 thi-1 recA1 relA1 gyrA96</i> <i>deoR nupG Φ80dlacZΔM15 Δ(lacZYA-</i> <i>argF)U169, hsdR17(r_K⁻ m_K⁺), λ-</i>	Sambrook <i>et al.</i> , 1989
XL1-Blue	<i>endA1 gyrA96(nal^R) thi-1 recA1 relA1 lac</i> <i>glnV44 F'[::Tn10 proAB⁺ lacI^q Δ(lacZ)M15]</i> <i>hsdR17(r_K⁻ m_K⁺)</i>	Karimova <i>et al.</i> , 2005

10.4. Analysis of the DEAD-box helicases CshB, DeaD and YfmL in *B. subtilis*

Introduction

DEAD-box RNA helicases are enzymes that can utilize ATP to unwind secondary structures on RNA molecules. While some of these secondary structures are needed for the RNA molecules to function properly in cell, other can have negative consequences. Therefore DEAD-box RNA helicases are an important for the physiology of every organism (Rocak & Linder, 2004). This is highlighted by the fact that RNA helicases can be found in all domains of life and eukaryotic organisms like *Saccharomyces cerevisiae* encodes 26 of these enzymes, of which 18 are essential (Linder *et al.*, 2000).

But RNA helicases also play an important role in the physiology of bacteria. The Gram negative model organism *E. coli* contains five different DEAD-box proteins. These enzymes play an important role in the ribosome biogenesis and mRNA decay (Iost & Dreyfus, 2006).

While *E. coli* encodes five different RNA helicases, the Gram positive model organism *B. subtilis* contains four enzymes: CshA, CshB, DeaD and YfmL. All four RNA helicases have a conserved catalytic core and, with the exception of YfmL, an additional C-terminal domain. While the RNA helicase CshA was already investigated with regard to its participation in the RNA degradosome and its physiological roles in chapter three and four, this short part will focus on the roles of CshB, DeaD and YfmL.

Results

Construction of individual and multiple RNA helicase mutant strains

To get insight into in physiological functions of CshB, DeaD and YfmL, single RNA helicase mutants were constructed by long-flanking homology PCR. As none of the individual genes were essential, *B. subtilis* mutant strains carrying multiple RNA helicase deletions were also constructed. Combining the deletions of the single RNA helicase mutants enabled us to construct strain GP1063. This mutant strain is devoid of all four annotated RNA helicases in *B. subtilis*. This strain is viable under laboratory conditions (37°C, rich medium).

Impact of RNA helicase deletions on growth at low temperatures

In its natural habitat (the upper layers of the soil) *B. subtilis* is exposed to broad range of temperatures. While high temperatures (37°C) rarely prevail, lower temperatures (20°C and below) are very common. To investigate whether RNA helicases have an impact on cell growth at lower (more physiological) temperatures, the different mutant strains were exposed to 42°C and 20°C.

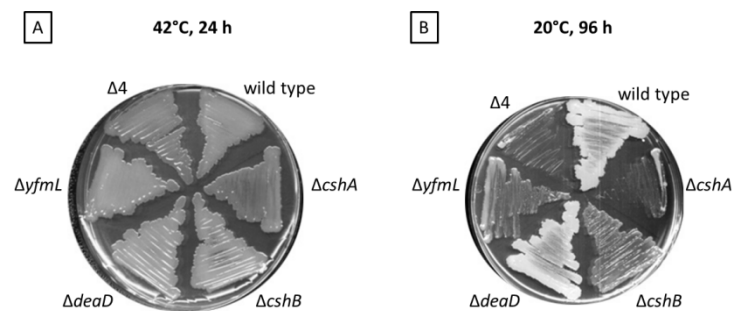


Fig 52. Influence of deletion of RNA helicase genes on growth at different temperatures. *B. subtilis* wild type and RNA helicase mutants were grown at (A) 42°C for 24 h or (B) 20°C for 96 h on LB-agar-plates. The quadruple mutant devoid of all RNA helicase is labeled “Δ4”.

As shown in Fig. 52, all strains grew indistinguishably on LB-agar-plates at 42°C. In contrast, when incubated at 20°C clear differences in the growth behavior emerged. While the wild type and the *deaD* mutant strain exhibited similar growth, the *yfmL* and *cshB* mutant strains were impeded in growth compared to the wild type. For the quadruple mutant strain (devoid of all RNA helicases) virtually no growth was detectable on LB-agar-plates. Therefore CshB and YfmL are important for the ability of the cell to cope with lower temperatures.

Interaction of RNA helicases CshB, DeaD and YfmL with cold shock proteins (CSPs)

The previous experiments revealed that CshB and YfmL are required for growth at lower temperatures. It was already known that the RNA helicase CshB interacts with the cold shock protein B (CspB), suggesting that both proteins work in conjunction to rescue misfolded mRNA molecules and maintain proper initiation of translation at low temperatures in *B. subtilis* (Hunger *et al.*, 2006). To detect primary protein-protein

interactions between the DEAD-box RNA helicases and the three cold shock proteins CspB, CspC and CspD, we conducted bacterial two-hybrid analysis.

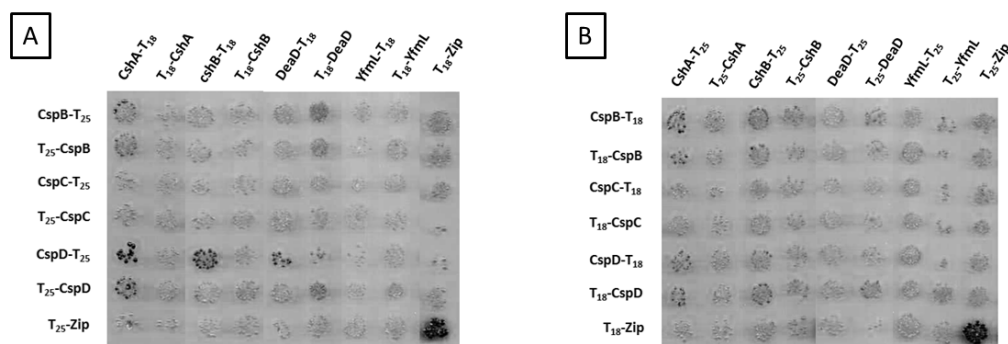


Fig 53. Analysis of interactions among the RNA helicases and the cold shock proteins in *B. subtilis*. All genes were cloned in the vectors of the bacterial two hybrid system. These plasmids allow the expression of the gene of interest fused to either the N- or C-terminus to the T18 or T25 domain of the *B. pertussis* adenylate cyclase. The *E. coli* transformants harboring both vectors were incubated for 48 h at 30°C. Degradation of Xgal indicates interaction due to the presence of a functional adenylate cyclase. A. Genes encoding the RNA helicases CshA, CshB, DeadD and YfmL were present in the high copy vectors (pUT18 and pUT18C), whereas the genes encoding the three cold shock proteins CspB, CspC and CspD were present in the low-copy vectors (p25N and pKT25). B. Genes coding for the cold shock proteins were present in the high copy vectors, whereas genes encoding RNA helicases were present in the in low-copy vectors.

Our two-hybrid analysis revealed strong interactions between the cold shock protein CspD and the RNA helicases CshB. In addition, CspD might also interact with DeadD. The anticipated interaction between CspB and CshB was only minor and did not meet our stringency criteria for interaction. The RNA helicase YfmL and the cold shock protein CspC did not exhibit any interaction with all proteins tested.

Analysis of the interactions between CshB, DeadD and YfmL with ribosomal proteins

Pull down experiments and bacterial two hybrid analysis of CshA revealed interactions with the ribosomal proteins RplA and RplC. To test whether CshB, DeadD and YfmL are also able to interact with both ribosomal proteins bacterial two hybrid analysis were conducted.

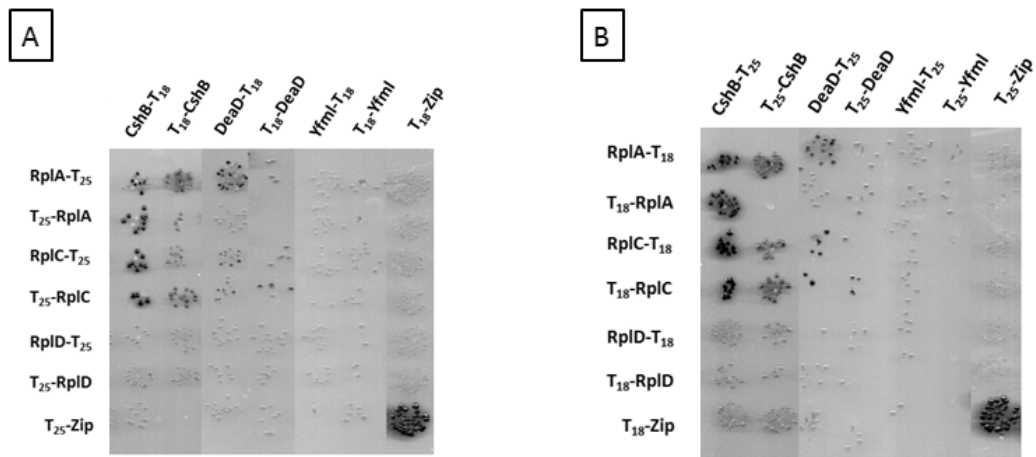


Fig 54. Analysis of interactions among the RNA helicases CshB, DeaD and YfmL and the ribosomal proteins RplA, RplC and RplD in *B. subtilis*. All genes were clones in the vectors of the bacterial two hybrid system. For details see Figure 53.

A. Genes encoding the RNA helicases CshB, DeaD and YfmL were present in the high copy vectors (pUT18 and pUT18C), whereas the genes encoding the ribosomal proteins RplA, RplC and RplD were present in the low-copy vectors (p25N and pKT25). B. Genes coding for the ribosomal proteins were present in the high copy vectors, whereas genes encoding RNA helicases were present in the in low-copy vectors.

Our two-hybrid screen demonstrates that the RNA helicase CshB is able to directly interact with the ribosomal proteins RplA and RplC. Slight interactions can also be observed for DeaD and the two ribosomal proteins. YfmL is not interacting with any of the tested ribosomal proteins. Again, no RNA helicase interacted with RplD.

Discussion

This short studied dealing with the RNA helicases CshB, DeaD and YfmL investigated the impact of the loss of these enzymes for the growth at lower temperatures and the binding ability of the three RNA helicases to ribosomal and cold shock proteins.

RNA helicases are important for the unwinding of secondary structures of RNAs. The emergence of these structures is thermodynamically favored at lower temperatures. Therefore it is well known that RNA helicases are important proteins helping the cell to adapt to the cold. In agreement, we found that the deletion of *cshB* and *yfmL* resulted in an impaired growth under conditions of reduced temperatures. It is interesting to note, that deletion of only one single RNA helicase already comprises growth. Thus, the different RNA helicases are not able to compensate the loss of another, suggesting that the proteins have specific functions to promote growth a lower temperatures. The implication of CshB and YfmL in the process of cold adaption also was previously found in the closely related bacterium *B. cereus* (Pandiani *et al.*, 2010).

In addition we were able to reveal interactions of CshB with the cold shock protein CspB. This co-operation between these two enzymes is thought to be beneficial for the cell as the two proteins can work in conjunction to rescue misfolded mRNA molecules. Nevertheless we were not able to confirm the reported interaction between CshB and CspB (Hunger *et al.*, 2006). This might be due to fact that two very different techniques were used to verify the interaction. While we performed bacterial two hybrid analysis, the interaction between CshB and CspB was demonstrated by FRET.

At last, we revealed that CshB and to a very minor extend also DeaD were able to interact with the ribosomal proteins RplA and RplC. So far these interactions have only been investigated in two hybrid experiments. Whether they indeed occur *in vivo* remains to be elucidated.

With this study we reveal that CshB and YfmL are important for *B. subtilis* to grow at lower temperatures. Furthermore our two hybrid experiments suggest interactions of CshB with ribosomal and cold shock proteins.

10.5. Supplementary material for RNase Y microarray analysis

List of microarray results

This list comprises all transcripts that are changed in abundance by RNase Y depletion in all replicates with an average fold change of at least 1.5. All 37 essential genes are highlighted in grey.

mRNA with increased abundance			mRNAs with decreased abundance		
Locus Tag	Gene name	Average fold change	Locus Tag	Gene name	Average fold change
BSU22680	<i>trpE</i>	13.1	BSU17600	<i>xylA</i>	-108.5
BSU22670	<i>trpD</i>	12.7	BSU17610	<i>xylB</i>	-39.7
BSU22660	<i>trpC</i>	12.3	BSU17570	<i>xynP</i>	-23.9
BSU22650	<i>trpF</i>	11.4	BSU16960	<i>rny</i>	-13.2
BSU22640	<i>trpB</i>	9.9	BSU17580	<i>xynB</i>	-9.4
BSU08990	<i>yhbI</i>	7.1	BSU16970	<i>ymdB</i>	-8.0
BSU09000	<i>yhbJ</i>	7.1	BSU38760	<i>cydA</i>	-5.4
BSU09010	<i>yhcA</i>	7.0	BSU03050	<i>ldh</i>	-5.3
BSU28910	<i>ysbA</i>	6.8	BSU34380	<i>slrR</i>	-4.3
BSU09020	<i>yhcB</i>	6.2	BSU34370	<i>epsA</i>	-4.1
BSU09030	<i>yhcC</i>	5.4	BSU34250	<i>epsL</i>	-4.0
BSU27200	<i>yrhG</i>	5.2	BSU34270	<i>epsK</i>	-4.0
BSU20080	<i>yosL</i>	5.0	BSU34360	<i>epsB</i>	-4.0
BSU20100	<i>yosJ</i>	4.9	BSU34280	<i>epsJ</i>	-3.9
BSU20110	<i>yosI</i>	4.8	BSU12080	<i>ctaO</i>	-3.9
BSU20070	<i>yosM</i>	4.7	BSU34300	<i>epsH</i>	-3.8
BSU37050	<i>maeA</i>	4.7	BSU34320	<i>epsF</i>	-3.8
BSU09680	<i>nhaC</i>	4.5	BSU34290	<i>epsI</i>	-3.8
BSU20230	<i>yorW</i>	4.4	BSU34230	<i>epsN</i>	-3.6
BSU19830	<i>yotM</i>	4.1	BSU24620	<i>tasA</i>	-3.6
BSU37040	<i>ywkB</i>	4.0	BSU34240	<i>epsM</i>	-3.4
BSU20140	<i>yosF</i>	4.0	BSU33770	<i>sdpC</i>	-3.3
BSU19850	<i>yotK</i>	4.0	BSU34220	<i>epsO</i>	-3.2
BSU20250	<i>mtbP</i>	3.9	BSU21460	<i>bdbA</i>	-3.2
BSU20150	<i>yosE</i>	3.9	BSU38060	<i>ywcJ</i>	-3.1

BSU20060	<i>nrdEB</i>	3.8	BSU34310	<i>epsG</i>	-3.0
BSU20130	<i>yosG</i>	3.7	BSU02700	<i>lip</i>	-3.0
BSU21060	<i>yonK</i>	3.5	BSU24630	<i>sipW</i>	-3.0
BSU32130	<i>guaC</i>	3.5	BSU21470	<i>sunT</i>	-3.0
BSU20120	<i>yosH</i>	3.5	BSU17590	<i>xylR</i>	-3.0
BSU04170	<i>ydaB</i>	3.5	BSU31980	<i>dhbE</i>	-2.9
BSU20160	<i>yosD</i>	3.4	BSU34330	<i>epsE</i>	-2.9
BSU20240	<i>yorV</i>	3.4	BSU40170	<i>yydG</i>	-2.9
BSU28900	<i>ysbB</i>	3.4	BSU31970	<i>dhbB</i>	-2.9
BSU31580	<i>maeN</i>	3.4	BSU31960	<i>dhbF</i>	-2.8
BSU38770	<i>cimH</i>	3.3	BSU37560	<i>thrZ</i>	-2.8
BSU18110	<i>ynfC</i>	3.3	BSU07480	<i>yfmG</i>	-2.7
BSU20180	<i>yosB</i>	3.2	BSU03060	<i>lctP</i>	-2.7
BSU27220	<i>yrhE</i>	3.2	BSU21450	<i>yolJ</i>	-2.7
BSU20370	<i>yorI</i>	3.2	BSU31990	<i>dhbC</i>	-2.7
BSU20380	<i>yorH</i>	3.2	BSU33760	<i>sdpB</i>	-2.6
BSU20400	<i>yorF</i>	3.1	BSU33750	<i>sdpA</i>	-2.6
BSU11490	<i>yjbC</i>	3.1	BSU10770	<i>wprA</i>	-2.6
BSU21050	<i>yonN</i>	3.0	BSU24640	<i>tapA</i>	-2.6
BSU20260	<i>yorT</i>	3.0	BSU39500	<i>yxeM</i>	-2.6
BSU21070	<i>yonJ</i>	3.0	BSU34340	<i>epsD</i>	-2.5
BSU29010	<i>speD</i>	3.0	BSU39510	<i>yxeL</i>	-2.5
BSU19920	<i>yotD</i>	3.0	BSU39890	<i>yxbB</i>	-2.5
BSU27210	<i>yrhF</i>	3.0	BSU39490	<i>yxeN</i>	-2.4
BSU10230	<i>yhfH</i>	2.9	BSU39900	<i>yxbA</i>	-2.4
BSU20030	<i>yosR</i>	2.9	BSU39910	<i>yxnB</i>	-2.4
BSU00750	<i>pabA</i>	2.9	BSU13240	<i>thiU</i>	-2.4
BSU06380	<i>yebC</i>	2.9	BSU32000	<i>dhbA</i>	-2.4
BSU22630	<i>trpA</i>	2.8	BSU21440	<i>bdbB</i>	-2.3
BSU20410	<i>yorE</i>	2.8	BSU14890	<i>ctaC</i>	-2.3
BSU20270	<i>yorS</i>	2.8	BSU39720	<i>iolE</i>	-2.3
BSU32590	<i>frlN</i>	2.8	BSU31080	<i>yuaB</i>	-2.3
BSU20200	<i>yorZ</i>	2.8	BSU08790	<i>thiC</i>	-2.3
BSU32580	<i>frlM</i>	2.8	BSU14350	<i>yknX</i>	-2.3
BSU19820	<i>yotN</i>	2.8	BSU12460	<i>xlyB</i>	-2.3

BSU32600	<i>frlO</i>	2.8	BSU13230	<i>thiV</i>	-2.3
BSU31480	<i>yuxJ</i>	2.8	BSU39920	<i>asnH</i>	-2.3
BSU20210	<i>yorY</i>	2.8	BSU14360	<i>yknY</i>	-2.3
BSU02680	<i>lmrA</i>	2.7	BSU38750	<i>cydB</i>	-2.3
BSU19860	<i>yotJ</i>	2.7	BSU14370	<i>yknZ</i>	-2.2
BSU27180	<i>yrhH</i>	2.7	BSU39480	<i>yxeO</i>	-2.2
BSU08060	<i>acoA</i>	2.7	BSU13220	<i>thiW</i>	-2.2
BSU00760	<i>pabC</i>	2.7	BSU38320	<i>ywbH</i>	-2.2
BSU21040	<i>yonO</i>	2.7	BSU39950	<i>yxaJ</i>	-2.2
BSU27230	<i>yrhD</i>	2.7	BSU13210	<i>thiX</i>	-2.2
BSU20090	<i>yosK</i>	2.7	BSU12670	<i>xkdN</i>	-2.2
BSU23050	<i>ribU</i>	2.7	BSU15960	<i>ylqB</i>	-2.1
BSU25000	<i>pbpA</i>	2.6	BSU02310	<i>ybfO</i>	-2.1
BSU19980	<i>yosW</i>	2.6	BSU12800	<i>xhlB</i>	-2.1
BSU20220	<i>yorX</i>	2.6	BSU14900	<i>ctaD</i>	-2.1
BSU20390	<i>yorG</i>	2.6	BSU24670	<i>comGG</i>	-2.1
BSU29540	<i>ytdI</i>	2.6	BSU40600	<i>yybL</i>	-2.1
BSU09640	<i>yhdY</i>	2.5	BSU38330	<i>ywbG</i>	-2.1
BSU11500	<i>spx</i>	2.5	BSU39470	<i>yxeP</i>	-2.1
BSU38080	<i>ywcl</i>	2.5	BSU38740	<i>cydC</i>	-2.1
BSU20170	<i>yosC</i>	2.5	BSU12620	<i>xkdH</i>	-2.1
BSU20050	<i>yosQ</i>	2.5	BSU39940	<i>yxaL</i>	-2.1
BSU20350	<i>yorK</i>	2.5	BSU12660	<i>xkdM</i>	-2.1
BSU33950	<i>cggR</i>	2.5	BSU37460	<i>rapF</i>	-2.1
BSU07570	<i>yflS</i>	2.5	BSU12180	<i>yjhA</i>	-2.1
BSU22620	<i>hisC</i>	2.5	BSU31250	<i>tlpA</i>	-2.1
BSU02670	<i>lmrB</i>	2.5	BSU12790	<i>xhlA</i>	-2.1
BSU20020	<i>yosS</i>	2.4	BSU39460	<i>yxeQ</i>	-2.1
BSU19890	<i>yotG</i>	2.4	BSU37350	<i>sboA</i>	-2.1
BSU19900	<i>yotF</i>	2.4	BSU34350	<i>epsC</i>	-2.1
BSU08740	<i>ygzB</i>	2.4	BSU37310	<i>fnr</i>	-2.0
BSU27540	<i>yrvM</i>	2.4	BSU29530	<i>sppA</i>	-2.0
BSU20360	<i>yorJ</i>	2.4	BSU18540	<i>yoaB</i>	-2.0
BSU32570	<i>frlD</i>	2.4	BSU14910	<i>ctaE</i>	-2.0
BSU39010	<i>yxjB</i>	2.4	BSU12760	<i>xkdW</i>	-2.0

BSU32610	<i>frlB</i>	2.4	BSU12810	<i>xlyA</i>	-2.0
BSU38130	<i>ywcE</i>	2.4	BSU12610	<i>xkdG</i>	-2.0
BSU20330	<i>yorM</i>	2.4	BSU39730	<i>iolD</i>	-2.0
BSU11520	<i>mecA</i>	2.4	BSU40590	<i>yybM</i>	-2.0
BSU05060	<i>lrpB</i>	2.4	BSU12770	<i>xkdX</i>	-2.0
BSU31950	<i>yukJ</i>	2.4	BSU14920	<i>ctaF</i>	-2.0
BSU30060	<i>ytfP</i>	2.4	BSU14170	<i>ykuP</i>	-2.0
BSU21110	<i>yonF</i>	2.3	BSU12650	<i>xkdK</i>	-2.0
BSU24010	<i>bmr</i>	2.3	BSU18550	<i>yoaC</i>	-2.0
BSU23060	<i>ypzE</i>	2.3	BSU39520	<i>yxeK</i>	-2.0
BSU19880	<i>yotH</i>	2.3	BSU02200	<i>ybfG</i>	-2.0
BSU19940	<i>yotB</i>	2.3	BSU40610	<i>yybK</i>	-2.0
BSU00770	<i>sul</i>	2.3	BSU14340	<i>yknW</i>	-2.0
BSU12830	<i>spolISA</i>	2.3	BSU06210	<i>ydjI</i>	-2.0
BSU01750	<i>ybbP</i>	2.3	BSU39740	<i>iolC</i>	-2.0
BSU02240	<i>mpr</i>	2.2	BSU02140	<i>glpT</i>	-2.0
BSU25100	<i>zur</i>	2.2	BSU24680	<i>comGF</i>	-2.0
BSU09860	<i>yhaT</i>	2.2	BSU12700	<i>xkdQ</i>	-1.9
BSU15660	<i>yloC</i>	2.2	BSU06560	<i>yerA</i>	-1.9
BSU21090	<i>yonH</i>	2.2	BSU12600	<i>xkdF</i>	-1.9
BSU14630	<i>speA</i>	2.2	BSU29520	<i>yteJ</i>	-1.9
BSU28640	<i>pheS</i>	2.2	BSU12640	<i>xkdJ</i>	-1.9
BSU19910	<i>yotE</i>	2.2	BSU37360	<i>sboX</i>	-1.9
BSU00780	<i>folB</i>	2.2	BSU30660	<i>ytkA</i>	-1.9
BSU07960	<i>yfkA</i>	2.2	BSU32010	<i>besA</i>	-1.9
BSU20570	<i>yoqN</i>	2.2	BSU12630	<i>xkdI</i>	-1.9
BSU28630	<i>pheT</i>	2.2	BSU39870	<i>yxbD</i>	-1.9
BSU07830	<i>yfkO</i>	2.2	BSU02010	<i>ybdK</i>	-1.9
BSU04950	<i>yddF</i>	2.1	BSU12690	<i>xkdP</i>	-1.9
BSU40790	<i>yyaO</i>	2.1	BSU07190	<i>yezD</i>	-1.9
BSU04990	<i>yddJ</i>	2.1	BSU12190	<i>yjhB</i>	-1.9
BSU30350	<i>yttB</i>	2.1	BSU37370	<i>albA</i>	-1.9
BSU27370	<i>yrrL</i>	2.1	BSU06200	<i>ydjH</i>	-1.9
BSU00570	<i>yabM</i>	2.1	BSU24660	<i>yqzE</i>	-1.9
BSU23290	<i>ypuE</i>	2.1	BSU06190	<i>ydjG</i>	-1.9

BSU33830	<i>opuCA</i>	2.1	BSU12750	<i>xkdV</i>	-1.9
BSU21240	<i>yomS</i>	2.1	BSU30650	<i>dps</i>	-1.9
BSU32870	<i>mdtR</i>	2.1	BSU02780	<i>ycdA</i>	-1.9
BSU19870	<i>yotI</i>	2.1	BSU23150	<i>resA</i>	-1.9
BSU21140	<i>yonC</i>	2.1	BSU14160	<i>ykuO</i>	-1.9
BSU39790	<i>yxcE</i>	2.1	BSU12740	<i>xkdU</i>	-1.9
BSU33800	<i>opuCD</i>	2.1	BSU24690	<i>comGE</i>	-1.9
BSU32550	<i>yurJ</i>	2.1	BSU40660	<i>yybF</i>	-1.9
BSU09400	<i>spoVR</i>	2.1	BSU12780	<i>xepA</i>	-1.9
BSU21390	<i>yomE</i>	2.1	BSU24720	<i>comGB</i>	-1.9
BSU35710	<i>tagG</i>	2.1	BSU07470	<i>yfmH</i>	-1.9
BSU09500	<i>yhdK</i>	2.1	BSU39710	<i>iolF</i>	-1.8
BSU16040	<i>rplS</i>	2.1	BSU24700	<i>comGD</i>	-1.8
BSU33810	<i>opuCC</i>	2.1	BSU12050	<i>yjdH</i>	-1.8
BSU33980	<i>yvbT</i>	2.1	BSU23140	<i>resB</i>	-1.8
BSU15670	<i>remA</i>	2.0	BSU06180	<i>pspA</i>	-1.8
BSU04940	<i>conE</i>	2.0	BSU03300	<i>nasD</i>	-1.8
BSU20040	<i>yosP</i>	2.0	BSU13180	<i>metE</i>	-1.8
BSU33820	<i>opuCB</i>	2.0	BSU12720	<i>xkdS</i>	-1.8
BSU19190	<i>desK</i>	2.0	BSU11710	<i>thiD</i>	-1.8
BSU25820	<i>yqcl</i>	2.0	BSU26890	<i>csn</i>	-1.8
BSU07180	<i>yezB</i>	2.0	BSU02050	<i>ybdO</i>	-1.8
BSU16680	<i>rpsO</i>	2.0	BSU18590	<i>yoaG</i>	-1.8
BSU21400	<i>yomD</i>	2.0	BSU37470	<i>phrF</i>	-1.8
BSU13850	<i>zosA</i>	2.0	BSU21480	<i>sunA</i>	-1.8
BSU17630	<i>yncC</i>	2.0	BSU04510	<i>ydbL</i>	-1.8
BSU36710	<i>fdhD</i>	2.0	BSU31900	<i>yukD</i>	-1.8
BSU04980	<i>yddl</i>	2.0	BSU37300	<i>ywiC</i>	-1.8
BSU05970	<i>rex</i>	2.0	BSU39610	<i>yxeB</i>	-1.8
BSU20480	<i>yoqX</i>	2.0	BSU24070	<i>buk</i>	-1.8
BSU22600	<i>aroE</i>	2.0	BSU31880	<i>yukB</i>	-1.8
BSU21100	<i>yonG</i>	2.0	BSU12730	<i>xkdT</i>	-1.8
BSU35700	<i>tagH</i>	2.0	BSU24710	<i>comGC</i>	-1.8
BSU39980	<i>qdol</i>	2.0	BSU31890	<i>yukC</i>	-1.8
BSU38110	<i>nfrA</i>	2.0	BSU37390	<i>albC</i>	-1.8

BSU14210	<i>ykuT</i>	2.0	BSU24060	<i>lpdV</i>	-1.8
BSU09520	<i>sigM</i>	2.0	BSU28250	<i>leuD</i>	-1.8
BSU00370	<i>abrB</i>	2.0	BSU26830	<i>zinT</i>	-1.8
BSU08700	<i>ygaE</i>	2.0	BSU36780	<i>ywzB</i>	-1.8
BSU38120	<i>rodA</i>	2.0	BSU11690	<i>thiG</i>	-1.8
BSU40400	<i>walkK</i>	2.0	BSU37380	<i>albB</i>	-1.8
BSU27780	<i>yrzF</i>	2.0	BSU14150	<i>ykuN</i>	-1.8
BSU20280	<i>yorR</i>	2.0	BSU37790	<i>rocG</i>	-1.8
BSU30020	<i>ytzE</i>	2.0	BSU24730	<i>comGA</i>	-1.7
BSU29600	<i>braB</i>	2.0	BSU25890	<i>yqxI</i>	-1.7
BSU09870	<i>yhaS</i>	1.9	BSU39750	<i>iolB</i>	-1.7
BSU32180	<i>yutK</i>	1.9	BSU12010	<i>manP</i>	-1.7
BSU12100	<i>yjeA</i>	1.9	BSU40100	<i>ahpF</i>	-1.7
BSU40190	<i>fbp</i>	1.9	BSU11700	<i>thiF</i>	-1.7
BSU07170	<i>yetI</i>	1.9	BSU40580	<i>yybN</i>	-1.7
BSU09850	<i>yhaU</i>	1.9	BSU39700	<i>iolG</i>	-1.7
BSU32880	<i>mdtP</i>	1.9	BSU18560	<i>yoaD</i>	-1.7
BSU21230	<i>yomT</i>	1.9	BSU15360	<i>ylmC</i>	-1.7
BSU10410	<i>yhzC</i>	1.9	BSU37400	<i>albD</i>	-1.7
BSU15680	<i>gmk</i>	1.9	BSU40180	<i>yydF</i>	-1.7
BSU34000	<i>yvbV</i>	1.9	BSU26200	<i>yqaS</i>	-1.7
BSU05510	<i>ydfQ</i>	1.9	BSU37260	<i>narJ</i>	-1.7
BSU04970	<i>cwlT</i>	1.9	BSU18170	<i>yngA</i>	-1.7
BSU16990	<i>tdh</i>	1.9	BSU25190	<i>cccA</i>	-1.7
BSU23880	<i>mifM</i>	1.9	BSU13170	<i>guaD</i>	-1.7
BSU34940	<i>yvpB</i>	1.9	BSU13140	<i>ohrA</i>	-1.7
BSU40410	<i>walR</i>	1.9	BSU01930	<i>skfC</i>	-1.7
BSU22170	<i>ypsC</i>	1.9	BSU11680	<i>thiS</i>	-1.7
BSU38470	<i>ywaD</i>	1.9	BSU38850	<i>yxkC</i>	-1.7
BSU21130	<i>yonD</i>	1.9	BSU01920	<i>skfB</i>	-1.7
BSU00790	<i>folK</i>	1.9	BSU39310	<i>yxiC</i>	-1.7
BSU13300	<i>mgtE</i>	1.9	BSU34430	<i>racX</i>	-1.7
BSU13670	<i>mhqR</i>	1.9	BSU23130	<i>resC</i>	-1.7
BSU21220	<i>yomU</i>	1.9	BSU22560	<i>qcrA</i>	-1.7
BSU05980	<i>tatAY</i>	1.9	BSU38930	<i>yxjJ</i>	-1.7

BSU13500	<i>ktrD</i>	1.9	BSU25570	<i>comEC</i>	-1.7
BSU21150	<i>yonB</i>	1.9	BSU11670	<i>thiO</i>	-1.7
BSU25900	<i>cwlA</i>	1.9	BSU12560	<i>xpf</i>	-1.7
BSU36790	<i>ywmA</i>	1.9	BSU39300	<i>yxiD</i>	-1.7
BSU07940	<i>yfkC</i>	1.9	BSU21610	<i>yokF</i>	-1.7
BSU21210	<i>yomV</i>	1.9	BSU22550	<i>qcrB</i>	-1.7
BSU21200	<i>yomW</i>	1.9	BSU38790	<i>yxzE</i>	-1.7
BSU06400	<i>yebE</i>	1.9	BSU32990	<i>mrgA</i>	-1.6
BSU10520	<i>glcP</i>	1.9	BSU29380	<i>tcyJ</i>	-1.6
BSU37990	<i>ywdE</i>	1.9	BSU12680	<i>xkdO</i>	-1.6
BSU31920	<i>yukF</i>	1.9	BSU37280	<i>narG</i>	-1.6
BSU06580	<i>yerC</i>	1.9	BSU32090	<i>yuiA</i>	-1.6
BSU20470	<i>yoqY</i>	1.9	BSU37290	<i>arfM</i>	-1.6
BSU22610	<i>tyrA</i>	1.9	BSU29390	<i>ytmI</i>	-1.6
BSU33340	<i>sspJ</i>	1.9	BSU37480	<i>ywhH</i>	-1.6
BSU19200	<i>desR</i>	1.8	BSU09890	<i>yhaQ</i>	-1.6
BSU01760	<i>ybbR</i>	1.8	BSU11530	<i>coiA</i>	-1.6
BSU39970	<i>yxaH</i>	1.8	BSU24100	<i>bkdR</i>	-1.6
BSU12820	<i>spoIISB</i>	1.8	BSU17160	<i>pksH</i>	-1.6
BSU24520	<i>mntR</i>	1.8	BSU40620	<i>yybJ</i>	-1.6
BSU23890	<i>yqjG</i>	1.8	BSU06830	<i>rapH</i>	-1.6
BSU18000	<i>citB</i>	1.8	BSU11650	<i>tenA</i>	-1.6
BSU15690	<i>yloH</i>	1.8	BSU14930	<i>ctaG</i>	-1.6
BSU20640	<i>yoqG</i>	1.8	BSU21620	<i>yokE</i>	-1.6
BSU36700	<i>moaA</i>	1.8	BSU10420	<i>comK</i>	-1.6
BSU23370	<i>ypuA</i>	1.8	BSU25830	<i>rapE</i>	-1.6
BSU21080	<i>yonI</i>	1.8	BSU11010	<i>yitJ</i>	-1.6
BSU20520	<i>yoqT</i>	1.8	BSU03960	<i>ycnK</i>	-1.6
BSU21250	<i>yomR</i>	1.8	BSU17240	<i>ymzB</i>	-1.6
BSU20620	<i>yoqI</i>	1.8	BSU33440	<i>cysJ</i>	-1.6
BSU34670	<i>yvdA</i>	1.8	BSU11040	<i>yitM</i>	-1.6
BSU21420	<i>bhlA</i>	1.8	BSU39690	<i>iolH</i>	-1.6
BSU25810	<i>arsR</i>	1.8	BSU16950	<i>pbpX</i>	-1.6
BSU09510	<i>yhdL</i>	1.8	BSU09300	<i>glpD</i>	-1.6
BSU08620	<i>yfhP</i>	1.8	BSU40090	<i>ahpC</i>	-1.6

BSU04930	<i>yddD</i>	1.8	BSU33270	<i>yvrO</i>	-1.6
BSU00670	<i>tilS</i>	1.8	BSU39320	<i>yxiB</i>	-1.6
BSU35750	<i>tagA</i>	1.8	BSU05480	<i>mhqN</i>	-1.6
BSU19970	<i>yosX</i>	1.8	BSU10790	<i>asnO</i>	-1.6
BSU36650	<i>ureB</i>	1.8	BSU11660	<i>tenI</i>	-1.6
BSU00700	<i>coaX</i>	1.8	BSU20580	<i>yoqM</i>	-1.6
BSU40390	<i>yycH</i>	1.8	BSU13550	<i>mtnA</i>	-1.6
BSU35760	<i>tagB</i>	1.8	BSU11410	<i>yjbA</i>	-1.6
BSU22430	<i>panB</i>	1.8	BSU24990	<i>pstS</i>	-1.6
BSU38480	<i>ywaC</i>	1.8	BSU37780	<i>rocA</i>	-1.6
BSU37010	<i>prfA</i>	1.8	BSU08760	<i>spo0M</i>	-1.6
BSU05990	<i>tatCY</i>	1.8	BSU17170	<i>pksI</i>	-1.6
BSU13030	<i>ykhA</i>	1.8	BSU34440	<i>pbpE</i>	-1.6
BSU24570	<i>gcvT</i>	1.8	BSU16660	<i>truB</i>	-1.6
BSU32190	<i>yuzB</i>	1.8	BSU12400	<i>yjnA</i>	-1.6
BSU30560	<i>pckA</i>	1.8	BSU17250	<i>ymaE</i>	-1.6
BSU06570	<i>yerB</i>	1.8	BSU39930	<i>yxam</i>	-1.6
BSU00320	<i>yaaT</i>	1.8	BSU24040	<i>bkdAB</i>	-1.6
BSU22160	<i>yptA</i>	1.8	BSU05490	<i>mhqO</i>	-1.6
BSU40110	<i>bglA</i>	1.8	BSU07150	<i>yetG</i>	-1.6
BSU35530	<i>tagO</i>	1.8	BSU22540	<i>qcrC</i>	-1.6
BSU39800	<i>yxcd</i>	1.8	BSU12550	<i>xtrA</i>	-1.6
BSU03150	<i>aroK</i>	1.8	BSU18840	<i>xynA</i>	-1.6
BSU19310	<i>dhaS</i>	1.8	BSU37250	<i>narI</i>	-1.6
BSU21160	<i>yonA</i>	1.8	BSU26120	<i>yqbG</i>	-1.6
BSU12860	<i>steT</i>	1.8	BSU27580	<i>yrvJ</i>	-1.6
BSU21410	<i>blyA</i>	1.8	BSU03940	<i>ycnI</i>	-1.6
BSU40370	<i>walJ</i>	1.8	BSU19410	<i>cwlS</i>	-1.6
BSU19990	<i>yosV</i>	1.8	BSU08580	<i>yfhL</i>	-1.6
BSU14250	<i>yknT</i>	1.8	BSU28950	<i>thrS</i>	-1.6
BSU25800	<i>yqcK</i>	1.8	BSU27770	<i>yrbE</i>	-1.6
BSU17470	<i>ynxB</i>	1.8	BSU08590	<i>yfhM</i>	-1.6
BSU36330	<i>ywpF</i>	1.8	BSU24030	<i>bkdB</i>	-1.6
BSU05470	<i>ydfM</i>	1.8	BSU15350	<i>ylmB</i>	-1.6
BSU40380	<i>yycI</i>	1.7	BSU12020	<i>manA</i>	-1.6

BSU03870	<i>ycnE</i>	1.7	BSU00950	<i>mrnC</i>	-1.6
BSU03550	<i>ycxC</i>	1.7	BSU26130	<i>yqbF</i>	-1.6
BSU04230	<i>ydaH</i>	1.7	BSU25880	<i>yqxJ</i>	-1.6
BSU11560	<i>yjbl</i>	1.7	BSU12710	<i>xkdR</i>	-1.6
BSU24560	<i>gcvPA</i>	1.7	BSU24050	<i>bkdAA</i>	-1.6
BSU28600	<i>yshB</i>	1.7	BSU26190	<i>yqaT</i>	-1.6
BSU17300	<i>ebrA</i>	1.7	BSU25360	<i>yqfC</i>	-1.5
BSU19480	<i>yojE</i>	1.7	BSU38800	<i>yxkH</i>	-1.5
BSU00800	<i>yazB</i>	1.7	BSU28260	<i>leuC</i>	-1.5
BSU20590	<i>yoqL</i>	1.7	BSU37270	<i>narH</i>	-1.5
BSU16980	<i>spoVS</i>	1.7	BSU29370	<i>tcyK</i>	-1.5
BSU40980	<i>yyaB</i>	1.7	BSU02590	<i>ycbP</i>	-1.5
BSU21180	<i>yomY</i>	1.7	BSU38400	<i>epr</i>	-1.5
BSU03860	<i>ycnD</i>	1.7	BSU00960	<i>yacO</i>	-1.5
BSU03850	<i>ycnC</i>	1.7	BSU21310	<i>yoZP</i>	-1.5
BSU38490	<i>menA</i>	1.7	BSU04240	<i>ydzA</i>	-1.5
BSU22590	<i>ypiA</i>	1.7	BSU34020	<i>yvbX</i>	-1.5
BSU25790	<i>arsB</i>	1.7	BSU21530	<i>yolB</i>	-1.5
BSU13150	<i>ohrR</i>	1.7	BSU33280	<i>yvrP</i>	-1.5
BSU36750	<i>spoIID</i>	1.7	BSU24080	<i>bcd</i>	-1.5
BSU20700	<i>yoqA</i>	1.7	BSU19400	<i>yojM</i>	-1.5
BSU19930	<i>yotC</i>	1.7	BSU25050	<i>yqgA</i>	-1.5
BSU05290	<i>ydeP</i>	1.7	BSU28470	<i>lysC</i>	-1.5
BSU29970	<i>ytkP</i>	1.7	BSU07380	<i>yfmQ</i>	-1.5
BSU17000	<i>kbl</i>	1.7	BSU02390	<i>ybgE</i>	-1.5
BSU20660	<i>yoqE</i>	1.7	BSU03950	<i>ycnJ</i>	-1.5
BSU09210	<i>yhcT</i>	1.7	BSU32080	<i>yuiB</i>	-1.5
BSU20650	<i>yoqF</i>	1.7	BSU28800	<i>araA</i>	-1.5
BSU03910	<i>gabD</i>	1.7	BSU03420	<i>nin</i>	-1.5
BSU24550	<i>gcvPB</i>	1.7	BSU29400	<i>ytlI</i>	-1.5
BSU20610	<i>yoqJ</i>	1.7	BSU00970	<i>yacP</i>	-1.5
BSU10570	<i>yhjN</i>	1.7	BSU20420	<i>yorD</i>	-1.5
BSU21690	<i>msrA</i>	1.7	BSU11020	<i>yitK</i>	-1.5
BSU21120	<i>yonE</i>	1.7	BSU28770	<i>araL</i>	-1.5
BSU26480	<i>yrkK</i>	1.7	BSU12540	<i>xkdD</i>	-1.5

BSU14620	<i>slp</i>	1.7	BSU27750	<i>bofC</i>	-1.5
BSU00810	<i>yacF</i>	1.7	BSU29360	<i>tcyL</i>	-1.5
BSU31300	<i>yugS</i>	1.7	BSU38940	<i>yxjI</i>	-1.5
BSU20740	<i>yopW</i>	1.7	BSU34010	<i>yvbW</i>	-1.5
BSU07720	<i>yfID</i>	1.7	BSU03350	<i>yciB</i>	-1.5
BSU21360	<i>yomH</i>	1.7	BSU35940	<i>rbsA</i>	-1.5
BSU33370	<i>yvgK</i>	1.7	BSU17150	<i>pksG</i>	-1.5
BSU20690	<i>yoqB</i>	1.7	BSU26140	<i>yqbE</i>	-1.5
BSU27940	<i>rpmA</i>	1.7	BSU21540	<i>yolA</i>	-1.5
BSU32060	<i>yuiD</i>	1.7	BSU00130	<i>serS</i>	-1.5
BSU28610	<i>zapA</i>	1.7	BSU32930	<i>yusU</i>	-1.5
BSU24210	<i>yqiG</i>	1.7	BSU33700	<i>opuBD</i>	-1.5
BSU05960	<i>ydiG</i>	1.7	BSU33260	<i>yvrN</i>	-1.5
BSU40120	<i>yyzE</i>	1.7	BSU37410	<i>albE</i>	-1.5
BSU20630	<i>yoqH</i>	1.7	BSU19160	<i>yocC</i>	-1.5
BSU26590	<i>blt</i>	1.7	BSU34870	<i>hisF</i>	-1.5
BSU21680	<i>msrB</i>	1.7	BSU27190	<i>yrzI</i>	-1.5
BSU21270	<i>yomP</i>	1.7	BSU36800	<i>atpC</i>	-1.5
BSU29920	<i>ytmP</i>	1.7	BSU12070	<i>yjdJ</i>	-1.5
BSU27360	<i>yrrM</i>	1.7	BSU27560	<i>hisS</i>	-1.5
BSU23950	<i>yqjA</i>	1.7	BSU17520	<i>ynaD</i>	-1.5
BSU02770	<i>yccK</i>	1.7	BSU28230	<i>tig</i>	-1.5
BSU07710	<i>ltaS</i>	1.7	BSU34860	<i>hisI</i>	-1.5
BSU36580	<i>ywnF</i>	1.7	BSU14580	<i>pdhA</i>	-1.5
BSU09690	<i>nhaX</i>	1.7	BSU28270	<i>leuB</i>	-1.5
BSU21020	<i>yonR</i>	1.7	BSU04000	<i>ycaA</i>	-1.5
BSU40360	<i>yyxA</i>	1.7	BSU39880	<i>yxbC</i>	-1.5
BSU21170	<i>yomZ</i>	1.7	BSU14590	<i>pdhB</i>	-1.5
BSU27350	<i>yrrN</i>	1.7	BSU01610	<i>feuC</i>	-1.5
BSU11900	<i>yjcL</i>	1.7	BSU32070	<i>yuiC</i>	-1.5
BSU21190	<i>yomX</i>	1.7	BSU18470	<i>proj</i>	-1.5
BSU36560	<i>ywnH</i>	1.7	BSU19580	<i>yodF</i>	-1.5
BSU22420	<i>panC</i>	1.7	BSU36810	<i>atpD</i>	-1.5
BSU02250	<i>ybjf</i>	1.7	BSU38730	<i>cydD</i>	-1.5
BSU01820	<i>adaB</i>	1.7	BSU04600	<i>ydbT</i>	-1.5

BSU04910	<i>yddB</i>	1.7	BSU01620	<i>feuB</i>	-1.5
BSU05670	<i>ydgJ</i>	1.7	BSU17130	<i>acpK</i>	-1.5
BSU09750	<i>sspB</i>	1.7	BSU26150	<i>yqbD</i>	-1.5
BSU38090	<i>vpr</i>	1.7	BSU12000	<i>manR</i>	-1.5
BSU06060	<i>ydiO</i>	1.7	BSU10740	<i>yisJ</i>	-1.5
BSU20670	<i>yoqD</i>	1.7	BSU29510	<i>ytfI</i>	-1.5
BSU14050	<i>ykuE</i>	1.6	BSU37430	<i>albG</i>	-1.5
BSU23830	<i>yqjL</i>	1.6	BSU16650	<i>rbfA</i>	-1.5
BSU04920	<i>yddC</i>	1.6	BSU35930	<i>rbsD</i>	-1.5
BSU20680	<i>yoqC</i>	1.6	BSU30700	<i>ytiA</i>	-1.5
BSU05340	<i>aseA</i>	1.6	BSU25260	<i>glyS</i>	-1.5
BSU26600	<i>bltD</i>	1.6	BSU01510	<i>ybaJ</i>	-1.5
BSU24020	<i>bmrR</i>	1.6	BSU35950	<i>rbsC</i>	-1.5
BSU05040	<i>yddN</i>	1.6	BSU26210	<i>yqaR</i>	-1.5
BSU00330	<i>yabA</i>	1.6	BSU39170	<i>yxzG</i>	-1.5
BSU31120	<i>lytG</i>	1.6	BSU39140	<i>yxiK</i>	-1.5
BSU08980	<i>yhbH</i>	1.6	BSU30750	<i>mntC</i>	-1.5
BSU39020	<i>nupG</i>	1.6	BSU28280	<i>leuA</i>	-1.5
BSU25780	<i>arsC</i>	1.6	BSU24090	<i>ptb</i>	-1.5
BSU00710	<i>yacC</i>	1.6	BSU02710	<i>yczC</i>	-1.5
BSU29900	<i>trmB</i>	1.6	BSU36090	<i>ywrE</i>	-1.5
BSU08210	<i>yfiB</i>	1.6	BSU04120	<i>yczI</i>	-1.5
BSU25140	<i>cshB</i>	1.6	BSU03340	<i>folE2</i>	-1.5
BSU29590	<i>nifZ</i>	1.6			
BSU31150	<i>yubB</i>	1.6			
BSU14990	<i>yIbF</i>	1.6			
BSU15310	<i>spoIIIGA</i>	1.6			
BSU22980	<i>ypbG</i>	1.6			
BSU05330	<i>aseR</i>	1.6			
BSU27300	<i>yrrS</i>	1.6			
BSU20600	<i>yoqK</i>	1.6			
BSU23980	<i>artP</i>	1.6			
BSU25090	<i>yqfW</i>	1.6			
BSU29580	<i>ytbj</i>	1.6			
BSU33010	<i>cssR</i>	1.6			

BSU34680	<i>yvcT</i>	1.6
BSU27950	<i>ysxB</i>	1.6
BSU20530	<i>yoqS</i>	1.6
BSU38000	<i>ywdD</i>	1.6
BSU02330	<i>ybfQ</i>	1.6
BSU30340	<i>ytvA</i>	1.6
BSU08560	<i>yfhJ</i>	1.6
BSU40440	<i>dnaC</i>	1.6
BSU21010	<i>yonS</i>	1.6
BSU36230	<i>ugd</i>	1.6
BSU02970	<i>yceK</i>	1.6
BSU32560	<i>frlR</i>	1.6
BSU31800	<i>yueF</i>	1.6
BSU07400	<i>yfmO</i>	1.6
BSU23970	<i>artQ</i>	1.6
BSU04880	<i>ydcS</i>	1.6
BSU14040	<i>ldt</i>	1.6
BSU10800	<i>yizA</i>	1.6
BSU35740	<i>tagD</i>	1.6
BSU03840	<i>ycnB</i>	1.6
BSU14950	<i>yIbB</i>	1.6
BSU40540	<i>yybR</i>	1.6
BSU08220	<i>yfiC</i>	1.6
BSU23560	<i>mleN</i>	1.6
BSU04900	<i>yddA</i>	1.6
BSU35510	<i>yvyE</i>	1.6
BSU13700	<i>clpE</i>	1.6
BSU37150	<i>pyrG</i>	1.6
BSU05430	<i>ydfJ</i>	1.6
BSU15330	<i>sigG</i>	1.6
BSU19470	<i>yojF</i>	1.6
BSU27530	<i>yrvN</i>	1.6
BSU04890	<i>ydcT</i>	1.6
BSU23240	<i>ribT</i>	1.6
BSU40330	<i>rocE</i>	1.6

BSU20010	<i>yosT</i>	1.6
BSU17900	<i>sirA</i>	1.6
BSU00280	<i>tmk</i>	1.6
BSU36980	<i>ywlA</i>	1.6
BSU03970	<i>ycnL</i>	1.6
BSU00310	<i>holB</i>	1.6
BSU37000	<i>ywkE</i>	1.6
BSU08540	<i>yfhI</i>	1.6
BSU20440	<i>yorB</i>	1.6
BSU00270	<i>yaaO</i>	1.6
BSU19460	<i>bshB2</i>	1.6
BSU03090	<i>ycgF</i>	1.6
BSU07310	<i>yfnD</i>	1.5
BSU31430	<i>yugE</i>	1.5
BSU00290	<i>yaaQ</i>	1.5
BSU20980	<i>yonV</i>	1.5
BSU05950	<i>ydiF</i>	1.5
BSU06420	<i>purE</i>	1.5
BSU26730	<i>yrdF</i>	1.5
BSU15370	<i>ylmD</i>	1.5
BSU08030	<i>yfnN</i>	1.5
BSU05230	<i>ydeK</i>	1.5
BSU05360	<i>ydfC</i>	1.5
BSU13650	<i>eag</i>	1.5
BSU08520	<i>yfhG</i>	1.5
BSU28180	<i>ysxD</i>	1.5
BSU21260	<i>yomQ</i>	1.5
BSU19130	<i>yocA</i>	1.5
BSU06430	<i>purK</i>	1.5
BSU04870	<i>nicK</i>	1.5
BSU22270	<i>yppE</i>	1.5
BSU25160	<i>ispH</i>	1.5
BSU17480	<i>ynzF</i>	1.5
BSU04860	<i>ydcQ</i>	1.5
BSU20510	<i>yoqU</i>	1.5

BSU01810	<i>adaA</i>	1.5
BSU31310	<i>yugP</i>	1.5
BSU03230	<i>ycgP</i>	1.5
BSU00820	<i>lysS</i>	1.5
BSU13660	<i>kinD</i>	1.5
BSU01800	<i>alkA</i>	1.5
BSU03080	<i>ycgE</i>	1.5
BSU06070	<i>ydiP</i>	1.5
BSU14550	<i>ykrA</i>	1.5
BSU24490	<i>yqhQ</i>	1.5
BSU15380	<i>ylmE</i>	1.5
BSU00300	<i>yaaR</i>	1.5
BSU20450	<i>yorA</i>	1.5
BSU11550	<i>yjbH</i>	1.5
BSU21380	<i>yomF</i>	1.5
BSU09830	<i>yhaX</i>	1.5
BSU22030	<i>dynA</i>	1.5
BSU05700	<i>ydhC</i>	1.5
BSU27400	<i>yrzL</i>	1.5
BSU09480	<i>yhdI</i>	1.5
BSU17290	<i>ebrB</i>	1.5
BSU20730	<i>yopX</i>	1.5
BSU36970	<i>spoIIR</i>	1.5
BSU20300	<i>yorP</i>	1.5
BSU00190	<i>dnaX</i>	1.5
BSU35730	<i>tagE</i>	1.5
BSU05080	<i>yddR</i>	1.5
BSU17880	<i>ynzC</i>	1.5
BSU22580	<i>ypiB</i>	1.5
BSU09970	<i>yhaJ</i>	1.5
BSU13760	<i>ykvN</i>	1.5
BSU33020	<i>cssS</i>	1.5
BSU35260	<i>ftsE</i>	1.5
BSU40760	<i>yyaP</i>	1.5
BSU20540	<i>yoqR</i>	1.5

BSU29660	<i>rpsD</i>	1.5
BSU00680	<i>hprT</i>	1.5
BSU18400	<i>yoeD</i>	1.5
BSU27340	<i>yrrO</i>	1.5
BSU09590	<i>yhdT</i>	1.5
BSU07140	<i>yetF</i>	1.5
BSU14430	<i>ykpA</i>	1.5
BSU16490	<i>rpsB</i>	1.5
BSU20960	<i>yopA</i>	1.5
BSU26660	<i>yrdN</i>	1.5
BSU23040	<i>fer</i>	1.5
BSU21700	<i>ypoP</i>	1.5
BSU08970	<i>prkA</i>	1.5
BSU03100	<i>ycgG</i>	1.5
BSU36740	<i>ywmC</i>	1.5
BSU17830	<i>yndM</i>	1.5
BSU40340	<i>rocD</i>	1.5
BSU10010	<i>trpP</i>	1.5
BSU15390	<i>sepF</i>	1.5
BSU40510	<i>yybT</i>	1.5
BSU05110	<i>ydeA</i>	1.5
BSU33420	<i>nhaK</i>	1.5
BSU40050	<i>gntR</i>	1.5
BSU17670	<i>cotU</i>	1.5
BSU22010	<i>ypcP</i>	1.5
BSU28490	<i>uvrC</i>	1.5
BSU17450	<i>glnR</i>	1.5
BSU15700	<i>yloI</i>	1.5
BSU26470	<i>yrkL</i>	1.5
BSU07260	<i>yfnI</i>	1.5
BSU26520	<i>yrkG</i>	1.5
BSU14770	<i>ylaG</i>	1.5
BSU27240	<i>yrhC</i>	1.5
BSU23640	<i>yqkD</i>	1.5
BSU05350	<i>ydfB</i>	1.5

BSU28930	<i>lytS</i>	1.5
BSU18790	<i>yoaZ</i>	1.5
BSU40750	<i>yyaQ</i>	1.5
BSU29000	<i>yticG</i>	1.5
BSU08690	<i>ygaD</i>	1.5
BSU27390	<i>yrrK</i>	1.5
BSU27500	<i>trmU</i>	1.5
BSU20970	<i>yonX</i>	1.5
BSU07420	<i>yfmM</i>	1.5
BSU22690	<i>aroH</i>	1.5
BSU30070	<i>opuD</i>	1.5
BSU22840	<i>yphC</i>	1.5
BSU07700	<i>nagP</i>	1.5
BSU40520	<i>yybS</i>	1.5
BSU24500	<i>yqhP</i>	1.5
BSU13770	<i>ykvO</i>	1.5
BSU08530	<i>yfhH</i>	1.5
BSU27960	<i>rplU</i>	1.5
BSU04200	<i>ydaE</i>	1.5
BSU23350	<i>ypzD</i>	1.5
BSU09760	<i>yheE</i>	1.5
BSU40910	<i>rpsF</i>	1.5
BSU13630	<i>ykvA</i>	1.5
BSU17950	<i>yneJ</i>	1.5
BSU24120	<i>yqiQ</i>	1.5
BSU36570	<i>ywnG</i>	1.5
BSU40900	<i>ssbA</i>	1.5
BSU35360	<i>hag</i>	1.5
BSU35520	<i>yvhJ</i>	1.5
BSU04850	<i>ydcP</i>	1.5
BSU15970	<i>ylxM</i>	1.5

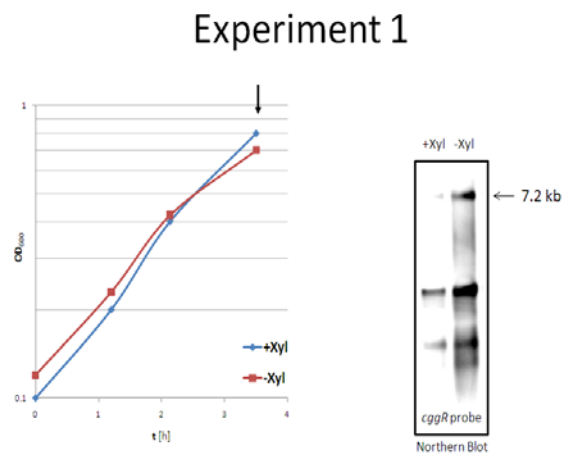
Supplemental figure: S1

Growth curves and Northern blot analysis of cultivations for transcriptome analysis. *Bacillus subtilis* strain GP193 was grown in CSE minimal media supplemented with 0.5% glucose. In this strain the expression of the *rny* gene is controlled by a xylose inducible promoter.

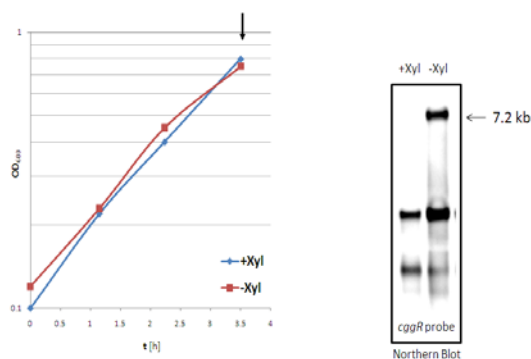
To deplete the essential RNase Y from this strain exponentially growing cells were used to inoculate two cultures to an optical density of 0.1. Whereas one culture contained xylose the other one was devoid of the inducer to restrict transcription of the *rny* gene. At the first sign of reduced growth of the culture without xylose (around OD 0.8), cells were immediately harvested for RNA isolation.

For every experiment the isolated RNA was tested for reduced processing of the *gap*-operon, a known target of RNase Y (Commichau *et al.* 2009). The depletion of the RNase stabilizes the operon, leading to higher amounts of *cggR* seen in the accumulation of the full length 7.2 kb transcript of the operon.

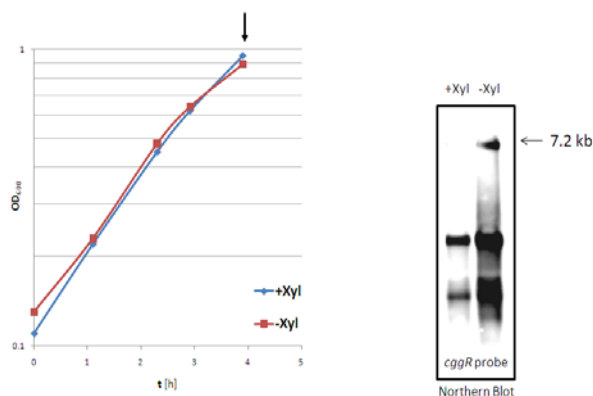
The arrow indicates the time point of cells harvest for RNA isolation.



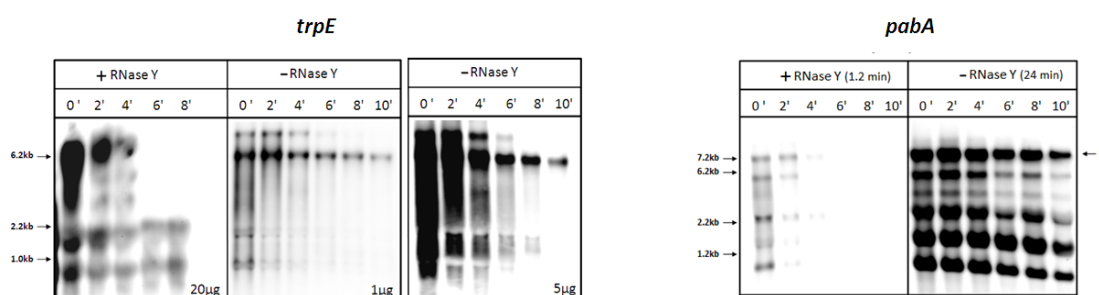
Experiment 2



Experiment 3



Supplemental figure: S2



Stability of the tryptophan and folate mRNA. Total RNA was isolated from a *P_{xyI}-rny* strain in the presence and absence of xylose. RNA was prepared from cells grown in minimal media supplemented with 0.5% glucose before (0') and after the addition of rifampicin (2, 4, 6, 8 and 10 min). For *trp*, 20 μ g, 1 μ g or 5 μ g of total RNA was loaded. The Northern blot with the *pabA* specific probe contained 5 μ g of total RNA per lane.

Supplemental Table: S2

Influence of RNase Y depletion on different mRNA transcripts.

For microarray analysis, *B. subtilis* GP193 was used. In this strain the potential downstream gene *ymdB* might be depleted, too. Therefore we used *B. subtilis* GP1015 in which *ymdB* is complemented in the *amyE* locus to verify the transcriptome data by quantitative reverse transcriptase PCR. In all cases, similar fold changes were obtained irrespective of depletion of *ymdB*.

Transcription unit	Fold regulation upon RNase Y depletion	
	Microarray	RT reverse transcriptase PCR
mRNAs stabilized upon depletion of RNase Y		
<i>trpEDCFBA-hisC-tyrA-aroE</i>	13.1	26
<i>yhbIJ-yhcABCDEFGHI</i>	7.1	16
<i>maeA-ywkB</i>	4.7	6
<i>ribU</i>	2.7	3
<i>yhdY</i>	2.5	3
<i>yorW</i>	4.4	4
mRNAs destabilized upon depletion of RNase Y		
<i>slrR</i>	0.2	0.4
<i>epsA-O</i>	0.2	0.2
<i>sunT-bdbA-yolJ</i>	0.3	0.3
<i>tapA-sipW-tasA</i>	0.4	0.3
<i>thrZ</i>	0.4	0.2
<i>sdpABC</i>	0.4	0.3

10.6. Curriculum vitae

Personal information

Name	Martin Lehnik-Habrink
Date of birth	4 th February, 1981
Place of birth	Berlin
Nationality	Germany

Education

1993-2000	Friedrich-Wilhelm-Gymnasium; Königs Wusterhausen
2000-2001	Basic military service
2001- 2007	Study of Biochemistry, Ernst-Moritz-Arndt-University of Greifswald, Diploma thesis in the group of Prof. Dr. Uwe Völker, Interfaculty Institute for Genetics and Functional Genomics
2005-2006	Attendance of the University of Texas, Health Science Center at San Antonio, USA
2008-2011	PhD project: “An mRNA degradation complex in <i>Bacillus subtilis</i> ” in the group of Prof. Dr. Jörg Stülke, Department of General Microbiology at the Georg-August-University Göttingen